Contribution of the Anconeus Muscle to the Elbow Kinematics: Range of Motion of 90° of Flexion-Extension and Pronation-Supination

A Thesis Submitted to the University of Manchester for the Degree of Doctor of Philosophy in the Faculty of Engineering and Physical Sciences

2016

Israel Miguel Andres

SCHOOL OF MECHANICAL, AEROSPACE AND CIVIL ENGINEERING

TABLE OF CONTENTS

Final word count 49117

LIST OF FIGURES

8

13

LIST OF TABLES

LIST OF ABBREVIATIONS

AP	Action potential
ATP	Adenosine triphosphate
ARV	Average rectify value
Br	Brachialis muscle
BR	Brachioradialis muscle
CNS	Central nervous system
CT scan	Computed tomography scan
CAD	Computer-aided design
CC	Contractile component
dB	Decibel
DICOM	Digital imaging and communicated in medicine
EMG	Electromyography
Eq	Equation
ECRB	Extensor carpi radialis brevis muscle
ECRL	Extensor carpi radialis longus muscle
ECU	Extensor carpi ulnaris muscle
EDC	Extensor digitorum communis muscle
FFT	Fast Fourier transformation
FEM	Finite element method
FIR	Finite impulse response
FCR	Flexor carpi radialis muscle
FDS	Flexor digitorum superficialis muscle
IMUs	Inertial motion units
IIR	Infinite impulse response
LACL	Lateral annular collateral ligament
LCL	Lateral collateral ligament
LRCL	Lateral radial collateral ligament
LUCL	Lateral ulnar collateral ligament
MRI	Magnetic resonance imaging
MVC	Maximum voluntary contraction
MNF	Mean frequency
MACL	Medial anterior collateral ligament

16

MCL	Medial collateral ligament
MPCL	Medial posterior collateral ligament
MTCL	Medial transverse collateral ligament
MDF	Median frequency
MEMS	Micro-electro-mechanical systems
MUAP	Motor unit action potential
PEC	Parallel elastic component
PCS	Physiological cross-section
PCSA	Physiological cross-sectional area
PSD	Power spectrum density
PT	Pronator teres muscle
RoM	Range of motion
RNS	Repetitive nerve stimulation
RMS	Root mean square
SEC	Series elastic component
Ag	Silver
AgCl	Silver chloride
sEMG	Surface electromyography
3D	Three dimensions
2D	Two dimensions
MTw	Wireless motion tracker

NOMENCLATURE

$\vec{\alpha}$	Angular acceleration vector
θ	Angular displacement
$\vec{L}$	Angular momentum
$\vec{\omega}$	Angular velocity vector
cm	Centimetre
cos	Cosine function
$\vec{F_c}$	Coriolis force
$^{\circ}$	Degree
$\vec{F}$	Force vector
G	Global coordinate system
Hz	Hertz
J	Joule
kg	Kilogram
$\vec{a}$	Linear acceleration vector
$\vec{v}$	Linear velocity vector
S	Local coordinate system
log	Logarithm
I	Mass moment of inertia
m	Metre
ml	Millilitre
mm	Millimetre
mV	Millivolts
N	Newton
P	Net joint power
$\vec{T}$	Net joint torque
q	Quaternion
q^{*}	Quaternion conjugate
rad	Radian
R	Rotational matrix
R_{GS}	Rotational matrix to rotate a vector from local to global system
Fs	Sample frequency

s	Second
sin	Sine function
SD	Standard deviation
k	Stiffness of the spring
σ	Stress
t	Time
Δt	Time increment
W	Watts
E	Young's modulus

ABSTRACT

The anconeus, a small triangular muscle positioned on the posterolateral part of the elbow joint, has been the subject of considerable research without a satisfactory conclusion being reached regarding the role it plays during normal elbow kinematics.

The aim of this investigation was to elucidate the function of the anconeus muscle and find the relative contribution that it makes to elbow kinematics by examining relative electrical muscle activity and elbow kinematics both before and after anconeus defunctioning carried out using a local anaesthetic (lidocaine). The study was performed through an examination of the myoelectric activity of the representative elbow flexor and extensor muscles (biceps brachii and triceps brachii) and the elbow kinematics and kinetics. Right-handed, healthy volunteers performed elbow flexion-extension and supination-pronation movements in both horizontal and sagittal planes before and after blocking of the anconeus. The kinematics and kinetics of the elbow were assessed using inertial sensors, and muscle electrical activity was recorded using surface electromyography.

In the following stage of the study, the anconeus muscle was blocked through an injection of lidocaine and then the flexion-extension and pronation-supination movements were repeated. The relative electrical activity results from the anconeus before blocking clearly indicate that the activity of the muscle was higher during the extension portion of the flexion-extension cycle, suggesting that it behaves as an extensor muscle. However, from the paired sample t-test analysis, it was found that blocking of the anconeus had no effect on the kinematics and kinetics of the elbow, including the angular velocity, net torque, power and net joint work. Moreover, the angular velocity data for the elbow, before and after the blocking for all movements, showed a linear trend with slopes and Pearson's correlations close to unity, indicating no apparent difference on the elbow kinematics. In addition, the relative electrical activity of the biceps and triceps brachii muscles did not alter significantly following blocking of the anconeus. These findings suggest that the anconeus muscle is a relatively weak elbow extensor as it is likely that the small contribution that the anconeus provides during extension before blocking is compensated by the triceps brachii after the anconeus is deactivated.

In order to provide additional weight and support to the findings of the experimental study, a computational model of the elbow joint was created in Abaqus CAE with the aim of investigating the contribution of the anconeus during the flexion-extension motion. In particular, the effect on the range of motion and contact area of the elbow joint was investigated both before and after anconeus blocking. The analysis was done in a range of motion of 90°, starting with the elbow extended 30° and ending flexed 120°. The elbow joint model considered cortical bone, trabecular bone, cartilage, collateral ligaments, the anconeus, biceps brachii and triceps brachii. The results of the investigation indicated that the anconeus muscle does not produce a significant change in the range of motion and contact area in the articulation, an outcome that supports the findings of the experimental investigation.

DECLARATION

No portion of the work referred to in the thesis has been submitted in support of an application for another degree or qualification of this or any other university or other institute of learning.

COPYRIGHT STATEMENT

i. The author of this thesis (including any appendices and/or schedules to this thesis) owns certain copyright or related rights in it (the "Copyright") and s/he has given The University of Manchester certain rights to use such Copyright, including for administrative purposes.

ii. Copies of this thesis, either in full or in extracts and whether in hard or electronic copy, may be made only in accordance with the Copyright, Designs and Patents Act 1988 (as amended) and regulations issued under it or, where appropriate, in accordance with licensing agreements which the University has from time to time. This page must form part of any such copies made.

iii. The ownership of certain Copyright, patents, designs, trade marks and other intellectual property (the "Intellectual Property") and any reproductions of copyright works in the thesis, for example graphs and tables ("Reproductions"), which may be described in this thesis, may not be owned by the author and may be owned by third parties. Such Intellectual Property and Reproductions cannot and must not be made available for use without the prior written permission of the owner(s) of the relevant Intellectual Property and/or Reproductions.

iv. Further information on the conditions under which disclosure, publication and commercialisation of this thesis, the Copyright and any Intellectual Property and/or Reproductions described in it may take place is available in the University IP Policy (see http://documents.manchester.ac.uk/DocuInfo.aspx?DocID=487), in any relevant Thesis restriction declarations deposited in the University Library, The University Library's regulations (see http://www.manchester.ac.uk/library/aboutus/regulations) and in The University's policy on Presentation of Theses

ACKNOWLEDGEMENTS

Above all, I want to express my sincere gratitude to Professor Teresa Alonso Rasgado, Dr Alan Walmsley and Professor Adam Watts for their support, advice, knowledge transmitted and excellent guidance during the development of this research. I want to thank Professor Adam Watts for helping in the development of the experimental protocol and during the experimental tests, I am grateful for his support.

I would like to thank my wife Juana for her personal support and great patience at all times. Besides, I want to thank my parents, brothers and sisters for their endless love, encouragement and confidence in this stage of my life.

A special thanks to my colleagues of the Bioengineering Research Group and the friendly people around of me for their help and support.

I want to thank Dr David Jimenez Cruz and Dr Jaya Nemchand for their help, suggestions and technical guidance.

I would also like to thank Wrightington Hospital for the facilities to carry out this project.

I want to express my gratitude to The National Council of Science and Technology of Mexico (CONACYT) for the scholarship and financial support to accomplish this research.

Last but not least, I would like to acknowledge The Secretaria de Educacion Publica of Mexico (SEP) for the scholarship during the last two years of this project.

Thanks God

CHAPTER ONE

1 INTRODUCTION

1.1 Background

The anconeus, a small triangular muscle located in the posterolateral part of the elbow, has been the subject of debate concerning the role it plays in human elbow kinematics. The anatomy and function of the anconeus have been studied since 1867, when Duchenne suggested that the muscle was involved in extension of the forearm and abduction of the ulna during pronation [1]. Since then, there have been several studies regarding the function of anconeus muscle; however, nobody has given a proper explanation of its function in the elbow kinematics. Consequently, some surgeons view this muscle as unimportant and it is frequently denervated during surgical approaches to the elbow [2]. Moreover, the anconeus has been harvested as a local flap for the treatment of conditions around the elbow [3-10].

It has also been used to repair the radiocapitellar and radioulnar joint dysfunction [11-14]. Repetitive nerve stimulation of the anconeus muscle has been used to detect neuromuscular transmission disorders, such as myasthenia gravis [15-19]. Anconeus has been associated with the lateral epicondylitis at the elbow and compartment syndrome of the forearm [20-21].

Electromyographic studies have found that the electrical activity of the anconeus was higher in extension [22-28], suggesting that this muscle was an elbow extensor muscle. However, other studies rejected the idea that the anconeus was an extensor muscle, concluding that it was an abductor of the ulna during pronation [29-30]. The assertion that the anconeus is an abductor has itself been refuted by other researchers, notably Pauly and Basmajian, who suggested that instead it could be a stabiliser of the joint [23, 31].

Other studies observed that the anconeus was active during the resisted pronation-supination movement, implying that it could provide elbow stability [22-23, 32]. In addition, it has been suggested that the contribution of the anconeus on elbow

kinematics could be more significant as an active stabiliser than as an elbow extensor muscle [31, 33].

Recent investigations found that the anconeus could contribute up to 15% of the extension moment during isometric contractions that require small joint torques of less than 13 Nm [34]. However, more recent anatomical studies have reported that the role of anconeus during extension is merely an accessory [35].

On the other hand, the physiological cross-sectional area and the moment arm of anconeus indicates that it should behave as an extensor muscle [36]. Moreover, because it is a pennate muscle, the anconeus would appear to be more suited to force production rather than motion production [37], and hence, could be considered as an active lateral stabiliser of the elbow joint [33, 35, 38-39].

Finally, new electromyographic studies have suggested that anconeus should be considered as a multifunctional muscle at the elbow, which could produce extension of the forearm, abduction of the ulna and stability of the joint [40].

These studies suggest that the anconeus is an important component of the joint and may play a significant role in the kinematics of the elbow. However, lack of agreement remains among the researchers to define a specific function for this muscle.

1.2   Aims and objectives

The aim of the investigation presented in this thesis was to study the function and contribution of the anconeus muscle on the elbow kinematics and kinetics in order to elucidate its function and stop the long debate within the research community regarding the function of anconeus muscle. Surface electromyography was used to measure the electrical activity of anconeus, biceps and triceps brachii. Inertial measurement units were employed to record the kinematics of the elbow joint.

In order to find the contribution of the anconeus muscle on the elbow kinematics, the anconeus muscle was deactivated with local anaesthesia (lidocaine). The contribution

of the anconeus muscle on the elbow movement was measured comparing the kinematics and kinetics of the elbow before and after blocking the anconeus. In addition, the effect on the myoelectric activity was done by comparing the electrical activity of biceps and triceps brachii before and after applying the anaesthetic.

1.3   Thesis overview

The anconeus muscle is generally described as a small, penniform muscle located in the posterolateral part of the elbow, connecting the humeroulnar joint from the lateral epicondyle to the proximal ulna [37, 41-42]. Although there are several studies regarding anconeus, the specific function and contribution of this muscle on the elbow kinematics remain unclear. Its anatomy and function have been studied since 1867, when Duchenne suggested for the first time that the muscle was involved in the extension of the forearm and abduction (lateral translation) of the ulna during pronation [1]. Since then, there has been little agreement among researchers to define the specific function of the anconeus muscle.

Anatomically, the orientation of the fibres of anconeus implies that the muscle is designed for force production, but it cannot produce large displacement [37]. Therefore, anconeus could play an important role in the stability of the elbow joint [31, 33, 35, 43]. Other anatomical and biomechanical studies of this muscle suggests that it can produce extension of the elbow up to a certain flexion angle because the moment arm of one of its fibres reverses the direction to produce flexion [38]. Recent electrical studies suggest that the anconeus should be considered as a multifunctional muscle at the elbow [40].

Muscles play an important role in the human body because they allow daily life activities to be performed, such as running, dancing, eating, and so on. There are three types of muscle: skeletal, cardiac and smooth muscles [44]. This investigation is focused on studying the function of the anconeus muscle, a skeletal muscle placed at the back of the elbow joint. It is connected from the posterior-inferior aspect of the lateral epicondyle of the humerus to the radial side of the olecranon and proximal ulna. The elbow is a synovial joint integrated by three bones: the humerus, ulna and radius. The elbow is an important joint of the upper limb, which allows the hand to

be placed in anywhere around the body to perform daily life activities, such as feeding, touching the face, using a screwdriver, so on [45]. The elbow stability is provided by passive and active components; bones and ligaments are the passive components and muscles crossing the elbow are the active components [46].

Flexion-extension and pronation-supination are the main movements of the elbow joint. There is a small angular deviation of the forearm when the flexion-extension movement is performed. This deviation is called the carrying angle and is formed by the longitudinal axis of the humerus and the axial axis of the forearm. This angle is greater in females than males [47]. The superficial muscles working in flexion and extension movements are biceps and triceps brachii. As their functions at the elbow are well known, they are considered in this study by comparing them with anconeus activity to find out the function of anconeus.

Even though there are several electromyographic, anatomical studies of the anconeus muscle, it is clear that its specific function in the elbow kinematics remains unknown.

Figure 1.1 shows the flow chart of the methodology of the experimental research, which was divided in two stages with the purpose of clarifying the role of the anconeus on the elbow kinematics. In the first part of the methodology, the muscle electrical activity of the anconeus, biceps and triceps brachii were recorded using surface electromyography and the kinematics and kinetics of the elbow joint were calculated using inertial sensors. The muscle electrical activity and the kinematics and kinetics of the elbow were compared to analyse the muscle activity on the elbow movement.

Subsequently, the second part of the methodology involved the use of a local anaesthetic to deactivate the anconeus muscle and study the effect on the elbow movement. The outcomes were compared before and after applying the anaesthesia. Moreover, the electrical activity of biceps and triceps brachii were compared before and after blocking anconeus to see the effect of anconeus defunctioning on the electrical activity of the superficial flexor and extensor muscles of the elbow.

The final stage of this investigation was to create a computational model of the elbow joint with muscles, cartilage, ligaments, trabecular and cortical bone with the aim of study the effect of the anconeus muscle on the range of motion of the joint.
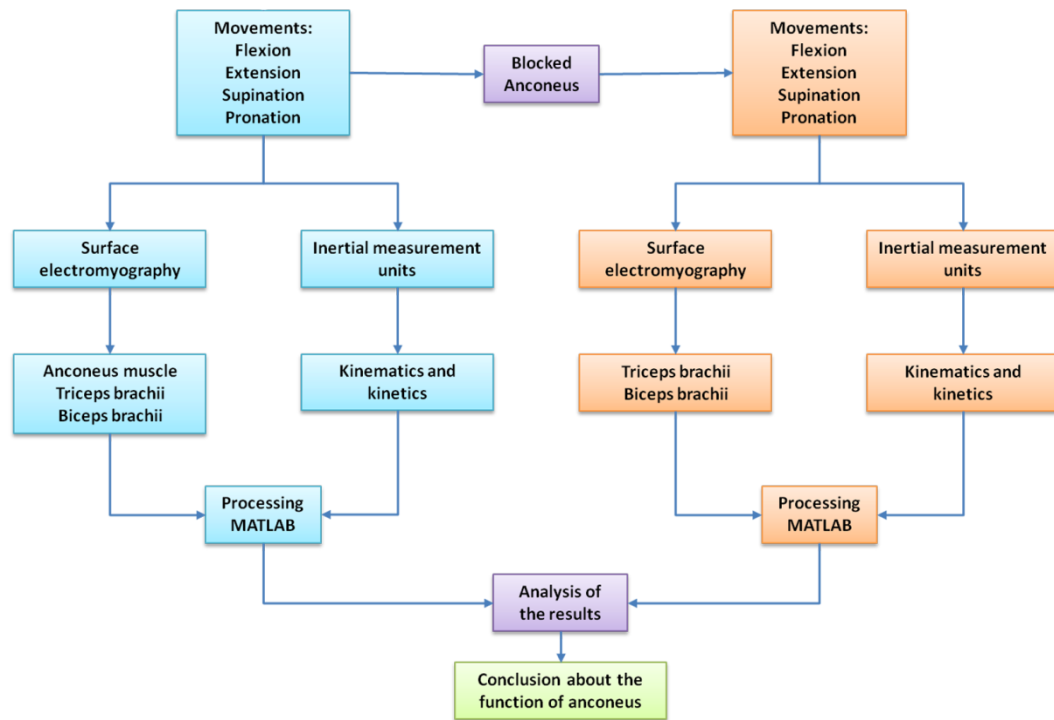
Figure 1.1 low chart of the experimental methodology

Following the introductory section, the remaining chapters of this thesis are presented as follows:

Chapter II describes the structure, function and the main components of the elbow joint in order to understand and become familiar with the anatomy and biomechanics of the elbow. This chapter provides information regarding the planes of the human body and the kinematics and kinetics of the elbow. Additionally, it is reported the mechanical properties of the skeletal muscles with the purpose of understanding the physiology of muscle contraction. A review of the most important studies regarding anconeus, biceps brachii and triceps brachii is described. The anatomy and biomechanics of the anconeus, biceps and triceps brachii muscles are presented in this chapter to understand how the main elbow flexor and extensor muscles are involved in the elbow movement. The theoretical background regarding signal processing in electromyography is presented. The components of an inertial

measurement unit are described in this section with the aim of understanding how these sensors track human motion. Furthermore, some mathematical operations using quaternions, Euler angles and the direction cosine matrix are explained by calculating relative movements and rotations with respect to a reference system. At the end of this chapter, some techniques of imaging processing are presented in order to know their technical features.

Chapter III explains the methodology, results and analysis of the flexion-extension and pronation-supination movements in the horizontal and vertical planes. The electrical activity of anconeus, biceps and triceps brachii muscles was recorded using surface electromyography (a non-invasive method) and the kinematics of the elbow was measured using inertial sensors. The kinematics and kinetics of the elbow were analysed in relation to the myoelectric activity to find how the muscles were activated during the elbow movement. The aim of this chapter is to clarify the relationship between the muscles and elbow movements in order to explain the role of anconeus in the elbow kinematics.

Chapter IV reports the results of the muscle electrical activity and elbow movements, before and after blocking the anconeus, in healthy volunteers. The aim of this chapter is to find the effect of the anconeus on the elbow kinematics and kinetics when the anconeus was deactivated with a local anaesthesia. The anconeus muscle was blocked by giving an injection of a local anaesthetic at the middle point between the lateral epicondyle and the olecranon tip of the ulna. The flexion-extension and pronation-supination movements were performed in the sagittal and horizontal planes. The analysis was performed by comparing the data of the movements and the myoelectric activity before and after deactivating anconeus.

Chapter V describes the methodology and results of the computational model of the elbow joint during flexion-extension motion. The model was created considering the cortical bone, trabecular bone, cartilage, collateral ligaments, the anconeus, biceps brachii and triceps brachii. The muscles were modelled using connector sections. The objective of this chapter is to simulate the natural flexion-extension motion of the elbow and study the effect of the anconeus muscle in the range of motion of the joint. The aim was achieved by applying four different loads to the anconeus and

comparing the effect in the range of motion. The normal movement of the joint was modelled with the anconeus having a force of 15% of the total extension force. Then, the deactivation of the muscle was simulated by applying no force to the muscle. The range of motion of the elbow model was analysed from 30 to 120 degrees. This range of motion was chosen to avoid the bones touch each other when the elbow is completely flexed or extended and to be able to compare the computational model analysis with the experimental part.

Finally, Chapter VI presents the conclusions, analysis of the outcomes and the future work of this investigation.

CHAPTER TWO

2 ANATOMY AND BIOMECHANICS OF THE ELBOW JOINT: ELECTROMYOGRAPHY, INERTIAL MEASUREMENT UNITS AND IMAGING PROCESSING

2.1 Introduction

The elbow is a trochoginglymoid articulation with two degrees of freedom: flexion-extension and pronation-supination. It is one of the most important joints of the human body due to the significant role it plays in daily life activities, such as eating, touching the face, using a screwdriver, personal care and so on [45, 48]. In comparison with the shoulder, the elbow is a stable joint formed by three bones: the humerus, ulna and radius [49]. The stability is provided by its passive and active components: the three bones and ligaments being the passive components and the muscles crossing the joint the active elements [45, 48, 50].

Due to its intricate structure, the function of the anconeus muscle has been studied for more than a century with different hypotheses being put forward about the probable role of this muscle in elbow kinematics. Anatomical and electromyographic studies have tried to address the function of the anconeus muscle, but none of them have clarified the specific role and contribution of this muscle in elbow kinematics. Meanwhile, the anconeus has been used as a muscle flap for the treatment of conditions affecting the elbow [3-9]. This chapter describes the anatomy and biomechanics of the elbow joint. The anatomy of the humerus, ulna and radius is presented with the aim of identifying the main bony landmarks and geometries of the bones. The structure of the three bones shows how the bones assemble in order to allow motion of the limb. Subsequently, muscles across the elbow joint are described to identify their anatomy and location in the articulation. The ligaments and articulations around the elbow are described so that the structure and function of the joint can be understood. Furthermore, the planes of the human body are illustrated to reference the movements of the elbow. The kinematics and kinetics of the elbow are presented in order to understand the orientation, angular velocity, the net torque,

31

power and work of the joint. This research assumed that the segments of the upper limb behave as rigid bodies.

Furthermore, in this chapter, the physiology of the muscular system is discussed in more detail. There are several muscles across the elbow joint, which contribute in the movement and stability of the articulation. The current study employs surface electromyography and evaluates the electrical activity of the superficial flexor and extensor muscles (biceps and triceps brachii). The brachialis is a deep flexor muscle and it is not considered in this study as it is not the major flexor muscle [51]. This chapter presents relevant information regarding the anatomy and biomechanics of the representative elbow flexor and extensor muscles, biceps brachii and triceps brachii. The function and myoelectric activity of the biceps and triceps brachii muscles are well known within the research community. Therefore, the myoelectric activity of the anconeus can be compared to them in order to be able to determine the role of the anconeus muscle in elbow kinematics.

The current chapter describes the different types of muscles in the human body and the various roles they play when they contract. As the skeletal muscles are the most important in this investigation, their mechanical properties are presented with the aim of understanding how the muscles contract in relation to the neuroelectrical system. Additionally, the structure and physiology of muscle contraction is explained in order to understand the chemical reaction that is developed inside the muscles to perform the contraction process. This chapter describes the theoretical background required for the signal processing of surface electromyography and some techniques employed in the analysis of human body movement. At the end of this chapter, the finite element method and the imaging analysis is presented in order to explain the imaging techniques to create the bone geometry.

2.2 Structure of the elbow joint

The elbow is an elaborate joint integrated by three bones, collateral ligaments and a fibrous capsule. The humerus, radius and ulna are the three bones, which produce three different articulations at the elbow: the humeroulnar, humeroradial and proximal radioulnar joint [52]. The complex shape of the articulations, in conjunction

with the medial and lateral collateral ligaments, gives the primary stability to the joint [49]. All muscles that cross the joint are considered to be dynamic stabilisers because they can give stability to the articulation when they contract. Furthermore, they are responsible for producing motion of the joint to perform daily life activities [48]. To have a better idea of the bony landmarks of the elbow, the anatomy of the three bones of the elbow is presented below.

2.2.1   Humerus

The humerus is the longest bone of the upper limb. Its proximal part articulates with the scapula to create the shoulder joint and the distal part articulates with the ulna and the radius to form the elbow [44]. The trochlea, the capitulum, lateral epicondyle, olecranon fossa, medial epicondyle and coronoid fossa are the representative bony landmarks of the humerus in the distal part, as shown in Figure 2.1. Most of the flexor and extensor muscles of the wrist emerge from the medial and lateral epicondyle, respectively.
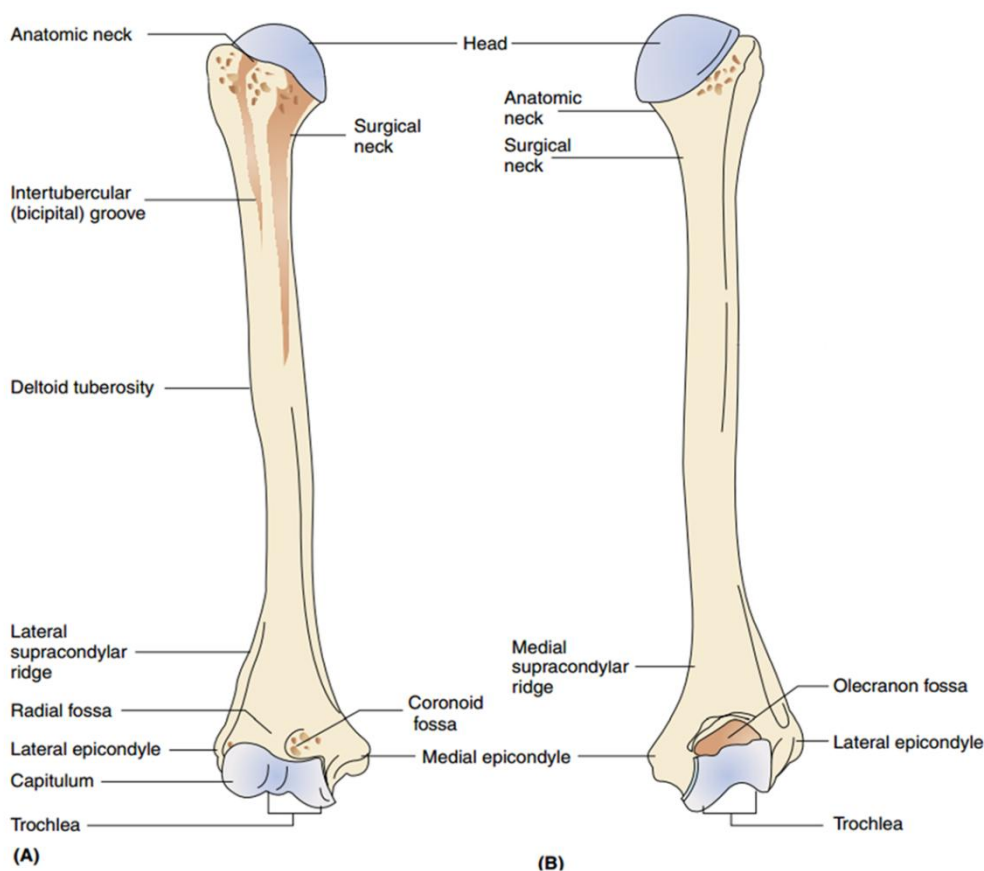
Figure 2.1 Bony landmarks of the humerus, (A) Anterior and (B) Posterior view. Adapted from [44].

33

The major bony landmarks in the proximal part of the humerus are the semi-spherical head and the greater and lesser tuberosities. The supraspinatus, infraspinatus and teres minor muscles are attached to the greater tuberosity. The bony landmarks of the humerus can be seen in Figure 2.1. The distal and proximal parts are primarily made of trabecular bone, surrounded by a small compact layer of cortical bone, the middle part (or shaft) is mainly made of cortical bone [53]. The small helical shape of the trochlea of the humerus allows the ulna to produce a small deviation from valgus to varus when the elbow is flexed or extended. This movement is known as the carrying angle.

2.2.2 Ulna

The ulna is the largest bone of the forearm. It is located in the medial side of the forearm and runs parallel with the radius [53]. The triceps brachii tendon is inserted in the proximal part of the olecranon. The olecranon has been considered as an important passive stabiliser of the elbow [54]. In addition, the coronoid process of the ulna also plays an important role in providing stability to the articulation [55-57].

The greater sigmoid notch articulates with the trochlea of the humerus allowing flexion and extension movement. Furthermore, the lesser sigmoid notch articulates with the head of the radius allowing rotation of the forearm. In the distal part, the ulna articulates with the radius forming the distal radioulnar joint. Figure 2.2 illustrates the main bony landmarks of the ulna in the proximal and distal parts.

2.2.3 Radius

The radius is smaller than the ulna and is placed in the lateral side of the forearm, as illustrated in Figure 2.2. It is attached to the ulna through the interosseous membrane, which connects the shafts of the two bones. Its proximal part is called the radial head which articulates with the humerus and ulna bones [44]. In the proximal part, the radius articulates with the capitulum of the humerus creating the humeroradial joint and in the distal part, it articulates with the carpal bones creating the radiocarpal joint. Furthermore, it has been suggested that the head of the radius plays an important role in posterolateral rotatory stability of the elbow [58].
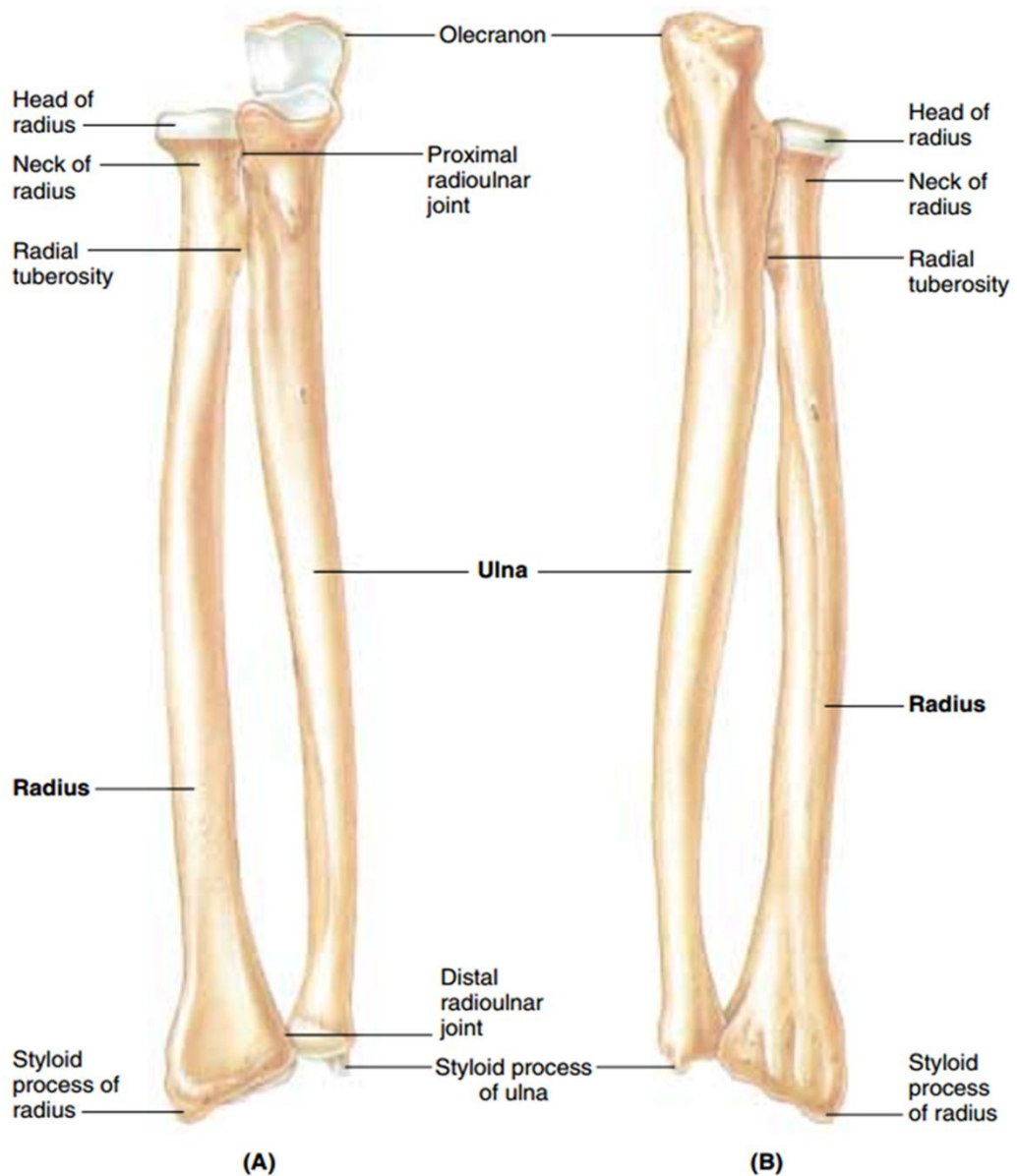
Figure 2.2 Bony landmarks of the ulna and radius bones, (A) Anterior and (B) Posterior view of the forearm [44].

2.2.4   Ligaments of the elbow

Lateral and medial collateral ligaments, in conjunction with the anterior and posterior synovial capsule of the elbow, play an important role in passive stability of the elbow [49, 59]. The lateral collateral ligament (LCL) complex is formed by an ulnar, a radial and an annular ligament and the anterior, posterior and transverse ligaments form the medial collateral ligament (MCL) complex [48-49]. It has been suggested that the lateral collateral ligament complex plays an important role in varus and posterolateral rotatory stability [48-49, 58, 60-61]. Furthermore, the medial collateral

35

ligament complex provides stability when valgus forces are trying to dislocate the elbow [62].

The lateral ulnar collateral ligament (LUCL) has been considered to be an intricate ligament of the LCL complex because of the structure of the fibres, Figure 2.3a. It arises from the lateral epicondyle and inserts on the tubercle of the supinator crest of the ulna [63]. It has been proposed that the LUCL plays an important role in posterolateral rotatory stability and in varus stability [49, 61, 63]. Furthermore, in an anatomical study, it was found that the LUCL could work together with the annular ligament because the fibres blend together [64].

The lateral radial collateral ligament (LRCL) emerges from the inferior area of the lateral epicondyle and blends with the annular ligament, as shown in Figure 2.3a. It is located in the anterior part of the LUCL and possesses a fan shape [64]. This ligament, in conjunction with the LUCL and annular ligament, provide posterolateral rotatory stability [60].

The lateral annular collateral ligament (LACL) encircles the head of the radius (Figure 2.3a) and is linked with the LUCL and LRCL to create the LCL complex [64]. It is attached to the anterior and posterior sides of the radial notch of the ulna [45]. The rupture of this ligament and the LUCL produces instability in varus stress and in resisted pronation-supination motion [65].

The medial anterior collateral ligament (MACL) is located on the ulnar side of the elbow. It arises from the lower part of the medial epicondyle and inserts on the sublime tubercle of the coronoid process of the ulna, as illustrated in Figure 2.3b. When it is evaluated at macroscopic scale, it appears to be divided into two bands [66-67]. It is more prominent than the posterior ligament and is considered as the major stabiliser of the elbow in valgus stress [68].

The medial posterior collateral ligament (MPCL) is placed between the anterior and transverse ligaments, as shown in Figure 2.3b. It emerges from the inferior area of the medial epicondyle and inserts in the medial olecranon [66]. It seems that this ligament bundle provides minimum stability to valgus stress [68].

The medial transverse collateral ligament (MTCL) arises from different areas of the ulna bone, as shown in Figure 2.3b. Although this ligament bundle seems to make a negligible contribution to the stability of the elbow, it has been hypothesised that MTCL could provide resistance to medially directed transverse translation [56, 62], perpendicular to the axis of elbow rotation [59]. This ligament is also called as oblique portion.
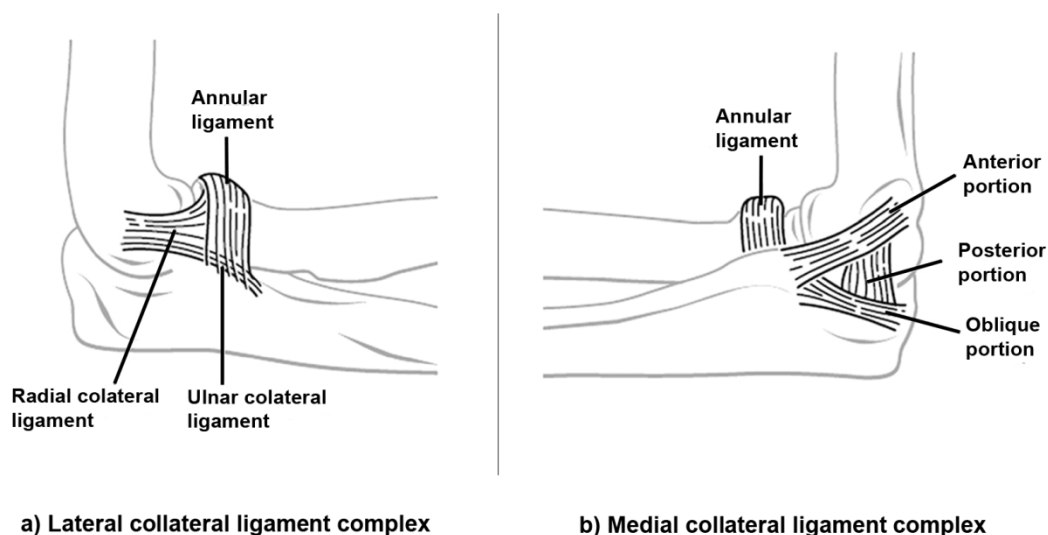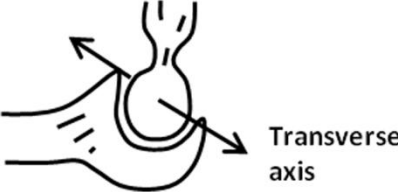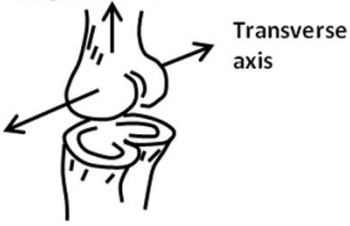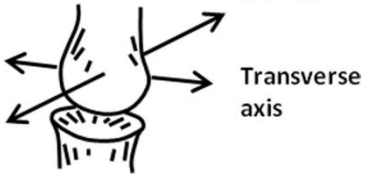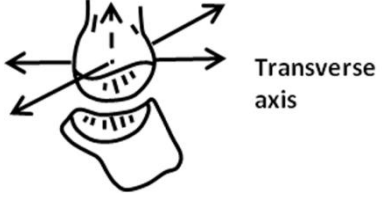
Figure 2.3 a) Lateral collateral ligament (LCL) complex; lateral view of the elbow and b) Medial collateral ligament (MCL) complex; medial view of the elbow [62].

2.2.5   Synovial joints

The synovial joints provide the greatest range of motion between one bone and the other. Table 2.1 presents the structure of all types of synovial joints in the human body [47]. These types of joints contain a lubricant between the bones called synovial fluid. This fluid is contained in a fibrous membrane, which surrounds the articulation. Furthermore, the contact between the bones is through a special material called cartilage. The cartilage is made of water and collagen. When the cartilage is damaged, the contact between the bones becomes painful. The function of cartilage is to absorb the impact of the forces transmitted within the joints. The synovial fluid reduces the friction among the bones [69].

Table 2.1 Synovial joints of the human body. Adapted from [47].

Type of joint		Examples
Hinge: allowing flexion-extension only, through transverse axis		Humero-ulnar joint (elbow)
Pivot: allowing rotation only, through longitudinal axis		Proximal-radio-ulnar joint (elbow)
Condylar/bicondylar: allowing flexion-extension through transverse axis with limited rotation through longitudinal axis		Tibiofemoral joint (knee)
Ellipsoid: allowing flexion-extension through transverse axis and abduction/adduction through A-P axis		Metacarpophalangeal joint (hand)
Saddle (sellar): as ellipsoid, but more open surfaces may allow some rotation through longitudinal axis; the reciprocal surfaces are concavo-convex like a saddle		1st carpometacarpal joint (thumb)

2.3   Articulations of the elbow joint

The elbow is mainly created by three articulations which are covered by the synovial capsule, collateral ligament complexes and muscles crossing the elbow. These three articulations comprise the humeroulnar, humeroradial and the radioulnar joints. They have special anatomical features, which enable flexion-extension and pronation-supination of the forearm to be performed.

2.3.1   Humeroulnar joint

The humeroulnar is the biggest and most important articulation of the elbow. It is considered to be one of the primary static stabilisers of the elbow [49]. It is formed by the trochlea of the humerus and trochlear notch of the ulna. Sometimes, this articulation is considered to be a pure hinge joint for practical studies. However, the anatomy of the trochlea generates a deviation known as the carrying angle, Figure 2.4. This angle is approximately of 10° to 15° in men and between 20° and 25° in women [41]. The medial and lateral collateral ligament complexes, muscles crossing the elbow and the synovial membrane connect this joint. The principal movement performed by the humeroulnar articulation is flexion-extension of the forearm.
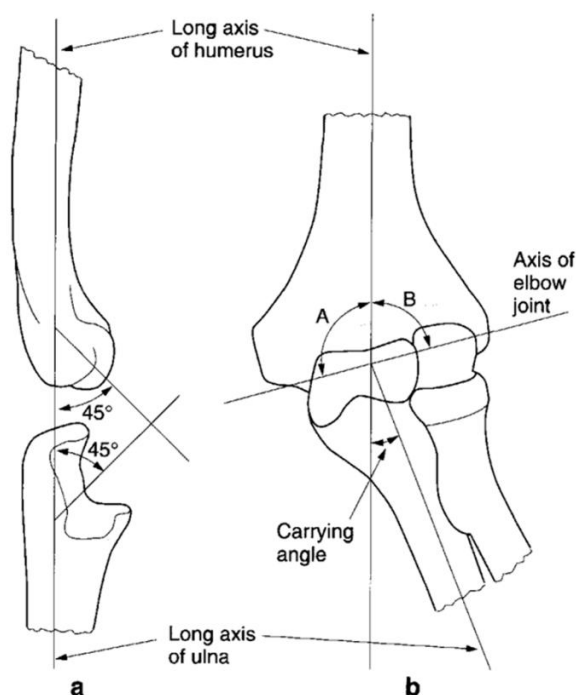
Figure 2.4 a) Relation of the axes of the elbow joint and b) the carrying angle [41].

39

2.3.2 Humeroradial joint

The capitulum of the humerus and the head of the radius are the two components of the humeroradial articulation. The lateral radial collateral ligament and the synovial membrane connect this joint. Flexion-extension is the movement allowed by this joint [45]. One important feature of the humeroradial joint is that the contact of the capitulum and the head of the radius increase when the forearm is completely flexed, as illustrated in Figure 2.5 [41]. Furthermore, 57% of the axial force applied to the forearm is transmitted to the humerus through this joint [70].

Humerus

Radius

Ulna

Full Extension   90° Flexion   Full Flexion
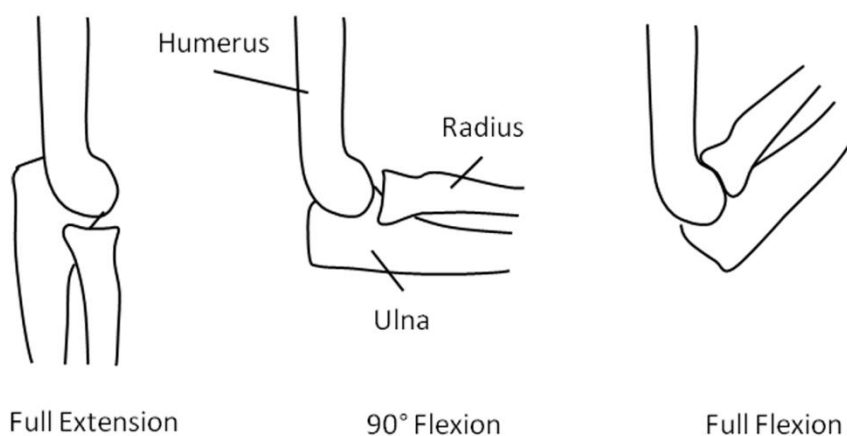
Figure 2.5 Contact area between the head of the radius and the capitulum of the humerus becomes prominent in full flexion. Adapted from [41].

2.3.3 Radioulnar joint

The radioulnar articulation is responsible for producing pronation-supination of the forearm [45]. Figure 2.6 displays the three components of this joint, the head of the radius, the radial notch of the ulna and the annular ligament. The flexibility of the annular ligament allows free rotation of the oval head of the radius. Although the annular ligament is the principal support of the radioulnar articulation, it is not enough to maintain the stability. The quadrate ligament and the interosseous membrane contribute to the stability of the forearm during the pronation-supination movement [41].
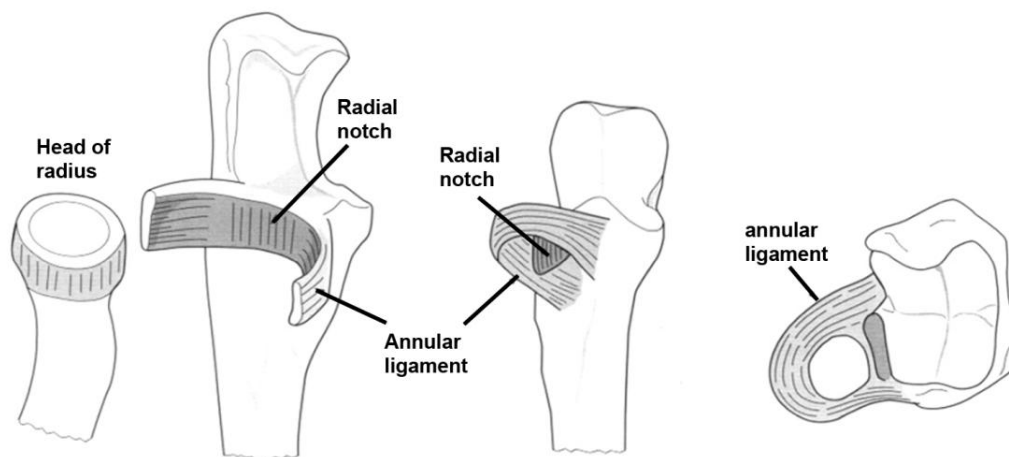
Figure 2.6 Radioulnar joint of the elbow. Adapted from [41].

2.4   Muscles of the upper arm and forearm

The muscle contraction process gives movement to the human body, allowing the execution of daily life activities. Humans could not move the limbs or perform physical activities without them. They are joined to the bones, ligaments, cartilage and skin, either directly or through the tendons [53]. There are different ways of classifying muscles. Sometimes they can be categorised by their location in relation to the skin, like deep and superficial muscles. They can be organised by their structure and role, like skeletal, smooth and cardiac muscles, and due to the orientation of their fibres, like fusiform and penniform muscles. They can also be classified by their geometry, like triangular, quadrilateral and spiral muscles.

The anatomy of the muscles varies in relation to the body. For example, muscles located in the limbs are large in order to produce movement and to protect the joints [53]. The arrangement or structure of the muscle fibres is important to produce force or movement [71]. The muscle force is clearly related to the physiological cross-section (PCS), an area, which passes throughout all fibres of the muscle. Muscles with the fibres orientated in a different axis of the tendon are able to produce more force. This type of muscles is usually called penniform, Figure 2.7. Conversely, the muscles with the fibres aligned in the same axis of the tendon are called fusiform muscles [53].

A, fusiform; B, unipinnate; C, bipinnate;
PCS, physiological cross-section.
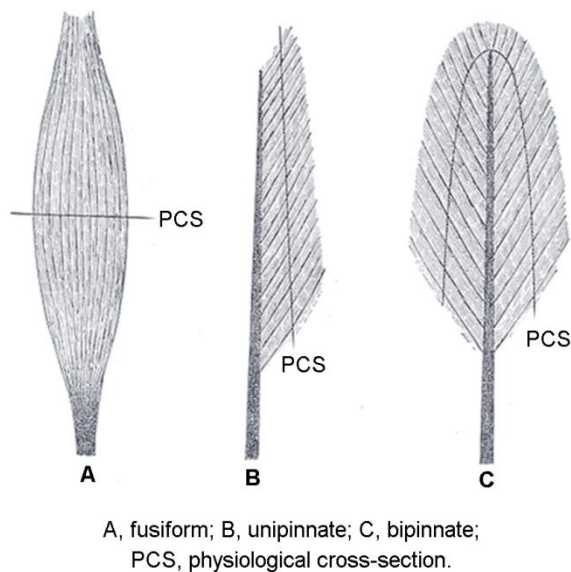
Figure 2.7 Physiological cross section (PCS) of the skeletal muscle. Adapted from [53].

Muscles of the arm and forearm play a significant role in the kinematics of the elbow joint. There are some muscles related with the flexion and extension movement. Others are responsible for rotating the forearm and some of them give stability to the articulation when they contract. These muscles will be described below to familiarise the reader with the muscle anatomy of the elbow.

There are eight muscles directly related with the kinematics of the elbow joint: biceps brachii, brachialis, brachioradialis, triceps brachii, anconeus, pronator teres, pronator quadratus and supinator muscles [72]. It has been suggested that all muscles crossing the elbow provide stability to the joint [48]. Therefore, flexor and extensor muscles of the wrist could give stability to the joint by adding compressive forces in the articular surface when they contract [45-46, 73].

Biceps brachii

Biceps brachii contains two heads placed in the anterior part of the arm. They arise from different parts of the scapula and finish in a single tendon inserted in the radial tuberosity. Its main function is flexion and supination of the forearm [74-75]. This muscle is explained in more detail in the following section 2.10.

Brachialis

The brachialis muscle is located in the anterior side of the humerus under the biceps brachii, as illustrated in Figure 2.8a. It has two heads, which arise from just below the middle part of the anterior humeral cortex. It is inserted in the inferior part of the coronoid process of the ulna. Although the brachialis is an important flexor muscle at the elbow, it cannot be studied using surface electromyography [41, 75]. The role of brachialis could be insignificant when the elbow is completely extended because its lever arm is small at this position [76].

Brachioradialis

Brachioradialis is a fusiform muscle placed in the lateral side of the forearm [41]. It arises from the lateral supracondylar ridge of the humerus and inserts into the styloid process of the radius, as shown in Figure 2.8b. It has been considered as a flexor muscle in conjunction with biceps brachii and brachialis muscles [75].
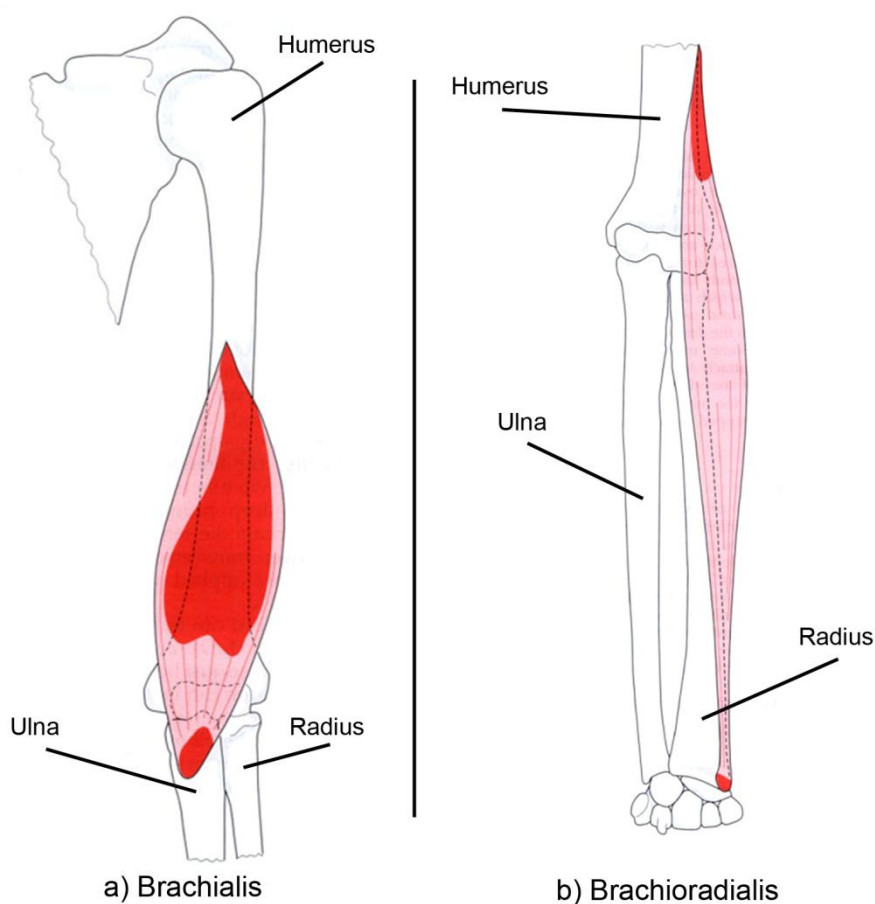
Figure 2.8 Muscles crossing the elbow joint: a) Brachialis and b) Brachioradialis. The shaded areas represent the attachment points. Adapted from [41].

43

Triceps brachii

Three heads integrate the triceps brachii muscle: the long, lateral and medial heads. It is a bi-articular muscle placed at the posterior part of the arm. The medial and lateral heads arise from the posterior part of the humerus and the long head begins from the infraglenoid tubercle of the scapula. The three heads combine in a tendon, which is inserted into the olecranon of the ulna [74].

Anconeus

The anconeus muscle is located in the posterolateral part of the elbow. It arises from the lateral epicondyle and inserts into the proximal part of the ulna [41, 74]. It has been the subject of debate regarding its function on elbow kinematics. Although there are several studies about the anconeus muscle, its role remains unclear. The anatomy and structure of the anconeus are analysed in more detail in the following section 2.9.

Pronator Teres

Pronator teres is a muscle located in the anterior side of the forearm. It emerges from two heads: the humeral and ulnar head. The humeral head begins from the superior part of the medial epicondyle of the humerus and the ulnar head arises from the coronoid process of the ulna [41]. Both heads blend in a tendon, which is inserted in the lateral side of the radius, Figure 2.9a.

Pronator Quadratus

Pronator quadratus is a quadrangular muscle located in the anterior part of the forearm, near to the wrist joint between the radius and ulna bones, as shown in Figure 2.9a. It arises from the volar surface of the ulna and it is inserted into the volar surface of the radius [41, 53]. The pronator quadratus has been considered to be the major pronator muscle of the forearm [77].

Supinator

The supinator muscle is located in the posterior side of the forearm and is integrated by two heads: the humeral and ulnar head. The humeral head arises from the lateral epicondyle and the ulnar head begins from the supinator crest of the ulna [41]. Both heads inserts in the posterior, lateral and anterior aspects of the radius, as presented

44

in Figure 2.9b. It has been considered to be the principal supinator muscle due to its high electrical activity during supination movement [78].
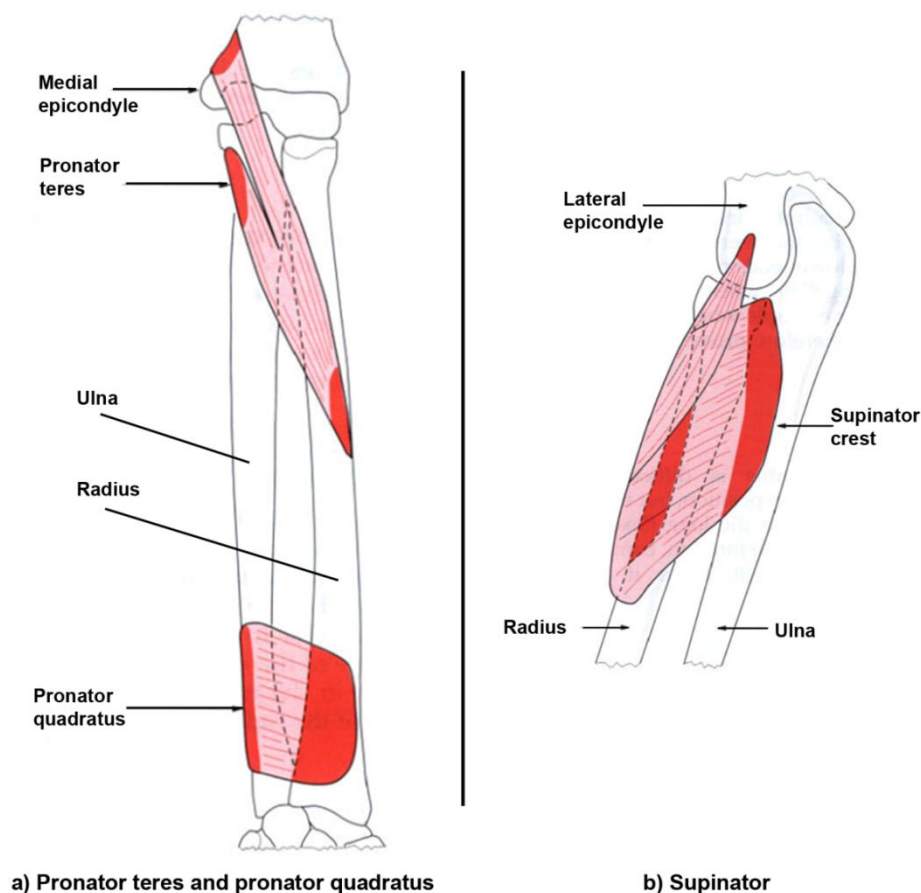
Figure 2.9 a) Pronator teres and pronator quadratus, b) Supinator. Adapted from [41].

Flexor and extensor muscles of the hand

Most of the flexor and extensor muscles of the hand arise from the medial and lateral epicondyle of the humerus, respectively. They insert into different regions of the hand. Flexor carpi radialis, flexor carpi ulnaris and palmaris longus are superficial muscles that are considered to be flexors of the wrist. These muscles can be easily palpated in the anterior part of the forearm. Extensor carpi radialis longus, extensor carpi radialis brevis and extensor carpi ulnaris are superficial muscles that are considered to be the extensors of the wrist. They are located in the posterior part of the forearm [52]. It has been suggested that all muscles that cross the elbow could give stability to the joint when they contract [33, 48]. Thus, flexor and extensor muscles of the hand could be considered to be dynamic stabilisers because they could give stability to the elbow, therefore producing compression to the joint when they

are activated [45]. Table 2.2 presents more details about the innervation, origin and insertion points of some muscles of the forearm and hand.

Table 2.2 Muscles of the elbow and hand [52].

Muscles that move the forearm and Hand				
Muscle	Origin	Insertion	Action	Innervation
ACTION AT THE ELBOW				
Flexors				
Biceps brachii	Short head from the coracoid process; log head from the supraglenoid tubercle [both on the scapula]	Tuberosity of radius	Flexion at elbow and shoulder; supination	Musculocutaneous nerve [C5-C6]
Brachialis	Anterior, distal surface of humerus	Tuberosity of ulna	Flexion at elbow	As above and radial nerve [C7-C8]
Brachioradialis	Ridge superior to the lateral epicondyle of humerus	Lateral aspect of styloid process of radius	As above	Radial nerve [C5-C6]
Extensors				
Anconeus	Posterior, inferior surface of lateral epicondyle of humerus	Lateral margin of olecranon on ulna	Extension at elbow	Radial nerve [C7-C8]
Triceps brachii				
Lateral head	Superior, lateral margin of humerus	Olecranon of ulna	As above	Radial nerve [C6-C8]
Long head	Infraglenoid tubercle of scapula	As above	As above, plus extension and adduction at the shoulder	As above
Medial head	Posterior surface of humerus inferior to radial groove	As above	Extension at elbow	As above
Pronators/Supinators				
Pronator quadratus	Anterior and medial surfaces of distal portion of ulna	Anterolateral surface of distal portion of radius	Pronation	Median nerve [C8-T1]
Pronator teres	Medial epicondyle of humerus and coronoid process of ulna	Midlateral surface of radius	As above	Median nerve [C6-C7]
Supinator	Lateral epicondyle of humerus, annular ligament, and ridge near radial notch of ulna	Anterolateral surface of radius distal to the radial tuberosity	Supination	Deep radial nerve [C6-C8]
ACTION AT THE HAND				
Flexors				
Flexor carpi radialis	Medial epicondyle of humerus	Bases of second and third metacarpal bones	Flexion and abduction at wrist	Median nerve [C6-C7]
Flexor carpi ulnaris	Medial epicondyle of humerus; adjacent medial surface of olecranon and anteromedial portion of ulna	Pisiform bone, hamate bone, and base of fifth metacarpal bone	Flexion and adduction at wrist	Ulnar nerve [C8-T1]
Palmaris longus	Medial epicondyle of humerus	Palmar aponeurosis and flexor retinaculum	flexion at wrist	Median nerve [C6-C7]
Extensors				
Extensor carpi radialis longus	Lateral supracondylar ridge of humerus	Base of second metacarpal bone	Extension and abduction at wrist	Radial nerve [C6-C7]
Extensor carpi radialis brevis	Lateral epicondyle of humerus	Base of third metacarpal bone	As above	As above
Extensor carpi ulnaris	Lateral epicondyle of humerus	Base of fifth metacarpal bone	Extension and adduction at wrist	Deep radial nerve [C6-C8]

46

2.5   Biomechanics of the elbow joint

The elbow joint represents an important mechanical connection between the wrist and shoulder joints. It allows the hand to move in the air to perform many daily life activities. The elbow is integrated by three joints: the humeroulnar, humeroradial and radioulnar joints. The humeroulnar and humeroradial joints are responsible for producing flexion and extension movements with a small deviation called carrying angle. The radioulnar joint helps to produce pronation-supination motion [47, 56]. Most of the time, the elbow movements are described in relation to the planes of the human body in order to have a comprehensible reference system.

2.5.1   Planes of the human body

The movements of the human body are usually described in relation to a reference system. This reference system involves three planes known as the sagittal, frontal and horizontal planes. It is necessary to know about these three planes to understand the movements of the human body. Furthermore, there are some common terms related to these planes, which help to locate some parts of the anatomy of the body, as shown in Figure 2.10. In order to identify the three planes, the human body has to be in standing position with the thumbs of the hands pointing to the lateral side (away from the body) and with the head straight [41].

The sagittal plane

The sagittal plane divides the human body into two symmetrical parts, left and right. The flexion-extension movement of the elbow is parallel to this plane. However, the rotational axis of flexion-extension is not completely perpendicular to this plane due to the carrying angle at the elbow. The sagittal plane is also known as median plane and it is the only plane which produces two identical parts of the body [41, 69].

The frontal plane

The frontal plane separates the human body into two sections: the anterior and posterior. It runs from top to bottom creating an orthogonal angle with the sagittal plane, as illustrated in Figure 2.10. It is also called the coronal plane and any parallel plane related to it is called by the same name [41, 69].

The transverse plane

The transverse plane divides the human body into two pieces, superior and inferior. It passes from the anterior to the posterior part forming a right angle with the sagittal and coronal planes, as shown in Figure 2.10. It is also known as the horizontal plane [41, 69].
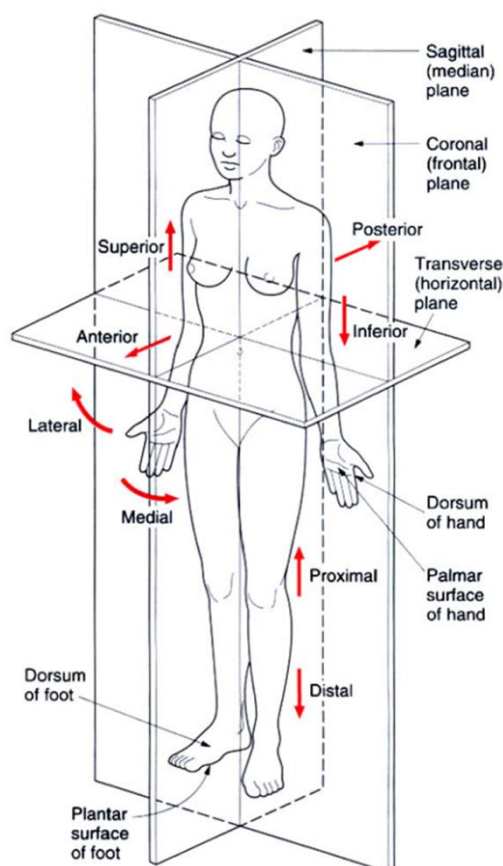
Figure 2.10 Planes of the human body [41].

2.5.2 Elbow movements

The three articulations of the elbow, described before, allow flexion-extension and pronation-supination movements of the forearm. Moreover, the geometry of the trochlea of the humerus and the trochlear notch of the ulna are designed to perform flexion-extension motion with a small deviation called the carrying angle, which is bigger in females [47, 56]. Loss or reduction of one of these movements represents a severe disability in the human body, limiting the performance of the daily life activities [56].

Flexion and extension movements of the elbow

Flexion-extension is the movement performed parallel to the sagittal plane. It is performed through the humeroulnar and radiocapitellar joints. This movement is one of the most important motions of the elbow and is responsible of many daily life activities. It has been found that the range of motion is 145° for active movement and 160° for passive motion [41]. The flexion-extension movement can be constrained by the soft tissue and the bony landmarks of the humeroulnar joint. Sardelli and colleagues found that the active range of motion for some common activities was between 27° ± 7° and 149° ± 5° while Morrey et al. noticed slightly different values between 30 and 130 degrees [79-80]. The rotational axis for flexion-extension motion passes through the centre of the trochlea and the capitulum [81]. Flexion is the action of the arm and forearm getting closer together and extension is the action of the arm and forearm getting further apart, as illustrated in Figure 2.11.
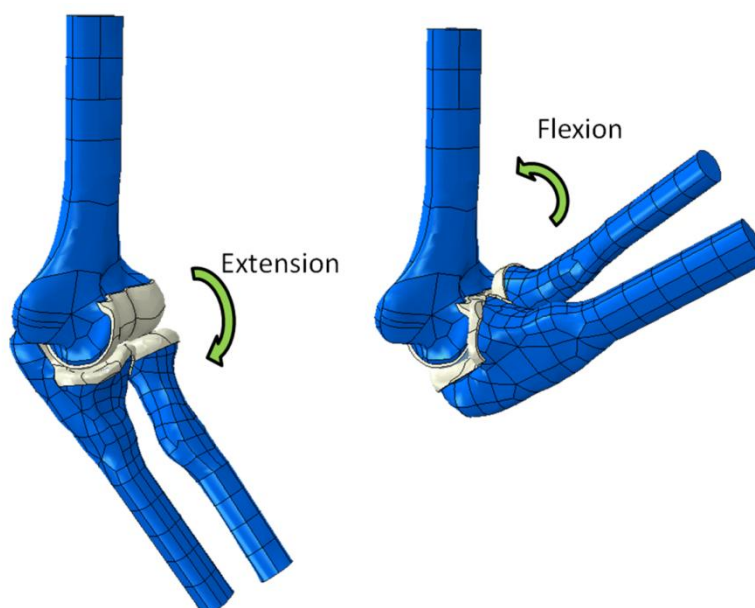
Figure 2.11 Flexion and extension movement of the elbow joint.

Pronation and supination movements of the forearm

The rotation of the forearm is performed by the proximal and distal joints between the radius and ulna bones. This movement becomes more powerful when the elbow is flexed at 90 degrees because the muscles that produce the motion have the optimal length and moment arm at that position [36, 82]. Furthermore, the interosseous

membrane plays an important role in the rotation of the forearm because it keeps the two bones together and helps to transmit forces to the ulna [41].

It has been suggested that under specific circumstances the radius rotates around the ulna whilst the ulna moves in a lateral plane [29-30, 41, 83]. The lateral movement of the ulna depends on the rotational axis during pronation-supination motion. This axis passes through the head of the radius and the distal part of the ulna. Pronation is the movement of the forearm until the palm of the hand faces backwards and supination is the opposite motion until the palm faces forwards, as illustrated in Figure 2.12 [41]. Cadaveric studies have shown measurements of $70 \pm 5°$ for pronation and $85 \pm 4°$ for supination with the elbow flexed at 90 degrees [84].

Supinated position   **Mid pronation-supination**

Pronated position
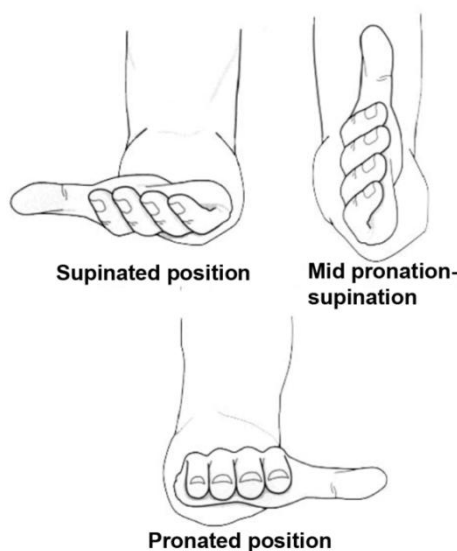
Figure 2.12 Pronation and supination of the forearm. Adapted from [41].

Abduction and adduction of the forearm

The abduction and adduction movement is performed parallel to the frontal plane, where the lower or upper limbs move away or get closer to the sagittal plane, as shown in Figure 2.13 [69]. Although flexion-extension and pronation-supination are the two major movements of the elbow, the abduction and adduction motion (lateral or medial displacement) of the ulna occurs during pronation-supination movement [29, 41]. This movement becomes more visible in the distal part of the ulna and depends upon the rotational axis.
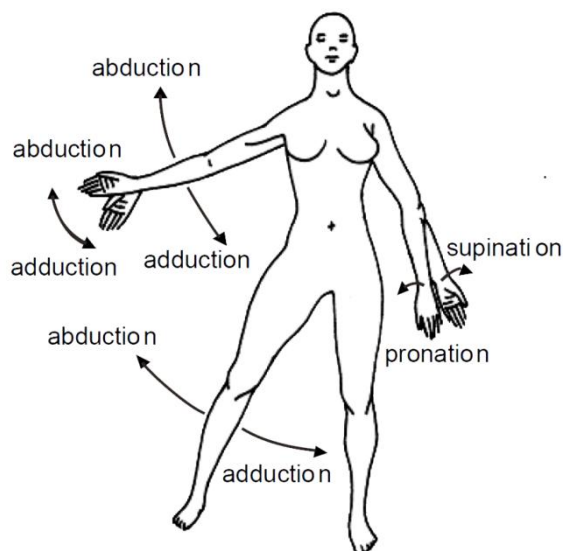
Figure 2.13 Abduction and adduction movement [69].

2.6 Kinematics and kinetics of the elbow

Once the anatomy and the main components of the elbow have been described, it is necessary to understand how the elbow articulation works from the mechanical point of view. Kinematics and kinetics are two branches of mechanics, which allow the interpretation of the movement of any segment of the human body. Kinematics describes the motion of a body in the space without considering the forces that have produced the movement. Kinetics studies the movement by considering the forces that produce the movement [74].

2.6.1 Kinematics

Kinematics is the study of the movement of the body in the space without considering the forces that produce it [85]. The description of the linear or angular displacement, velocity and acceleration of a particle are the most important parameters studied in this field. This research considers the movement of the forearm in relation to the arm in the sagittal and horizontal planes. It was assumed that the arm and forearm segments of the upper limb behave as rigid bodies.

Angular displacement

There are two ways of describing the angular position of a body in the space. In the first case, the segment is described in relation to the global reference system and in

51

the second one; the movement is measured with respect to other proximal segment. The orientation of the angular displacement in both cases follows the right hand rule where positive rotations are counter clockwise and negative rotations are clockwise [85]. The selection of the method to describe the motion of a particle depends upon the requirements and aims of the study.

Angular velocity

Angular velocity is the rate of change of the angular displacement with respect to time. This rate of change can be calculated with the following equation (2.1). Furthermore, the integration of the angular acceleration with respect to time produces the angular velocity [85].

$$\vec{\omega_i} = \frac{\theta_{i+1} - \theta_{i-1}}{2\Delta t} \tag{2.1}$$

Where $\vec{\omega}$ is the angular velocity of the segment, θ represents the angular position, Δt indicates the time increment and i is the specific instant in the time analysed.

Angular acceleration

The angular acceleration is the rate of change of the angular velocity with respect to time. It can be obtained from equation (2.2). This parameter, in conjunction with the angular displacement and angular velocity, helps to describe the angular movement of a rigid body in the space [85].

$$\vec{\alpha_i} = \frac{\vec{\omega}_{i+1} - \vec{\omega}_{i-1}}{2\Delta t} \tag{2.2}$$

Where $\vec{\alpha}$ is the angular acceleration of the rigid body, $\vec{\omega}$ represents the angular velocity, Δt is the time increment and i signifies the specific instant in the time analysed.

2.6.2   Kinetics

Kinetics is the study of the causes that produce the movement of a body [85]. The body segment parameters and anthropometric data are important properties of a body

to calculate its mass moment of inertia. Subsequently, the mass moment of inertia is used to obtain the torque that produces the angular movement of a segment. The investigation performed in this thesis considered the body segment parameters from Dempster and Zatsiorsky [86-87].

Mass moment of inertia

The mass moment of inertia is the opposition of a segment to change its rotational movement [85]. To calculate the mass moment of inertia of a body with respect to its centre of gravity, it is necessary to estimate the radius of gyration of the segment using Dempster's body segment parameters, equation (2.3). Then, the mass moment of inertia can be calculated using equation (2.4).

$$k_{cg} = K_{cg}l \tag{2.3}$$

Where k_{cg} is the radius of gyration in metres, K_{cg} is the length of the radius of gyration in relation to the length of the segment and l is the length of the segment in metres.

$$I_{cg} = mk_{cg}^2 \tag{2.4}$$

Where I_{cg} represents the mass moment of inertia with respect to the centre of gravity (cg) in kilogram square metres, m is the mass of the segment in kilograms and k_{cg} is the radius of gyration in metres.

The mass moment of inertia of the segment with respect to the centre of gravity has to be calculated with respect to the centre of rotation of the joint. The parallel axis theorem helps to calculate the mass moment of inertia in relation to the rotational axis of the joint, equation (2.5).

$$I_{axis} = I_{cg} + mr^2 \tag{2.5}$$

Where I_{axis} represents the mass moment of inertia in relation to an axis of the joint, I_{cg} represents the mass moment of inertia with respect to the centre of gravity (cg), m is the mass of the segment in kilograms and r is the distance between the axis and centre of gravity of the body in metres.

Net joint torque

The net joint torque is the result of all forces acting on the joint, which produce the rotation movement. There are many elements working in the kinetics of the joint, such as friction forces, muscles, ligaments, inertial forces and the gravitational force. It is difficult to measure every single element because there are many unknown variables and just a few equilibrium equations [85]. Therefore, net joint torque is a useful tool to quantify the behaviour of the articulation, equation (2.6).

$$\vec{T} = [I] \times \vec{\alpha} \qquad (2.6)$$

Where $\vec{T}$ is the net joint torque in Nm, I is the mass moment of inertia of the segment and $\vec{\alpha}$ represents the angular acceleration of the joint.

Net joint power

The net joint power is the result of the multiplication between the net joint torque and the angular velocity of the articulation, equation (2.7). The net joint power, the angular velocity and the net joint torque describe the angular movement of the articulation. The net torque and power are directly related to the muscular contraction and the type of motion performed. That is, these two parameters indicate when the muscles in the articulation of the elbow are working in a concentric or eccentric way [85].

$$P = \vec{T} \cdot \vec{\omega} \qquad (2.7)$$

Where P is the net joint power in watts, $\vec{T}$ represents the net joint torque in Nm and $\vec{\omega}$ is the angular velocity of the joint in radians per second.

Net joint work

Work is defined as the energy flow of one body to another, and it takes time for the work to occur. For example, a muscle can make a bone move and the work takes place as the energy passes from the muscle to the bone [88]. The net joint work represents the area below the net joint power, equation (2.8).

The net joint work helps to quantify and describe the mechanical behaviour of the joint. The total net joint work represents the absolute area below the net power curve, equation (2.9) [89].

$$Net\ joint\ work = \int P\ dt = \int \vec{T} \cdot \vec{\omega}\ dt = \frac{1}{2}I\vec{\omega}^2 \qquad (2.8)$$

$$Total\ net\ joint\ work = \int |P|\ dt \qquad (2.9)$$

Where $Net\ joint\ work$ represents the net joint work of the joint in joules, P is the net joint power in watts, dt represents the time increment, $\vec{T}$ is the net joint torque in Nm, $\vec{\omega}$ is the angular velocity of the joint in radians per second, I is the mass moment of inertia and $Total\ net\ joint\ work$ is the absolute area below the power curve in joules.

2.7   The muscular system

The muscles play a significant role in daily life activities. They are responsible for giving movement to the bones and keeping the stability of the human body. There are three types of muscle tissue: skeletal, cardiac and smooth muscles. Every single muscle tissue has a different structure in a microscopic scale and plays diverse activities in the human body. Moreover, muscles represent between 40% and 50% of human body weight [44].
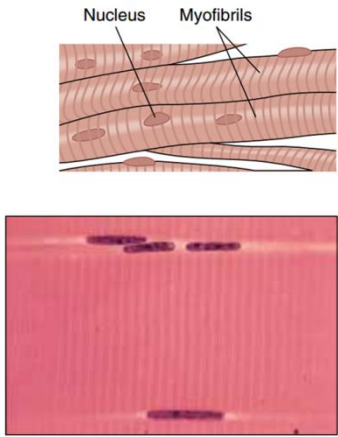
2.7.1   Muscle tissue types

A tissue is a group, or aggregation of cells, which are joined together to perform a specific task. There are four types of tissue in the human body, the epithelial, connective, muscle and nervous. The most important tissue in this work is the muscle tissue. This tissue is also classified in three different categories; they are skeletal, cardiac and smooth muscle [44]. Among these three categories, the most important muscle tissue for this particular study is the skeletal. This research is focused on the analysis of the anconeus muscle, which is a skeletal muscle attached to the humerus and ulna bones.

In contrast to the structures of buildings, bridges, buses, planes, etc., the skeleton of the human body would collapse under the effect of gravity without the support of the skeletal muscles [69]. The muscles play a significant role to perform activities of the human body, such as walking, dancing, running, eating, breathing, speaking and so on. For this reason, it is important to know their function and structure.

The *skeletal muscles* are attached to the bones and help to produce movement of the articulations in the human body [44]. They are also called striated muscles because they present a banding pattern at microscopic scale. Furthermore, skeletal muscles are considered to be voluntary muscles because the contraction mechanism is controlled by the brain. Table 2.3 explains some features of this type of muscle tissue.
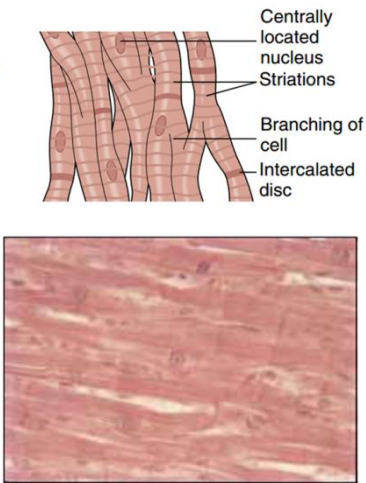
Table 2.3 Morphological features of the skeletal muscles. Adapted from [44].

Function	Characteristics and location	Morphology
Skeletal (striated voluntary) These muscles are attached to the movable parts of the skeleton. They are capable of rapid, powerful contractions and long states of partially sustained contractions, allowing for voluntary movement.	Skeletal muscle is: striated (having transverse bands that run down the length of muscle fibre); voluntary, because the muscle is under conscious control; and skeletal, since these muscles are attached to the skeleton (bones, tendons and other muscles).	

The *cardiac muscle* produces the rhythmic contractions of the heart. It is instinctive because it generates its own reactions to begin muscle contraction process [44]. Furthermore, it is also called striated muscles because it presents a banding pattern like the skeletal muscles. This type of muscles can be found only in the heart. Its morphological features can be seen in Table 2.4.
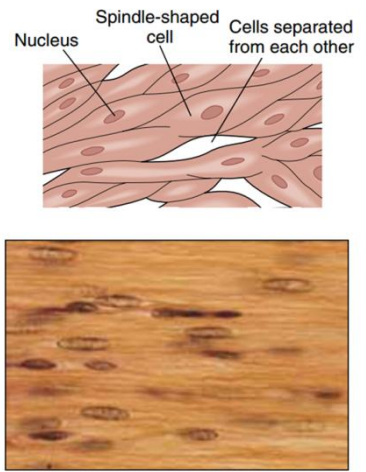
Table 2.4 Morphological features of the cardiac muscles. Adapted from [44].

Function	Characteristics and location	Morphology
Cardiac These cells help the heart contract in order to pump blood through and out of the heart.	Cardiac muscle is a striated (having a cross-banding pattern), involuntary (not under conscious control) muscle. It makes up the walls of the heart.	

The *smooth muscles* cover the internal area of hollow organs. They are considered to be involuntary muscles because they cannot be controlled by the brain [44]. These muscles line the blood vessels and the digestive tract where they help to move the substances, like the food. Table 2.5 shows some features of the smooth muscle.

Table 2.5 Morphological characteristics of the smooth muscles. Adapted from [44].

Function	Characteristics and location	Morphology
Smooth (Nonstriated involuntary) These provided for involuntary movement. Examples include the movement of materials along the digestive tract, controlling the diameter of blood vessels and the pupil of the eyes.	Smooth muscle is nonstriated because it lacks the striations (bands) of skeletal muscles; its movement is involuntary. It makes up the walls of the digestive, genitourinary, respiratory tracts, blood vessels, and lymphatic vessels.	

2.7.2 Skeletal muscle functions

There are five functions of the skeletal muscles in the human body. The first one and the most important is movement. Muscle contractions produce the motion of the bones. Without these contractions, the human would not be able to perform any daily life activities. The second function is posture. The body would collapse, due to the effect of gravity, if the skeletal muscles were not there to keep the balance. The third function is protection. The muscles cover some regions of the abdomen, protecting some internal organs. The fourth function is thermogenesis. The muscle contractions increase the temperature of the human body, keeping it warm when the weather is cold. Vascular pump is the last function of the skeletal muscles. The muscle contractions help to move the blood through the veins and blood vessels [90].

2.7.3 Structure of the skeletal muscle

The cells of the skeletal muscles are the longest and most slender muscle fibres. Its range in size is going from 1 to 50 mm in length and 40 to 50 micrometres in diameter [44]. Figure 2.14 shows the anatomy and structure of the skeletal muscle at microscopic level. The whole muscle is covered by a membrane called facia which is visible to the naked eye. Every muscle fibre is surrounded by a cell membrane named sarcolemma, which is electrically polarised.

There are three types of connective tissue, which connect and cover the muscle fibres; these tissues are endomysium, perymysium and epimysium. The main role of this connective tissue is to maintain the muscle fibres together [44]. When the muscle fibres are viewed at microscopic scale, they appear to have a dark and light banding pattern. This pattern is known as cross-striations. The overlapping of the dark and light bands of protein on the myofibrils produces the striation pattern. The dark bands are made of the protein myosin and they are called A bands. The light bands are made of the protein actin and they are named I bands [44]. There is another pattern at the middle of the A bands, called the H zone, which is slightly dark. There is a dark staining pattern found in the central region of the I bands that looks like a series of Z letters, one on top of another. This pattern is named Z line. The myosin and acting filaments are localised between two Z lines. The region between two Z lines is called sarcomere. This is where the most important process of muscle

contraction occurs via chemical interactions. This chemical reaction is developed within the cross-bridges integrated by the actin and myosin filaments.
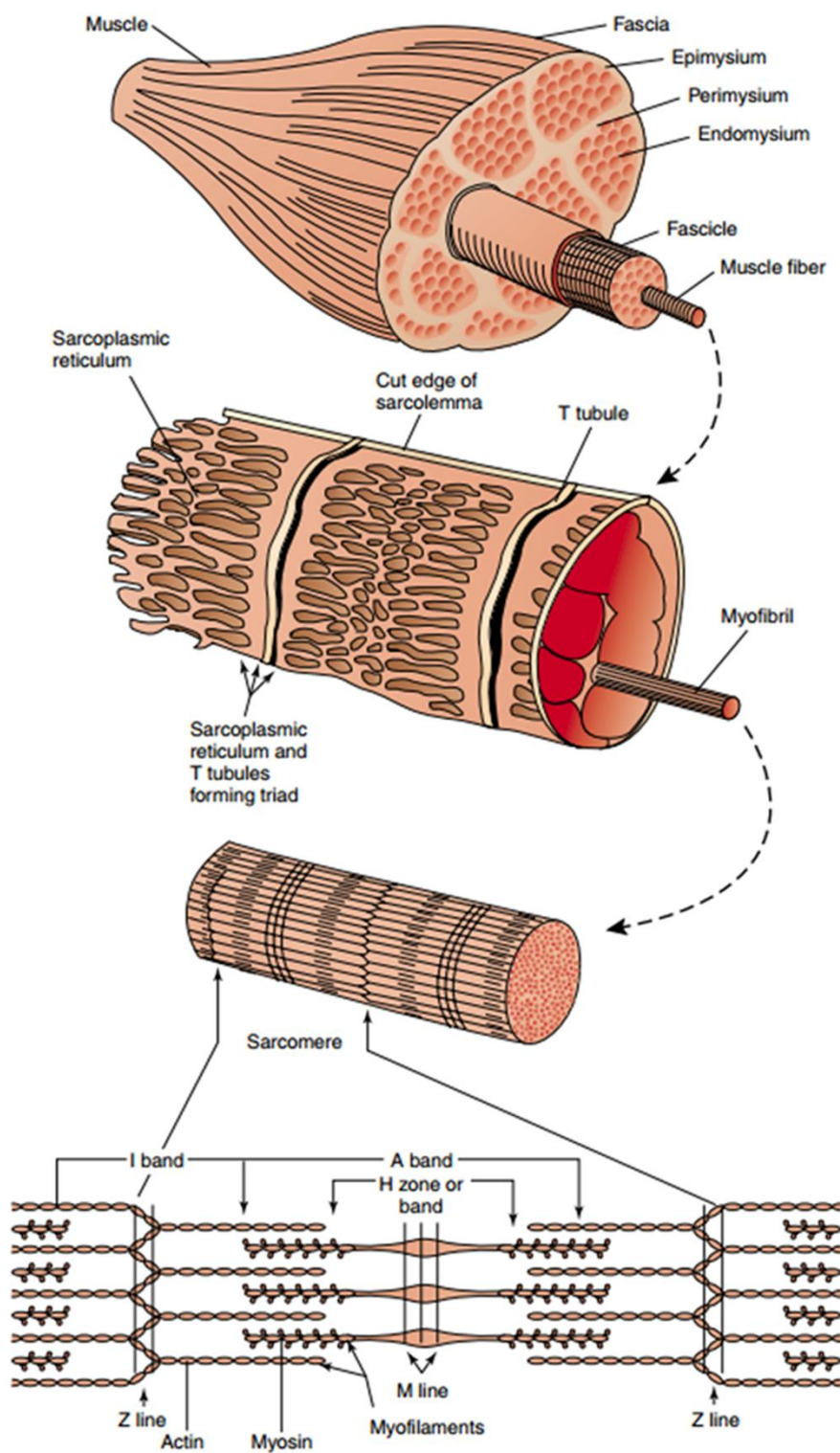
Figure 2.14 The structure of the skeletal muscle at the microscopic, cellular and molecular levels [44].

2.7.4 The physiology of muscle contraction

Once the structure of the muscle contraction and the region where the contraction of the muscle occurs are known, it is necessary to understand the physiology of muscle contraction to be able to interpret how the muscle works. To identify how the muscle produces movement in the human body, it is necessary to know some properties of the muscle cells and to describe what a motor unit is.

A motor unit refers to all muscle fibres, which are fed or innervated by one motor neuron [44]. This innervation excites the muscle fibres and contracts them. It is important to know that the terminal divisions of a motor neuron are distributed throughout the belly of the whole muscle. Excitability, conductivity, contractility and elasticity are four properties that the muscle cells present. These four properties describe the functioning of the muscle. The contraction process is the most important property of the muscle cells. This process is produced by the interaction of three factors: neuroelectrical factors, chemical interactions and energy sources.

The neuro-electrical factor refers to the distribution of the ions in the superficial and internal area of the muscle cell (sarcolemma). The distribution of the ions inside of the cell can be seen in Figure 2.15. There is a chemical substance named acetylcholine, which affects the membrane of the muscle cell releasing the sodium ions outside the membrane. This activity creates an electrical potential or action potential, which travels in both directions along the muscle cell at a rate of five meters per second [44].

The chemical interactions refer to the interaction that exists among the proteins contained in the muscle cell like myosin, actin and actomyosin. The combination of actin and myosin proteins generates the actomyosin, which is released during the contraction process [44].

The energy sources are all substances that a muscle cell can absorb to develop the contraction process. The muscle cell transforms chemical energy (Adenosine triphosphate ATP) into mechanical energy (contraction). Furthermore, the muscle cells produce heat as a waste product during the contraction process [44].
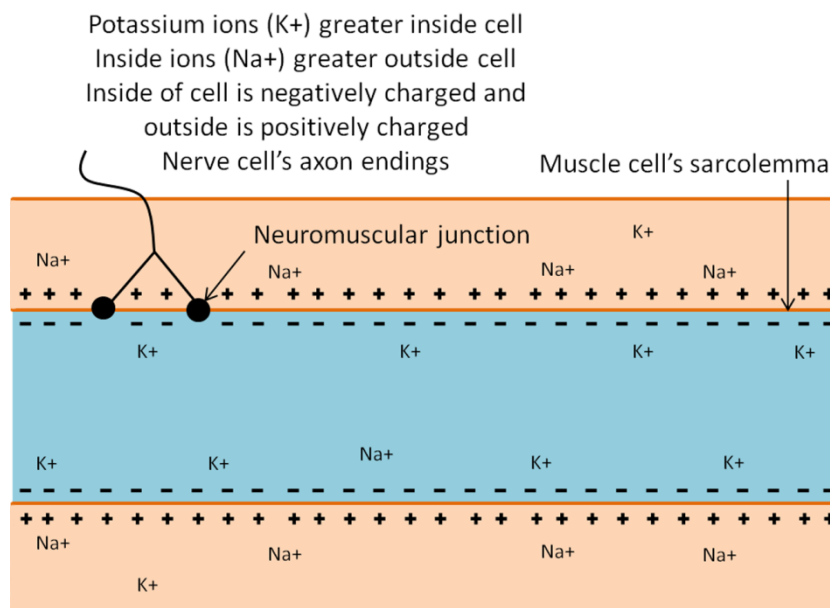
Figure 2.15 Ionic and neuro-electrical factors affecting the skeletal muscle cell. Adapted from [44].

2.7.5 Types of muscle contractions

There are two types of muscle contraction, isometric and isotonic. The isometric contraction occurs when the muscle length does not change during loading conditions, this type of contraction is also called static contraction. On the other hand, the muscle length in isotonic contractions changes during load conditions. There are two types of isotonic contractions, concentric and eccentric. The concentric contraction takes place when the muscle length decreases during loading conditions. Conversely, the muscle length increases during the eccentric contraction [91-92].

2.8 Mechanical properties of the skeletal muscles

Skeletal muscles play an important role in the motion of the human body. They transform chemical energy into movement, allowing the execution of complex movements of the body. The skeletal muscles can be shortened, lengthened or stay the same length depending on the external or internal forces applied to them.

According to Hill's model, the skeletal muscle is integrated by three elements: the contractile component (CC), the series elastic component (SEC) and the parallel elastic component (PEC) [85, 93]. The CC consists of the muscle fibres, which transform the neurological signals of the nervous system in muscle force. The tendon

that connects the muscle fibres with the bones represents the SEC. The PEC is the soft tissue that surrounds the muscle fibres, such as the fascia [85]. The contractile or active component is characterised by four mechanical relationships, which are described as follows.

Stimulation-activation relationship

The mechanical property of stimulation-activation of the contractile component of the skeletal muscle represents how the central nervous system sends the signals (stimulation) to activate the motor units and produce the contraction process (activation). This relationship is difficult to quantify because it is not possible to measure the specific amount of the stimulation or activation in the muscle contraction process [85].

Force-activation relationship

Another mechanical property of the contractile component is the force-activation relationship. This property is difficult to quantify because the force produced by the stimulation depends on the mechanical properties of the contractile component, such as the type and orientation of the fibres [85].

Force-velocity relationship

The force-velocity relationship is the most important mechanical property of the skeletal muscles. This relation is based on Hill's model, which indicates that the muscle force decreases if the velocity of muscle contraction increases during concentric contraction, as illustrated in Figure 2.16. It also indicates that the highest muscle force is produced during eccentric contractions [69, 85, 92-94].
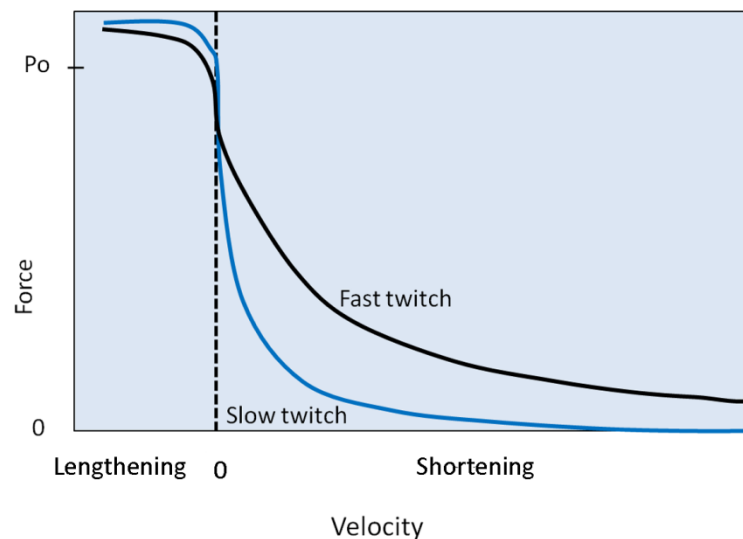
Figure 2.16 Force-velocity relationship of the contractile component for fast and slow twitch muscles. Po is the maximum force when the velocity of contraction is equal to zero. Adapted from [85].

Force-length relationship

The force-length relationship is another important mechanical property of the skeletal muscles. It indicates that the muscle produces the highest force (Po) when the muscle is in resting position (Lo, the optimal length when the muscle is not shortened or lengthened). Conversely, when the muscle is shortened or lengthened, it produces the lowest muscle force, as shown in Figure 2.17.
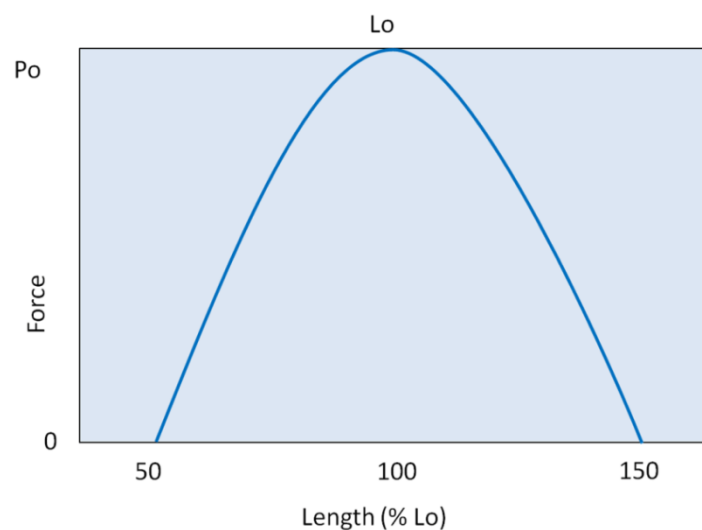
Figure 2.17 Force-length relationship of the contractile component (CC), where the maximum amount of force that the CC can produce is when the muscle is not shortened or lengthened, Lo. Adapted from [85].

63

This is more easily understood if the muscle fibres are observed at a microscopic level in the sarcomere zone. The force is reduced when the actin and myosin filaments are separated or overlapping, reducing the connection between the filaments [69, 85, 92, 94].

2.9   Anconeus muscle

Anconeus is a small and slim triangular muscle located in the posterior part of the elbow; that appears to be a continuation of the triceps brachii [35, 41, 53]. It arises from the lateral epicondyle of the humerus and inserts in the lateral side of the proximal ulna, as illustrated in Figure 2.18. The radial nerve innervates anconeus and triceps brachii [95]. In 1981, An et al. developed an anatomical study to measure the fibres length of the muscles crossing the elbow [36]. They found that the length of the fibres of the anconeus was approximately 2.7 cm with a moment arm of 0.62 cm with the forearm extended and in neutral position [36]. Moreover, in 2009, Coriolano and colleagues found similar lengths. However, Coriolano et al. identified that one of the borders (lateral inferior margin) of anconeus measured 8.2 cm [37].
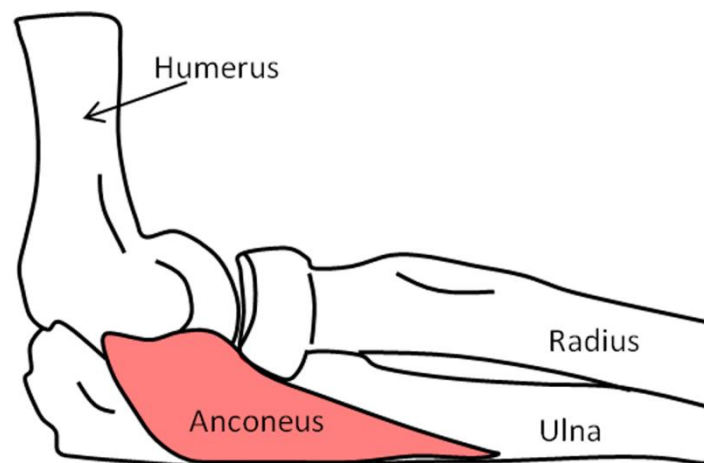
Figure 2.18 Anconeus muscle, lateral view of the elbow. Adapted from [6].

The major uncertainty regarding this muscle is that its specific function has not been clarified. Some researchers [22-23, 25] have suggested that this muscle could be an extensor of the elbow, while others believe that the anconeus could be an abductor of the ulna [1, 29-30]. Moreover, it has been thought that this muscle could produce dynamic stability to the joint [33, 35, 43]. More recent studies have suggested that

the contraction of the anconeus muscle could tense the elbow joint capsule to avoid being pinched by the bones when the elbow is extended [42, 95-96].

2.9.1   Anatomy of the anconeus muscle

The anconeus is a small triangular muscle located in the posterolateral part of the elbow. It arises from the lower part of the lateral epicondyle of the humerus and inserts in the lateral part of the olecranon of the ulna [35, 37-38, 41-42, 53]. Although the anconeus has been described as a triangular muscle, some anatomy books still represent the muscle as a fusiform shape [41, 97]. Its anthropometric measurements are 73.11 ± 10.32 mm, 27.39 ± 3.29 mm and area 2002.48 ± 33.95 mm^2 [98].

There are few specific studies regarding the anatomy of this muscle. In 2009, Coriolano et al. performed an anatomical research with the purpose of discovering the anatomical structure of this muscle and tried to establish its function. They found four different types of fibres (proximal, medial, distal and terminal fibres) oriented in different directions of the tendon, as illustrated in Figure 2.19. They calculated a design index of 0.3, a ratio between the length of the fibres (2.52) and the length of the anconeus muscle (8.2 cm). This ratio suggests that this muscle could produce force with small displacement [37]. Moreover, the architecture of the fibres supports the idea that the anconeus is a penniform muscle (penniform: feather form).

The anatomy and structure of the elbow and muscles crossing the joint were analysed in order to see the effect of the muscles in the stability of the joint. All muscles crossing the elbow joint could contribute in the stability of the articulation by compressing the articular surface when they contract. Anconeus was considered to be a stabiliser muscle [46]. This study should be developed during dynamic conditions to support the idea that the anconeus is a stabiliser of the joint [46].

In addition, based on the anatomy of the muscles crossing the elbow joint, O'Driscoll and colleagues suggested that the anconeus, triceps brachii and brachialis muscles participate in stability of the joint [33]. They mentioned that dynamic stability was the major role of the anconeus muscle on the elbow. However, none of these studies

provided enough evidence to support their statements regarding the anconeus function as a stabiliser muscle [33, 46].
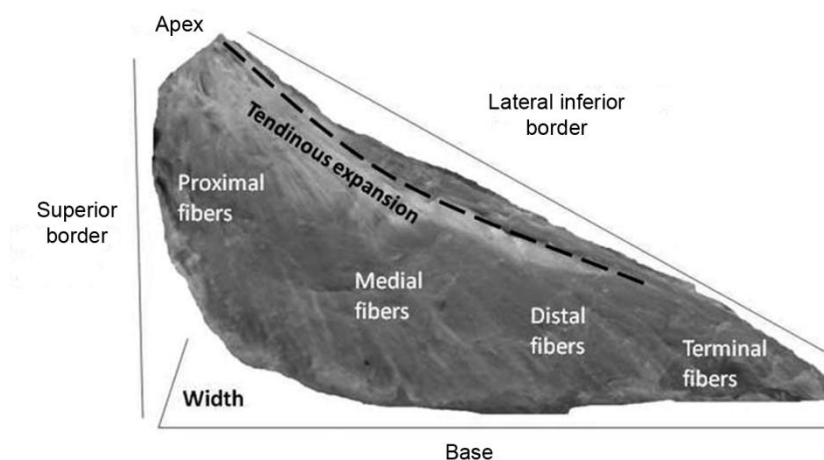
Figure 2.19 The anconeus with the muscle fibres and the tendinous expansion [37].

In 2010, Molinier and colleagues developed a cadaveric study where they found a strong relationship between the lateral head of the triceps brachii and the anconeus fibres [35]. This anatomical investigation suggested that anconeus should be considered as an extension of the triceps brachii, as illustrated in Figure 2.20. The major contribution of this research was to support the argument that anconeus was a dynamic lateral stabiliser of the elbow [35]. This idea was previously mentioned by Basmajian and Griffin [31] and O'Driscoll [33].
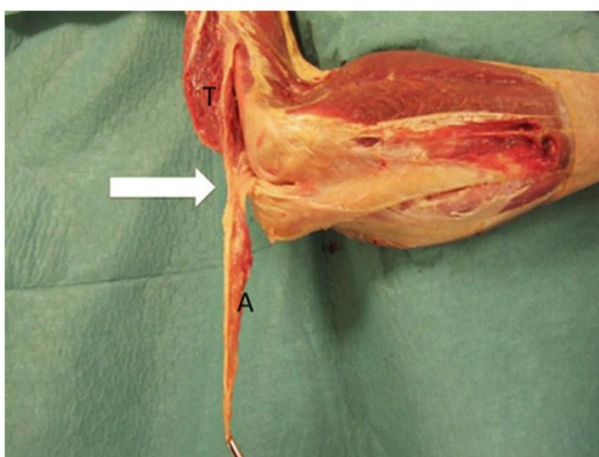
Figure 2.20 Right elbow, anconeus was removed. The arrow shows the continuity of the triceps brachii, lateral view (A anconeus and T Triceps brachii) [35].

Molinier et al. disagreed on the idea that the anconeus muscle should play an important role during extension of the forearm. They concluded that the role of anconeus in extension motion was merely an accessory [35].

In 2010, Harwood and colleagues performed a pilot investigation to study some anatomical features of the anconeus muscle. They found that the fascicle length of anconeus increased as the elbow is flexed and the pennation angle decreased as the elbow is flexed [99].

The elbow has been considered as a tensegrity (tension-integrity) structure because its stability is provided by the continuous tension of the soft tissue. In 2012, Graham Scarr suggested that the anconeus and brachioradialis muscles could play an important stabiliser role in the structure of the elbow [100]. As the anconeus remains active during all movements of the elbow, it could contribute to the concept of tensegrity of the elbow [22-23, 32, 100].

Four years after the first pilot study regarding the fascicle length and pennation angle using ultrasonography, Stevens et al. developed a complete method to study these anatomical features of anconeus. The study was carried out in vivo throughout the full range of motion of the elbow joint. The outcomes showed that the pennation angle decreases as the flexion angle increases. The maximum pennation angle in full extension was 16 degrees and decreased up to 11 degrees in full flexion. On the other hand, it was reported that the fascicle length of anconeus increases as the flexion angle increases [101].

2.9.2   Biomechanics of the anconeus muscle

In 2012, Pereira conducted another study of the anatomy and biomechanics of this muscle with the aim of investigating the importance of anconeus in the elbow. He found two different compartments in the muscle (one in the anterior edge and the other in the posterior edge of anconeus). The length of the fibres in these compartments seems to be similar to the lengths measured by Coriolano et al. [37-38]. Moreover, because the anterior fibres of anconeus followed the same trajectory

of the lateral collateral ligament, the anconeus was considered to be a lateral stabiliser of the elbow [38].

In a two dimensional (2D) analysis of the two compartments of the moment arm, it was found that the posterior edge did not change its role of being an extensor muscle from 0-120 degrees. However, the anterior edge of the muscle changed from being an extensor muscle to a flexor muscle at around 80 degrees of flexion. The maximum moment arm obtained was 14 mm at 0 degrees of flexion [38]. There were some limitations in the study performed by Pereira. One of them was to consider the lateral epicondyle as a fixed rotational axis of the flexion-extension motion of the elbow. The lateral epicondyle is not the real axis of rotation, which crosses throughout the centre of the trochlea of the humerus [102]. In addition, the population considered in the research was elderly people and the analysis was carried out in a 2D plane. The range of motion considered in this study was from 0 degrees to 120 degrees [38].

The anatomical studies of the anconeus muscle provided a lot of information regarding the structure and biomechanics of this muscle in the elbow. However, it seems that this information is not enough to define a clear role of the anconeus. Furthermore, since all anatomical studies were performed in cadavers, this could present a disadvantage because the muscles behave in a different way when they are alive [38].

2.9.3   Electromyography of the anconeus muscle

Electromyography (EMG) represents a reliable approach to determine the function of the anconeus muscle among living subjects. EMG could lead a better understanding of the behaviour of the muscles. A brief description of EMG research of the anconeus muscle is described as follows.

In 1867, Duchenne speculated the first idea about the role of anconeus. In his book named "Physiology of motion demonstrated by means of electrical stimulation and clinical observation and applied to the study of paralysis and deformities", he commented that this muscle was involved in the extension of the forearm and it could abduct the ulna during pronation [1].

The second idea of Duchenne was later supported by Ray et al. [29]. In his study of the rotation of the forearm (pronation and supination), Ray and colleagues found that the contraction of the anconeus could produce abduction of the ulna (lateral movement) and under specific circumstances, the ulna could be abducted during pronation and adducted in supination. The ulna stayed relatively stationary and aligned to the fifth finger when the rotation of the forearm was performed. Nevertheless, the distal part of the ulna presented lateral or medial displacement when the rotation was performed with the index digit of the hand. They implied that the importance of this muscle during extension of the forearm was insignificant [29].

In 1959, eight years after the discoveries of Ray and colleagues, Hora described that the muscle could contract during extension. Moreover, he determined that the muscle could contract during resisted and unresisted pronation and supination of the forearm [32]. In the following years, Travill [22] speculated similar ideas of Hora, but he did not find electrical activity of anconeus during unresisted pronation-supination motion. Travill compared the two important extensors of the elbow (Triceps brachii and anconeus) and he observed that anconeus was active during all extension movements, as shown in Figure 2.21. Nevertheless, he concluded that the greatest electrical activity of the anconeus occurred during extension of the forearm [22].
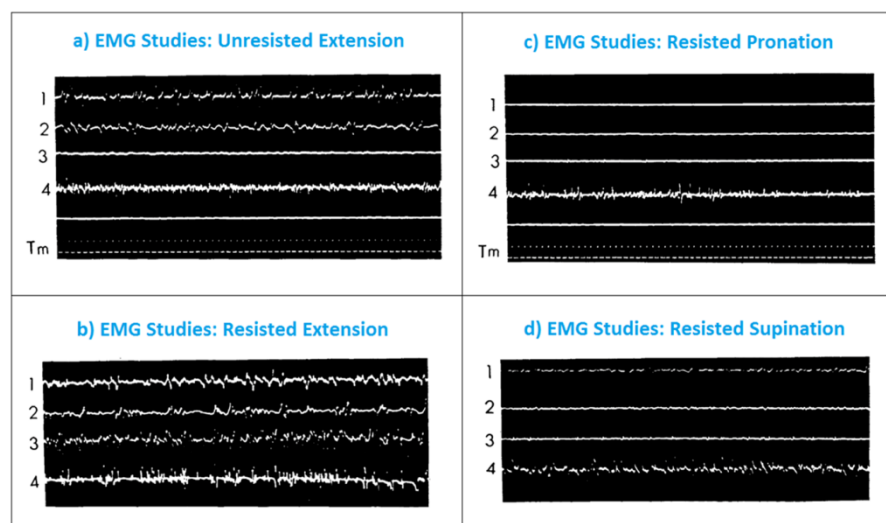
Figure 2.21 Electrical activity of the anconeus and triceps brachii: a) Unresisted extension, b) Resisted extension, c) Resisted pronation and d) Resisted supination. 1 Triceps brachii medial head, 2 lateral head, 3 long head and 4 anconeus muscle. Adapted from [22].

Considering all disagreements previously established [1, 22, 29, 32] about the function of the anconeus muscle in the elbow, Pauly et al. [23] developed an electromyographic study of some muscles crossing the elbow joint in order to re-examine their functions. From the investigation, they found that the extension of the forearm is the prime function of the anconeus and the secondary role could be the stability of the elbow. The electrical activity of anconeus during pronation-supination movement was identified only if the motion was resisted. Moreover, they noticed that the electrical activity of this muscle diminished when the powerful triceps brachii was contracted [23].

With the aim of giving a better explanation about the function of the anconeus, Basmajian and Griffin [31] performed another electromyographic study to understand the behaviour of this muscle during the motion of the elbow. They found that anconeus was involved in the pronation, supination and extension movements, as illustrated in Figure 2.22. Nevertheless, they concluded that the importance of this muscle in the rotation of the forearm was insignificant due to its low level of electrical activity. At the end, they suggested that anconeus could act as a stabiliser of the elbow [31].
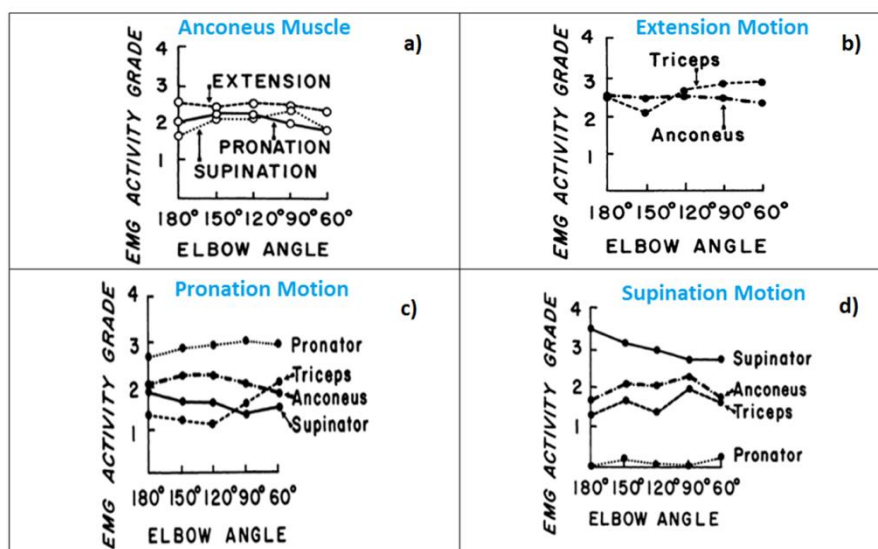
Figure 2.22 Electrical activity of the anconeus and triceps brachii: a) EMG of the anconeus during extension, pronation and supination, b) EMG of the anconeus and triceps brachii during extension, c) EMG during pronation and d) EMG during supination. Adapted from [31].

Following the trend of considering anconeus as an extensor muscle, Le Bozec and colleagues [24] investigated the relationship between the three heads of the triceps brachii and anconeus during isometric contractions. They concluded that the anconeus was an extensor muscle and played an important role when the torque was less than 1.17 Nm. Moreover, to support the previous findings about the synergy between the anconeus and triceps brachii, Le Bozec et al. [25] developed a dynamic study of the extension motion of the elbow. They concluded that the activation time of the anconeus muscle was different from the triceps brachii. The electrical activity of the anconeus appeared during low values of external work (< 1 J) and stayed linear with less intensity for higher values than 1 J [25]. They suggested that the anconeus muscle should play an important role during slow movements of extension. They implied that one of the three heads of triceps brachii should not be considered as a representation of the whole extensor group.

Trying to find the contribution of the anconeus muscle during extension of the elbow, Le Bozec and Maton [26] simulated the deactivation of this muscle using anaesthesia. They suggested that blocking the anconeus did not change the kinematics of the elbow. The only difference was that the three heads of the triceps brachii were activated at different time [26]. Although this investigation represented a good approach to the problem of the anconeus, it had the disadvantage of a lack of motion control in the tests and the low amount of participants involved. Furthermore, other disadvantage was that the analysis of the electrical activity of anconeus and the range of extension motion was limited to 40 degrees [26].

It was reported that the anconeus could be an extensor of the elbow. However, some authors [28, 31, 103] added the role of lateral stabiliser of the elbow. This argument brought new questions regarding the specific function of the anconeus muscle. In 1985, Gleason and colleagues disagreed on the idea of considering the anconeus as an extensor and stabiliser muscle. They suggested that there was an axis formed by the head of the radius and the middle finger of the hand, which causes that the anconeus abducts the ulna during pronation [30]. This idea was in agreement with those ideas of Duchenne [1] and Ray et al. [29].

Two years later, Funk et al. [104] performed another electromyographic study of the muscles crossing the elbow. The investigation was performed during resisted isometric contractions at three different flexion angles, 30, 90 and 130 degrees. The outcomes showed that the major electrical activity of the anconeus was during extension [104]. They found that the major flexor muscles of the elbow (biceps brachii, brachialis and brachioradialis) were activated during isometric flexion contractions [104].

The extensor muscles (triceps brachii and anconeus) were activated during isometric extension contractions. The results of Funk and colleagues showed that the anconeus was the only muscle activated during varus and valgus stress. Therefore, they suggested that the structure of the joint and the ligaments were the main responsible components of the varus and valgus stability. The results showed that the myoelectric activity was variable between subjects performing the same activity; however, the muscle activity followed a similar trend [104].

In 1991, Naito et al. carried out an electromyographic study of the main flexor (biceps brachii, brachialis and brachioradialis) and extensor muscles (triceps brachii and anconeus) of the elbow joint [105]. Although the myoelectric activity changed from each participant, it was found that the electrical activity of the flexor muscles was more active during flexion motion. The biceps brachii muscle was less active when the forearm was placed in pronation. On the other hand, although the triceps brachii is considered the major extensor muscle, its activity was not significant in some volunteers during extension motion. It was suggested that the effect of gravity on the posture of the elbow could be the reason of the small amplitude of the triceps brachii activity. The myoelectric activity of anconeus muscle was presented in almost all participants during the extension movement [105].

Two years after the studies of Naito and colleagues, Werner et al. studied the biomechanics of the elbow joint during baseball pitching. They mentioned that the activity of the anconeus, triceps brachii and wrist flexor muscles helped the ligaments to stabilise the joint and prevent dislocation of the elbow [39]. In 1994, Naito et al. studied the flexion-extension motion of the elbow produced by electrical stimulation of the main flexor (biceps brachii, brachialis and brachioradialis) and

extensor (triceps brachii and anconeus) muscles. They found that functional electrical stimulation of the flexor muscles produced flexion of the joint and stimulation of the extensor muscles generated extension movement. Moreover, they found that electrical stimulation of the long head of the triceps brachii produced extension of the shoulder joint [106].

Previous attempts to evaluate the myoelectric activity of the anconeus involved using electromyography either alone or in conjunction with additional experimental equipment, such as accelerometers and potentiometers. However, they provided only qualitative results instead of quantitative ones hence limiting the understanding [22-23, 28, 31]. Moreover, some of them limited the investigation considering a short range of motion [25-26].

Investigations from the last decade have indicated that the anconeus could contribute up to 15% of the extension moment during isometric contractions of the elbow flexed at 90 degrees [34]. It is clear from the results that the importance of this muscle cannot be negligible. It was also found that the uniarticular muscles (short and medial head of triceps brachii) contributed more during extension torques. The long head of triceps brachii contributed less during the isometric torques. However, due to the small amount of volunteers considered and the isometric contractions used in that work, further investigation considering non-isometric contractions is needed to support the evidence [34]. One limitation of this investigation was that the results regarding the contribution of the anconeus during isometric torques was variable among participants. In some individuals was less than 5% the contribution that anconeus contributed during the torques [34].

Another similar study was performed by Davison and Rice [107], with the purpose of investigating the electrical activity of the extensor muscles during fatigue contractions. The electrical activity of the three heads of the triceps brachii and anconeus was measured with needle electrodes during fatigue isometric contractions at two different positions of the shoulder (0° and 90° of flexion). The EMG results showed that one head of the triceps brachii was not representative during extension, so one head of the triceps brachii should not be considered to be a whole group of extensor muscles [107].

Furthermore, the electrical activity of the anconeus did not increase during fatigue contractions. This behaviour could be explained by the structure of the fibres in the extensor muscles. The anconeus has 62.9% of type I fibres whereas the triceps brachii has 63.8% of type II fibres [107-109]. Muscles with type I fibres have great resistance to fatigue and are activated first [108].

In 2013, Bergin et al. developed an electromyographic research of the extensor muscles at two particular regions of the anconeus muscle, as illustrated in Figure 2.23 (transverse AT and longitudinal fibres AL). Triceps brachii and both compartments of the anconeus all presented electrical activity during extension [40].

Moreover, the findings indicated that the activity of the transverse fibres was higher in pronation than in supination, but the longitudinal fibres did not show any difference during the rotation [40]. They concluded that the electrical activity of both compartments depended on the rotational axis of the forearm. These results suggested that the anconeus should be considered to be a multifunctional muscle of the elbow and forearm [40]. In another electromyographic study, it was reported that the anconeus, extensor carpi ulnaris and the lateral head of the triceps brachii could play an important role during a forward fall [110]. These muscles could be activated before falling onto the ground and minimise the effects of the impact [110].
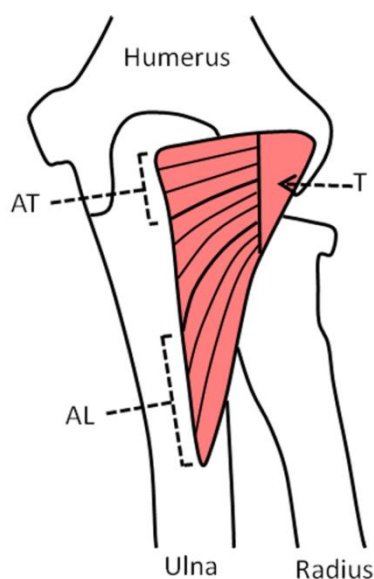
Figure 2.23 Posterior view of the elbow demonstrating the tendon (T), transverse fibres (AT) and longitudinal fibres (AL) of anconeus. Adapted from [40].

2.9.4 Clinical applications of the anconeus muscle for the treatment of injuries at the elbow joint

It has been a long debate within the research community to give the best explanation regarding the function of the anconeus muscle; however, there is no agreement. Some surgeons view this muscle as unimportant and it is frequently denervated during surgical approaches to the elbow [2]. Some authors [3, 5-6, 111] have considered the anconeus for the treatment of lateral epicondylitis (tennis elbow) after failing conservative treatment. This technique seems to be prominent for pain relief of the elbow (Figure 2.24), showing good results in most of the treated patients. Furthermore, changes in the range of motion of the elbow (flexion-extension and pronation-supination) after the surgery were insignificant [3, 6].
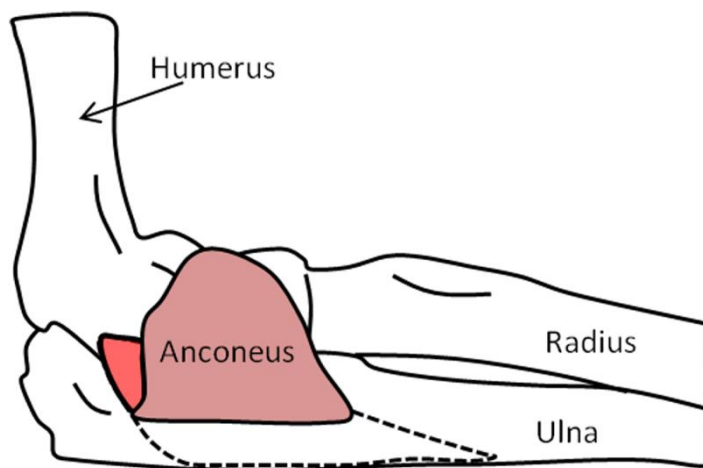
Figure 2.24 Rotation of the anconeus muscle on the humeroradial joint. Adapted from [6].

The anconeus muscle has been also used to detect neuromuscular transmission disorders, using repetitive nerve stimulation (RNS). The main common illness is myasthenia gravis, a neuromuscular disease leading to muscle weakness and fatigue [15-17, 19]. Maselli and colleagues found that the anconeus could be used to detect neuromuscular disorders. They removed some fibres of the anconeus for in-vitro study and reported that none of the patients presented functional deficit because of the partial removal of the muscle [18].

Anatomical studies performed by Schmidt et al. [4] have demonstrated that anconeus could have clinical applications in the treatment of injures around the elbow. The muscle has been harvested as a local flap for covering some areas around the elbow

(the radiocapitellar joint, the distal triceps tendon and over the olecranon) with no loss of motion or extension strength of the elbow [4, 7-8, 112-113]. Furthermore, it has been considered for the treatment of the radiocapitellar and radioulnar joints after trauma [11-14].

Other authors studied the morphological features of anconeus, concluding that the anconeus might be used as a free flap to repair soft tissue (abductor pollicis brevis) defects in the thumb [9, 98]. Moreover, the anconeus muscle has been used for the treatment of injures in the synovial membrane around the radiocapitellar joint, as shown in Figure 2.25 [114]. Although the function of the anconeus muscle is not well defined, some surgeons perform surgical approaches to the elbow joint preserving the arteries, veins and nerve of the anconeus muscle [115]. The anconeus flap transolecranon approach is a surgical technique, which helps to access the humerus fractures preserving the innervation of the anconeus muscle intact [115]. The anconeus muscle has been used for the treatment of the radioulnar synostosis. The fusion of the radius and ulna in the proximal part becomes common during radius fractures. Therefore, the anconeus muscle is considered as a pedicle flap for being placed between these two bones. This stops formation of synostosis and prevents loss of pronation [116-117].
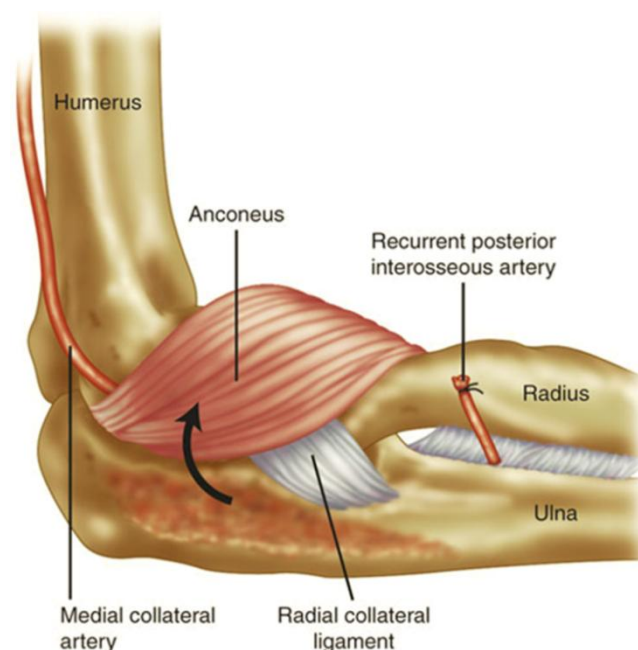
Figure 2.25 The anconeus muscle is folded back to cover injures around the radiocapitellar joint [114].

Due to lack of universal agreement in the research community about the specific function of anconeus, it has been hypothesized that the anconeus has lost its function on the elbow motion due to an evolutionary process. It seems that the muscle used to play a significant role when humans used to crawl and climb the trees to obtain food. Nowadays, the elbow joint is more stable due to the geometry of the bones and ligaments. Therefore, the anconeus seems to play an important role in the early stage of life but becomes an accessory when humans learn to walk [118-119].

2.10 Biceps brachii

Biceps brachii is a long fusiform bi-articular muscle situated in the anterior part of the humerus, as shown in Figure 2.26. It is integrated by two heads, long and short, which give the name of biceps brachii. The short head arises from the coracoid process of the scapula and the long head begins from the supraglenoid tubercle of the scapula. Both heads are inserted in the radial tuberosity of the radius [41, 74, 90]. It has been considered to be one of the main flexor muscles of the elbow joint [75, 104, 106, 120]. Furthermore, this muscle is involved in the stability of the shoulder joint and is considered to be a supinator muscle of the forearm [41, 78, 121].

2.10.1 Anatomy of the biceps brachii

Anatomical studies have suggested that the two heads of biceps brachii can be separated from each other, implying that each head has its own function. The tendon of the short head is inserted more distally from the tuberosity of the radius, suggesting that the short head of biceps brachii is more powerful in flexion than the long head. On the other hand, the tendon of the long head is inserted in the radial tuberosity, indicating that the long head of biceps brachii is more powerful in supination [122-123].

The biceps brachii is a superficial muscle, which is usually considered to have a fusiform structure [74, 90]. However, it has been reported that every head has different structure. The fibres of the long head of biceps brachii are aligned in the same axis of the tendon. Therefore, the long head could be considered as a fusiform head. On the other hand, the fibres of the short head of biceps brachii are not aligned

in the same axis of the tendon. Then, the short head could be considered as a unipinnate head [82].
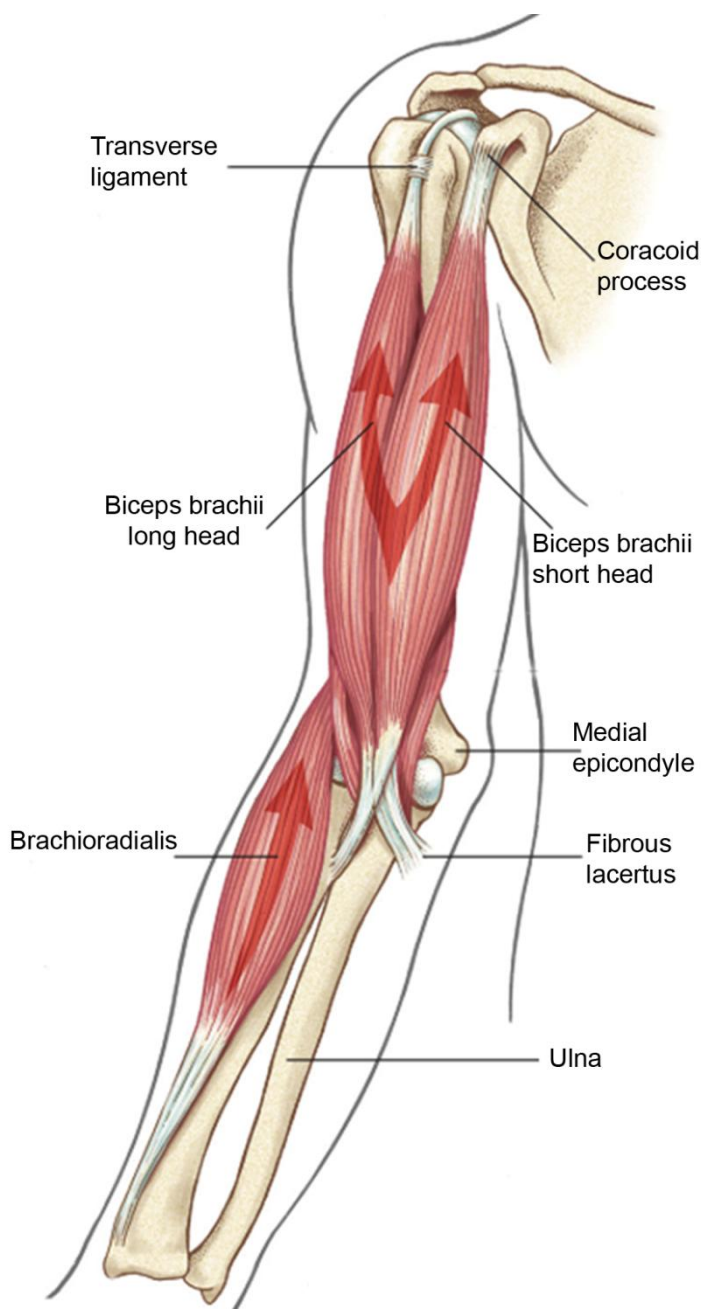
Figure 2.26 Biceps brachii muscle: short and long heads. Adapted from [74].

The biceps brachii muscle has two different neuromuscular compartments, one for each head. Two different branches of the musculocutaneous nerve innervate the long and short heads. Furthermore, each head has smaller neuromuscular compartments originated from the same musculocutaneous nerve [124]. The biceps brachii muscle

is formed mainly by type II fibres. This type of fibres are considered fast twitch fibres [108].

2.10.2 Biomechanics of the biceps brachii

As the two heads of biceps brachii cross the shoulder and elbow joints of the upper limb, it seems that the muscle could contribute to more than one function. It is usually know that the biceps brachii works as flexor muscle at the elbow and it contributes in supination of the forearm [75, 78, 121-123, 125]. Nevertheless, the biceps brachii cannot supinate the forearm when the elbow is completely extended unless the rotation is resisted [75, 103]. The explanation for this behaviour is that the lever arm of biceps brachii, for rotation of the forearm, decreases when the elbow is extended due to having less capability to produce supination motion [36, 82]. Similarly, the moment arm of biceps brachii for flexion of the elbow decreases, when the forearm is completely extended or completely flexed, but increases up to its highest level when the elbow is flexed approximately 100 degrees [82]. Moreover, due to the biceps brachii muscle crosses the shoulder joint, it has been suggested that the contraction of biceps brachii could contribute to the movement and stability of this joint [74, 126].

The isometric moment-generating capacity of the muscles is the combination of the moment arm, physiological cross-sectional area and pennation angle. Biceps brachii has the greatest isometric moment-generating capacity at the elbow. The moment arm and physiological cross-sectional area generate the greatest isometric moment-generating capacity of biceps brachii. Although brachialis has the greatest physiological cross-sectional area, it is not the muscle with the greatest moment-generating capacity. This is because brachialis has the smallest moment arm among the flexor muscles [51].

2.10.3 Electromyographic studies of biceps brachii

Electromyographic studies of the biceps brachii reported that the muscle was activated during supination of the forearm when the elbow is placed at 90 degrees and the rotation is resisted [23, 78]. This suggests that the biceps brachii assists the

supination movement [78]. Moreover, the myoelectric activity of biceps brachii during movement of the glenohumeral joint indicated that it plays an important role in shoulder movement [127]. It is clear from the anatomy and electromyographic studies that the biceps brachii is a multifunctional muscle at the elbow and shoulder joints. Furthermore, the electrical activity of the biceps brachii muscle has been used for the control of the electromechanical devices, which could improve the rehabilitation of the upper limbs after neurological injury [128].

2.11 Triceps brachii

The triceps brachii muscle is considered as the principal extensor muscle of the elbow joint. It is placed in the posterior compartment of the arm and contains three heads. Its anatomical structure provides great advantage to produce extension motion of the elbow [22-23, 82, 104, 106]. Moreover, the triceps brachii is a bi-articular muscle, which crosses the elbow and shoulder joints. It could contribute in adduction of the shoulder [90].

2.11.1 Anatomy of the triceps brachii

Triceps brachii is a muscle that is integrated by three heads, medial, lateral and long, situated in the posterior compartment of the arm. The medial head arises from the posterior part of the humerus below the spiral groove, as illustrated in Figure 2.27. The lateral and long head arise from the posterior part of the humerus and from the infraglenoid tubercle of the scapula, respectively. The three heads are fused in a single tendon, which is inserted on the olecranon of the ulna [41, 74].

Amis et al. found that the structure of the medial and long heads of triceps brachii is unipinnate. The fibres of the lateral head of triceps brachii are orientated in a bipinnate structure [82]. The orientation of the fibres of triceps brachii indicate that it is a muscle for force production [90]. Although the three heads fused in a single tendon inserted on the olecranon of the ulna, each head contains different anatomical structure.
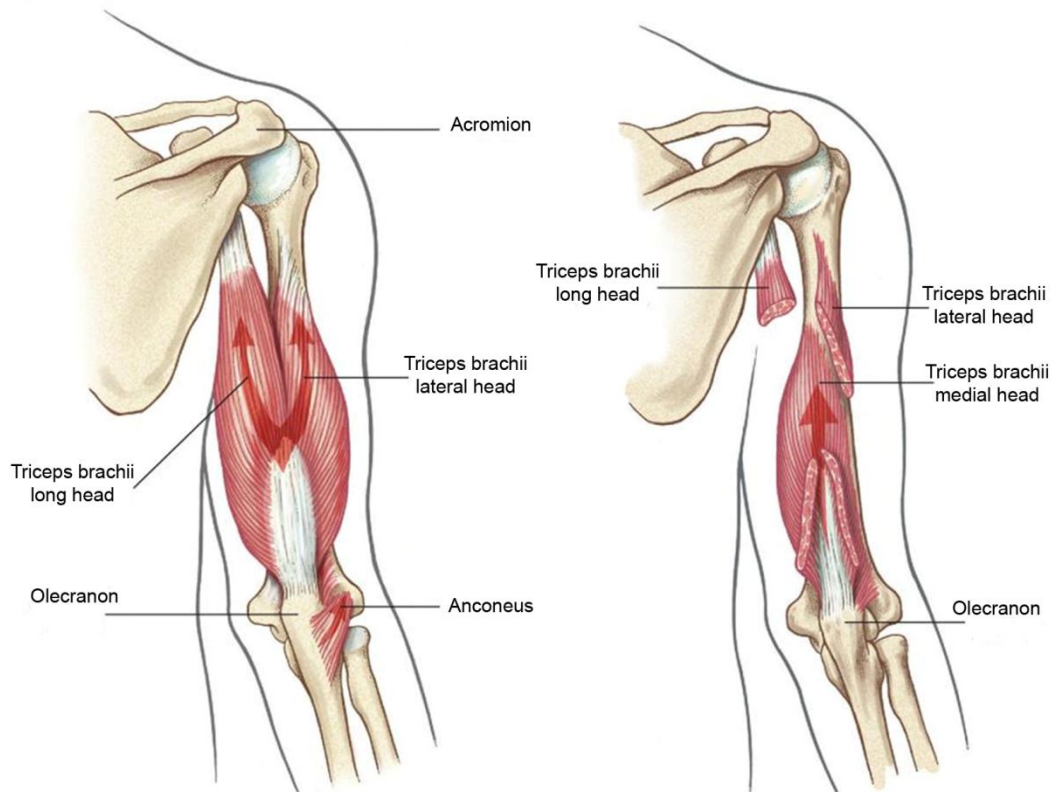
Figure 2.27 Triceps brachii muscle: long, lateral and medial heads. Adapted from [74].

The triceps brachii muscle has different neuromuscular compartments innervated by the radial nerve. The radial nerve spreads their branches through the three heads of the muscle [41, 56]. The branch to the medial head can be affected during posterior surgical approaches to the elbow. Surgeons should be aware that injuring the nerve of the medial head of the triceps brachii can reduce the strength of the muscle [95]. It has been documented that the triceps brachii has three different physiological cross-sectional areas (PCSA). This indicates that each head could have different mechanical properties [36, 82].

There are two types of fibres, which integrate the muscles, type I and type II fibres. The type of fibre is an important feature of the muscles to characterise the physiology of muscle contraction. Type I fibres are slow twitch fibres and have great resistance to fatigue. These fibres are activated first during the motion. On the other hand, type II fibres are fast twitch fibres [108-109]. The lateral head of the triceps brachii muscle is composed around of 36.2% of type I and 63.8% of type II fibres [109].

2.11.2 Biomechanics of the triceps brachii

Figure 2.28 demonstrates that the triceps brachii has the major moment arm of the elbow joint when the forearm is almost completely extended [36, 74, 82]. Conversely, it is clear from Figure 2.28 that the triceps brachii muscle reaches the lowest moment arm when the elbow is completely flexed [82]. Several studies have reported that the triceps brachii muscle has the greatest physiological cross-sectional area between elbow extensors [36, 51, 82]. Therefore, the combination of the moment arm, the physiological cross section and the pennation angle of triceps brachii indicates that this muscle has the greatest isometric moment capacity to extend the joint [51].
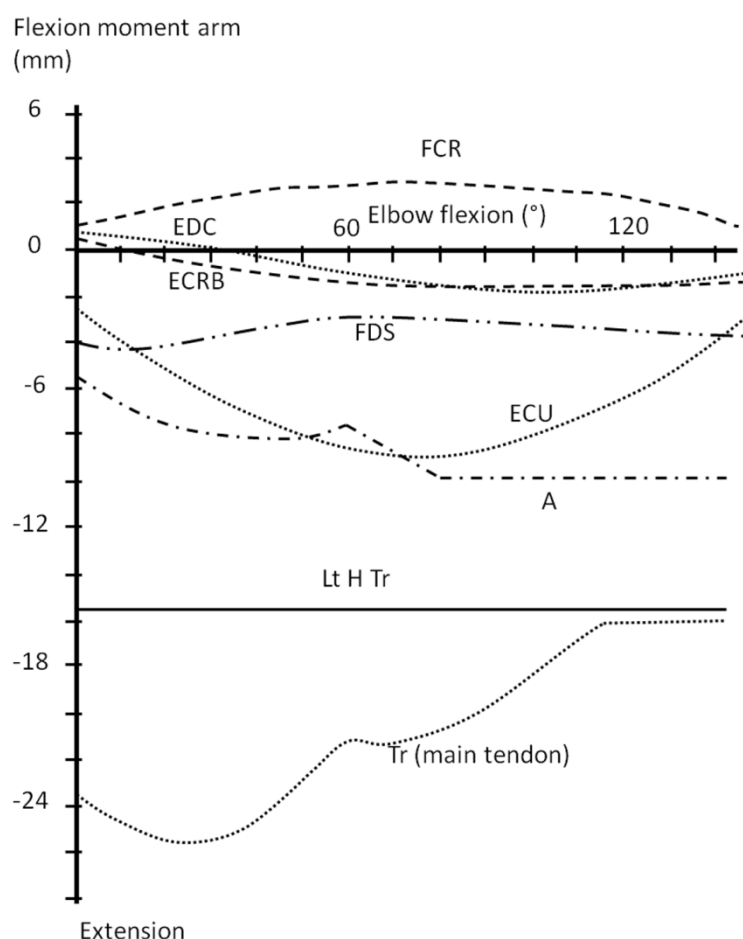
Figure 2.28 Changes of the moment arm of different muscles at the elbow during extension: FCR flexor carpi radialis, EDC extensor digitorum communis, ECRB extensor carpi radialis brevis, FDS flexor digitorum superficialis, ECU extensor carpi ulnaris, A anconeus, Lt H Tr lateral head of triceps and Tr triceps (main tendon). Adapted from [82].

82

The structure of triceps brachii indicates that the muscle is a powerful muscle. Because one head of the triceps brachii crosses the elbow and shoulder joints, it seems that the bi-articular triceps brachii could contribute to more than one function [129]. It has been suggested that the long head of triceps brachii could help to stabilise the glenohumeral joint [42].

2.11.3 Electromyographic studies of the triceps brachii

It is well known that the main function of the triceps brachii muscle is extension of the elbow joint [22-23, 103]. Moreover, it has been suggested that the medial head of triceps brachii is the principal head to produce extension and the other two heads assist the motion when more force is needed [22-23, 31]. However, other researchers reported that the lateral head could be the main head to produce extension because it is the first head to be activated during the motion [25-26, 130]. Electromyographic studies have reported that the three heads of triceps brachii are activated at different time during the extension movement, indicating that one head of the triceps brachii cannot be considered to be the whole muscle [22, 25-26]. Moreover, it has been reported that the electrical activity of the triceps brachii muscle could be used in rehabilitation, prosthesis control, sport and physiological exercise [131]. Another electromyographic study reported that the long head of triceps brachii could adduct the arm [23].

Landin et al. studied the contribution of the triceps brachii during extension of the shoulder at different joint angles. The electrical stimulation of the triceps brachii indicates that the muscle also works as an extensor of the shoulder [129].

2.12 Electromyography

Electromyography (EMG) studies the behaviour of the muscles through the myoelectric activity that they produce when they contract [85, 103, 132]. There are three types of muscles in the human body: skeletal, smooth and cardiac muscles. They are designed to perform different tasks in the human body. Skeletal muscles connect the bones through the joints and allow movement of the limbs.

EMG has been applied to understand the human body movement through the muscle activity [128, 133]. The electrical activity contains a lot of information regarding how the central nervous system activates the muscles to produce movement [134]. The process begins when the central nervous system (CNS) sends an electrical signal through a motoneuron to stimulate the fibres in the muscle and produce a contraction. This structure is named a motor unit and the result is called action potential (AP). The amount of electrical activity of the fibres innervated by a motor unit is known as motor unit action potential (MUAP) and the total amount of electrical activity of all motor units is the electrical muscle activity $\sum$(MUAP), Figure 2.29 [85, 134].
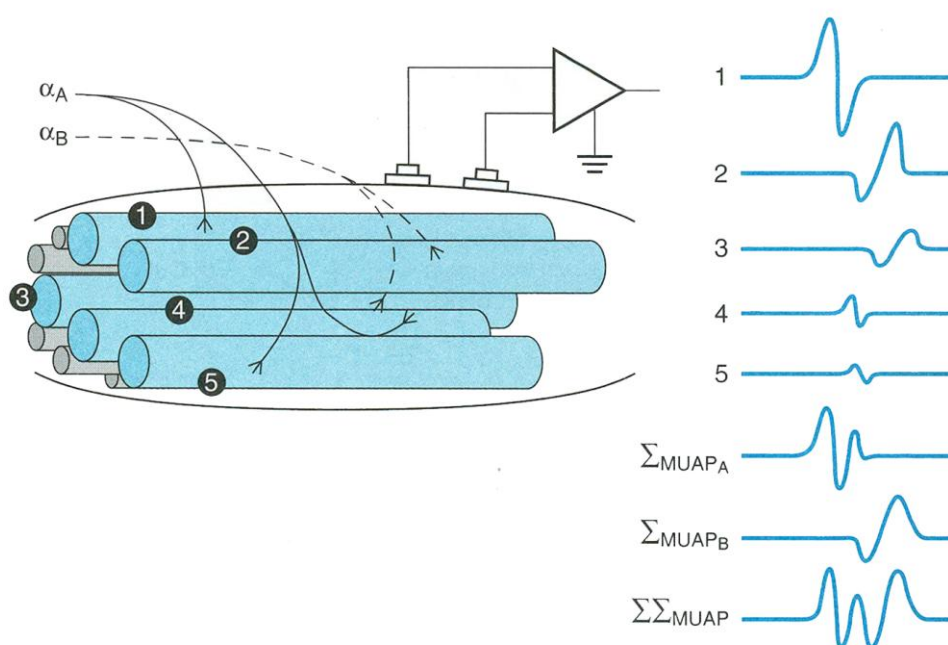
Figure 2.29 Two motor units α_A and α_B innervate different fibres in the muscle (1-5). The total amount of electrical activity recorded from this muscle is called motor unit action potential (MUAP) and it is integrated by the sum of the two individual MUAP from A and B [85].

There are invasive and non-invasive methods to evaluate the myoelectric activity of the muscles. The invasive methods involve needle electrodes during the acquisition of the signal. This type of electrodes is used specially in small and deep areas of the muscle fibres, Figure 2.30. One disadvantage of these electrodes is that they can produce pain to the participants. Other disadvantage is that special care has to be taken in order to protect the participants and avoid any contamination between them [135]. Then, a special protocol with disposable materials has to be used during the

experiments. The recording area of the needle electrodes is small in comparison with the surface electrodes.
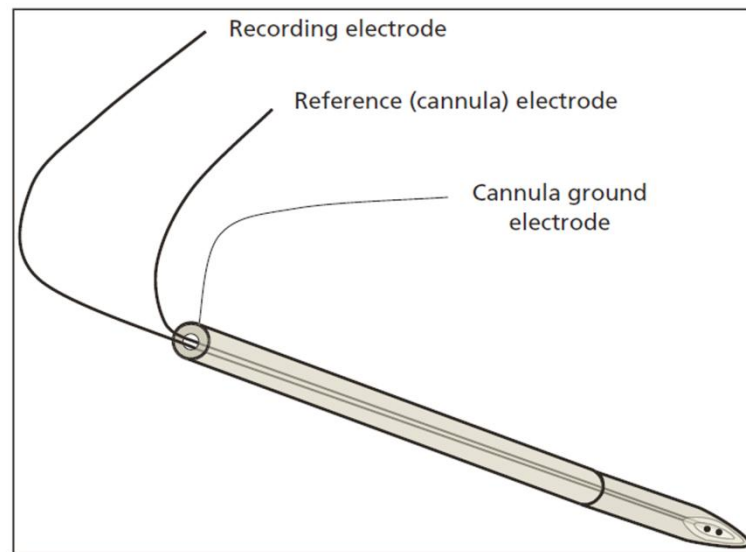
Figure 2.30 Bipolar concentric needle electrode [135].

The non-invasive methods consider the use of surface electrodes for the acquisition of the electrical activity, as illustrated in Figure 2.31. These electrodes do not produce any injury on the skin of the participant and are used specially for muscles that are close to the skin surface [134]. The fat tissue between the muscle and the surface electrode placed over the skin could be a limitation of these electrodes because the fat tissue attenuates the electrical signal of the muscle.
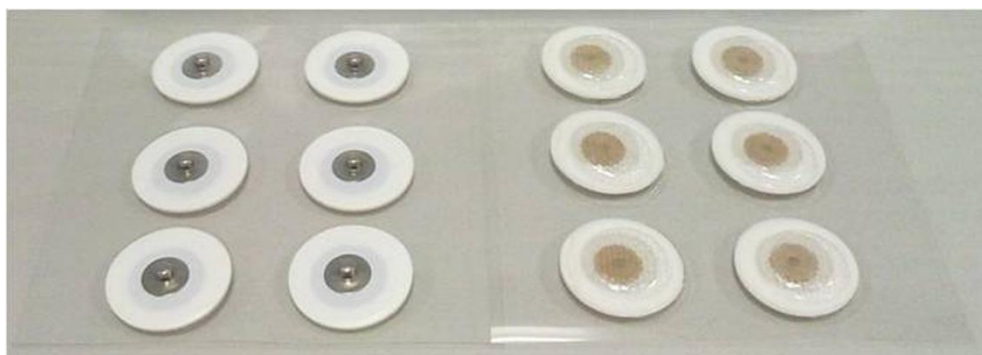
Figure 2.31 Disposable surface EMG electrodes Ag/AgCl.

The amplitude and frequency are the most important parameters of the electromyographic signal to characterise the behaviour of a muscle contraction [85].

The amplitude indicates the intensity of the electrical muscle activity generated by the increment of the motor units. This factor is related to the frequency in such way that the increment of the motor units will increase the frequency of the electromyographic signal [85, 136-137].

Although surface electromyography represents an acceptable way to measure the electrical activity of the superficial muscles, it requires a long process with caution to obtain reliable results in the analysis of the signals. Several factors affect the features of the EMG signal, such as internal structure of the subject, muscle type, fat, skin formation, blood flow velocity, body temperature, so on [138]. Furthermore, there are factors that can affect the acquisition process of the electrical signals [108]. If these factors are not considered in the methodology, it will produce misleading results [139-140].

In 1997, De Luca developed a study of the different factors, which can affect the electrical signal of a muscle contraction. He classified these factors in three different categories; causative, intermediate and deterministic factors [141]. The causative factors have an elemental effect on the signal; they are classified in two categories, intrinsic and extrinsic. The intrinsic causative factors are related with the anatomy, physiology and biomechanics of the muscle. The extrinsic causative factors are related to the features of the electrode and the position over the muscle [141-142].

These causative factors have a direct relationship with the intermediate factors. The intermediate factors represent physical and physiological phenomenon. The last group is the deterministic factors, which have a direct relation to the interpretation of the EMG signals. If all these factors can be addressed properly during the acquisition of the electrical signal, the surface EMG represents a good tool for the study of the muscle biomechanics [141].

Some authors [143] have used the surface electromyography with the idea of extracting information regarding the anatomical and physiological structure of the muscle during isometric contractions. Furthermore, it has been found that there is a direct relation between the electrical activity during an isometric contraction (no shortening of the muscle) and the muscle force [136, 144]. However, it is not

possible to predict the muscle force from the electrical activity because it is not possible to directly measure the force in a muscle [144-145]. Furthermore, the muscle strength is influenced by several factors, such as the number of motor units recruited, fibre arrangement, muscle length and muscle cross-sectional area [90].

The study of the frequency domain of the electrical signals can predict a fatigue index, which in ergonomics is a valuable tool for performing tasks. Some activities have to be performed within a limited time because the quality of the work can be affected negatively due to muscle fatigue [146].

Surface electrodes present an opportunity for the collection of the electrical activity of the superficial muscles without producing any injury to the skin. There have been several studies [134, 147-149] regarding the reliability of these electrodes. In 1984, Webster found that the electrodes made of silver/silver chloride (Ag/AgCl) could eliminate the motion artefact and noise produced between the skin and electrode [147].

In 1994, Winter and colleagues concluded that the reduction of the diameter of the electrodes could diminish the crosstalk noise [148]. Furthermore, in the last decade there have been new types of surface electrodes with new features, which allow a reliable collection of data. The secure skin attachment and small dimension of the surface electrodes reduce the motion artefact and the crosstalk noise of the surrounding muscles, respectively [149].

2.12.1 EMG applications

Neuromuscular disorders

Electromyography is a practical tool to detect neuromuscular disorders by analysing the electrical activity that the muscles produce when they contract. The analysis of the motor unit action potentials provides the diagnostic to detect problems, which affect the performance of the muscles. Myasthenia gravis is an illness that produces muscle weakness and fatigue. Other common problem, which can be identified with the use of electromyography is the injury of the nerves. Proper identification of these injures is important in formulating treatment [16-17, 134].

Kinesiology

Kinesiology is the study of the movement of human body. Muscles are responsible of producing movement of the limbs. Figure 2.32 shows the electrical activity of the biceps brachii muscle during five cycles of flexion. It is clear from the image infer the number of cycles performed by the participant and the time when the muscle was inactive. Clinicians can evaluate the elbow movement and detect abnormalities from the activation time of the muscle. Moreover, the electrical activity can be related with the gait analysis and detect any abnormality during walking [134].
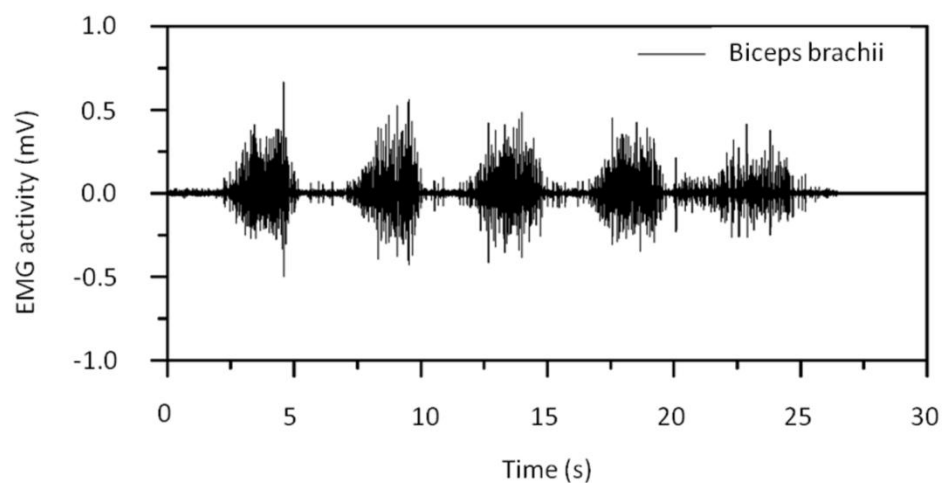
Figure 2.32 Electrical activity of the biceps brachii muscle. The signal was recorded using surface electromyography.

Prosthesis control

The electrical activity of the muscles can be used to control prosthesis of amputated limbs. The evolution of technology and the development of new data processing techniques have improved the design and performance of the prostheses. Nowadays, there are several types of prostheses with more than one degree of freedom. The myoelectric activity is obtained in real time by placing surface electrodes on the muscles of the remained limb. This signal is processed and sent it to the prosthesis as an input signal to produce movement [134, 150].

Ergonomics

The electrical muscle activity provides information to detect fatigue during repetitive tasks. The analysis of the myoelectric activity in the frequency domain is performed by comparing the mean and median frequencies during long periods of work. This

analysis helps to identify muscle abnormalities, which affect the performance of the activities. Therefore, the development of new strategies can be established with this analysis in order to improve the performance and productivity [132, 134].

2.12.2 Signal processing in electromyography

Surface electromyography represents a good approach to study the physiological mechanism of the muscles. However, it is important to know that the electrical activity can be affected from different sources of noise, such as power supply, movement artefact and crosstalk. To obtain reliable outcomes in the analysis, it is necessary to eliminate these sources of noise or apply specific types of filters to attenuate the unwanted frequencies of the sources of noise.

The power spectrum density of the electrical signals represents a powerful algorithm to investigate the frequencies, which are involved in the signal. Although several studies mention the types of filters and cut-off frequencies applied in the signal processing, it is important to understand how the muscle electrical activity can be affected [151-153]. The range of frequencies in the muscle activity is approximately between 0-400 Hz [151]. Furthermore, due to the fact that EMG signal has positive and negative values, the root mean square (RMS) and average rectify (ARV) values represent a good approach to quantify the amplitude of the signals, equations (2.10) and (2.11). The mathematical methods in conjunction with the computational software are an important tool for signal processing.

Root mean square equation:

$$RMS = \sqrt{\frac{1}{N}\sum_{n=1}^{N} EMG(n)^2} \qquad (2.10)$$

Where: N is the number of samples to be averaged, n indicates a specific sample of the signal and EMG is the electrical activity.

Averaged rectified value equation:

$$ARV = \frac{1}{N} \sum_{n=1}^{N} |EMG(n)| \qquad (2.11)$$

Where: N is the number of samples to be averaged and $|EMG(n)|$ is the absolute value of the electrical activity during a specific sample (n).

Power spectrum density

The power spectrum density represents the electrical activity of the signal in the frequency domain. This type of plot highlights the principal frequencies of the signal [85]. The muscle electrical activity can be transformed into sinusoidal form through the Fast Fourier Transformation (FFT). This allows the activity to pass from the time domain to the frequency domain. The most common use of the power spectrum density is the study of fatigue during isometric contractions [154-155].

The changes in the mean and median frequencies are the parameters used to determine the fatigue in the muscles [132]. Moreover, the analysis of the EMG signal in the frequency domain is important to identify the unwanted frequencies, which contaminate the electrical muscle activity. However, it is necessary to have caution when these frequencies are removed because the unwanted frequencies could overlap the muscular frequencies.

The mean frequency (MNF) is the average of the frequency calculated from the sum of the multiplication of the EMG spectrum frequency times the frequency divided by the sum of the spectrum frequency, as shown in equation (2.12) [155].

$$MNF = \frac{\sum_{j=1}^{N} F_j P_j}{\sum_{j=1}^{N} P_j} \qquad (2.12)$$

Where F_j is the frequency of the EMG spectrum at a particular point j, P_j is the EMG spectrum of the signal at a particular point j and N is the length of the data.

The median frequency (MDF) is the frequency, which divides the EMG spectrum in two equal sections, equation (2.13) [155].

$$\sum_{j=1}^{MDF} P_j = \sum_{j=MDF}^{N} P_j = \frac{1}{2}\sum_{j=1}^{N} P_j \qquad (2.13)$$

Where MDF is the median frequency, N is the length of the data, and P_j is the EMG spectrum of the signal.

Crosstalk and movement artefact noise

Crosstalk and movement artefact noise are two parameters that have to be considered in the analysis of the electrical activity of the muscles. Crosstalk noise is the unwanted electrical activity of the muscles, which are close to the recording area. In 1994, David A. Winter and colleagues developed a study to measure the crosstalk of some muscles (gastrocnemius/soleus, tibialis anterior/gastrocnemius, tibialis anterior/peroneus longus and peroneus longus/gastrocnemius) in the lower limb. They found that the reduction of the area and spacing of the electrodes could reduce the crosstalk from the surrounding muscles. In some cases, manual resistance could be enough to detect the activity from the unwanted muscles. However, in other cases a cross correlation technique should be applied [148]. Another common problem that affects the collection of the electrical activity is the movement artefact. This phenomenon occurs during dynamic trials when there is relative movement between the electrode and the muscle contraction [151, 156]. The analysis of the electrical activity in the frequency domain permits the identification of the low frequencies produced by the relative movement. In 2010, Carlo De Luca and colleagues suggested that a Butterworth band pass filter with cut-off frequencies of 20 and 400-450 Hz could eliminate the movement artefact noise without affecting the EMG activity [151].

Digital filtering

Digital filtering is an important tool for the EMG signal processing. The attenuation of the frequencies produced by sources of noise allows a better interpretation of the electrical muscle activity. Furthermore, these types of filters can smooth the signals

depending on the cut-off frequency applied. There are different types of filters, which attenuate the electrical signal depending on the power spectrum density of the signal and the unwanted frequencies [85, 88].

The low pass filter reduces all frequencies below the cut-off frequency. This filter is used to eliminate high frequencies. Conversely, the high pass filter reduces the low frequencies. Moreover, it is possible to define two cut-off frequencies, which allow passing the frequencies between them; this filter is called the band pass. Another filter used to remove the power supply frequency (50 or 60 Hz) is the notch filter [85, 157]. These types of filters can be classified by their impulse responses as a finite impulse response (FIR) or an infinite impulse response filter (IIR). The latter seems to be more efficient but can alter the signals. It is recommended to filter the electrical signals backwards and forwards to avoid any delay in the signals [85, 157].

MATLAB (The Mathworks, Inc. Massachusetts, U.S. version 7.10.0.499 R2010a) software provides a toolkit to design and analyse the outcome of the signal in the base of the attenuation and type of cut-off frequency used. Figure 2.33 and Figure 2.34 illustrate the parameters needed as inputs for this tool.
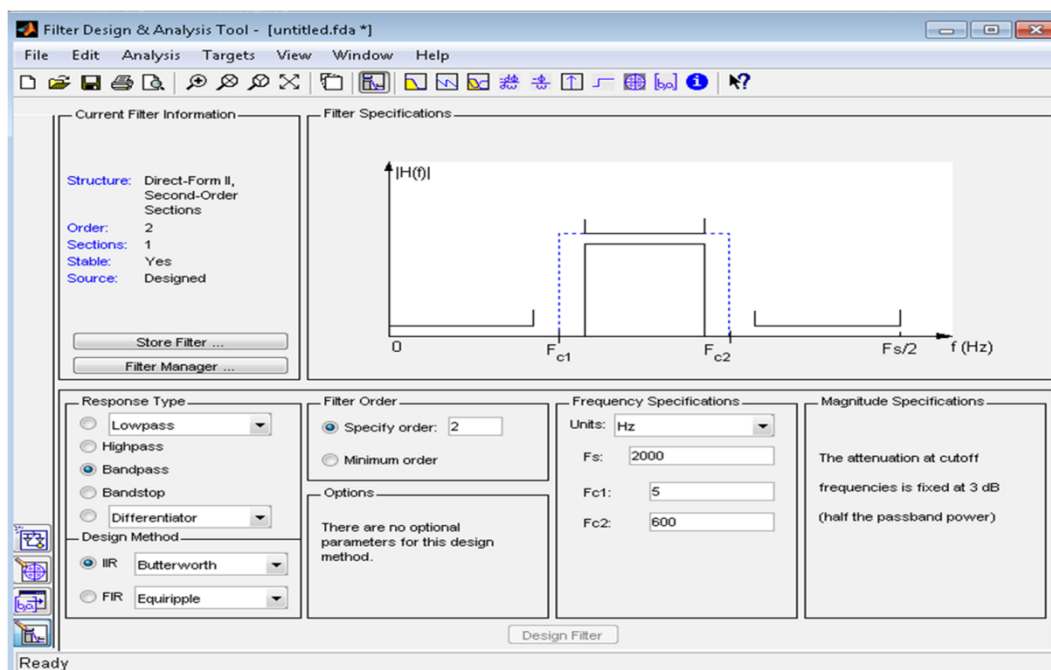
Figure 2.33 Filter design and analysis tool from MatLab software.

92
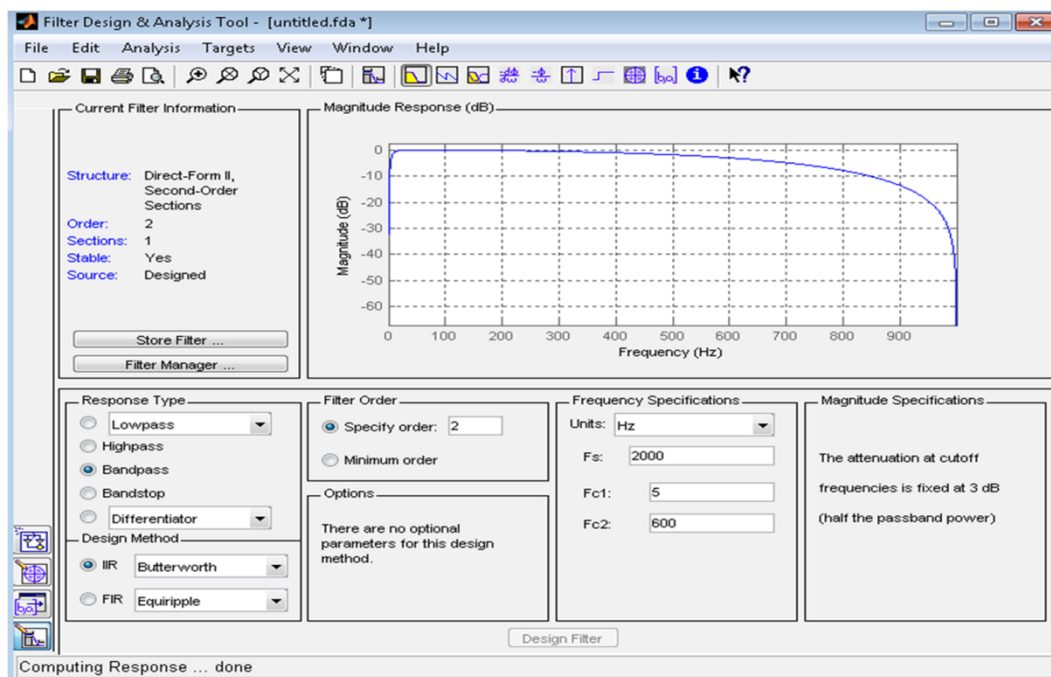
Figure 2.34 Butterworth band pass filter with cut-off frequencies of 5-600 Hz.

Normalisation of the electromyographic signal

To compare electrical activities among subjects, it is important to define a proper way to normalise the electrical activity of the muscle [103]. There are several methods of normalising the electrical activity. The most common method used to normalise the electrical signal is the maximum voluntary contraction (MVC). The MVC trials are commonly performed during isometric contractions.

The idea is to consider the electrical activity of the muscles during dynamic trials in relation to the maximum voluntary contraction. Another technique applied is the maximum peak of the dynamic trials. Furthermore, the muscles can be electrically stimulated and the maximum peak wave, produced during the stimulation, can be used to normalise the trials [85]. However, there is no standard method of normalising the signals. The normalisation method will depend on the aim of the investigation.

93

2.13 Inertial measurement units

The evolution of technology, especially in the field of electronics, has developed new equipment to measure the position and orientation of the human body. The objective of these devices is to understand and describe the behaviour of human movement to improve human life. There are several systems to measure human body movement, such as inertial, mechanical, optical and magnetic [158]. However, it is necessary to consider the advantages and disadvantages that every system has. In this investigation, inertial measurements units (IMUs) are applied to study the kinematics of the forearm in relation to the arm.

Tri-axial accelerometers, gyroscopes, magnetometers and a barometer integrates the inertial measurement unit [159]. The small size of these sensors gives free motion to the participants without any discomfort. Moreover, they can be used anywhere in a space that is free of magnetic disturbances. There are several studies regarding the movement of the human body using inertial units [160-164].

IMUs have been used in the rehabilitation field to study the movement of limbs of people who have suffered a stroke [165]. Furthermore, they are used to track the full body during walking, running and jumping [166]. Although some authors [167-168] have questioned their accuracy and reliability, it is possible to apply this type of sensors to measure human body movement under specific conditions [160, 169-170]. Moreover, additional signal processing of the raw data has to be applied to get reliable results [171].

2.13.1 Accelerometers

A single axis accelerometer can be explained by the combination of Hooke's law ($\vec{F} = k\vec{x}$) and the second law of Newton ($\vec{F} = m\vec{a}$). According to Hooke's law, a mass (m) attached to a spring will move a distance ($\vec{x}$) when acceleration ($\vec{a}$) is applied to the system, Figure 2.35 [158, 172]. The combination of these two laws $\left(\vec{a} = \frac{k\vec{x}}{m}\right)$ allows measuring the acceleration of the mass when it moves a distance $\vec{x}$, where k, $\vec{x}$ and m are known as spring constant, displacement, and mass of the system, respectively [158]. Due to the values of k, $\vec{x}$ and m usually being known in

the system, it is possible to calculate the acceleration ($\vec{a}$) of the system. Nowadays, it is possible to find smaller devices, with better accuracy; they are called micro-electro-mechanical systems (MEMS). These devices contain small electronic components that can measure the acceleration in a three dimensional space (3D) under the same principles.
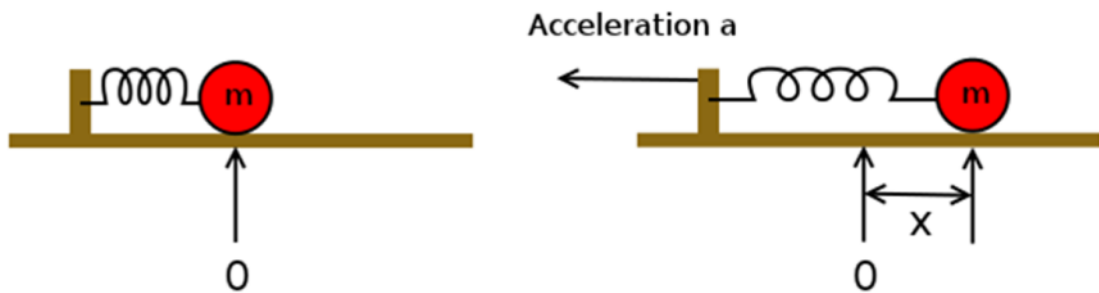
Figure 2.35 Spring-mass system of one single axis. The image in the left is in the static position and the image in the right shows how the mass is moved a distance x by an acceleration force [172].

2.13.2 Gyroscopes

A gyroscope is a device designed to measure the angular velocity of a body. Newton's second law $\left(\vec{\tau} = \frac{d\vec{L}}{dt} = \frac{d(I\vec{\omega})}{dt} = I\vec{\alpha} \right)$ can describe the behaviour of a gyroscope, where $\vec{\tau}$, $\vec{L}$, I, $\vec{\omega}$, dt and $\vec{\alpha}$ are the torque, angular momentum, mass moment of inertia, angular velocity, time increment and angular acceleration, respectively. This law indicates that the angular momentum ($\vec{L}$) of a body will not change unless a torque acts upon it. There are different types of gyroscopes, such as mechanical, optical and vibrating [158, 172-173].

Mechanical gyroscopes work on the basis of the conservation of momentum. In 1852, Foucault built the first mechanical gyroscope, Figure 2.36. This type of gyroscope has the disadvantage of the gimbal lock, the loss of one degree of freedom usually in a 3D gyroscope. Mechanical and optical gyroscopes are not usually used in the analysis of the human movement due to the large size and high cost. These types of gyroscopes have different applications in the research field [158, 172].
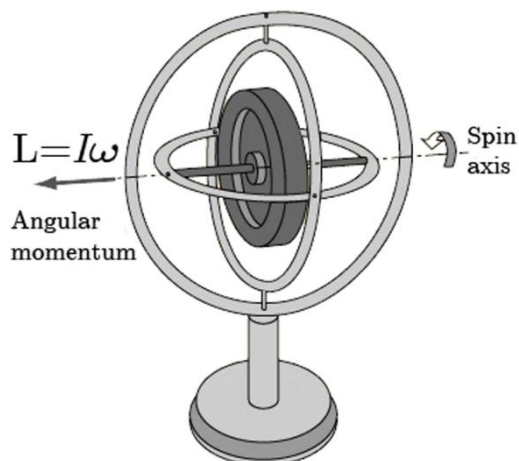
Figure 2.36 Mechanical Gyroscope. The angular velocity of the inner wheel will keep the orientation although the orientation of the outside framework changes [158].

The vibrating gyroscope is another type of gyroscope used to measure the angular velocity of a body. Due to its small size and low cost, they represent the best option for the analysis of human body motion. These gyroscopes are based on the Coriolis effect.

The function of these gyroscopes can be explained with the principle of the Coriolis force $\overrightarrow{F_C} = -2m(\vec{\Omega} * \vec{V})$; where m, $\vec{\Omega}$, and $\vec{V}$ are the mass of the system, the angular velocity and the linear velocity of the mass, respectively. This effect, in combination with Hooke's law, enables measuring of the angular rate of the body [158, 172-173]. Currently, there are smaller and inexpensive devices integrated by electronic components with better accuracy; they are called MEMS gyroscopes.

2.13.3 Magnetometers

Magnetometers are used to measure the intensity or direction of the magnetic field [172]. They can be used to establish the orientation of the IMU device because they can detect the magnetic field of the earth. However, they have to be used carefully because if the magnetic field is disturbed, it will produce misalignments of the reference system [173]. There are different types of magnetometers, which can be used in different research fields. Moreover, they can be manufactured in small dimension to be integrated in the IMU device.

2.13.4 Quaternions

The orientation of a rigid body in the space can be described with Quaternions, Euler angles and rotational matrix. Quaternions are an extension of the imaginary numbers [174]. They were described by William Rowan Hamilton in 1843. Although quaternions seem complicated, they represent an alternative solution to the rotation of bodies in space [175]. They have the advantage of avoiding the problem of gimbal lock. Quaternions have applications in computer graphics, computer vision, robotics, navigation, orbital mechanics and flight dynamics. They have one real part and three imaginary components as shown in equation below [176].

$$q = w + x\vec{\imath} + y\vec{\jmath} + z\vec{k} \tag{2.14}$$

Where w, x, y and z are real numbers and $\vec{\imath}, \vec{\jmath}$ and $\vec{k}$ represent three orthonormal axes.

Quaternions are usually represented by **q** or **H** in honour to Hamilton. They can be used to represent a rigid body in the space. Furthermore, they can rotate a vector from one reference system to another, using the mathematical expression of vector rotation as explained below.

Vector rotation: To rotate a vector $\vec{v}(x, y, z)$ by a quaternion q, it must be transformed to a pure quaternion, $v(w, \vec{v})$.

$$v = (0, \vec{v}) \tag{2.15}$$

Where v is the pure quaternion.

Then the pure quaternion v is rotated to the new reference system with the following mathematical expression:

$$v' = q \cdot v \cdot q^* = (0, \vec{v}') \tag{2.16}$$

Where v' is another pure quaternion with the rotated vector $\vec{v}'$.

2.13.5 Euler angles

The Euler angles named in honour to Leonhard Euler (1707-1783), represent a rotation sequence to describe the orientation of a rigid body in a 3D space with respect to a reference system [102, 177]. The three rotations are also known as roll, pitch and yaw or Cardan angles . These rotations are represented by the three angles known as Alfa (α), Beta (β) and Gama (γ). There are twelve different sequences of rotations to explain the orientation of a segment with respect to a reference system. Six sequences of rotations are known as classic Euler Angles, z-x-z, x-y-x, y-z-y, z-y-z, x-z-x and y-x-y. The other six sequences of rotations are known as Tait–Bryan angles, x-y-z, y-z-x, z-x-y, x-z-y, z-y-x and y-x-z. Where x, y and z represent the rotation axes.

The Euler angles have the disadvantage of having gimbal lock, which is the loss of a degree of freedom in a 3D space. This happens when one axis of the coordinate system aligns with other axis during the rotations, producing just two axes in the system. However, Euler angles are useful when the range of motion of the segment in the three axes is less than 90 degrees [159, 178].

2.13.6 Direction cosine matrix

Similar to the quaternions and Euler angles, the direction cosine matrix represents the orientation of a rigid body in a three-dimensional space. A local reference system can be described by a global reference system using a direction cosine matrix. The study of the different limbs of the human body sometimes require the use of a global reference system to have a common frame and be able to describe one segment with respect to other. The direction cosine matrix represents a good tool to transform vectors from a local system to a global system without having issues of gimbal lock [159, 179]. However, one disadvantage of direction cosine matrix is that there are nine numbers in the matrix, which could take more time in the calculations of the rotations.

Starting with defined rotations in a specific axis, X, Y or Z, a rotational matrix can be created as shown below.

Rotation in X axis, equation (2.17):

$$R_X(\alpha) = \begin{bmatrix} 1 & 0 & 0 \\ 0 & \cos\alpha & -\sin\alpha \\ 0 & \sin\alpha & \cos\alpha \end{bmatrix} \tag{2.17}$$

Where α is the rotation angle in X axis.

Rotation in Y axis, equation (2.18):

$$R_Y(\beta) = \begin{bmatrix} \cos\beta & 0 & \sin\beta \\ 0 & 1 & 0 \\ -\sin\beta & 0 & \cos\beta \end{bmatrix} \tag{2.18}$$

Where β is the rotation angle in Y axis.

Rotation in Z axis, equation (2.19):

$$R_Z(\gamma) = \begin{bmatrix} \cos\gamma & -\sin\gamma & 0 \\ \sin\gamma & \cos\gamma & 0 \\ 0 & 0 & 1 \end{bmatrix} \tag{2.19}$$

Where γ in the rotation angle in Z axis.

Finally, the product of three rotations to get the rotation matrix for the sequence X, Y', Z'' is demonstrated below, equations (2.20) and (2.21).

$$R = R_Z(\gamma)R_Y(\beta)R_X(\alpha) \tag{2.20}$$

$$= \begin{bmatrix} \cos\beta\cos\gamma & \sin\alpha\sin\beta\cos\gamma - \cos\alpha\sin\gamma & \cos\alpha\sin\beta\cos\gamma + \sin\alpha\cos\gamma \\ \cos\beta\sin\gamma & \sin\alpha\sin\beta\sin\gamma + \cos\alpha\cos\gamma & \cos\alpha\sin\beta\sin\gamma - \sin\alpha\cos\gamma \\ -\sin\beta & \sin\alpha\cos\beta & \cos\alpha\cos\beta \end{bmatrix} \tag{2.21}$$

Where R is the rotation matrix.

2.14 Finite element method (FEM)

The finite element method (FEM) is a numerical method commonly employed to solve complex problems in science and engineering. It is a numerical technique for finding approximate solutions to partial differential equations that involves dividing the structure of interest into smaller parts or elements. The individual behaviour of the elements and their relation to each other are readily determined and based on the understanding of this, the behaviour of the complete structure can be ascertained. FEM is commonly used in cases where an analytical problem is complex and a simple solution cannot be obtained. It was initially developed for the stress analysis of aircraft structures but it has found application in a wide range of different areas, such as heat transfer, electromagnetism and fluid dynamics [180-182].

The development of new and more powerful computers has increased the range, size and complexity of applications that the finite element method can be applied to. This has led to reduced solution times and improved accuracy for complex problems. To date, FEM has had a significant influence on the development of technology in a range of different engineering fields [181].

The finite element analysis performed in the current study was undertaken in the Abaqus CAE software (Abaqus/CAE Version 6.12-2, Dassault Systèmes Simula Corp, Providence, RI). The geometry of the elbow, created from computed tomography scan (CT scan) data of a healthy subject, was segmented generating a mesh of nodes and elements connected to each other. Newton's method was then applied to solve the resulting nonlinear system of finite element equations generated by the problem. The solver is based on the equation of Hooke's law, which describes the behaviour of a spring when a force is applied, equation (2.22). This principle is used to solve the system of equations generated from the nodes and elements of the mesh.

$$\{F\} = [K]\{u\} \tag{2.22}$$

Where $\{F\}$ represents the vector force, $[K]$ is the stiffness matrix and $\{u\}$ is the displacement vector.

2.15 Imaging analysis

The evolution of technology has increased the capabilities of computer equipment enabling improvements in imaging techniques, which have resulted in the production of better quality images with higher resolution. Plain radiography (X-ray), ultrasound, computed tomography scans (CT scans) and magnetic resonance imaging (MRI) are imaging methods, which are commonly used to examine fractures of the bones and abnormalities of the soft tissue. These methods have been shown to be of great value in the accurate diagnosis of joint diseases [56, 183-185].

Plain radiography consists of the taking of images usually in two planes, the anteroposterior and lateral view. This imaging based diagnosis technique is generally straightforward and capable of providing relatively high resolution 2-D images of bone and dense tissue.

Ultrasound is a diagnostic imaging technique that is performed in real time. This method allows assessment of the soft tissue in movement but the images produced are generally lower in resolution than X-rays and CT scans [56].

2.15.1 Computed tomography scan (CT scan)

Computed tomography scans show in detail the anatomy of the joints in different planes of the human body. CT imaging systems produce a series of cross sectional images or slices, which show the geometry of the bones and soft tissue, as illustrated in the example shown in Figure 2.37. These types of images provide high resolution for identifying abnormalities, such as fractures in the articulations. Moreover, they can be used to build up accurate, detailed 3D models of the bones. Surgeons can identify more easily abnormalities in the joints with the 3D view provided by CT scans [56, 183, 185].
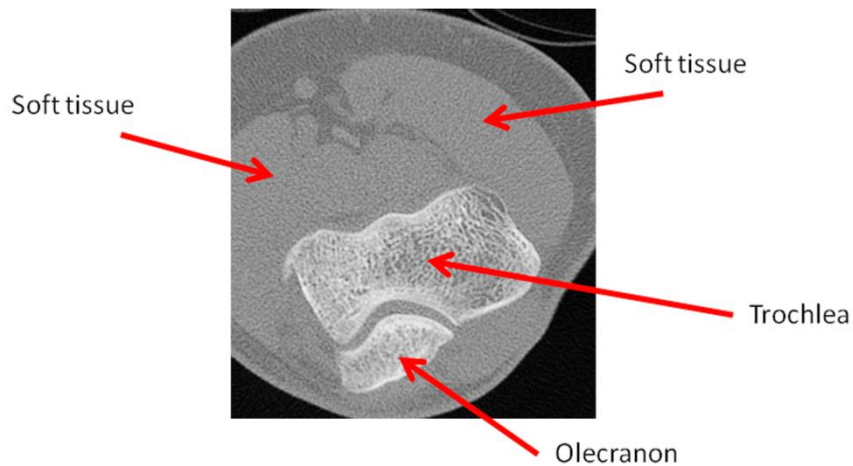
Figure 2.37 Computed tomography scan (CT scan) of the elbow joint.

2.15.2 Magnetic Resonance Imaging (MRI)

Magnetic resonance imaging (MRI) is the main method for the diagnosis of the abnormalities of soft tissue. It provides a series of images in different planes that show in detail the structure of the tissue [56, 184]. Moreover, as with CT scans, MRI shows in detail the structure of the bones. Therefore, it is possible to detect fractures of the bones and ruptures of the ligaments and tendons using this imaging technique. MRI shows in detail the structure of the veins, ligaments, arteries, tendons, muscles, fat layer, nerves, articular cartilage and bones, Figure 2.38. It uses magnetic fields and radio waves to create the images, which involves measuring the energy produced by hydrogen atoms when subjected to a strong magnetic field [56, 184, 186-187].
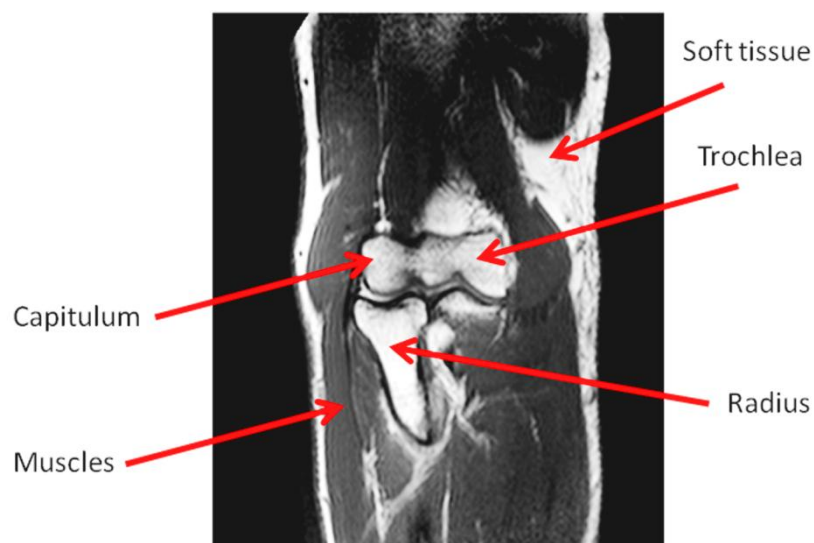
Figure 2.38 Magnetic resonance imaging (MRI) of the elbow joint.

102

This chapter presented the anatomy and biomechanics of the elbow joint with the aim of understanding the main components of the elbow and the role the elbow plays in daily life activities. Moreover, the main muscles involved in the movement of the elbow were presented to show their anatomy and function when they contract. The investigation presented in this thesis is based on the study of the anconeus muscle and the main flexor and extensor muscles of the elbow (biceps brachii and triceps brachii).

The literature presented in this chapter gives an overview of the information regarding the anconeus, biceps brachii and triceps brachii muscles. It includes the hypotheses and conclusions of previous studies about the probable function of the anconeus. Nevertheless, it is clear that none of the previous studies has given a well-justified explanation of the role of the anconeus in elbow kinematics. Furthermore, the anatomy and biomechanics of the biceps brachii and triceps brachii muscles were presented with the aim of understanding their function at the elbow. As these are the major elbow flexor and extensor muscles, their electrical activity will be compared with the anconeus activity during flexion-extension and pronation-supination movements. The electrical activity of the three muscles will be measured using surface electromyography.

Additionally, this chapter has discussed the theoretical background regarding signal processing in electromyography and inertial measurement units. In the next chapter, this background knowledge is utilised in undertaking an analysis of the movement of the elbow and myoelectric activity of the anconeus, biceps and triceps brachii. In particular, the experimental techniques discussed in this chapter are used to measure the elbow kinematics and kinetics and the muscle electrical activity, during flexion-extension and pronation-supination, in the horizontal and vertical planes.

CHAPTER THREE

3 EXPERIMENTAL STUDIES OF THE ELBOW JOINT: A KINEMATIC, KINETIC AND ELECTROMYOGRAPHIC ANALYSIS

3.1 Introduction

The anconeus, a small penniform muscle located in the posterolateral part of the elbow, has been the subject of debate concerning the role it plays in human elbow kinematics. Its anatomy and function have been studied since 1867 when Duchenne suggested that the muscle was involved in extension and abduction of the ulna [1]. Since then, the anconeus has been studied with the purpose of clarifying the role it plays in human elbow kinematics.

Several studies have reported that the greatest activity of the anconeus appears during elbow extension suggesting that it could be an extensor muscle of the elbow [22-27, 40]. Other studies concluded that the anconeus is an abductor of the ulna during pronation motion [29-30]. Furthermore, it has been mentioned that the anconeus could be an elbow stabiliser [22-23, 31-33]. It is evident from these and more recent studies that agreement has not yet been reached about the precise function of the anconeus.

Some surgeons view this muscle as unimportant and it is frequently denervated during surgical approaches to the elbow [2]. Moreover, the anconeus has been harvested as a local flap for the treatment of conditions around the elbow [3-9, 11-12].

This chapter presents the methodology, analysis and results of an investigation into electrical muscle activity (anconeus, biceps and triceps brachii) and elbow kinematics and kinetics with the aim of clarifying the specific function of the anconeus. Surface electromyography was applied, in conjunction with 3D inertial motion sensors, to relate the electrical activity of the muscles to the kinematics and kinetics of the elbow.

3.2   Methods and materials

The approach taken in this study consisted of examining and relating the data obtained from surface electromyography (EMG) and 3D inertial motion sensors (IMUs) during elbow movement trials on subjects in order to clarify the behaviour of the anconeus muscle during the various motions investigated. The data obtained during the trials on the participants was subsequently normalised and averaged to facilitate comparison and analysis of the results. The data was then analysed retrospectively so that anconeus behaviour could be compared to that of the biceps brachii and triceps brachii.

3.2.1   Participants and anthropometric data

Thirteen right-handed healthy volunteers, 8 men and 5 women, took part in this research. The number of participants included in this study was obtained with a confidence interval of 90% and an expected standard deviation of 10% [188]. A requirement for inclusion in the study was that the volunteers had no history of neuromuscular or musculoskeletal impairment. The mean and standard deviation (SD) of the participant anthropometric data are shown in Table 3.1. The forearm length was measured from the head of the radius to the radial styloid process [85]. All trials were evaluated on the dominant hand. The protocol was approved by the Ethics Committee of The University of Manchester (approval number 11335, Appendix II) and informed consent was obtained from all the participants.

Table 3.1 Anthropometric data; the forearm length was measured from the head of the radius to the radial styloid process.

MEASUREMENT	MEAN	SD
Height [m]	1.696	0.098
Forearm Length [m]	0.234	0.014
Mass [kg]	68.538	9.640
Age [years]	29.154	1.994

3.2.2 Equipment

3.2.2.1 Electromyography

The electrical activity of the muscles was recorded using surface electromyography (BTS Pocket EMG, BTS Bioengineering, Milan, Italy) with a sample frequency of 2 kHz. BTS Pocket EMG is a non-invasive medical device used to measure the electrical activity of muscles near to the skin surface, Figure 3.1. The skin was shaved and cleaned with 70% isopropyl alcohol. Subsequently, self-adhesive bipolar paediatric silver/silver chloride electrodes (Ag/AgCl) were positioned over the mid-point of the anconeus, triceps brachii and biceps brachii to measure the depolarization.

The mid-point of each muscle was found by palpation using the bony landmarks of the upper limb [90]. The electrodes were attached with approximately 25 mm between the centres. A reference electrode was placed on the styloid process of the ulna.

Figure 3.1 Pocket EMG medical device used to measure the electrical activity of the muscles near to the skin.

3.2.2.2 Inertial measurement units

The movements were recorded using 3D wireless Inertial Measurement Units (IMUs) with an acquisition frequency of 75 Hz. The IMUs combine tri-axial

accelerometers, gyroscopes, and magnetometers in a single sensing unit. Figure 3.2 illustrates 6 inertial measurement units plugged in the Awinda station [159]. Several studies have suggested that the use of IMUs is a reliable way to measure human body motion [160, 169-170].

Figure 3.2 Six inertial measurement units docked in an Awinda station; they were used to measure the elbow kinematics.

The wireless motion tracking devices (MTw) are micro-electro-mechanical systems with miniature components, like accelerometers, gyroscopes, magnetometers and a barometer. These units measure the orientation of a segment and provide its velocity and acceleration in real time. The size of these devices is less than 60 millimetres and weighs less than 27 grams [159]. These dimensions made them useful as tracking sensors of the human body without discomfort. Figure 3.3 displays the drawing with its dimensions of a wireless motion-tracking unit.

The data collected from these units is sent it to the Awinda station and then saved on the workstation (computer). The Awinda station has the capacity of data transmission up to 50 metres indoors and outdoors. An advantage of these devices is that the data can be observed in real time and an analysis of the movements can be obtained. Moreover, the inertial motion units or wireless motion tracking devices have several applications in biomechanics, sport, rehabilitation, virtual reality, animation and motion capture [159].
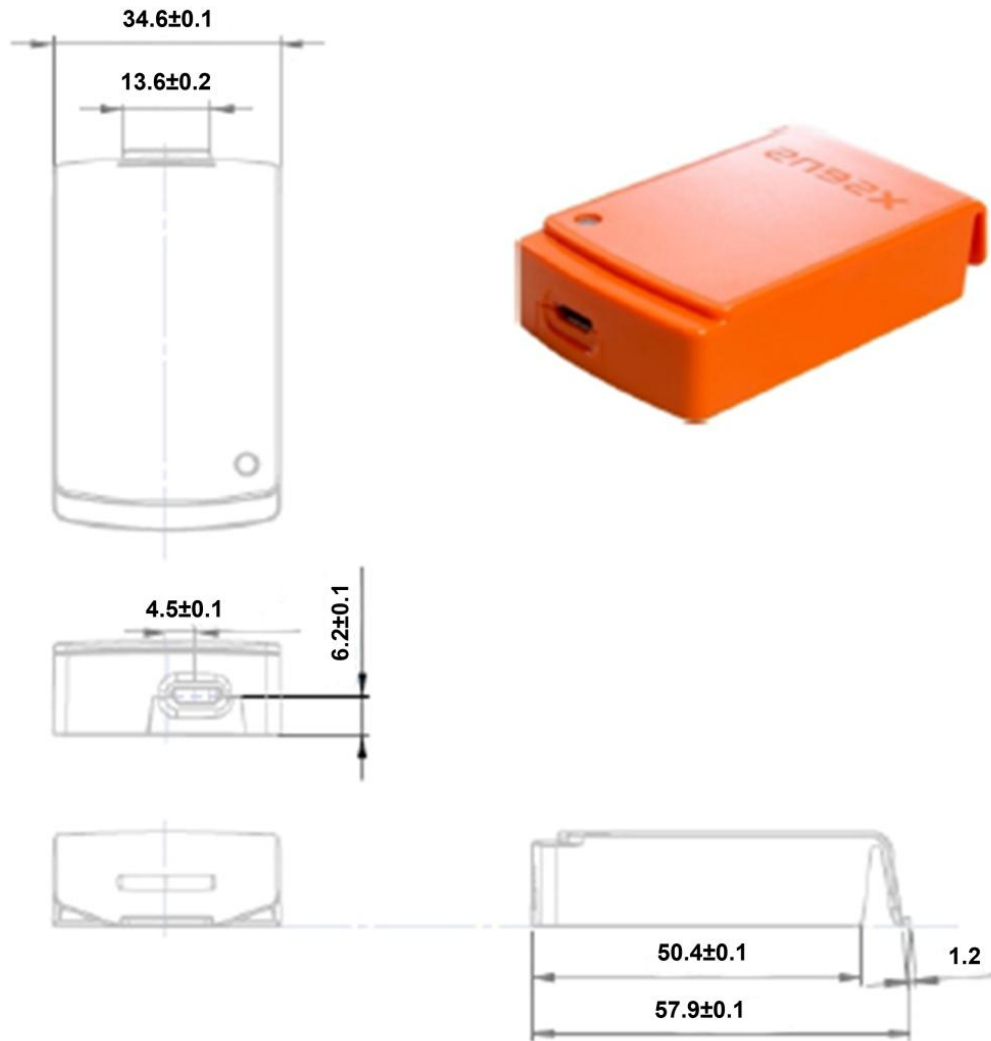
Figure 3.3 Drawing of a wireless motion-tracking unit; the dimensions are in millimetres [159].

To estimate the kinematics and kinetics of the joint, three MTw IMU sensors (Xsens Technologies, Enschede, Netherlands) were attached to the participant. The first IMU was fixed on the sternum, immediately below the sternal notch (IMU1). The second was at the midpoint between the acromion of scapula and the head of the radius on the lateral side of the arm (IMU2) and the third was placed on the posterior part of the wrist between the ulnar and radial styloid processes (IMU3), as illustrated in Figure 3.4. These sensors were fastened to the body using manufacturer supplied click-in straps and hypoallergenic double sided tape to allow free motion without discomfort to the participants.
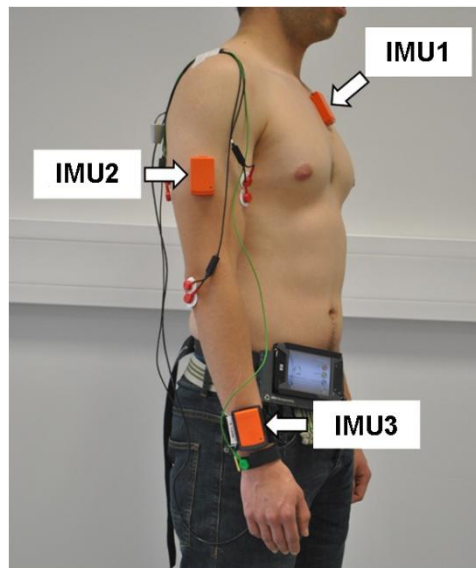
Figure 3.4 Participant preparation: electrodes and inertial measurement units (IMUs) were attached to the right upper limb and trunk.

3.2.3 Reference system calibration

The elbow kinematics was analysed using two coordinate systems. The first one is the global coordinate system (G) created from the magnetic north of the earth. The X-axis of the global system points to the magnetic north of the earth, the Z-axis points away of the centre of gravity (vertically to the ground), and the Y-axis is the result of the cross product of X and Z axes following the right hand rule. The second one is the local coordinate system of the sensor (S). The coordinate systems of the IMUs were calibrated with the global coordinate system. The local x-axis of the sensor was pointing to the magnetic north of the earth, as shown in Figure 3.5.

Furthermore, the local z-axis of the sensor was aligned vertically with the global Z-axis. Therefore, the orientation of the sensors is referenced with the global system. However, the raw data (acceleration, angular velocity, magnetic field and pressure) from the sensors are referenced with the local system of the sensor [159]. In order to calculate relative movements among the sensors, it is necessary to rotate the raw data into the global coordinate system using quaternions, as was explained in chapter two [175].
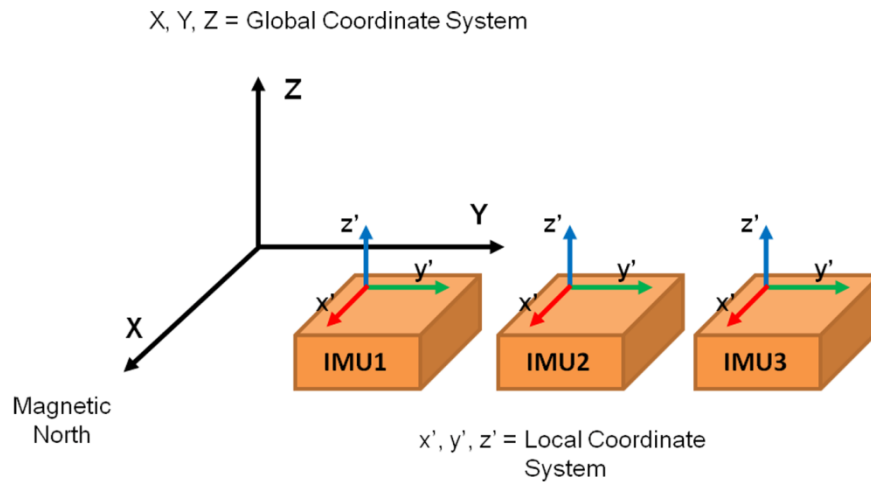
Figure 3.5 Calibration of the inertial sensor according to the Global coordinate system of the earth.

3.2.4 Motions

The participants performed the four following movements in different postures enabling the function of the anconeus to be investigated by analysing the results from the trials whilst taking into account the effect of gravity on elbow torque during the motions, Figure 3.6:

a) Flexion-extension with the shoulder abducted 90 degrees (horizontal plane),

b) Flexion-extension with the elbow close to the trunk (sagittal plane),

c) Flexion-extension with the spine bent forward 90 degrees (sagittal plane), the arm aligned in the horizontal plane, and

d) Supination-pronation with the elbow flexed 90 degrees.
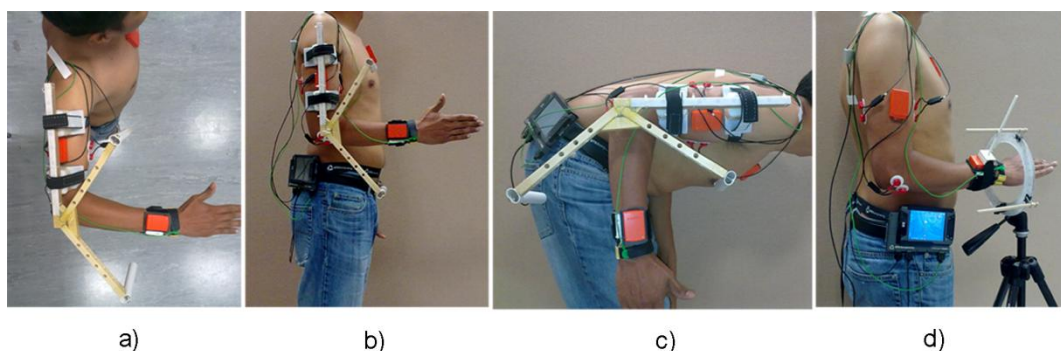
Figure 3.6 Movements of the elbow joint: a) flexion-extension in the horizontal plane, the shoulder abducted 90 degrees; b) flexion-extension in a sagittal plane, the elbow close to the trunk; c) flexion-extension in a sagittal plane, the spine bent forward 90 degrees and the arm placed horizontally to the ground; d) supination-pronation with the elbow flexed 90 degrees.

The range of motion for flexion-extension was constrained to 90 degrees by an adjustable custom-made frame (mass 196 grams) made of wood to eliminate any local magnetic interference with the IMU magnetometers, Figure 3.7a. The frame was designed to limit the flexion-extension movement to 90° by this reason the internal angle of the frame was more than 90°. Supination-pronation was constrained to the same range by a custom-made Perspex ring illustrated in Figure 3.7b. The frame used to constrain the flexion-extension movement was attached to the lateral side of the arm.

The participants performed the trials through the active range of motion limited by the frames, beginning with the elbow extended for flexion-extension and with the forearm pronated for supination-pronation movement. In order to have an anatomical reference point for flexion-extension, the forearm was placed in a neutral position with the thumb pointing up.

a)   b)
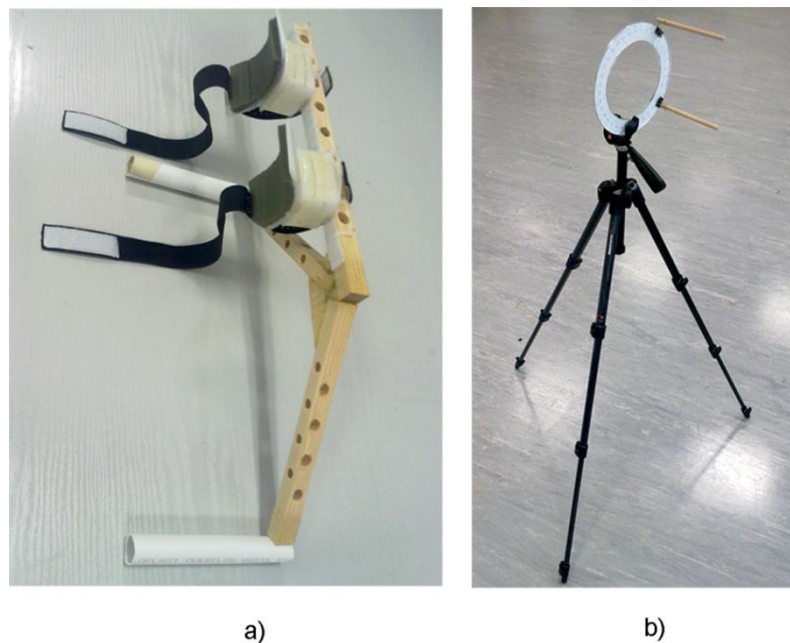
Figure 3.7 Frames to constrain the movements: a) adjustable custom-made frame made of wood used to constrain the flexion-extension motion and b) adjustable custom-made Perspex ring utilised to limit the supination-pronation movement.

3.2.5 Procedure

Three maximum voluntary contractions (MVC) of the anconeus, triceps brachii and biceps brachii were evaluated during a sustained maximal isometric contraction over

111

6 seconds (Appendix III). The root mean square (RMS) value of every contraction was calculated within a window of 1.5 seconds, as illustrated in Figure 3.8.

Each volunteer was asked verbally to perform three MVC trials and there were two minutes of rest between every trial to avoid muscular fatigue. The maximum RMS values of the MVC of each muscle were used to normalise the EMG signal during the four motions.
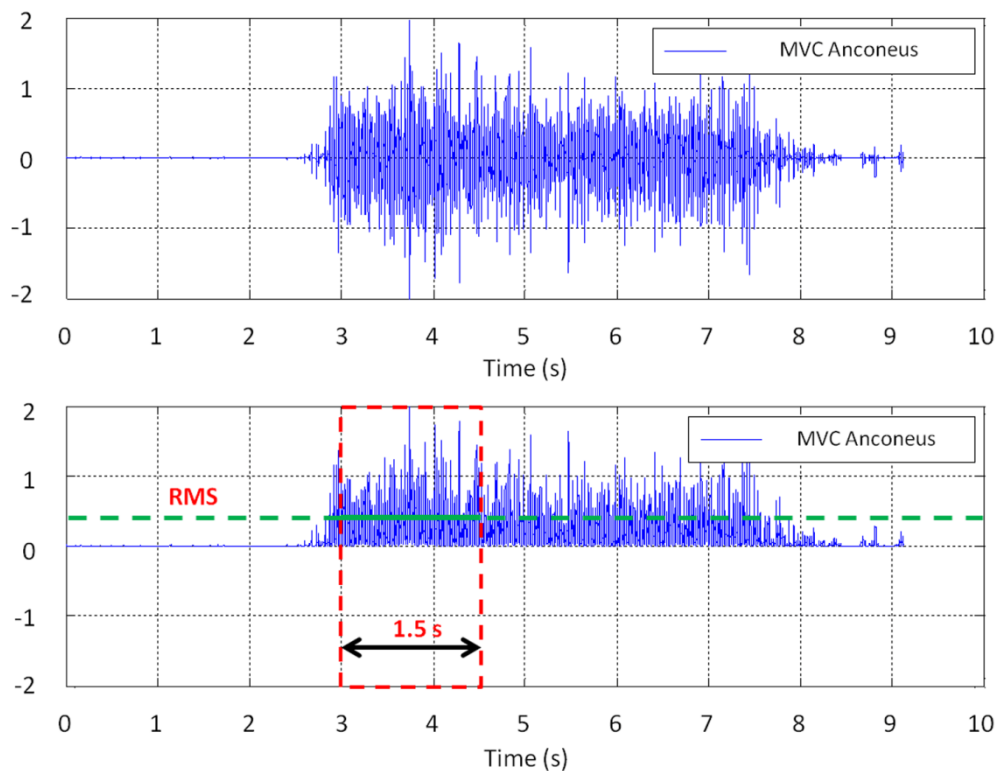
Figure 3.8 Root mean square value of the maximum voluntary contraction of anconeus muscle.

Each flexion-extension trial consisted of 5 cycles over a period of approximately 28 seconds paced using a metronome. Timing was indicated to the participant by four beeps for each cycle (one beep per second). The first and second beeps were to start and stop the flexion motion, respectively. Subsequently, the third and fourth beeps were to start and stop the extension movement, as shown in Figure 3.9.

The supination-pronation motion followed the same procedure with participants asked to perform the motion pointing at a fixed marker with the middle finger [30].

All participants performed three trials of 5 cycles for each motion, making a total of fifteen cycles. Visualisation of the Euler angles of the arm sensor, in real time during the tests, was used as feedback to check the correct posture of the elbow in the participants. When the participants were not able to maintain the correct posture, they repeated the trial.

Furthermore, two minutes of rest were given to the volunteers to help them to relax and maintain the posture in every test. The fifteen cycles were averaged and the time was normalised from zero to 100% of the movement time. In addition, the participants were trained prior to the tests by completing two practice trials to get used to the sound of the metronome and perfect the timing of the movements.
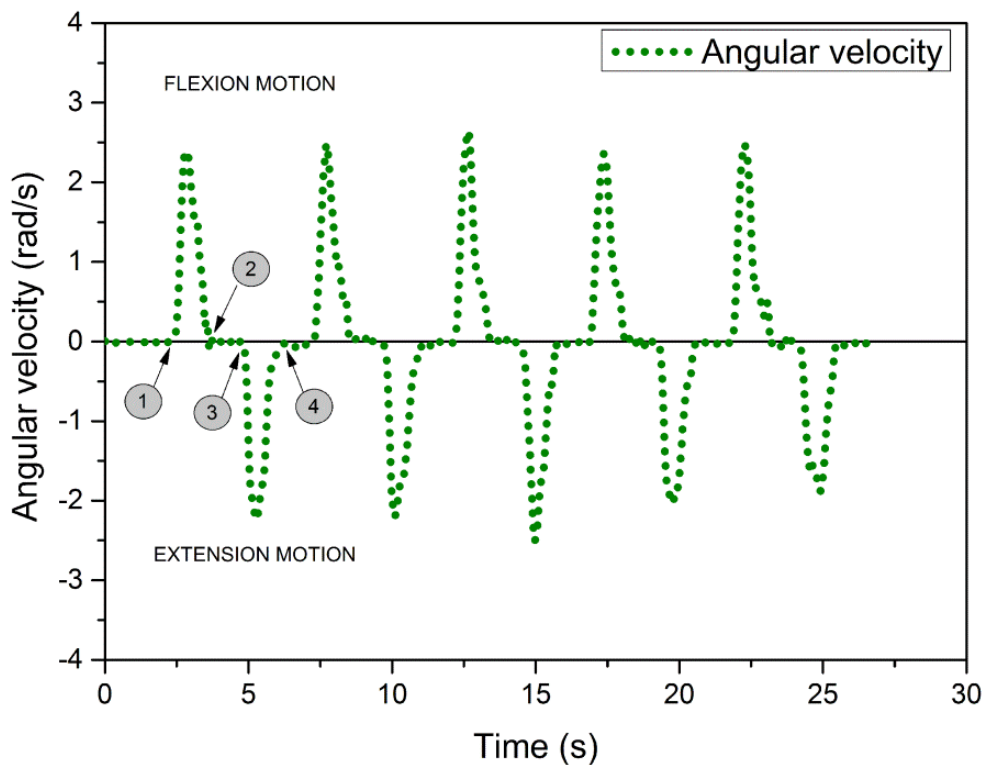
Figure 3.9 Five cycles performed during a flexion-extension trial. The circled numbers 1, 2, 3 and 4 represent the stages of the first cycle.

3.2.6 Data processing

Electromyography

The raw EMG signal was normalised using the RMS value of the MVC and then it was filtered with a 2-pole Butterworth band-pass filter (roll-off 40dB/decade) with

cut-off frequencies of 5 Hz and 600 Hz, which removed the movement artefact [153]. Subsequently, the signals of the three muscles were rectified and filtered with a 2-pole Butterworth low pass filter, (roll-off 40dB/decade) with a cut-off frequency of 6 Hz to obtain the EMG envelope [85], which gives a better idea of the timing and activation level of the muscle.

Filter Design

The filter design for the myoelectric activity was performed according to the attenuation of the output signal and the spectrum frequency. Assuming that the attenuation at cut-off frequencies is fixed at -3dB (half the pass band power), the equations (3.1) to (3.3) explain how to calculate the percentage of the output signal using the attenuation outcomes from different cut-off frequencies.

$$A_{dB} = 20\log\left(\frac{V_{out}}{V_{in}}\right) \tag{3.1}$$

$$\text{Where } \left(\frac{V_{out}}{V_{in}}\right) \leq 1 \tag{3.2}$$

Where A_{dB} is the attenuation signal in decibels (dB), V_{out} is the output signal in millivolts (mV) and V_{in} is the input signal in mV.

It was assumed that the input signal V_{in} represents 100% in order to facilitate the analysis and calculation. Simplifying equation (3.1) it is possible to calculate the percentage of the output signal, as demonstrated in equation (3.3).

$$V_{out} \ [\%] = 100\% \times \left[10^{\wedge}\left(\frac{A_{dB}}{20}\right)\right]^2 \tag{3.3}$$

Table 3.2 shows an example of this calculation for a Butterworth band pass filter with cut-off frequencies of 5-600 Hz, second order; the attenuation values were obtained from the MATLAB filter design tool. It is clear to observe from Table 3.2 that the frequencies 5 and 600 Hz have the attenuation of approximately 50% of the signal.

114

Table 3.2 Calculation of the output signal; the attenuation values were obtained from Matlab filter design and analysis tool.

Band-Pass Filter [5-600Hz]		
Frequency	Attenuation	Output signal
Hz	dB	%
1	-14.2	3.802
5	-3	50.119
6	-2.3	58.884
10	-0.9	81.283
20	-0.22	95.060
100	0	100.000
500	-1.8	66.069
600	-3	50.119
700	-4.8	33.113
800	-7.8	16.596
900	-13.5	4.467
1000	-72	0.000

From Figure 3.10 it is clear that the Butterworth band pass filter, with cut-off frequencies of 5-600 Hz, had less effect on the output signal. Conversely, the Butterworth band pass filter with cut-off frequencies of 20-500 Hz had a major effect on the activity. The percentage of the output signal represents how much the myoelectric activity is attenuated by different cut-off frequencies. The cut-off frequencies in Figure 3.10 were selected because the frequencies of the electrical activity stay among those values (0-500Hz approximately).
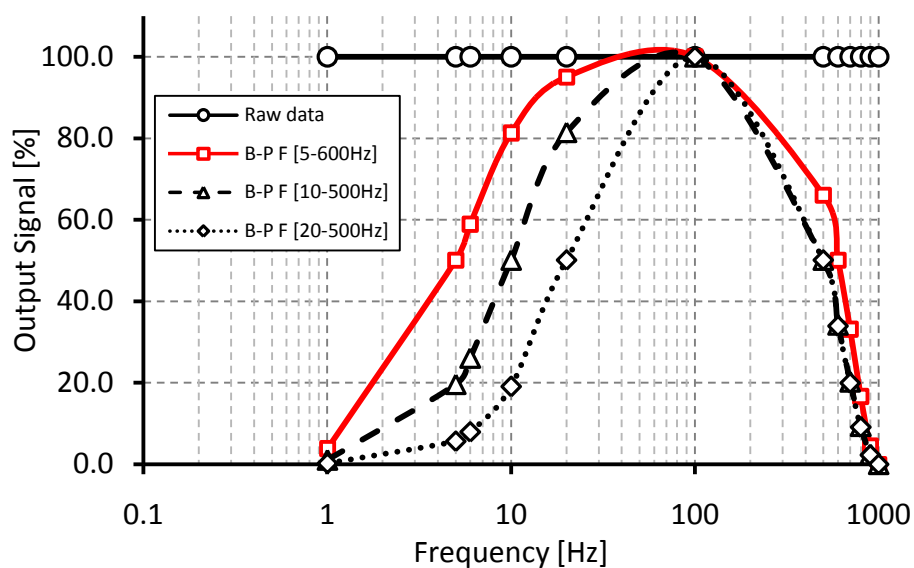
Figure 3.10 Filter design for the myoelectric activity. The cut-off frequencies have a different effect on the signal. B-P F means Band-Pass Filter.

In addition, the analysis of the power spectrum density of the electrical signals provided the major and minor frequencies of the myoelectric activity. The spectrum frequency was calculated in MATLAB software using Fast Fourier Transformations. The Butterworth band pass filter attenuated frequencies below 5 Hz and higher than 600 Hz, in order to try to keep as much of the muscle activity as possible. The power spectrum density (PSD) in Figure 3.11 shows the frequency spectrum of anconeus, triceps and biceps brachii during sagittal flexion-extension movements with the spine bent forward 90 degrees. Figure 3.11a shows the raw data before applying the Butterworth band pass filter and Figure 3.11b after filtering. The cut-off frequencies were 5 and 600 Hz.
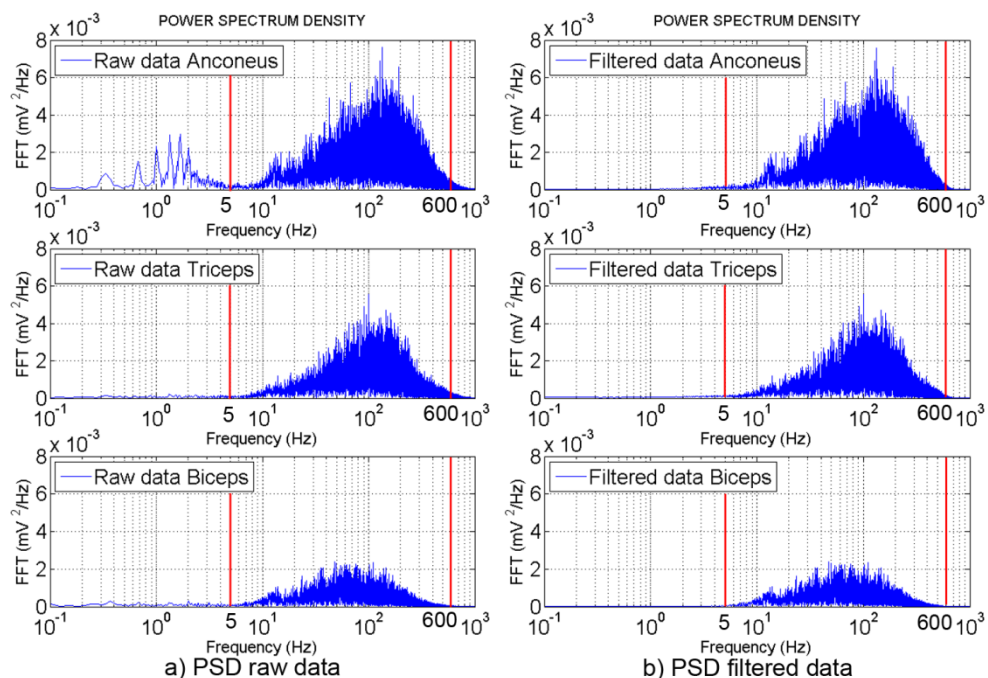
Figure 3.11 Power spectrum density of anconeus, triceps and biceps brachii before and after filtering with a Butterworth band pass filter, 5 Hz and 600 Hz.

An analysis of the RMS values of the muscle electrical activity for all movements was performed in order to determine the effect of the filters on the amplitude of the electrical activity. Figure 3.12 indicates that a Butterworth band pass filter with cut-off frequencies of 5 Hz and 600 Hz attenuated the signals less than 2% in relation to the raw data. However, a Butterworth band pass filter with cut-off frequencies of 20 Hz and 500 Hz affected the signals by more than 10% in some cases, Figure 3.12.

From the frequency analysis, it is known that the muscle activity in the frequency domain contains frequencies below 400-500 Hz [134]. Therefore, a Butterworth band pass filter with cut-off frequencies of 5 Hz and 600 Hz seems to attenuate less muscle activity.
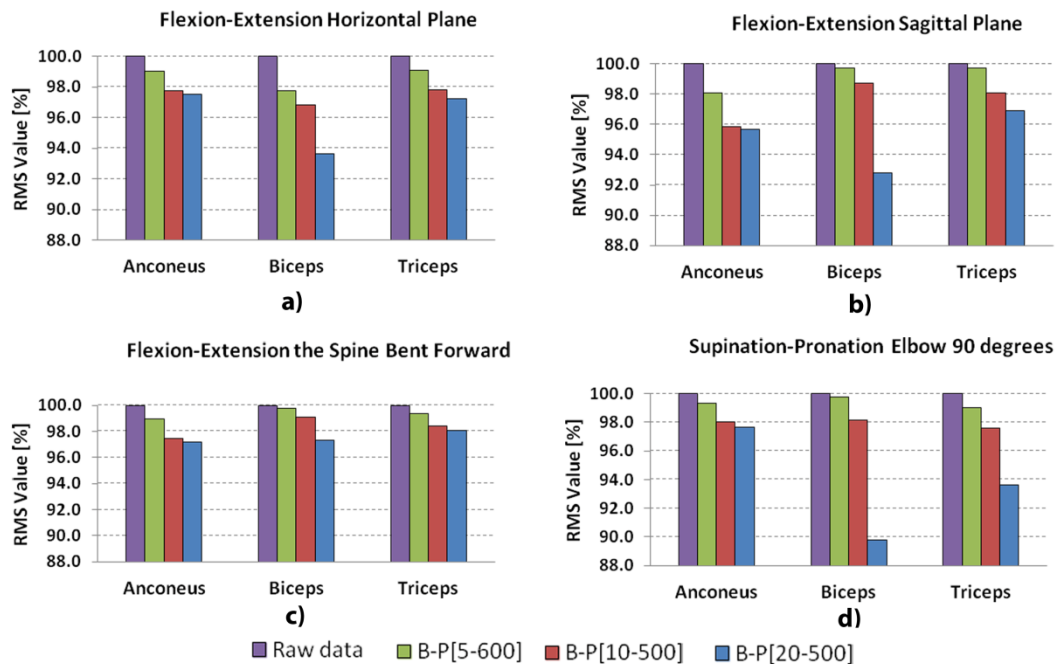
Figure 3.12 Filter analysis: Butterworth band pass filter with cut-off frequencies of 5 Hz and 600 Hz attenuated the electrical activity less than 2% in relation with the raw data.

Once the filter design was performed in the base of the spectrum frequency and the attenuation of the electrical signals, the signal processing of the myoelectric activity was carried out. The data of all the participants were analysed and processed in the same way.

The whole procedure of the signal processing from the raw data to the linear envelope is illustrated in Figure 3.13. The raw data of anconeus activity taken during a flexion-extension trial in the horizontal plane with the shoulder abducted 90 degrees is presented in Figure 3.13a. Subsequently, Figure 3.13b shows the filtered and the normalised activity of anconeus muscle (Butterworth band pass filter of 5-600 Hz). Finally, Figure 3.13c and Figure 3.13d illustrate the rectified activity and the linear envelope of anconeus obtained with a low pass filter with cut-off frequency of 6 Hz [85]. The same analysis was performed for all movements.
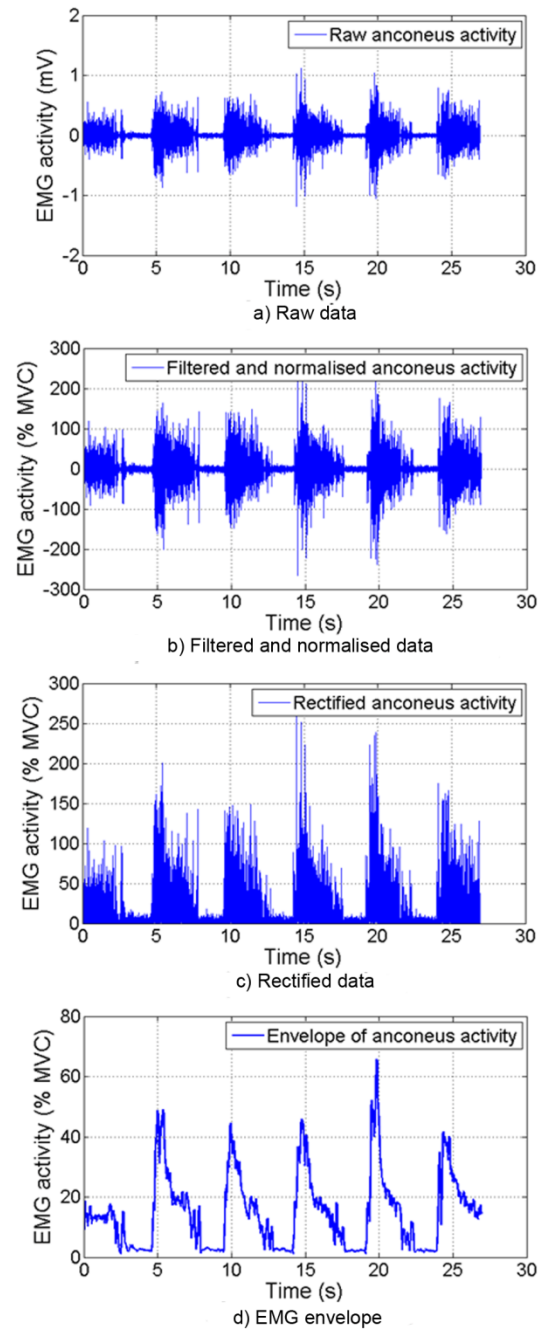
Figure 3.13 Signal processing: a) Raw data of anconeus; b) Filtered and normalised activity with the RMS of the MVC; c) Rectified data; and d) EMG envelope.

Kinematics and kinetics of the elbow

The linear acceleration and angular velocity data from the IMUs were filtered using a 2-pole Butterworth low pass filter (roll-off 40dB/decade) with a cut-off frequency of 2 Hz before calculating the net torque and power. The cut-off frequency applied to the raw data was calculated from a power spectrum analysis of the angular velocity,

as shown in Figure 3.14. All filters were zero-lag digital filters implemented using the MATLAB "filtfilt" function.

Figure 3.14a displays the frequency spectrum of the angular velocity, before and after filtering with Butterworth low pass filter, with a cut-off frequency of 2 Hz. This cut-off frequency was chosen due to an analysis of the spectrum frequency; it was obvious that most of the frequency data of the angular velocity was concentrated below 2 Hz. Furthermore, from the analysis of the movements, it was determined that the frequency of motion of the forearm was approximately 0.5 Hz. Figure 3.14b illustrates five cycles of the angular velocity of the elbow before and after applying the Butterworth low pass filter.
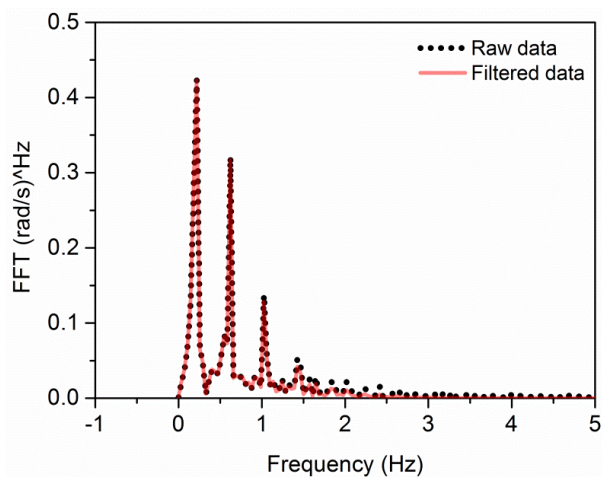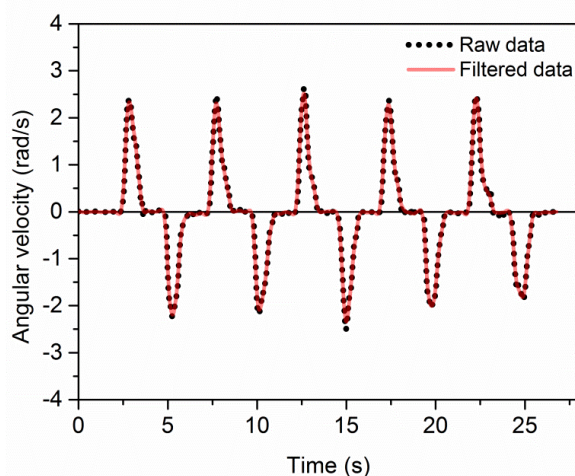
Figure 3.14 Power spectrum density of the angular velocity before and after applying a Butterworth low pass filter with a cut-off frequency of 2 Hz. a) spectrum frequency and b) angular velocity before and after filtering.

119

The net torque and power were important parameters for describing the muscle behaviour during the motion of the joint. They were calculated using equations (3.4) and (3.5) below, respectively. IMU and EMG data were synchronised using an external trigger. The percentage of the Maximum Voluntary Contraction (% MVC) of each muscle was analysed in relation to the net torque and power of the joint.

When the net torque and power were positive, it indicated flexor torque and concentric contraction of the muscles, respectively. Conversely, when the net torque and power were negative, this represented extensor torque and eccentric contraction, correspondingly [88].

The mass moment of inertia for flexion-extension was calculated using Dempster's parameters [85-86] and for supination-pronation data from Zatsiorsky [87]. The data processing was performed in MATLAB version 7.10.0.499 (R2010a).

$$\vec{T} = [I] \times \vec{\alpha} \qquad (3.4)$$

$$P = \vec{T} \cdot \vec{\omega} \qquad (3.5)$$

Where $\vec{T}$ is the net torque of the joint [Nm], I is the mass moment of inertia of the forearm-hand segment [kgm^2], $\vec{\alpha}$ is the angular acceleration of the segment [rad/s^2], P is the net power of the joint [W] and $\vec{\omega}$ is the angular velocity of the elbow [rad/s].

3.3   Results

Plots of the mean relative angular velocity, net joint torque, net joint power and the normalised EMG activity of the three muscles over one cycle during the motions are shown in Figures 5.15-5.18. These plots are explained below.

3.3.1   Flexion-extension in the horizontal plane

In horizontal flexion-extension movements (Figure 3.6a), gravity had minimal effect on the elbow kinematics because the gravity vector was perpendicular to the principal plane of motion. Consequently, the joint motion was a result of only muscle

activity. Figure 3.15a shows the relative angular velocity of the joint in the horizontal plane where positive values indicate flexion and negative values represent extension motion. Figure 3.15c shows the relative electrical activity of the anconeus in the horizontal flexion-extension movements and indicates that muscle activation was greater during extension.
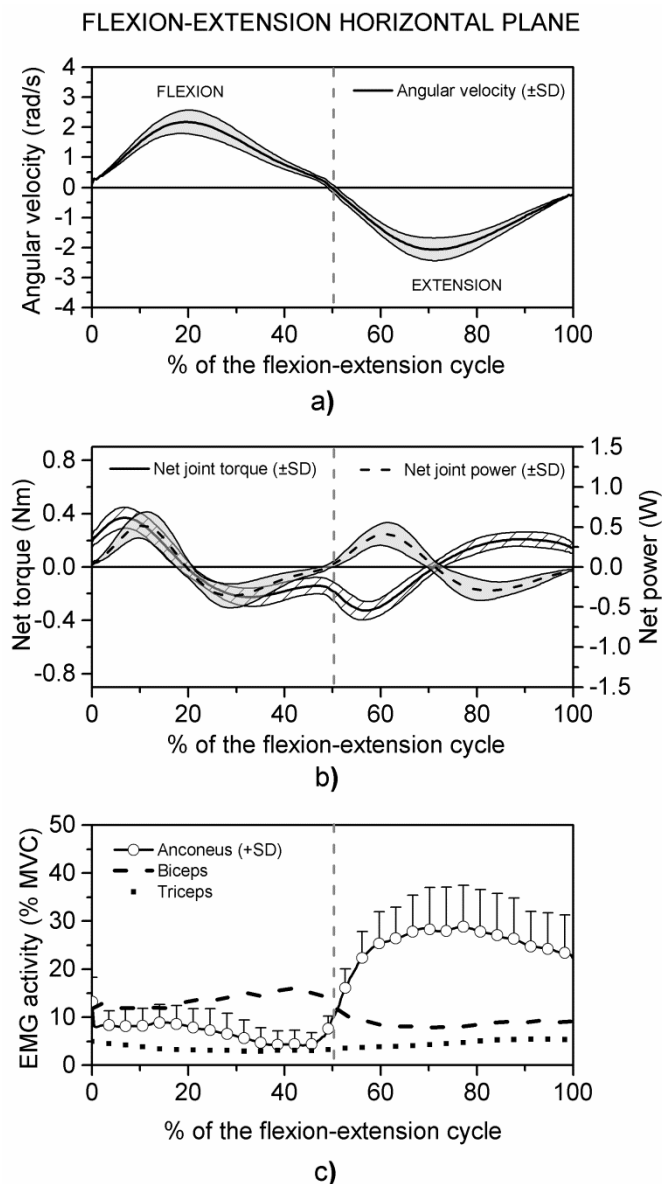
Figure 3.15 Flexion-extension in the horizontal plane, the shoulder abducted 90 degrees. Mean and standard deviation of a) the relative angular velocity of the elbow, b) net joint torque and power and c) the relative EMG activity of anconeus, biceps brachii and triceps brachii normalised with the maximum voluntary contraction (MVC). The increase in activity of anconeus was higher during extension between 46% and 60% of the cycle when the net torque was negative (extensor muscles were dominant) and net power was positive (concentric contraction), which suggests anconeus was acting as an elbow extensor muscle.

An increase in the activity of the anconeus muscle appeared at 46% of the cycle just before the angular velocity changed from positive to negative at 50% of the movement cycle. The anconeus activity increased from 9.9 ± 3.4% MVC to 28.2 ± 8.7% MVC between 50% and 70% of the flexion-extension cycle when the net torque was negative (extensor muscles were dominant) and the net power was positive (concentric contraction), which suggests that the anconeus was acting as an elbow extensor muscle (Figure 3.15b).

The maximum muscle activity of the anconeus was 28.8 ± 8.7% MVC at 77% of the flexion-extension cycle. The biceps brachii was active during flexion and triceps brachii was active during extension.

3.3.2   Flexion-extension in a sagittal plane

In sagittal plane flexion-extension movements (Figure 3.6b), gravity played a major role in elbow kinematics because the gravity vector was parallel to the main plane of motion. As a result, gravity exerted an extensor torque throughout the movement that assisted the extensor muscles. Conversely, the flexor muscles had to work against gravity in addition to producing joint torques.

Figure 3.16a shows the relative angular velocity of the joint in a sagittal plane and Figure 3.16c illustrates the relative electrical activity of anconeus, biceps brachii and triceps brachii muscles in a sagittal plane flexion-extension movement. The relative activity of the anconeus muscle increased from 5.4 ± 2% MVC to 10.6 ± 3.7% MVC between 50% and 63% of the cycle, again indicating that it was playing a role as an elbow extensor muscle.

However, the relative activity levels were lower than in the horizontal flexion-extension movements as, in this case, gravity was producing an extensor torque about the elbow which assisted extension. Moreover, the triceps brachii (the main agonist muscle during extension) showed minimal activity of 1.5% MVC throughout the extension motion, which implies that gravity was mainly responsible for extending the elbow joint.

FLEXION-EXTENSION SAGITTAL PLANE

a)

b)

c)
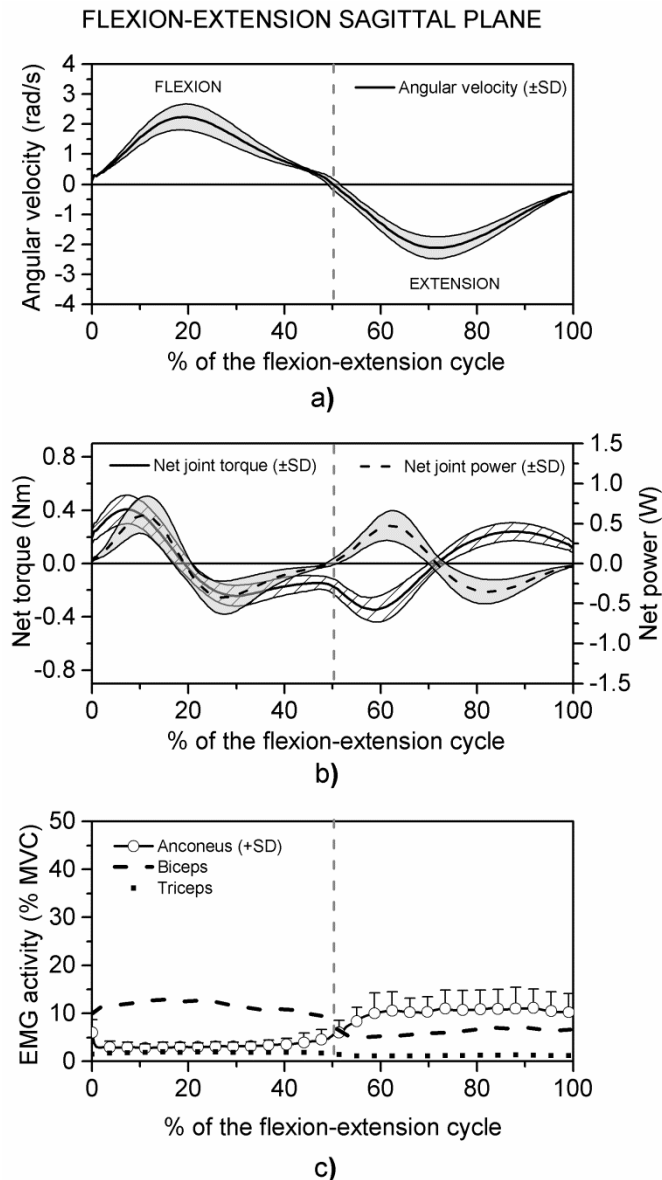
Figure 3.16 Flexion-extension in a sagittal plane, elbow close to the trunk. Mean and standard deviation of a) the relative angular velocity of the elbow, b) net joint torque and power and c) the relative EMG signal of anconeus, biceps brachii and triceps brachii normalised with the maximum voluntary contraction (MVC). The reduction of the relative electrical activity of anconeus during extension implies that gravity assisted anconeus.

3.3.3 Flexion-extension with the spine bent forward 90 degrees

Flexion and extension movements in a sagittal plane with the spine bent forward 90 degrees (Figure 3.6c) were also affected by gravity because the gravitational acceleration vector was again parallel to the plane of motion. However, in this case, gravity produced both flexor and extensor torques during different parts of the movement. The relative electrical activity of the anconeus, shown in Figure 3.17c, demonstrates that the muscle behaves as an extensor muscle. That is, the anconeus

123

was more active in early flexion (12.4 ± 4% MVC) when gravity was providing a flexor torque and was less active (4.5 ± 2.6% MVC) when gravity provided an extensor torque, as illustrated in Figure 3.17c.

FLEXION-EXTENSION SPINE BENT FORWARD
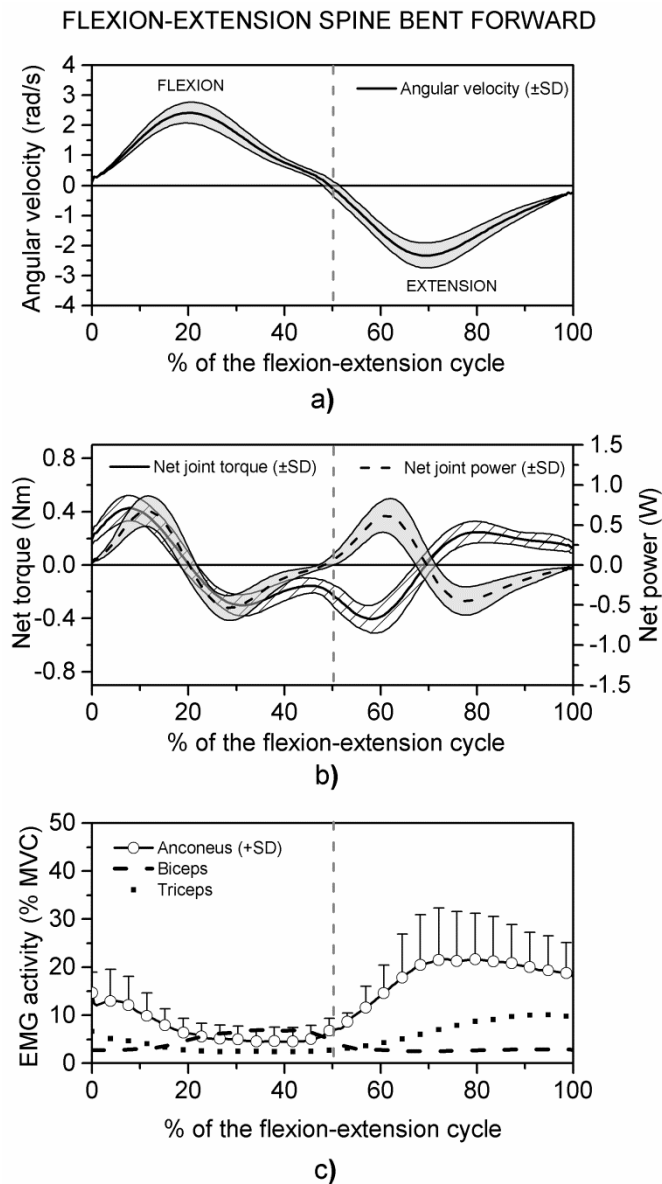
Figure 3.17 Flexion-extension in a sagittal plane, the spine bent forward 90 degrees and the arm placed horizontally to the ground. Mean and standard deviation of a) the relative angular velocity of the elbow, b) net joint torque and power and c) the relative EMG activity of anconeus, biceps brachii and triceps brachii normalised with the maximum voluntary contraction (MVC). The relative electrical activity of anconeus suggests that this muscle behaves as an extensor muscle because its activity increased when gravity provided a flexor torque in early flexion and decreased when gravity provided an extensor torque in late flexion.

Furthermore, in early extension, the activity of anconeus increased from 7 ± 2.6% MVC to 21.5 ± 10.8% MVC between 50% and 72% of the cycle, which suggests that

anconeus behaved as an extensor muscle. Similarly, the activity of both biceps and triceps brachii were modulated as expected by the effect of gravity, Figure 3.17c.

3.3.4   Supination-pronation with the elbow flexed 90 degrees

In supination-pronation movements with the elbow flexed 90 degrees (Figure 3.6d), gravity had a minimum effect on elbow kinematics because the angular velocity vector during axial rotation of the forearm was perpendicular to the gravity vector. Figure 3.18 shows the relative angular velocity, net torque, power and muscle EMG.
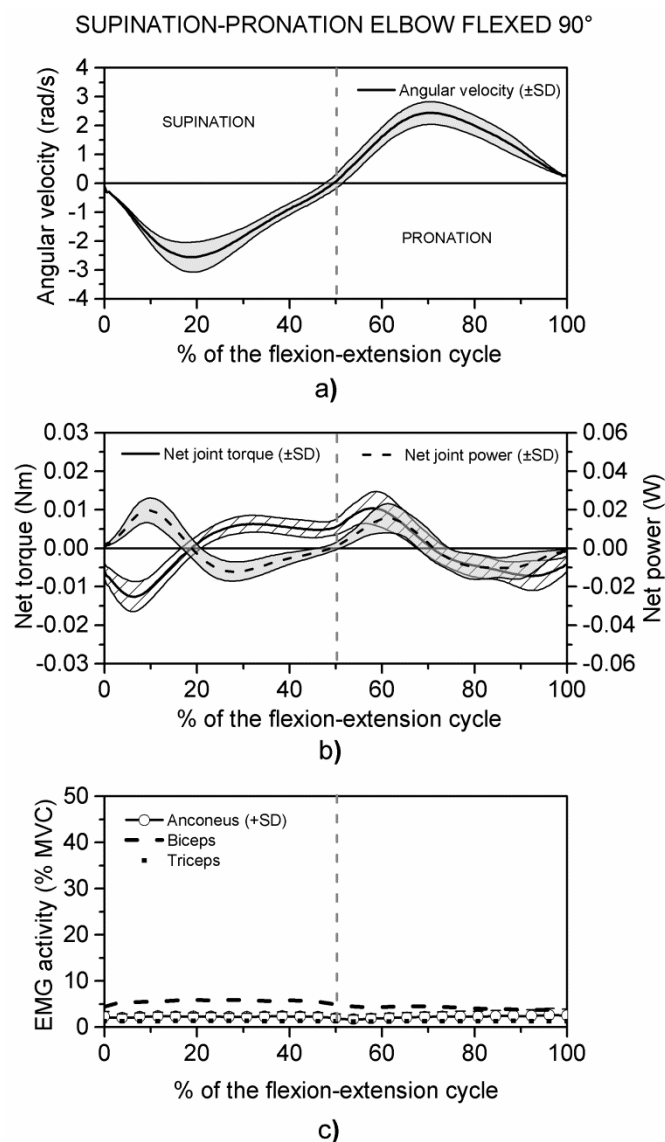
Figure 3.18 Supination-pronation with the elbow flexed 90 degrees. Mean and standard deviation of a) the relative angular velocity of the elbow, b) net joint torque and power and c) the relative EMG activity of anconeus, biceps brachii and triceps brachii normalised with the maximum voluntary contraction (MVC).

125

The joint motion was a result of only muscle activity because the gravity vector was perpendicular to the rotational axis of the forearm. There was no relative electrical activity of the anconeus muscle and triceps brachii during supination and pronation movements, indicating no contribution to the rotation of the forearm, Figure 3.18c. Furthermore, the relative EMG activity of biceps brachii was slightly elevated during supination.

3.4   Discussion

This study was designed to investigate the activity of the anconeus muscle during normal movement of the elbow and hence infer the probable function of the muscle. The relative electrical activity of the anconeus, triceps and biceps brachii muscles, in combination with the kinematics and kinetics of the elbow joint, provides evidence that indicates that the anconeus is an elbow extensor muscle.

In horizontal flexion-extension movements, the anconeus is most active during early extension when the net torque is negative (extensor muscles are dominant) and the net power is positive (concentric contraction), implying that the anconeus has an active role in extension. This concurs with previous observations reported by other researchers [22-25, 31].

In sagittal plane flexion-extension movements while standing, the relative amplitude of the EMG activity of the extensor muscles was reduced when gravity exerted an extensor torque, especially the triceps brachii. Here, it is clear that gravity assisted the function of anconeus because its electrical activity was reduced in the sagittal plane extension compared with horizontal extension.

Similarly, the anconeus activity during sagittal plane flexion-extension movements, with the spine bent forward 90 degrees, was affected by gravity in a way that indicated it was acting as an extensor muscle. As expected, the relative electrical activity increased when the muscle worked against gravity and decreased when it was assisted by gravity. Furthermore, the relative electrical activity of the anconeus and triceps brachii displayed a similar trend, indicating that they play a similar role.

The results of the current investigation showed that there was no electrical activity of the anconeus and triceps brachii during pronation and supination motions, suggesting that these muscles do not contribute to forearm rotation. These outcomes agree with those studies, which found that the anconeus was not active during unresisted pronation and supination movements [22-23]. In addition, the activity of biceps brachii was found to be elevated during supination, which is as expected, because the biceps brachii works as a supinator muscle when the elbow is flexed at 90 degrees [75, 78, 125].

The current investigation considered a number of movements, which were selected so as to be representative of those common in daily life activities. Furthermore, the movements were chosen so that an analysis of the effect of gravity on the movements could provide more information and insight into the anconeus muscle function.

In conclusion, the analysis of the relative electrical muscle activity and the kinematics and kinetics of the elbow joint leads us to consider the anconeus foremost as an elbow extensor muscle.

In this chapter, a complete analysis of the flexion-extension and supination-pronation movements at different elbow postures was performed and it was found that according to the EMG activity, the anconeus muscle behaves as an elbow extensor muscle. However, it is also important to know the contribution of the anconeus to elbow kinematics. The effect of the anconeus on elbow kinematics and kinetics is reported in the following chapter.

CHAPTER FOUR

4 EFFECT OF THE ANCONEUS MUSCLE TO THE KINEMATICS OF THE ELBOW JOINT: KINEMATIC AND ELECTROMYOGRAPHIC STUDY

4.1 Introduction

From the previous chapter, it was found that the relative electrical activity of the anconeus indicated that the muscle behaved as an elbow extensor muscle. In addition, it has been suggested that the muscle makes a significant contribution during low levels of extensor torques [26, 34]. Nevertheless, more recent anatomical studies have reported that the anconeus acts merely as an accessory during extension [35].

Other anatomical studies have been undertaken with the purpose of discovering new arguments to clarify the function of this muscle. For example, Coriolano et al. [37] found that the muscle fibres of the anconeus were penniform, a formation proficient for force production. Another anatomical and biomechanical research study observed that the anconeus behaves as an extensor muscle and provides posterolateral stability of the elbow [38]. Even though several electromyographic and anatomical studies have been performed on the anconeus, it is evident that its specific role and contribution in elbow kinematics remains unclear.

Based on the methodology of the previous section, the anconeus muscle was blocked with local anaesthesia with the aim of identifying the relative contribution of the anconeus in elbow kinematics and in the activity of biceps and triceps brachii. The human participants in this study followed an experimental protocol which consisted of three stages. In the first stage, the volunteers performed three isometric maximum voluntary contractions (MVC) for every muscle (anconeus, biceps brachii and triceps brachii). Subsequently, in the second stage, flexion-extension and supination-pronation movements were performed before applying the anaesthesia, and in the last stage, the same movements were repeated but this time with the anconeus blocked.

This chapter presents the results of the investigation into the relative electrical muscle activity and elbow kinematics before and after anconeus defunctioning in order to elucidate the effect of the anconeus on elbow movement.

4.2 Methods and materials

In order to clarify the contribution of the anconeus muscle in the motion of the elbow and its effect on the electrical activity of the biceps and triceps brachii, the anconeus muscle was blocked with lidocaine. Measurements were taken using surface electromyography (EMG) and motion tracking devices (3D inertial sensors) before and after blocking during the performance of 4 motions; flexion-extension and supination-pronation. The data obtained from the trials was analysed in order to further investigate the role of the anconeus.

4.2.1 Subjects

Ten right-handed healthy volunteers, aged 29.3 ± 2.21 years and mass 66.80 ± 9.56 kg, with no history of neuromuscular or musculoskeletal disease took part in this investigation. All trials were carried out using the dominant hand of the participant. The participants were informed about the procedures before the tests and the protocol was approved by the Ethics Committee of The University of Manchester, Appendix II.

Subject Preparation

The participant preparation was done in the same way as the previous chapter. For the trials where the anconeus was blocked, the skin was prepared with an alcoholic chlorhexidine solution. Then, 10 ml of plain lidocaine (Figure 4.1) was injected through a 25 gauge hypodermic needle by a trained orthopaedic surgeon into the soft tissue at a point midway between the tip of the olecranon and the lateral epicondyle of humerus. The injection was performed with the elbow flexed approximately 90 degrees. At least ten minutes were allowed for the local anaesthetic to work before the experimental protocol was initiated.

Figure 4.1 Lidocaine hydrochloride injection 1% used to deactivate the anconeus muscle

4.2.2   Equipment

Surface electromyography and inertial measurement units were used to record the muscle electrical activity and kinematics of the elbow joint as was explained in the previous chapter.

4.2.3   Motions

The participant performed flexion-extension and supination-pronation movements in the horizontal and sagittal planes, as illustrated in Figure 3.6. The motions were performed at four different postures enabling the role and contribution of the anconeus to elbow kinematics to be investigated. These movements were described in the previous chapter. The active range of motion for flexion-extension was constrained to 90 degrees by a custom-made frame constructed out of wood. The frame was attached to the lateral side of the arm. Supination-pronation motions were constrained to the same range by a custom-made Perspex ring, Figure 3.7.

4.2.4   Procedure

The EMG and IMU measurements for each participant were carried out in two steps: before and after the anconeus muscle was blocked. Before the tests began, a static trial was undertaken by each participant in order to determine the level of electrical activity resulting from cross talk from adjacent muscles, noise and soft tissue [156].

The electrical activity from the electrodes attached to the anconeus, biceps and triceps brachii muscles of each participant was measured over a period of 20 seconds with the subject standing still with their arms straight down by their side. The mean value of the background electrical activity obtained from the static trials undertaken by the participants was approximately 2%MVC.

4.2.4.1   Before blocking the anconeus muscle

Once the skin of the participant had been prepared and the bipolar paediatric electrodes (Ag/AgCl) placed on the belly of anconeus, biceps and triceps brachii muscles and the three IMUs attached. Then, the participant was asked to perform dynamic trials involving undertaking the flexion-extension and supination-pronation motions of the dominant arm while EMG and IMU data was recorded.

The flexion-extension movements were performed with the forearm placed in the neutral position. Every trial consisted of 5 cycles performed over a period of approximately 28 seconds paced using a metronome. Each cycle consisted of 4 beeps (one beep per second); the first and second beeps were to start and stop flexion and then, the third and fourth beeps were to start and stop the extension motion. The flexion-extension motion was constrained to an arc of 90 degrees by a custom-made wood frame to ensure repeatability (Figure 3.6a-c) and that all participants performed the same range of motion during the trials. The correct posture of the elbow and trunk during the tests was monitored by visualisation of the Euler angles of the arm and thorax sensors in real time. For the supination-pronation motion the participants performed three trials with the elbow flexed 90 degrees, pointing at a fixed reference with the middle finger [30]. The motion was constrained to 90 degrees using a Perspex ring, as shown in Figure 3.6d. The movements were paced using the metronome at the same speed as that used for the flexion-extension movements.

4.2.4.2   After blocking the anconeus muscle

Once the participants had undertaken the first set of dynamic trials, the anconeus muscle was blocked using 10 ml of plain lidocaine, which was injected at the mid-point between the lateral epicondyle and the tip of the olecranon of the ulna, as

shown in Figure 4.2. Ten minutes were allowed for the local anaesthetic to work before the second set of dynamic trials were started. To ensure that the anconeus muscle was effectively blocked, the electrical activity of the muscle was measured when the participants flexed and extended the elbow three times with the spine bent forward 90 degrees. This was because in this position the anconeus was clearly active before applying the anaesthesia.

The electrical activity of anconeus was measure in real time after the muscle being blocked to determine when the muscle was inactive. Once the anconeus muscle showed null activity, the second set of dynamic trials were initiated. These trials entailed participants undertaking a second set of flexion-extension and pronation-supination motion tests following the same procedure as was used for the first set of trials undertaken prior to blocking of the anconeus.

Figure 4.2 The local anaesthetic (lidocaine) was injected at the middle point between the olecranon tip of the ulna and the lateral epicondyle of the humerus.

4.2.5 Data processing

The electrical activity data of the muscles during the dynamic trials was normalised in order to enable a comparison of the results to be undertaken. Participants were asked to perform isometric maximum voluntary contractions (MVC) in order to detect the maximum electrical activity of the anconeus, biceps and triceps brachii muscles (Appendix III). To measure the MVC of the anconeus, participants were asked to raise their dominant arm, hold it straight out from the body, then flex the

elbow by 90 degrees and hold/restrain the arm with the non-dominant hand. They were then asked to try to extend the dominant arm, with as much force as possible, while constraining movement with the non-dominant hand, as illustrated in Figure 4.3a.

For the measurement of the MVC of the biceps and triceps brachii, participants were asked to stand with their arm straight down by their side, bend the elbow by 90 degrees and then restrain the wrist of the dominant arm with the non-dominant hand. For the biceps brachii, participants were asked to flex the dominant arm, with as much force as possible, while constraining the arm with the non-dominant hand, as shown in Figure 4.3b.

In the case of the triceps brachii, participants tried to extend the dominant arm with as much force as possible while the arm was constrained by the non-dominant hand, as illustrated in Figure 4.3c. Each participant performed three isometric maximum voluntary contractions (MVC) of 6 seconds duration for each muscle to detect the maximum electrical activity. Two minutes of rest between each MVC test were given to avoid muscle fatigue. In addition, the participants were encouraged verbally during the tests to get the maximum muscle activity.
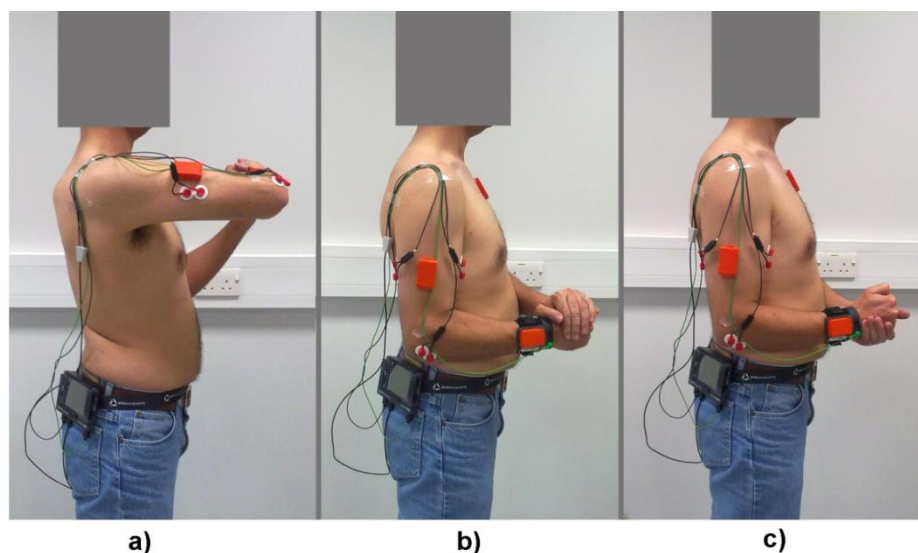
Figure 4.3 Isometric maximal voluntary contractions: a) MVC for anconeus muscle, b) MVC for biceps brachii and c) MVC for triceps brachii.

The root mean square (RMS) value of every MVC test was calculated within a window of 1.5 seconds and then the maximum RMS of each muscle was used to normalise the electrical activity during the dynamic trials in each volunteer. Once the normalization had taken place the data was then filtered with a 2-pole Butterworth band pass filter, with cut-off frequencies of 5 Hz and 600 Hz, in order to retain as much as possible of the electrical activity data [153].

Subsequently, the muscle activity data was rectified and filtered with a 2-pole Butterworth low pass filter with a cut-off frequency of 6 Hz [85]. The electrical activity data from the 15 cycles from the 3 trails undertaken by each participant for each motion were averaged and normalised with respect to time from zero to 100% of the movement time. Then the normalised and averaged data from all participants was analysed to give an overall average for all the participants.

The raw data from the IMUs was filtered with a 2-pole Butterworth low pass filter with a cut-off frequency of 2 Hz. This cut-off frequency was obtained from a frequency spectrum analysis of the elbow angular velocity [88]. The data processing was performed in MATLAB version 7.10.0.499 (R2010a).

The filtered IMU data from the 15 cycles from the 3 trails, undertaken by each participant for each motion, were averaged and normalised with respect to time from zero to 100% of the movement time. The normalised and averaged data from all participants was then analysed to give an overall average for all the participants.

The raw data from the IMUs (acceleration, angular velocity, magnetic field and pressure) was obtained in the default local system of the sensors [159]. In order to calculate relative movements, this raw data was then rotated into the global coordinate system using quaternions [175].

4.3 Results

4.3.1 Electrical Activity

4.3.1.1 Anconeus before and after the blocking

The relative electrical activity of the anconeus muscle during the flexion-extension movements, before and after anconeus blocking, is shown in Figure 4.4a-c. The first half of the cycle (0-50%) represented the portion of the cycle during which flexion took place and the second half (50-100%) indicated the portion of extension. The relative electrical activity of the anconeus, throughout the flexion-extension cycle, indicated that the anconeus activity before blocking was generally greater in extension than in flexion, as can be seen upon inspection of Figure 4.4a-c.

Before blocking, in the flexion-extension movement in the horizontal plane, the maximum anconeus activity was 8.4 ± 4% MVC in flexion at 15% of the cycle. When extension started the anconeus activity was 9.4 ± 3.5% MVC, this then increased reaching a maximum of 33 ± 7.5% MVC, as shown in Figure 4.4a.

From Figure 4.4b it can be seen that in the sagittal plane flexion-extension movement before blocking, in the flexion motion no anconeus activity was detected. In the extension motion the electrical activity of the anconeus increased from 5.2 ± 2.2% MVC to 11.4 ± 3.4% MVC between 50% and 82% of the cycle. In the sagittal plane flexion-extension movement with the spine bent forward 90º, the relative electrical activity of the anconeus (Figure 4.4c) was 14.1 ± 6% MVC at the beginning of flexion. The anconeus activity reduced towards the end of the flexion motion, before then increasing from 6.9 ± 3% MVC at the start of the extension to a maximum of 24.2 ± 12% MVC at 72% of the flexion-extension cycle.

In the case of the supination-pronation motions with the elbow flexed 90 degrees, no relative electrical activity was detected from the anconeus muscle. After the anconeus muscle was blocked the relative electrical activity recorded was 2 ± 0.5% MCV during the 4 motions tested. This level corresponded to the value of the background electrical activity obtained from the participants during the static trial prior to the test. Consequently, the anconeus was considered to be inactive.
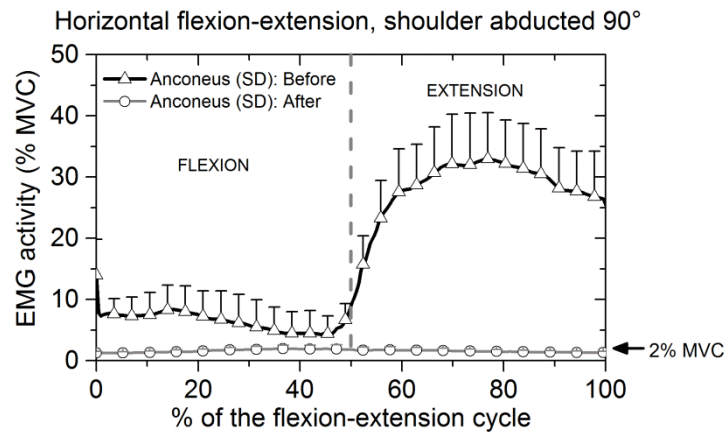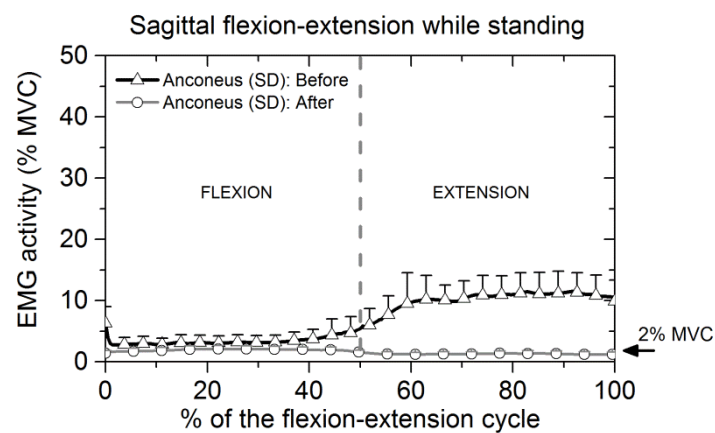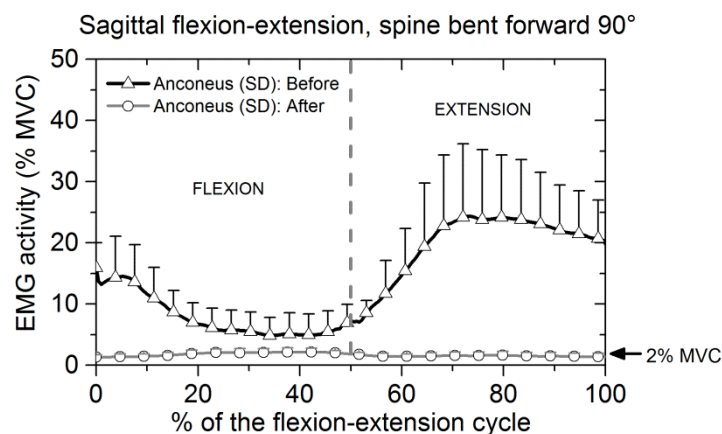
Figure 4.4 Mean and standard deviation of the relative electrical activity of anconeus muscle before and after applying anaesthesia: a) flexion-extension cycle with the shoulder abducted 90°, b) flexion-extension cycle in the sagittal plane while standing and c) flexion-extension cycle with the spine bent forward 90°. Anconeus activity was greater in extension movements.

4.3.1.2 Biceps brachii before and after the blocking

The relative electrical activity of the biceps brachii during the four motions under consideration, before and after blocking of the anconeus, is shown in Figure 4.5a-d. The relative electrical activity of the biceps brachii was generally higher in flexion than in extension and slightly higher in supination than in pronation. During flexion-extension in the horizontal plane before anconeus blocking, the activity decreased from $19.3 \pm 10\%$ MVC to $13.1 \pm 7.3\%$ MVC when the flexion motion changed to extension during the cycle (Figure 4.5a).

The relative electrical activity of biceps brachii, during flexion-extension in the sagittal plane, was higher in flexion than extension motion, as illustrated in Figure 4.5b. There was a small increment of the myoelectric activity of biceps brachii at the middle of extension at 75% of the cycle, which indicated that the muscle was counteracting the force of gravity and at the same time was slowing down the velocity of the elbow joint. The relative electrical activity of biceps brachii suggested the muscle was working eccentrically at that stage of the cycle.

In the flexion-extension movements with the spine bent forward, the maximum biceps brachii activity recorded was $8.6 \pm 4\%$ MVC during flexion at approximately 40% of the cycle (Figure 4.5c). During the supination-pronation motion, the relative electrical activity of biceps brachii was slightly higher in supination ($6.2 \pm 2\%$ MVC) than in pronation ($3.5 \pm 1.5\%$ MVC) (Figure 4.5d).

From Figure 4.5a-d it can be seen that the electrical activity of the biceps brachii was similar before and after applying anaesthesia to the anconeus. With a confidence interval of 95%, the difference of the electrical activity of biceps brachii before and after blocking anconeus was not significant according to the paired sample t-test analysis. Flexion-extension in the horizontal plane $t(9) = 0.0994$ (*p=0.923*), in the sagittal plane while standing $t(9) = 1.504$ (*p=0.1667*), in the sagittal plane with the spine bent forward $t(9) = 0.2953$ (*p=0.7744*) and pronation-supination $t(9) = 0.0887$ (*p=0.9312*). This indicated that the blocking of the anconeus had little or no effect on the electrical activity of the biceps brachii for all the movements considered.

Figure 4.5 Mean and standard deviation of the relative electrical activity of biceps brachii before and after applying anaesthesia: a) flexion-extension cycle with the shoulder abducted 90°, b) flexion-extension cycle in the sagittal plane while standing, c) flexion-extension cycle with the spine bent forward 90° and d) supination-pronation with the elbow flexed 90°. Biceps brachii activity remained approximately the same before and after anconeus defunctioning.

4.3.1.3   Triceps brachii before and after the blocking

Figure 4.6a-d shows the relative electrical activity of the triceps brachii during the four movements before and after blocking of the anconeus. In the horizontal flexion-extension movement before anconeus blocking, the electrical activity of the triceps brachii gradually decreased during flexion before then increasing in extension from $3.6 \pm 1.7\%$ MVC to $5.5 \pm 2.4\%$ MVC between 50% and 80% of the cycle (Figure 4.6a). In sagittal plane flexion-extension and supination-pronation motions, the relative electrical activity of the triceps brachii was of a level at which the muscle could be considered inactive (Figure 4.6b and d).

In flexion-extension with the spine bent forward, electrical activity of the triceps brachii reduced from $5.7 \pm 2.3\%$ MVC at the beginning of flexion to $3 \pm 0.8\%$ MVC at the end of flexion. The activity then increased during extension, reaching $10.6 \pm 3.6\%$ MVC at 90% of the flexion-extension cycle, as shown in Figure 4.6c. From

Figure 4.6a-d, it can be seen that blocking of the anconeus did not affect the electrical activity of the triceps brachii. With a confidence interval of 95%, the difference of the electrical activity of triceps brachii before and after blocking anconeus was not significant according to the paired sample t-test analysis. Flexion-extension in the horizontal plane t(9) = 2.1965 (*p=0.0557*), in the sagittal plane while standing t(9) = 1.6006 (*p=0.1439*), in the sagittal plane with the spine bent forward t(9) = 0.9564 (*p=0.3638*) and pronation-supination t(9) = 0.7480 (*p=0.4735*).
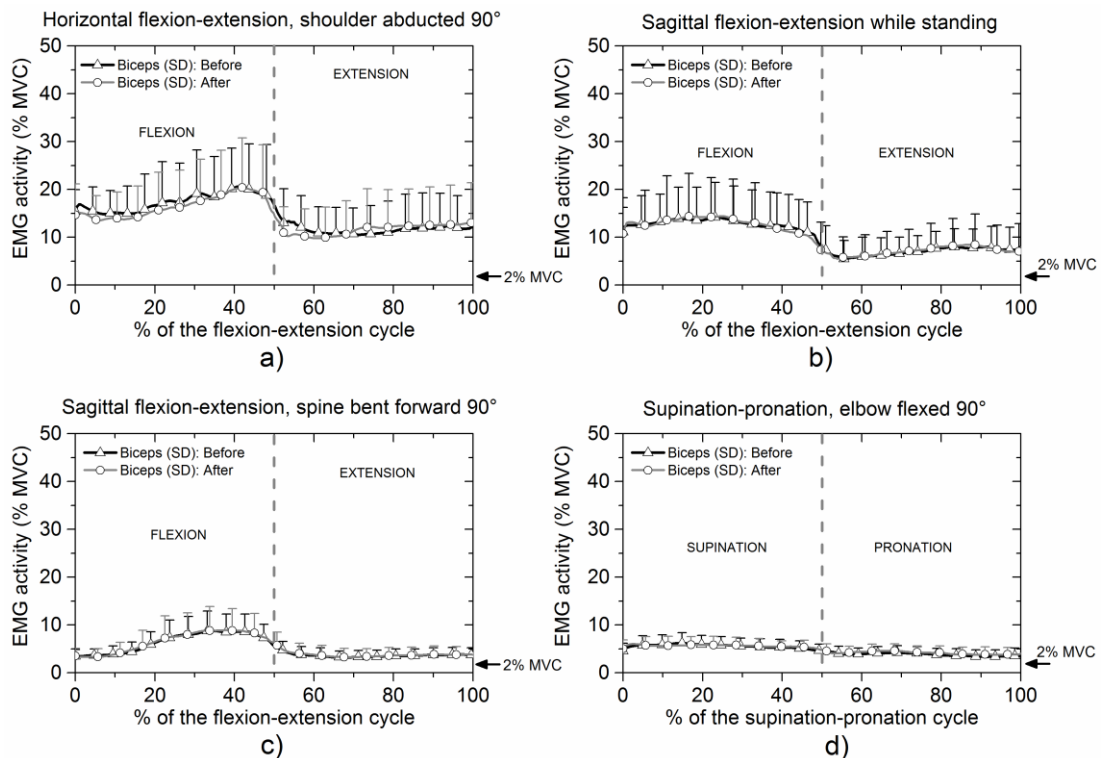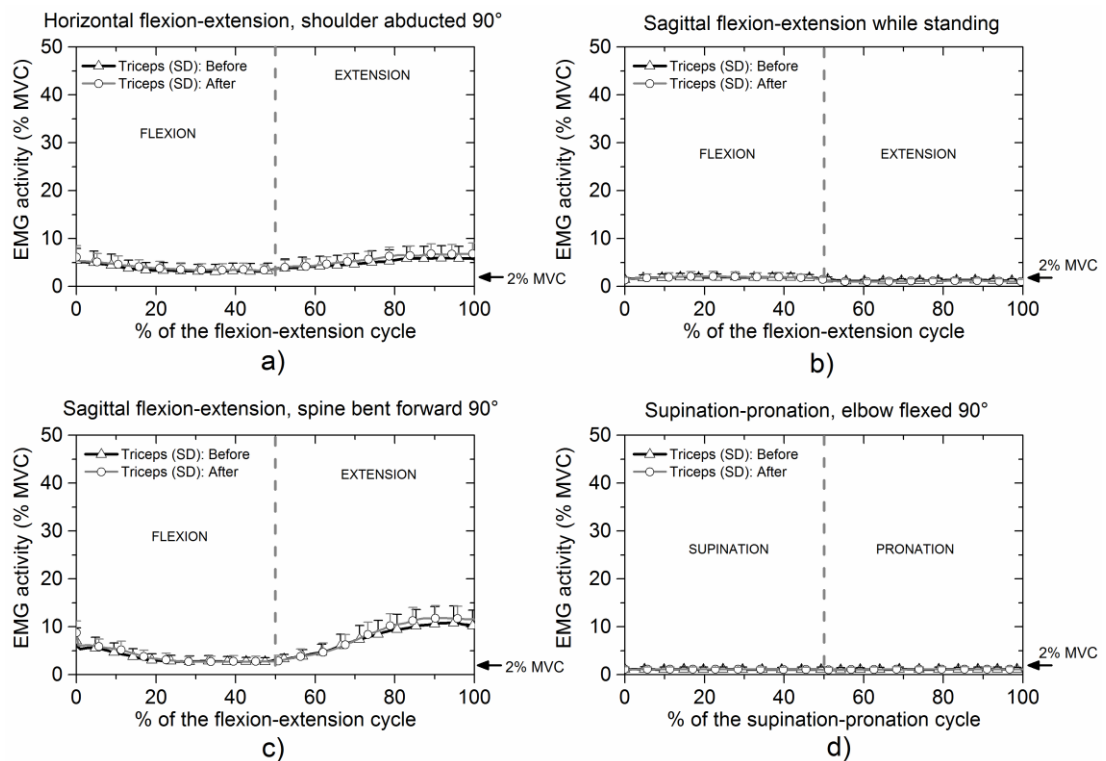

Figure 4.6 Mean and standard deviation of the relative electrical activity of triceps brachii before and after applying anaesthesia: a) flexion-extension cycle with the shoulder abducted 90°, b) flexion-extension cycle in the sagittal plane while standing, c) flexion-extension cycle with the spine bent forward 90° and d) supination-pronation with the elbow flexed 90°. Triceps brachii activity was approximately the same before and after blocking anconeus.

4.3.2   Kinematics and kinetics of the elbow

4.3.2.1   Kinematics before and after the anconeus defunctioning

The relationship between the angular velocity of the elbow for the four movements, before and after anconeus blocking, is shown in Figure 4.7a-d. In these plots, positive velocity indicates the flexion and pronation movements and negative velocity represents the extension and supination motions.

Figure 4.7 Relative angular velocity of the elbow before and after anconeus defunctioning: a) flexion-extension in the horizontal plane with the shoulder abducted 90º, b) sagittal flexion-extension while standing, c) flexion-extension in the sagittal plane with the spine bent forward 90º and d) supination-pronation with the elbow flexed 90º. The results in all movements showed a linear relationship with slope of approximately 1, suggesting the effect of anconeus defunctioning on elbow kinematics was not significant.

In the plots, for all the four movements, the angular velocity data for the elbow before and after anconeus blocking exhibited a near-linear relationship. It had a slope and Pearson's correlation coefficient (r) of 0.98 and 1 respectively for the horizontal flexion-extension motion (Figure 4.7a). For sagittal plane flexion-extension motion, while standing, a slope of 0.98 and Pearson's correlation of 1 was found (Figure 4.7b). Similarly, for flexion-extension movements in a sagittal plane with the spine bent forward 90º a slope of 1 and Pearson's correlation of 1 was found (Figure 4.7c). Finally, in supination-pronation a slope of 1 and Pearson's correlation 1 was found (Figure 4.7d). The near-linear relationship of the angular velocity data for the elbow, during the four motions, indicates that blocking of the anconeus made no significant

140

difference to the angular velocity of the elbow. Moreover, the difference of the relative angular velocity of the elbow joint before and after blocking anconeus was not significant according to the paired sample t-test analysis. Flexion-extension in the horizontal plane $t(9) = 0.2108$ (*p=0.8377*), in the sagittal plane while standing $t(9) = 0.5061$ (*p=0.6249*), in the sagittal plane with the spine bent forward $t(9) = 0.1262$ (*p=0.9023*) and pronation-supination $t(9) = 0.0984$ (*p=0.9238*).

In addition, a power spectral analysis [88] of the relative angular velocity indicated that there was no change in the spectral frequency components following application of the anaesthesia to the anconeus muscle. Thus, confirming that the angular velocity trace is essentially identical before and after blocking, as revealed in Figure 4.8. The main frequency of the angular velocity was approximately the same before and after the blocking for all movements, 0.5 Hz.

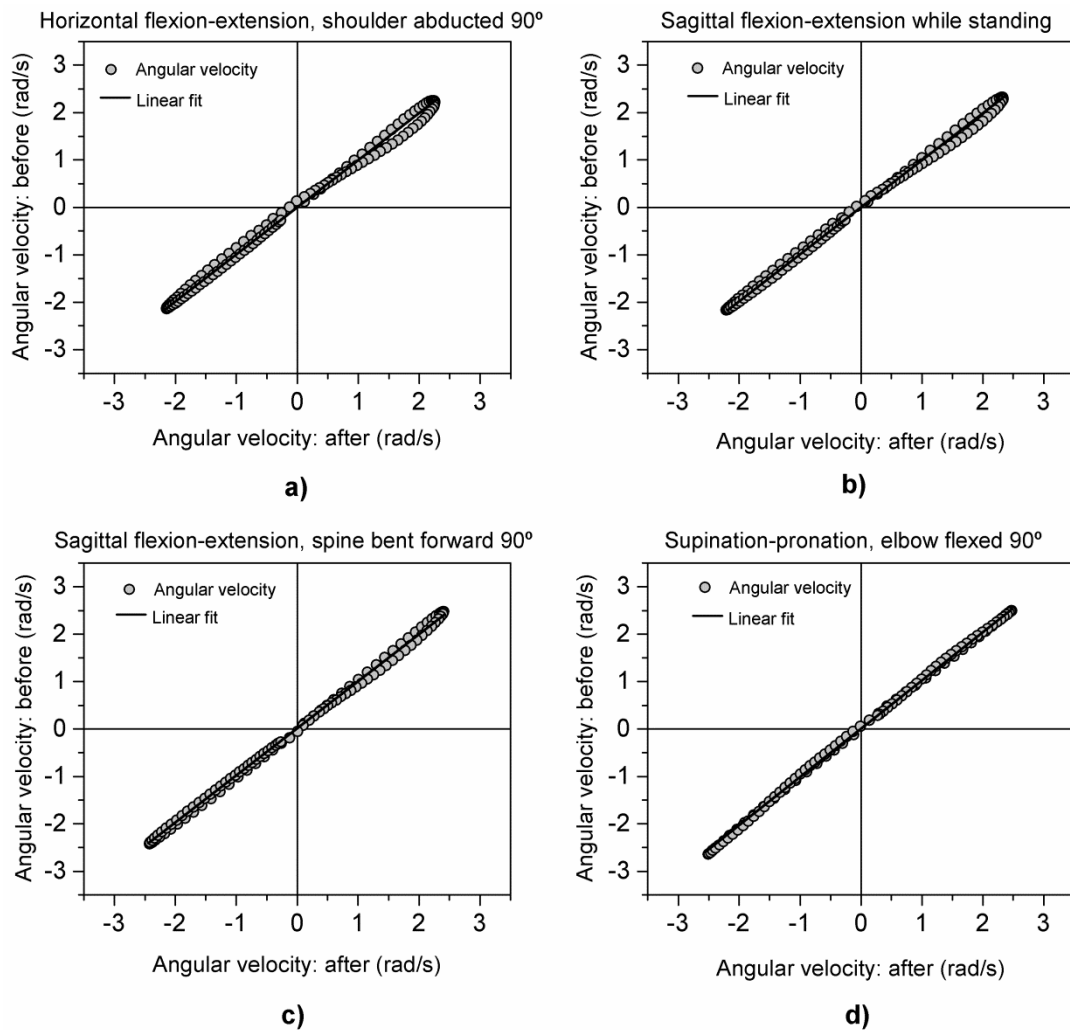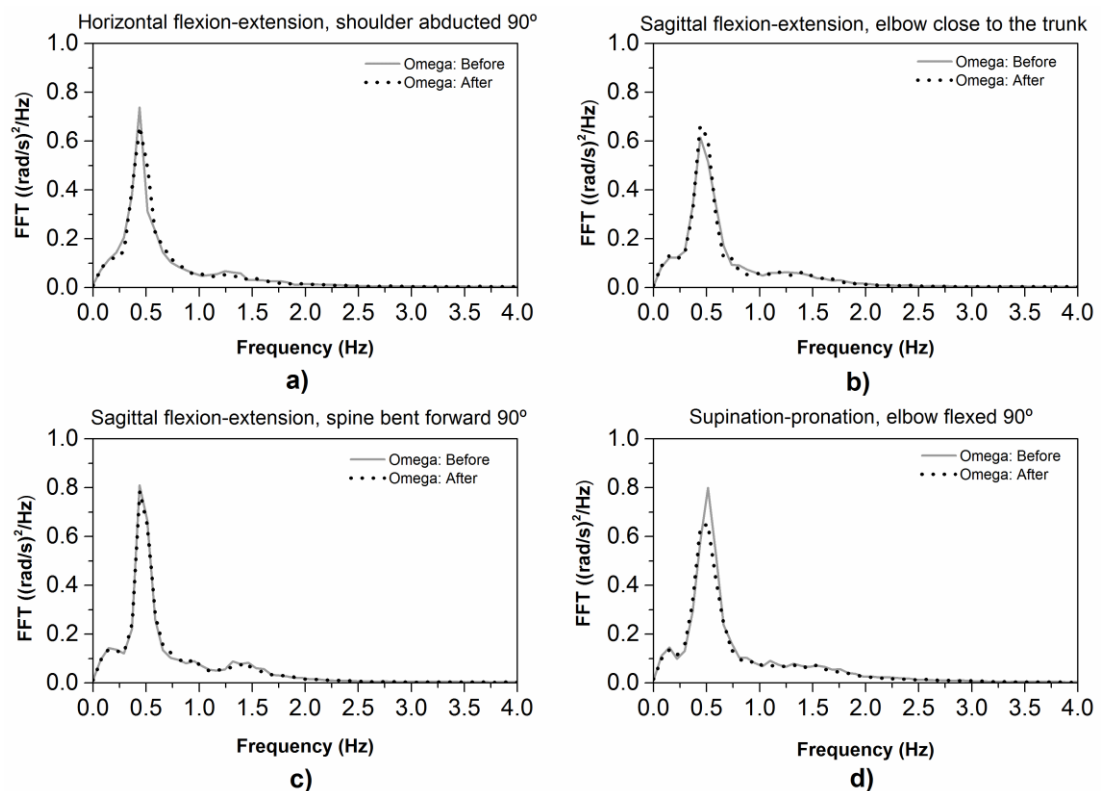Figure 4.8 Frequency spectrum of the relative angular velocity before and after anconeus defunctioning: a) flexion-extension in the horizontal plane with the shoulder abducted 90º, b) sagittal flexion-extension while standing, c) flexion-extension in the sagittal plane with the spine bent forward 90º and d) supination-pronation with the elbow flexed 90º. There was no significant difference in the spectral components before and after anconeus defunctioning.

The difference of the power spectrum frequency of the relative angular velocity of the elbow joint before and after blocking anconeus was not significant according to the paired sample t-test analysis. Flexion-extension in the horizontal plane t(9) = 0.8240 (*p=0.4312*), in the sagittal plane while standing t(9) = 0.8983 (*p=0.3923*), in the sagittal plane with the spine bent forward t(9) = 1.7626 (*p=0.1118*) and pronation-supination t(9) = 1.2142 (*p=0.2556*).

4.3.2.2   Kinetics before and after the anconeus defunctioning

The net torque and net power for the elbow joint for the four movements, before and after blocking of the anconeus, are shown in Figure 4.9 and Figure 4.10. Comparing the results for the net power and torque, before and after anconeus blocking for all the motions considered, suggests that blocking of the anconeus does not have an effect on the kinetics of the elbow joint.
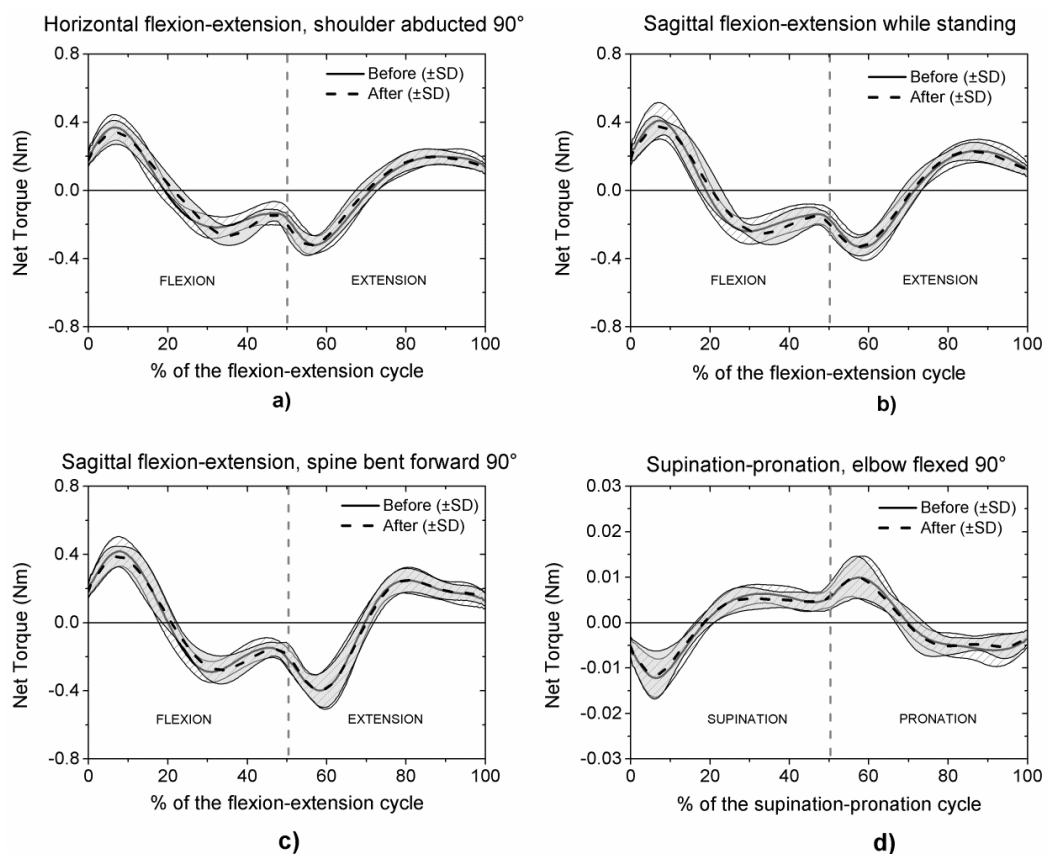
Figure 4.9 Net torque of the elbow joint before and after blocking anconeus: a) flexion-extension in the horizontal plane with the shoulder abducted 90º, b) sagittal flexion-extension while standing, c) flexion-extension in the sagittal plane with the spine bent forward 90º and d) supination-pronation with the elbow flexed 90º. The results showed no significant difference in the net joint torque before and after applying the anaesthesia.
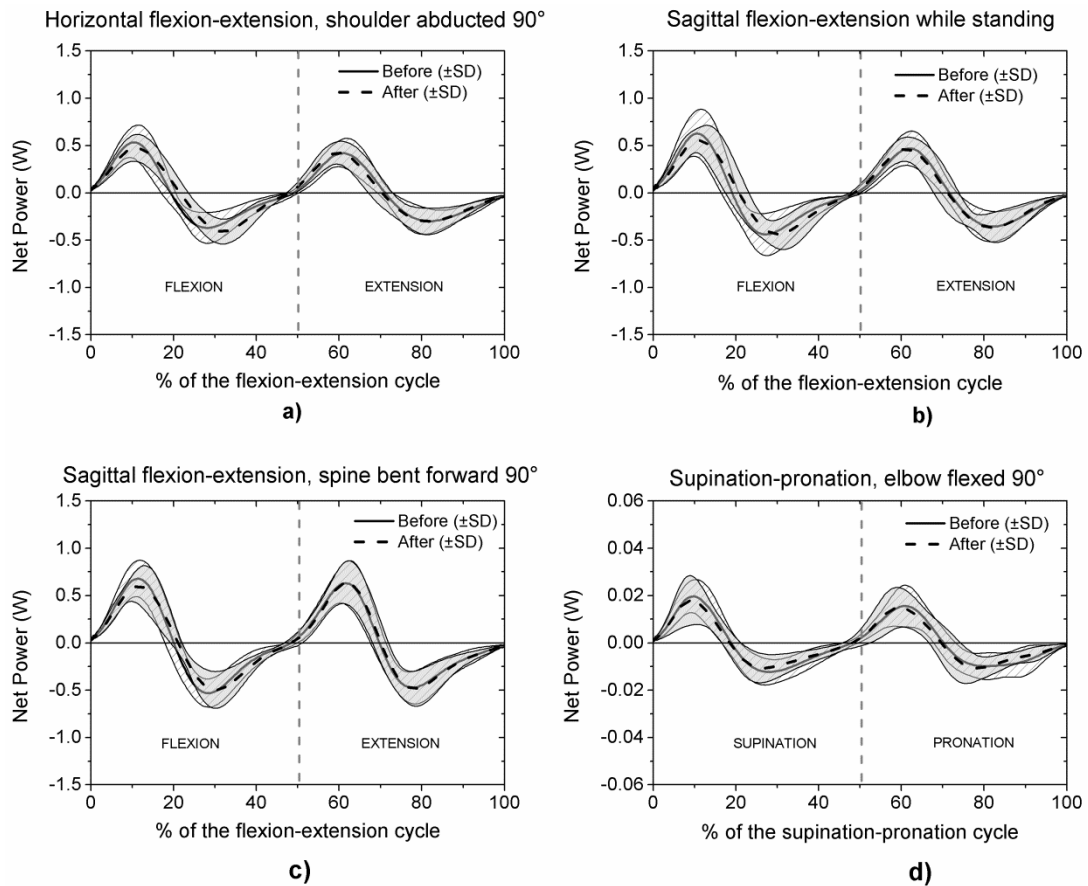
Figure 4.10 Net power of the elbow joint before and after the anconeus defunctioning: a) flexion-extension in the horizontal plane with the shoulder abducted 90°, b) sagittal flexion-extension while standing, c) flexion-extension in the sagittal plane with the spine bent forward 90° and d) supination-pronation with the elbow flexed 90°. There was no significant difference in the net joint power before and after applying the anaesthesia.

The net torque and power were compared before and after blocking the anconeus muscle. With a confidence interval of 95%, the paired sample t-test analysis indicated no significance difference of the net torque after blocking anconeus. Flexion-extension in the horizontal plane $t(9) = 0.0811$ ($p=0.9371$), in the sagittal plane while standing $t(9) = 0.1222$ ($p=0.9054$), in the sagittal plane with the spine bent forward $t(9) = 0.3760$ ($p=0.7156$) and pronation-supination $t(9) = 0.5063$ ($p=0.6248$). Similarly, the power did not show a significant difference. Flexion-extension in the horizontal plane $t(9) = 0.1395$ ($p=0.8920$), in the sagittal plane while standing $t(9) = 0.1980$ ($p=0.8474$), in the sagittal plane with the spine bent forward $t(9) = 0.0662$ ($p=0.9486$) and pronation-supination $t(9) = 0.3765$ ($p=0.7153$).

In addition, the total net joint work was calculated for each of the four movements, for both before and after blocking, by calculating the absolute area below the net power curve in order to confirm that anconeus blocking had no effect on elbow kinetics. The mean and standard deviation of the total net joint work at the elbow, for the four movements before and after blocking the anconeus, are presented in Figure 4.11.

TOTAL NET JOINT WORK FOR FLEXION & EXTENSION

a)

TOTAL NET JOINT WORK FOR SUPINATION & PRONATION

b)

Figure 4.11 Mean and standard deviation of the total net joint work at the elbow in the four movements before and after blocking anconeus: a) Mean values for flexion and extension movements and b) Mean values for supination and pronation motions. The results show that there is no effect of anconeus defunctioning on the elbow kinetics.

The flexion-extension and supination-pronation cycles were divided in two sections for ease of comparison. Upon inspection of Figure 4.11a-b, it can be determined that anconeus blocking does not have a significant effect on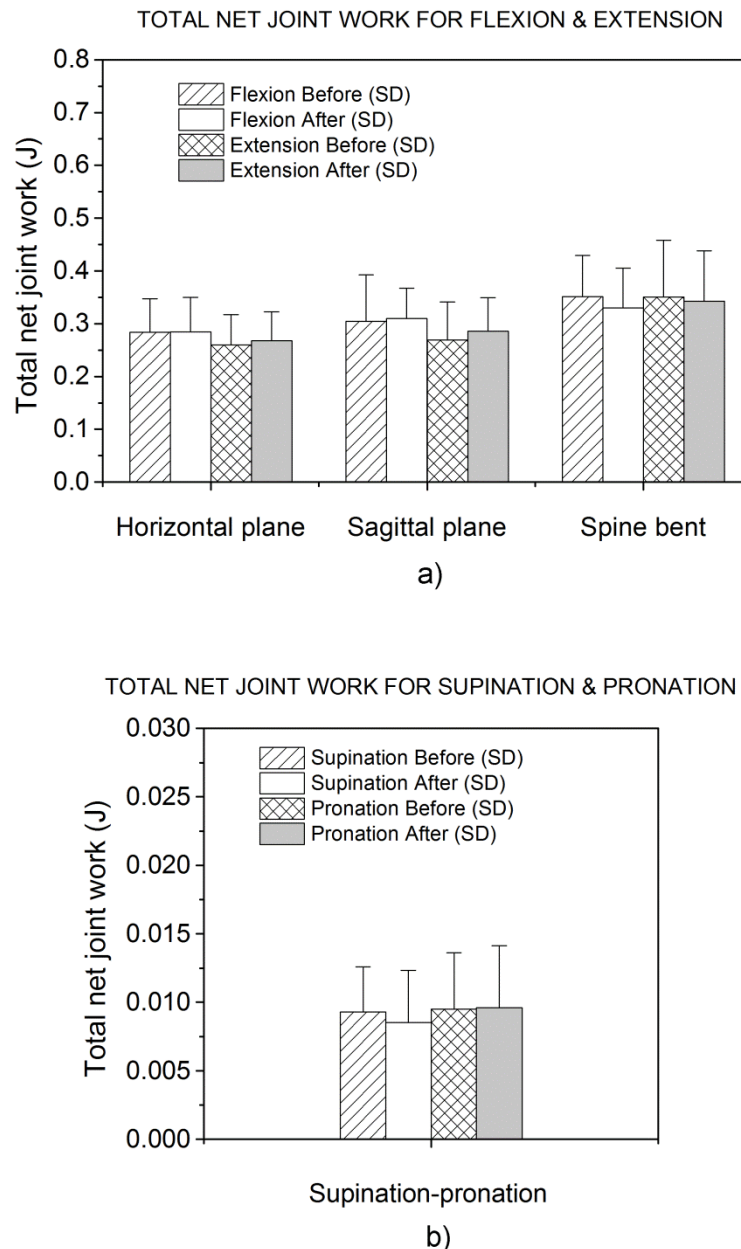 elbow joint work. The paired sample t-test analysis of the net work of the elbow joint indicated no significance difference after the muscle being blocked. Flexion-extension in the horizontal plane $t(9) = 0.3238$ ($p=0.7535$), in the sagittal plane while standing $t(9) = 0.5308$ ($p=0.6084$), in the sagittal plane with the spine bent forward $t(9) = 0.4318$ ($p=0.6760$) and pronation-supination $t(9) = 0.1606$ ($p=0.8759$).

4.4 Discussion

The aim of this study was to investigate the relative contribution that blocking of the anconeus might have on elbow kinematics, kinetics and the electrical activity of the biceps brachii and triceps brachii muscles. The results of the electrical activity of the muscles in combination with the elbow kinematics, before and after the blocking, provide evidence that suggests that the anconeus is an elbow extensor. The results of the current study clearly indicate that the relative electrical activity of the anconeus before blocking is higher during extension in the flexion-extension cycle as other researchers have observed [22-27, 31, 40].

The linear relationship between the relative angular velocity, before and after anconeus deactivation, suggests that the anconeus contribution to the elbow kinematics is not significant. Furthermore, the spectrum frequency analysis of the angular velocity, before and after blocking the anconeus, indicates that the frequency components do not change. The anconeus muscle and triceps brachii were inactive, during the unresisted pronation-supination movement, a finding consistent with previous studies [22-23], implying these muscles do not contribute to forearm rotation. The electrical activity of the biceps brachii indicates that the muscle contributes more in the flexion motion than extension, whereas the triceps brachii contributes more in extension. Blocking of the anconeus muscle did not have a significant effect on the relative electrical activity of the biceps and triceps brachii muscles. In addition, the net power, net torque and the total net work of the elbow joint before and after anconeus blocking remained the same. This indicated that the anconeus does not significantly contribute to the elbow kinetics.

Although the penniform structure of the anconeus indicates it is a muscle for force production, it is not able to produce large displacements as the triceps brachii does [37, 90]. This may be the reason why the anconeus does not have a significant effect on elbow kinematics. Moreover, the anconeus contains type I fibres, which allow it to be activated first [108-109, 189], but its activity will be overcome by the triceps brachii when more force is needed in the joint [23, 25-26]. In addition, the triceps brachii has a large moment arm 2.809 cm with the forearm extended and physiological cross section area of approximately 6 square centimetres per head, making it a powerful extensor muscle in relation to the small moment arm of anconeus, 0.622 cm [36, 74, 82]. The anconeus muscle has a physiological cross-sectional area of 2.5 ± 1.2 cm^2 and the whole physiological cross-sectional area of triceps brachii is approximately 18 cm^2 [36]. Moreover, the triceps brachii muscle can produce the same amount of force than the anconeus with a smaller activity level due to the higher moment arm [190].

This investigation considered a relatively limited number of movements; however, the selected movements were considered to be representative of those common in daily life activities. Moreover, the movements were chosen taking into consideration the effect of gravity on the elbow joint. This effect related with the electrical muscle activity helped to identify the function and contribution of the anconeus on the elbow kinematics. The results and conclusions are valid for the conditions previously established in the current experiment.

This chapter has presented the effect of the anconeus muscle in the elbow kinematics and kinetics. It was inferred from the results that the anconeus did not have a significant contribution in the elbow movement and in the electrical activity of the biceps and triceps brachii muscles. To support this experimental research, the following chapter presents the analysis of the computational model of the elbow joint with the effect of the anconeus muscle in the elbow movement. The range of motion and contact area are analysed in different scenarios, which represent the deactivation of the anconeus muscle during the extension movement in a range of motion of 90 degrees.

CHAPTER FIVE

5 COMPUTATIONAL MODEL OF THE ELBOW TO MEASURE THE CONTRIBUTION OF THE ANCONEUS MUSCLE ON THE RANGE OF MOTION AND CONTACT AREA OF THE JOINT

5.1 Introduction

Some anatomical studies have suggested that the anconeus is a muscle of power; others have implied that the muscle is an accessory at the elbow [35, 37]. It is clear from these studies that the specific function and contribution of the anconeus muscle to elbow kinematics is yet to be clearly established.

Although it has been argued that the anconeus is an accessory at the elbow, some researchers have suggested that the muscle could contribute up to 15% of the extension moment during isometric contractions [34]. In addition, it has been found that the anconeus plays an important role when torque values are low, less than 1 J [24-25]. In order to help clarify the effect of the anconeus on elbow kinematics and inform the debate about the function of the anconeus muscle, a computational model of the elbow joint was developed, the details of which are described in this chapter. The computational model was created with the aim of investigating the contribution of the anconeus during the flexion-extension motion, in particular the effect on the range of motion of the elbow joint, and thus to provide additional weight and support to the findings of the clinical study developed in chapter four. The study was focused on a range of motion of the elbow joint of around 90 degrees from 30° to 120° corresponding approximately to the range of motion employed for the flexion-extension experimental trials described in chapter four.

To the author's knowledge, the computational model of the elbow detailed in this chapter is the first to be developed and utilised to investigate the effect of the anconeus muscle on the range of motion of the elbow joint. The model includes cortical bone, cartilage, collateral ligaments, muscles and trabecular bone. Three-dimensional basic connector elements were employed to represent the muscle

behaviour of the anconeus, biceps brachii and triceps brachii. These elements model discrete physical connections between bodies and using a combination of two types of basic connector elements enabled muscle forces to be accurately simulated in the model.

The analysis consisted of examining the range of motion and contact area of the articulation when the anconeus muscle is subject to loads representing differing percentages of the total extension force, up to a maximum of 15%, which is based on the maximum that the anconeus can contribute in extension as reported in the literature [34]. The anconeus loads considered were 0%, 5%, 10% and 15% of the total extension force, with the 0% load effectively representing the case where the anconeus is deactivated.

5.2 Methods

To investigate the effect of the anconeus muscle in the elbow joint, the elbow geometry was created from CT scan data of a healthy patient. The left elbow of a male subject of 26 years old was analysed. The CT scan images of the elbow did not present any abnormality or musculoskeletal impairment and the subject had no history of either neuromuscular or musculoskeletal disorder. The model considered the cartilage, cortical and trabecular bone of the elbow joint. Linear spring elements were employed to simulate the lateral and medial collateral ligaments [191]. Furthermore, the anconeus, biceps and triceps brachii muscles were modelled using a combination of Cartesian and Cardan connector elements [191].

Using the model, the range of motion and contact area of the joint was determined when the anconeus muscle was subject to differing percentages of the total extension force.

The analysis started with the forearm extended at 30 degrees with respect to the humerus. This posture was the original position of the elbow joint generated from the CT scan data. Flexion motion was then simulated followed by extension. A load (152N) was applied to the biceps brachii connector that produced a range of motion (RoM) of approximately 90 degrees in flexion. Subsequently, this load was removed

and a load (180N) was then applied to the triceps brachii connector to simulate the extension movement. This load generated approximately the same RoM as in the flexion motion, thus placing the forearm back in the initial position (30 degrees with respect to the humerus). The loads of biceps and triceps brachii were calculated from an iterative process where the force required was enough to produce a range of motion of 90 degrees for flexion and extension. The range of motion was chosen so as to correspond to that employed for the flexion-extension experimental trials described in chapter four thus enabling the findings of the computational model analysis to be more readily considered in conjunction with those of the clinical study.

To study the effect of anconeus muscle on the elbow joint, four different loads were applied to the anconeus muscle connector, 0N, 9N, 18N and 27N, representing 0%, 5%, 10% and 15% of the total load applied to the triceps brachii, respectively. The 0N load corresponds to the case when the anconeus is deactivated or blocked and 27N represents the maximum contribution that the anconeus is able to provide to the overall extension force [34].

The computational model of the elbow consisted of six stages. First, 3D image visualisation and processing software was employed to generate the surface geometry of the bones and cartilage from the CT scan data. Computer-aided design (CAD) software was then utilised in stage 2, to create solid models from the surface geometry generated in the first stage. In the third stage, the solid models of the bone and cartilage were assembled to form the elbow joint model, the ligaments were added to the joint and the interaction between the cartilages was defined. In the fourth stage, the material properties of the bones, ligaments and cartilage were assigned to the model. In the fifth stage, model boundaries conditions were defined and muscle forces were applied to the joint. Finally, the bone and cartilage geometries were meshed with 3-Dimensional solid (continuum) elements.

5.2.1 Geometry

The 3-D volumetric CT scan data was imported into the ScanIP image processing software package (ScanIP^{TM} Version 3.2, Simpleware Ltd, Exeter, UK) where the surface geometry of the bones and cartilage was created through a segmentation

process. Subsequently, the segmented bone and cartilage surface data were exported in point cloud format then imported into SolidWorks (SolidWorks® Dassault Systèmes, SolidWorks Corp, Waltham, MA, USA), enabling solid models to be created from the surface data. The solid models (bones and cartilage) were imported into Abaqus CAE (Abaqus/CAE Version 6.12-2, Dassault Systèmes Simula Corp, Providence, RI) where pre-processing tools for solid geometry were employed to produce the final assembled model of the bone and cartilage. The ligament and muscle representations were then added to the model.

5.2.1.1 Bones

The humerus, ulna and radius bone geometries were created from CT scans in the ScanIP software. The CT scan data in Digital Imaging and Communicated in Medicine (DICOM) file format was read into ScanIP. The DICOM files provide a series of 2-D slices (planar images) at a specific resolution, containing information about the bone features, as illustrated in Figure 5.1.
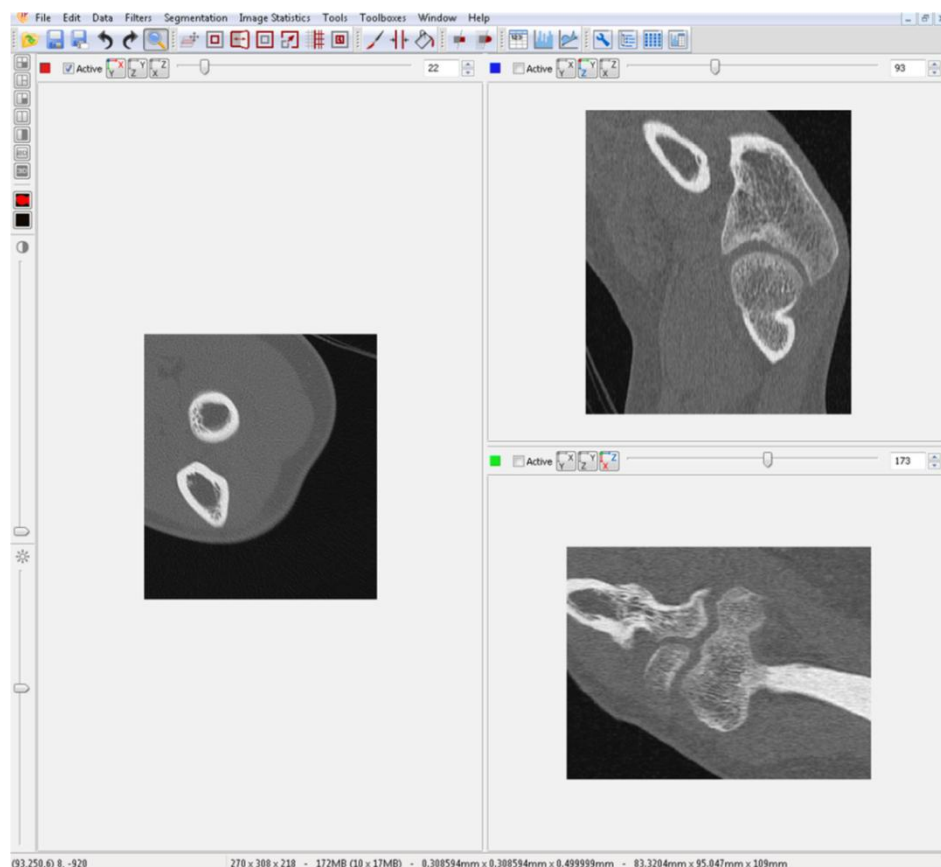

Figure 5.1 CT scans of the elbow joint showing three different planes (slices) in the ScanIP software.

A good resolution is required for the CT scans in order to obtain an accurate representation of the bone geometry therefore a narrow slice width is essential. The elbow joint CT scan data, from which the elbow joint model was created, consisted of two hundred and seventeen slices in the transversal plane at a thickness of 0.5 mm. Further details of the elbow joint CT scans are given in the following Table 5.1.

Table 5.1 Technical features of the CT scans of the elbow joint.

Format	DICOM
Colour type	Gray scale
Study description	Upper limb
Slices	217 slices in the transversal plane (X, Y)
Slice thickness	0.5 mm (transversal plane)
Slices	307 slices in the frontal plane (Z, X)
Slice thickness	0.3 mm (frontal plane)
Slices	269 slices in the sagittal plane (Y, Z)
Slice thickness	0.3 mm (sagittal plane)

In ScanIP, the 3D scan data for the elbow bones, the humerus, ulna and radius, were segmented into masks using a threshold tool. Three masks were created in each case. The slices were then examined individually and a paint tool employed in a manual segmentation operation to fill any gaps identified in the structures.

Once the masks had been created in ScanIP format (*.sip), morphological filters were applied to the model to smooth irregularities in the surfaces generated. These surfaces represent the outer tissue (cortical bone) of the elbow bone structures. Figure 5.2 shows the masks of the humerus, ulna and radius in three planes created from the CT scans alongside a 3D view of the elbow model. Trabecular bone and cartilage masks were then created by applying erode and dilate filters, respectively, to the cortical bone surfaces.
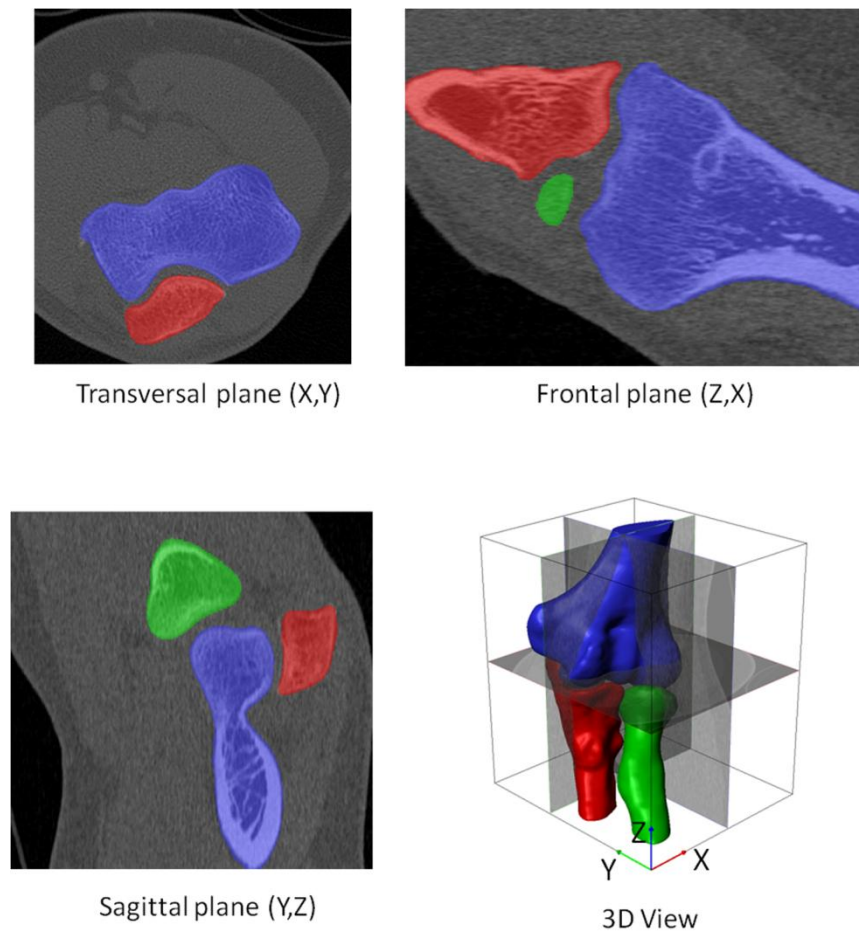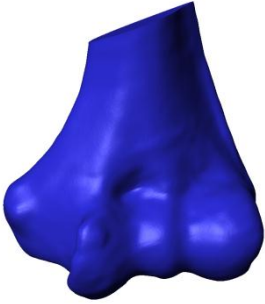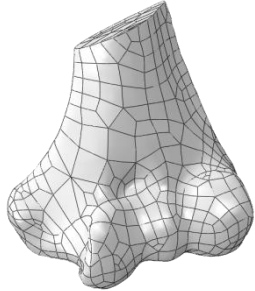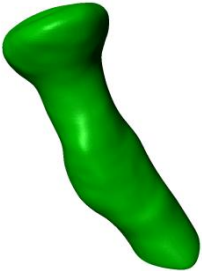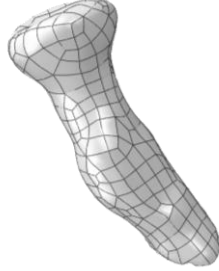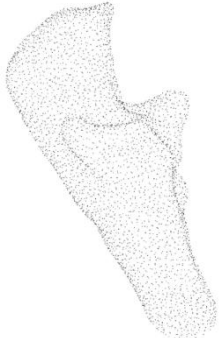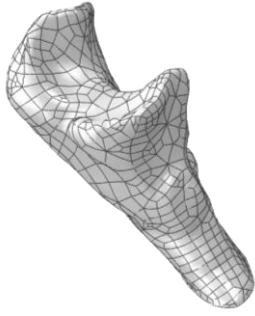
Figure 5.2 Masks of the humerus (blue), ulna (red) and radius (green) bones created from the CT scans.

The masks of the cortical bone, trabecular bone and cartilage were exported from ScanIP in point cloud format (*.xyz). These were then read into the SolidWorks software where the point cloud data were transformed into solid geometric models.

The solid geometry data was then exported from SolidWorks in Parasolid format (*.x_t) so that it could be imported into Abaqus CAE. Table 5.2 summarizes the geometry creation process for the elbow joint bones. The cartilage, cortical and trabecular bone were modelled to represent the real geometry of the elbow joint. For example, it is well known that the contact area of a joint will be affected by the mechanical properties of the cartilage [192-193], by that reason it is important to model the real geometry of the cartilage with its mechanical properties.
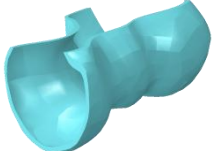
Table 5.2 Humerus, ulna and radius geometry creation: a) ScanIP format, b) Point cloud data from ScanIP and c) Solid geometry in Parasolid format from SolidWorks.

Bones	ScanIP (*.sip)	ScanIP (*.xyz)	SolidWorks (*.x_t)
Humerus			
Ulna			
Radius			
	a)	b)	c)

Having imported the solid geometry of the humerus, ulna and radius into Abaqus CAE pre-processing tools including Boolean operators were employed to produce the final representations of the cortical and trabecular bone. This operation produced a cortical bone layer of around two millimetre thickness [194-195]. The end of the cortical bone of the humerus, ulna and radius was extruded following the external shape of the bone in order to obtain regular surfaces and be able to apply the boundary conditions in the distal parts of the bones. The final geometries obtained for the cortical bone, trabecular bone and cartilage are shown in Table 5.3.

Table 5.3 Cortical, trabecular and cartilage geometries of the elbow joint.

Bones	Humerus	Ulna	Radius
Cortical			
Trabecular			
Cartilage			

5.2.1.2   Cartilage

Boolean operators were also employed in Abaqus CAE to obtain representations for the cartilage of the humerus, radius and ulna, illustrated in Table 5.3. The cartilages were created to have a more realistic geometry of the joint.

5.2.1.3   Muscles

The anconeus, biceps and triceps brachii muscles were modelled using connector elements in Abaqus CAE. Connector elements are useful tools to connect and

simulate the interaction between two different parts of an assembly. They can simulate forces, displacements, velocities, rotations, friction, translation and accelerations between two nodes [191]. Table 5.4 shows the different types of connector elements available in the Abaqus CAE software. The basic translational connectors allow displacement between two nodes and the basic rotational connectors allow rotation. The assembled connection elements represent a combination of the translation and rotation connectors [191].

Table 5.4 Connector elements: assembled and basic connectors [191].

Assembled	Basic translational	Basic rotational
BEAM	LINK	ALIGN
WELD	JOINT	REVOLUTE
HINGE	SLOT	UNIVERSAL
UJOINT	SLIDE-PLANE	CARDAN
CVJOINT	CARTESIAN	EULER
TRANSLATOR	RADIAL-THRUST	CONSTANT VELOCITY
CYLINDRICAL	AXIAL	ROTATION
PLANAR	PROJECTION CARTESIAN	FLEXION-TORSION
BUSHING		PROJECTION FLEXION-TORSION

The computational model developed utilised three-dimensional basic connector elements (CONN3D2, Connector 3D 2-nodes) to represent the muscle behaviour of the anconeus, biceps brachii and triceps brachii. Cartesian and Cardan type connectors were used to simulate the muscle force. The advantage of using these connector elements to represent the muscular behaviour is that they follow the local orientation defined by the two connected nodes.

The two nodes of each connector element represented the insertion points of the muscles and their positions were defined according to the literature [41, 44, 56, 90, 92]. By representing the muscle behaviour in this way, the force applied to the connector followed the relative position of the muscle anatomy during the flexion-

extension movement. That is, the direction of the muscle force changed according to the rotation of the elbow.

Cartesian connector element connects two nodes (a, b nodes) where the position of node b is measured according to the local coordinate system of node a, as illustrated in Figure 5.3a. A Cardan connector element allows rotation between two nodes (a, b nodes). Node b rotates with reference to the local coordinate system of node a, as shown in Figure 5.3b.
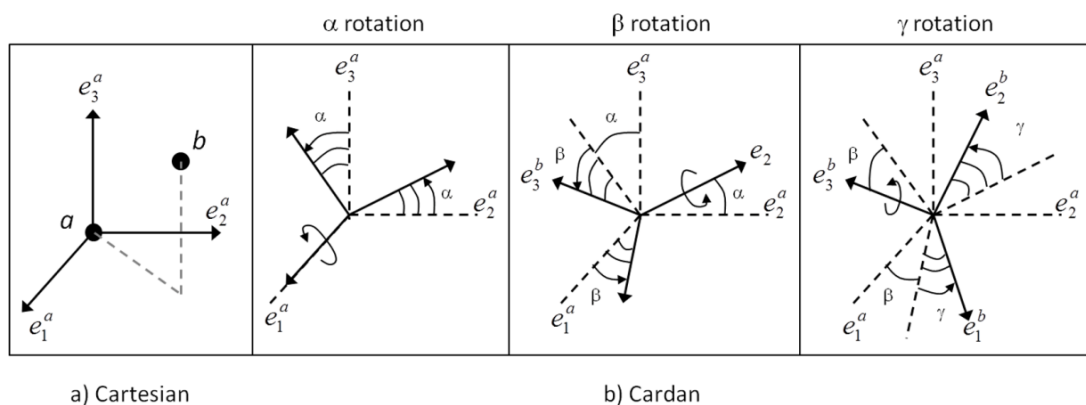
Figure 5.3 Connector elements: a) Cartesian connector for translation and b) Cardan connector for rotation. Adapted from [191].

5.2.1.4 Assembly

The geometric representations of the humerus, ulna and radius bones were assembled in the Abaqus CAE software. Figure 5.4 shows the assembled model. As the cartilage, cortical bone and trabecular bone of each had been created separately and the components brought together in the assembled model, this enabled the mechanical properties of the different bone type and cartilage to be defined and easily assigned.
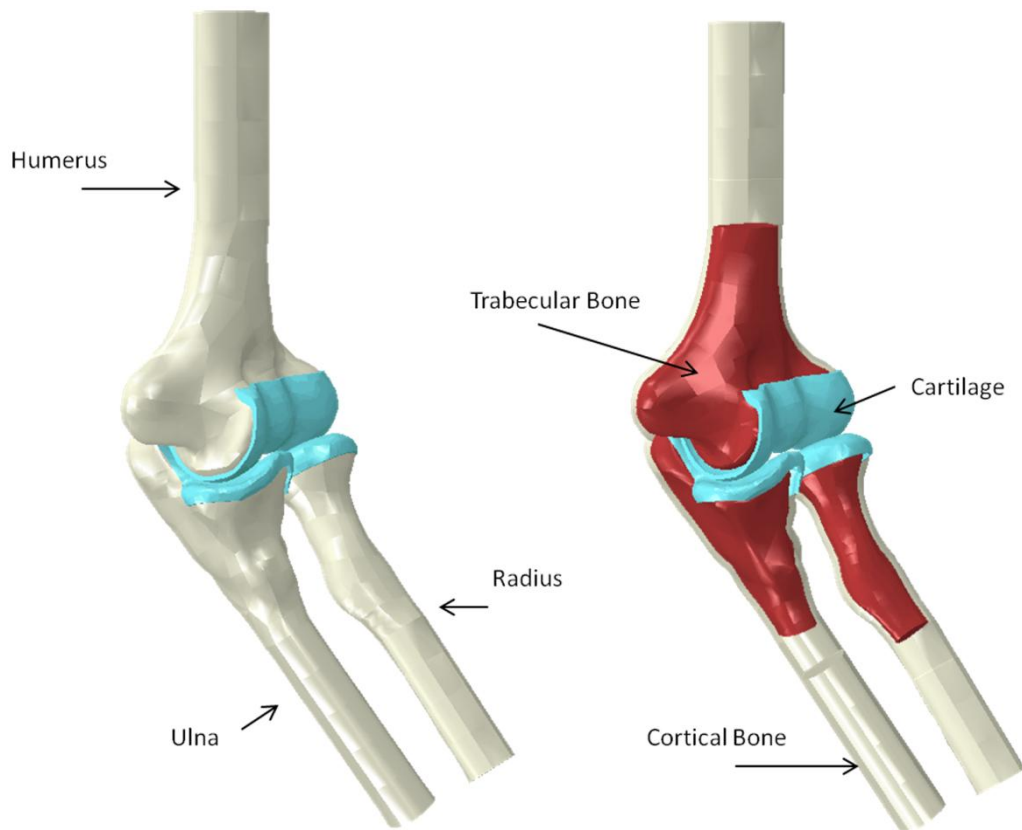
Figure 5.4 The elbow joint formed from the cartilage, cortical and trabecular bone.

5.2.2   Material properties

The mechanical properties of cortical bone, trabecular bone and cartilage were taken from the literature [196-199]. These describe the mechanical behaviour of the bone when it is exposed to external forces.

5.2.2.1   Mechanical properties of the bones and cartilage

The bone is one of the hardest structures of the human body, only the teeth being harder. The bones can resist large compressive or tensile forces. They protect internal organs, form part of the main structure of the body and play an important role in daily life activities. The high stiffness of the bones indicates that they do not allow large deformation when a load is applied to them. This enables them to be considered as effectively rigid bodies [41, 69, 92].

Bones are non-homogenous and anisotropic materials because they have an irregular internal structure. This means that bone has different properties, which change

157

according to their location. Furthermore, the mechanical properties of bones change with age and with activities performed by people. For example, people who undertake sports actively tend to have bones with higher density [41, 69, 91-92]. This study considered bone as exhibiting isometric, homogenous and continuous material behaviour. This assumption was considered sufficiently accurate as the analysis was focused on the contact area of the cartilage and the range of motion of the joint [195, 197, 200-202]. Bone is made of collagen and inorganic calcium salts. Its structure is formed by cortical bone, cancellous bone and a hollow space filled with bone marrow. Trabecular, cancellous or spongy bone is found in areas subjected to small stresses and compact or cortical bone is located in regions subjected to high stresses [41, 69, 92]. Table 5.5 shows the mechanical properties of the cortical bone, trabecular bone and cartilage applied to the elbow joint model.

Cartilage is an elemental part of the synovial joints. It covers the articular surface of the bones and reduces the friction between them. Furthermore, it can be found in different parts of the body, such as the ribs and spine. It is made of water, collagen and electrolytes. The friction in articulation increases when the cartilage is damaged producing pain in the joint. There are three types of cartilage in the human body, hyaline, yellow fibrocartilage and white fibrocartilage. The hyaline cartilage is also called articular cartilage and it is found in all synovial joints, such as the elbow, shoulder, knee and wrist. The main function of the articular cartilage is to reduce the friction between bones and decrease the impact of the forces transmitted by the joint. The white and yellow fibrocartilage helps to maintain the shape of the structures, such as the trachea and ear [41, 69, 92, 203]. The mechanical properties of the cartilage employed in the elbow model are listed in Table 5.5.

Table 5.5 Mechanical properties of cartilage, cortical and trabecular bone [196-199].

Material	Young's modulus E (MPa)	Poisson's ratio	Density (kg/m^3)
Cortical bone	17500	0.3	1997
Trabecular bone	309.8	0.3	330.5
Cartilage	12	0.4	1300

5.2.2.2 Mechanical properties of the collateral ligaments

Ligaments play a significant role in the passive stability of the joints. They connect the bones and constrain the movement of the articulations. They are composed of water, collagen and elastin. Ligaments are viscoelastic structures, which work mainly in tension [41, 69, 92, 94]. In this research, the collateral ligaments of the elbow were modelled as linear springs using SPRINGA elements in Abaqus CAE. Table 5.6 shows the stiffness of the lateral and medial collateral ligaments of the elbow employed for the model.

Table 5.6 Stiffness of the collateral ligaments of the elbow joint [204-208].

Elbow Ligaments	Stiffness [N/m]
Anterior Medial Collateral Ligament	k = 72 300
Posterior Medial Collateral Ligament	k = 52 200
Lateral Radial Collateral Ligament	k = 15 500
Lateral Ulnar Collateral Ligament	k = 57 000
Lateral Annular Collateral Ligament	k = 28 500

5.2.3 Boundary conditions

Loads and boundary conditions were applied to the elbow joint model in order to simulate the natural flexion-extension movement of the joint. The translation movement and rotation of the humerus in the global x, y and z axes were constrained in the distal part, as shown in Figure 5.5. The anconeus, biceps brachii and triceps brachii muscles were modelled with three connector elements, as illustrated in Figure 5.5 and Figure 5.6. The location and attachment points of the connectors were selected in accordance with the literature [41, 44, 56, 90, 92]. The biceps connector was placed in the anterior part of the elbow joint, arising from the radial tuberosity and ending fixed in the anterior side of the humerus, as illustrated in Figure 5.5. The triceps connector was placed in the posterior side of the humerus, starting from the olecranon tip of the ulna and finishing in the posterior side of the humerus. Although the biceps and triceps brachii muscles were not inserted in the scapula, they were inserted at the middle part of the humerus following the anatomical line of action. The anconeus muscle was placed in the posterolateral side of the elbow, arising from the lower part of the lateral epicondyle and inserted in the lateral side of the ulna.

The ends of the anconeus connector were attached to the bone geometry using a kinematic coupling, as illustrated in Figure 5.6. The attachment point of the biceps brachii connector in the radial tuberosity was simulated with a kinematic coupling and a kinematic coupling was also employed for the attachment point of the triceps brachii with the olecranon tip of the ulna. A force (152N) was applied to the biceps connector that generated around 90 degrees of flexion motion in the model. Subsequently, a force (180N) was applied to the triceps connector to produce an extension motion to return the elbow back to the initial position. The distal ends of the biceps and triceps connectors were fixed in the same way as the humerus, i.e. all translation and rotation motions were completely constrained.
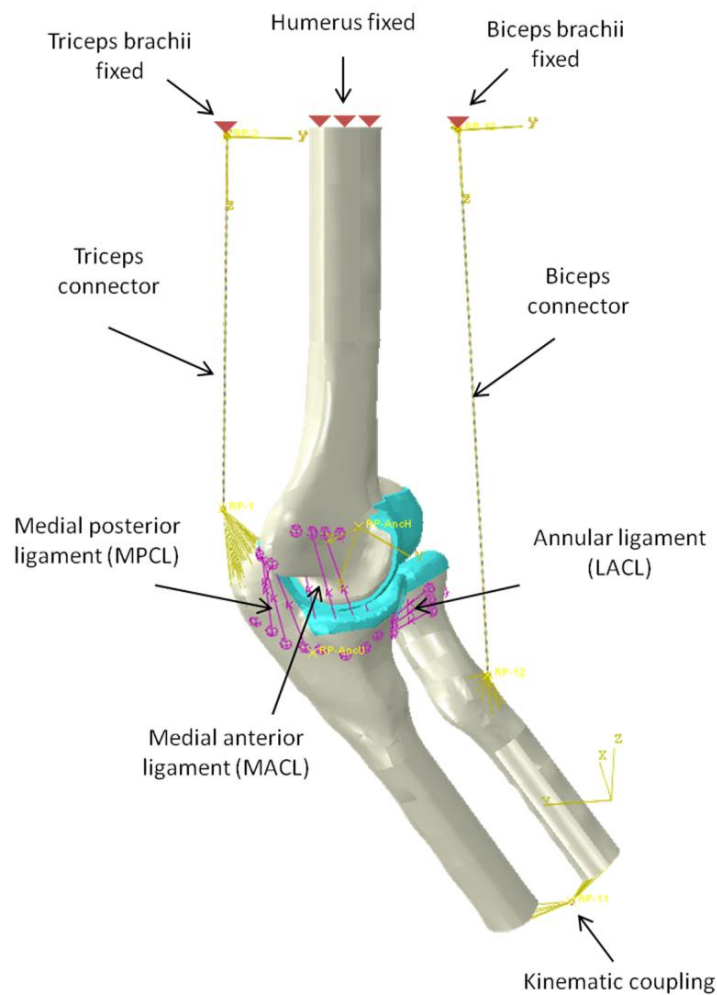
Figure 5.5 Boundary conditions of the elbow joint model (Medial view).

The origins and insertion points of the ligaments were located in the elbow model in accordance with the locations described and defined in the literature [48-49, 56, 59,

160

61-62]. Four springs were employed to represent for each ligament of the elbow. The annular ligament was represented with three springs. The interaction between cartilages was defined as a surface-to-surface interaction without friction. Based on the master-slave interaction, the degrees of freedom of the slave surface can be defined based on the master surface using kinematic constraints. The humerus cartilage was selected as the master surface because it underwent the minimum movement during the analysis. Conversely, the ulna and radius cartilage were defined as the slave surfaces because they underwent higher relative movement with respect to the humerus. This allocation of master and slave surfaces ensured rapid solution convergence in a low number of increments. Moreover, to ensure the ulna and radius bones moved at the same rate, the ends of the two bones were connected with a kinematic coupling, as illustrated in Figure 5.6.
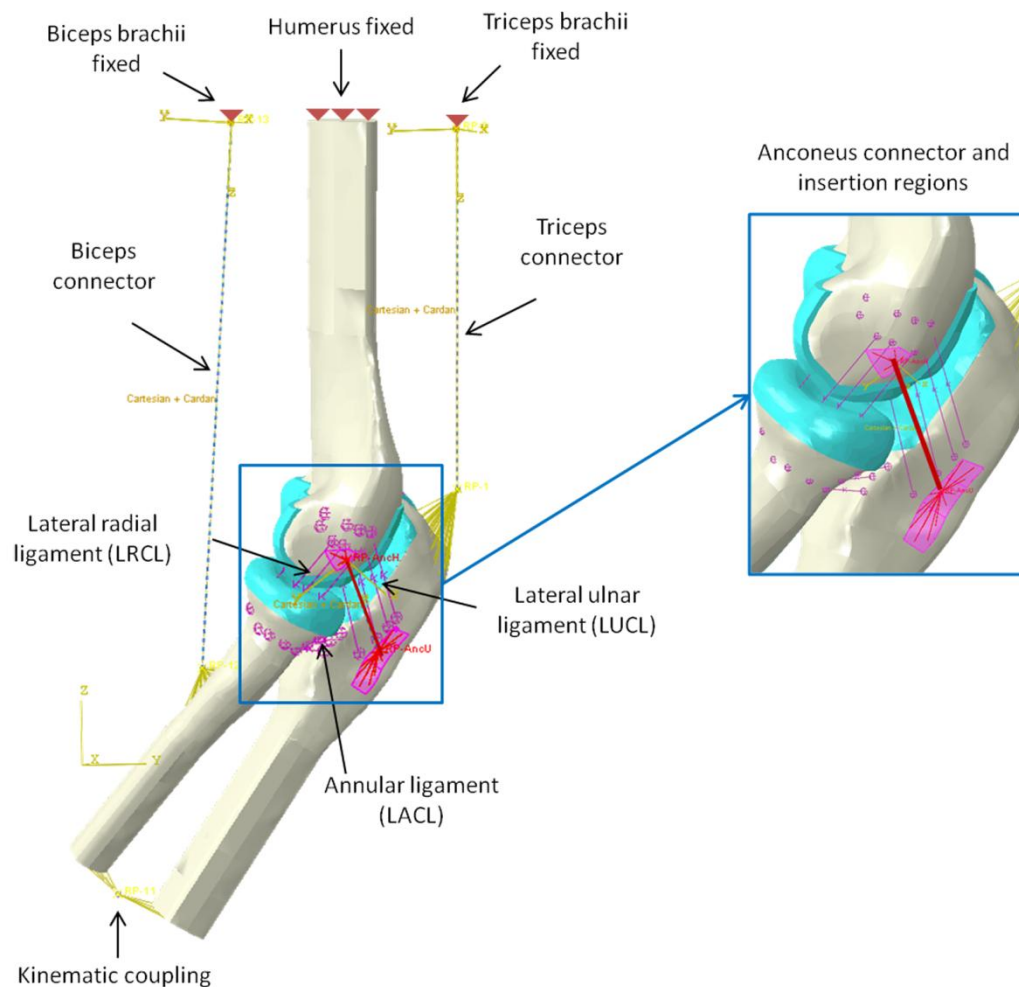
Figure 5.6 Boundary conditions of the elbow joint model: the red areas indicate the insertion regions of the anconeus muscle (Lateral view).

5.2.4   Mesh sensitivity analysis

A mesh sensitivity analysis is of paramount importance in finite element analysis. It enables a mesh density to be established that balances accuracy with computational requirements. In order to reduce the complexity of the elbow joint during the mesh sensitive analysis, the humerus and radius cartilage were only considered in the analysis. The geometry of the humerus and cartilage of the radius was meshed with 4-node linear tetrahedral elements, C3D4 (Continuum, 3D, 4-node).

The mesh of the bone and cartilage of the humerus was kept constant, as illustrated in Figure 5.7. The humerus cartilage was meshed with a global seed size of 0.5 mm and the humerus bone was meshed with a global seed of around 2 mm. Then, nine different mesh densities were selected for the radius cartilage leading to meshes with increasing numbers of elements, as illustrated in Figure 5.8.
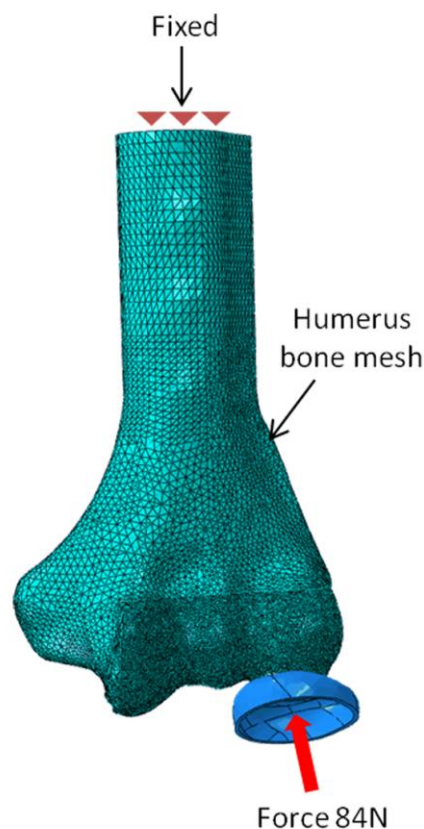
Figure 5.7 Mesh sensitive analysis of the radius cartilage: the mesh of the humerus was kept constant.

a) 507 Elements   b) 545 Elements   c) 653 Elements

d) 878 Elements   e) 2 240 Elements   f) 7 725 Elements

g) 48 380 Elements   h) 91 128 Elements   i) 197 545 Elements
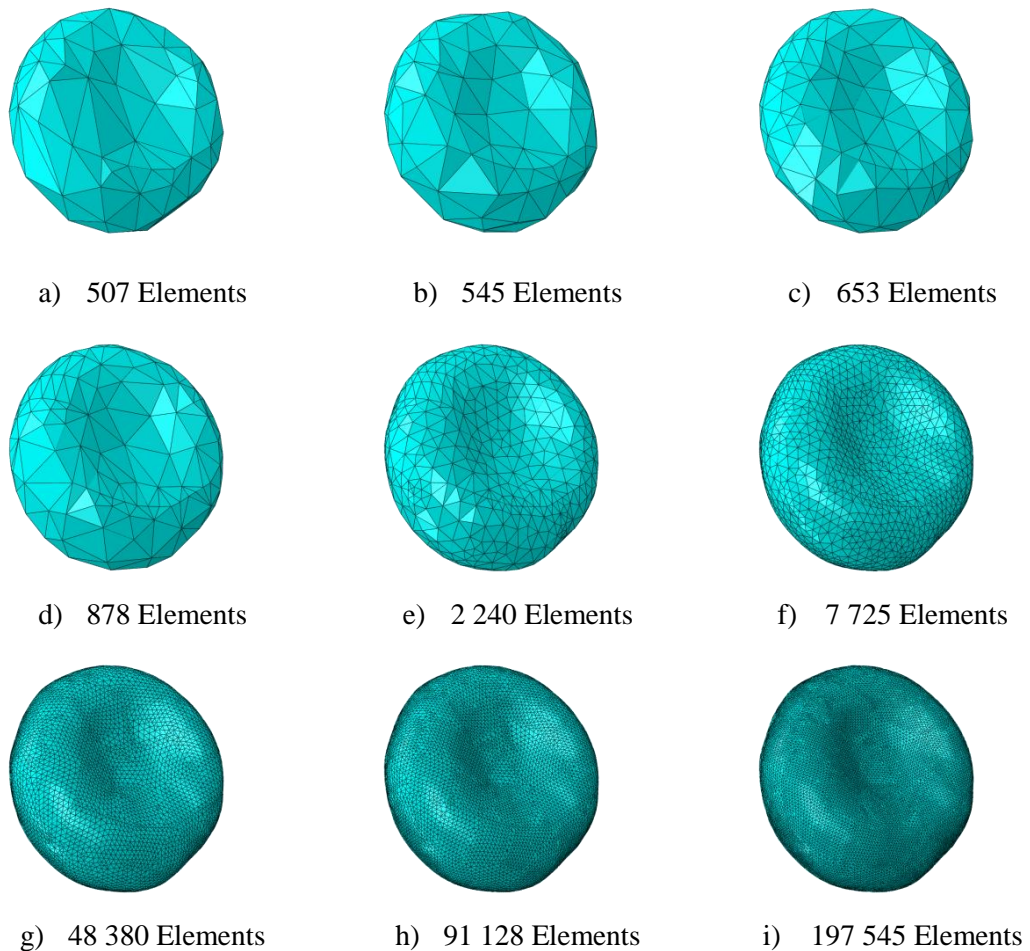
Figure 5.8 Cartilage of the radius with different number of elements.

Halls and Travill performed a study of the upper limb in human cadavers to investigate how the forces are transmitted from the hand to the humerus [70]. They applied a constant force of 147 N to the hand and measured the pressure in the humeroradial and humeroulnar joints using micro-transducers. They found that 57% of the force applied passed through the radiocapitellar joint and 43% of the force crossed on the humeroulnar joint [70]. Therefore, in the mesh sensitivity analysis 57% (84N) of a 147N force was applied to the radius.

The upper part of the humerus was fully fixed (displacement and rotation fully constrained in all directions). The force was applied and the analysis was run for the different mesh sizes with contact area calculated in each case. The contact area between cartilages was analysed because the range of motion and contact area in the articulation were the main focus when investigating the effect of the anconeus muscle on the elbow joint. Moreover, the contact area of the joint is an important

variable, which can be affected when the anconeus muscle is modelled with different loads conditions.

Table 5.7 shows the number of elements of the mesh of the radius cartilage, the total contact area, the global seed size of the elements and the percentage of variability of the contact area. The variability represents the difference in percentage of the contact area between one mesh and the next one. It was calculated from the following, equation (5.1).

$$Variability = \left| \frac{CA_i - CA_{i+1}}{CA_{i+1}} \right| * 100 \tag{5.1}$$

Where $Variability$ is the percentage of change of the contact area between one mesh and the next mesh size, CA_i represents the contact area for the number of elements (*i*) and CA_{i+1} is the contact area with the following number of elements (*i*+1).

Table 5.7 Elements and total contact area generated from different mesh densities.

Mesh	Mesh analysis		Global seed size		Variability
	Elements	Contact area (mm^2)	m	mm	%
Mesh a)	507	104.513	0.01	10	73.23
Mesh b)	545	60.332	0.008	8	37.06
Mesh c)	653	44.020	0.006	6	33.62
Mesh d)	878	66.315	0.004	4	58.08
Mesh e)	2240	41.951	0.002	2	11.35
Mesh f)	7725	37.675	0.001	1	4.01
Mesh g)	48380	39.250	0.0005	0.5	1.11
Mesh h)	91128	38.817	0.0004	0.4	0.75
Mesh i)	197545	39.110	0.0003	0.3	--

Figure 5.9 shows the total contact area of the humeroradial joint and the number of elements of the mesh. The contact area of the articulation changed by less than 2% when the number of elements employed in the radius cartilage mesh was 48 380 (global seed size of approximately 0.5mm) or more.
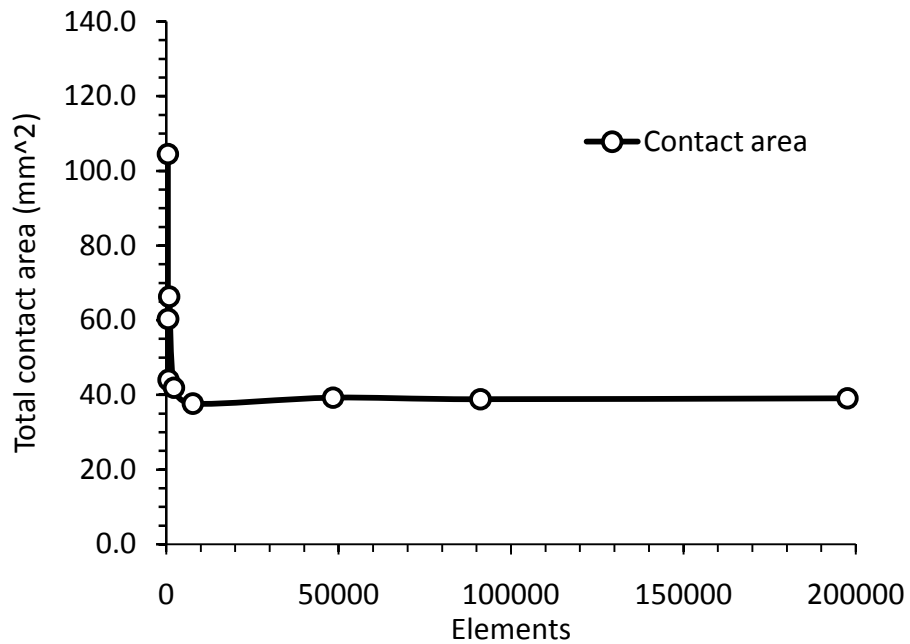
Figure 5.9 Number of elements versus total contact area of the humeroradial joint.

The mesh sensitivity analysis of the cartilage of the radius demonstrated that the number of elements required for the analysis should not be less than 48 000 elements in the cartilage region. In addition, the global seed size should be around 0.5 millimetres. Following the mesh sensitivity analysis, the finite element model of the elbow joint that was utilised for the study was meshed with C3D4, 4-node linear tetrahedral elements.

The element size of the cartilage region was 0.5 mm and the ends of the cortical bone of the humerus, ulna and radius was around 2 mm, as illustrated in Figure 5.10. This element size was used in the elbow joint model because in the mesh sensitivity analysis the contact area changed by less than 2% when the number of elements was increased beyond this level. Virtual topology was used to generate a uniform mesh and avoid distorted elements. The humerus was meshed with 207 402 elements, the ulna with 170 096 elements and the radius with 114 471 elements. The final assembled model consisted of a total of 491 969 4-node linear tetrahedral elements, 22 linear springs for the ligaments (SPRINGA) and 3 connector elements for the muscles (CONN3D2).
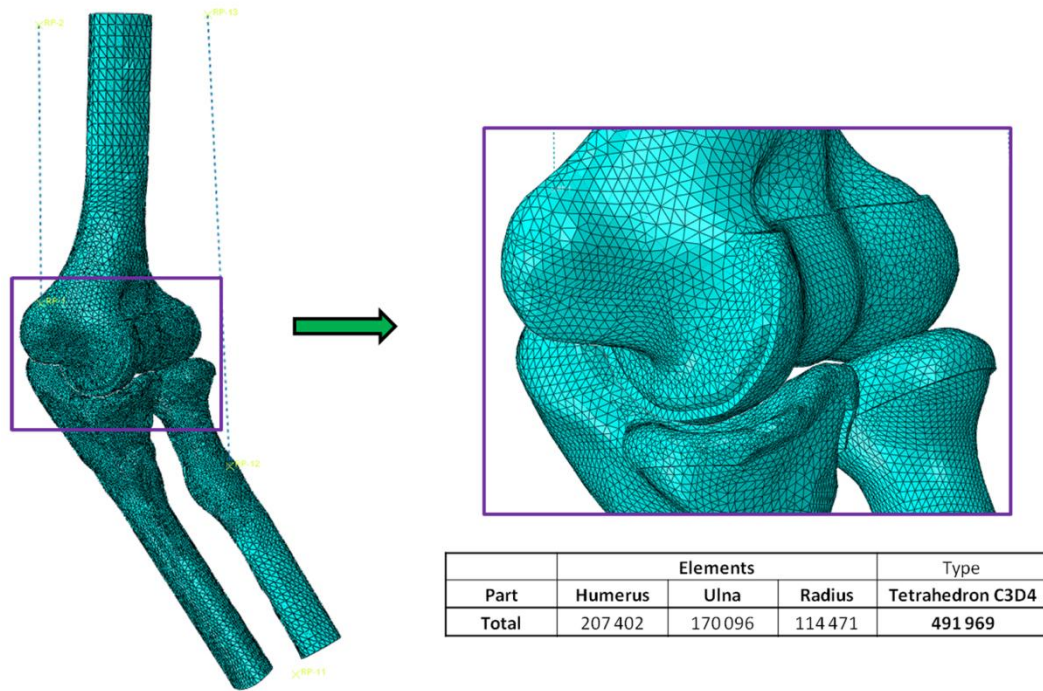
Figure 5.10 The elbow joint model meshed with tetrahedral elements C3D4.

5.3 Validation of the elbow model

The computational model of the elbow joint was validated by comparing the contact area pattern with the results from the experimental tests undertaken by Goto and colleagues [209]. The study undertaken by Goto et al. consisted in evaluating the contact area of three healthy elbows in vivo using a non-invasive technique and a markerless algorithm. The contact area of the articulation was measured at three different angles (0, 90, 135 degrees) with magnetic resonance imaging. The contact area obtained was found to be in the medial region of the ulna and humerus, as illustrated in Figure 5.11. The contact area of the radius was found to be in the central region of the head except at 135 degrees where it was in the anterior side of the head, as shown in Figure 5.12. It is worth to mention that the medial and lateral labels for the humerus in both figures (Figure 5.11and Figure 5.12) are misplaced.
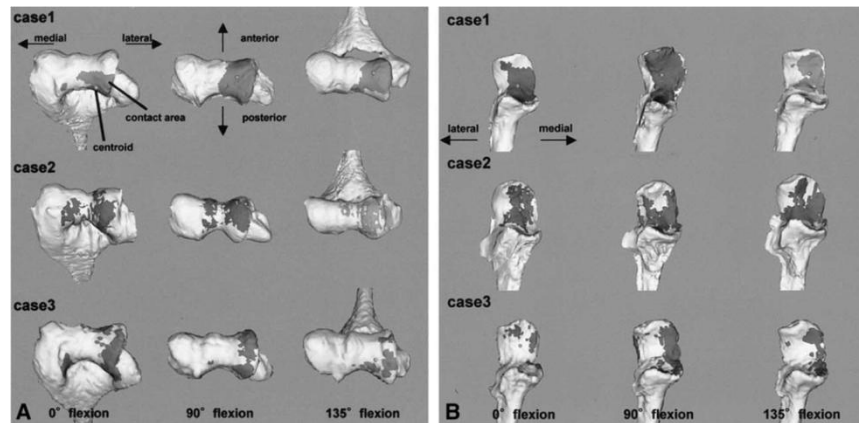
Figure 5.11 Contact area of the elbow joint: A) Contact area of the humerus, B) Contact area of the Ulna [209].
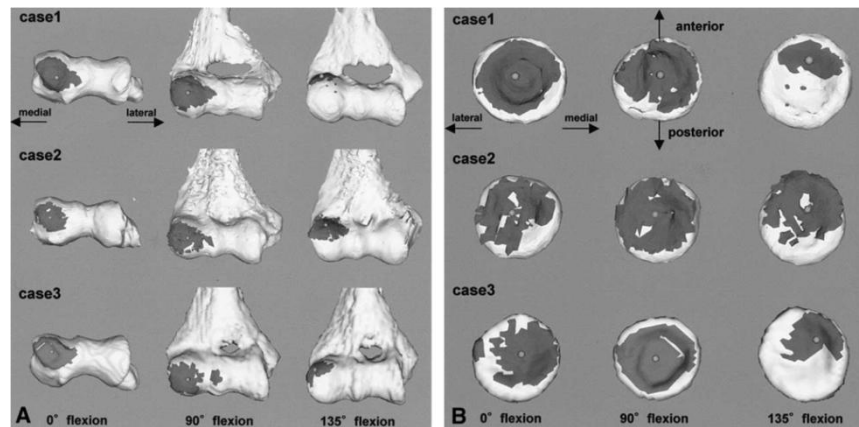
Figure 5.12 Contact area of the elbow joint: A) Contact area of the humerus, B) Contact area of the radius [209].

The contact area pattern predicted by the model was similar with the results of the experimental study performed by Goto and colleagues. In particular, the contact area in the trochlea notch of the ulna appeared in the medial side at the three angles, 0, 90 and 135 degrees. Moreover, the contact area of the radius at 0 degrees appeared in the centre of the head and moved to the edge at 90 degrees, as illustrated in Figure 5.13.

It is important to bear in mind that the contact area depends on several factors, such as load application and position of the joint [210-211]. Moreover, the mechanical properties used in the model could affect the contact area between the cartilages [192]. It is known that the contact area is reduced if the stiffness value of the material is too high [192-193]. Although the model considered just three muscles, the range of

motion and the contact area pattern accurately matched those obtained in previous studies [209]. Furthermore, springs and connector elements were considered in the model to simulate the collateral ligaments and muscles, respectively. These tools provided stability and allowed the natural flexion-extension movement of the joint.
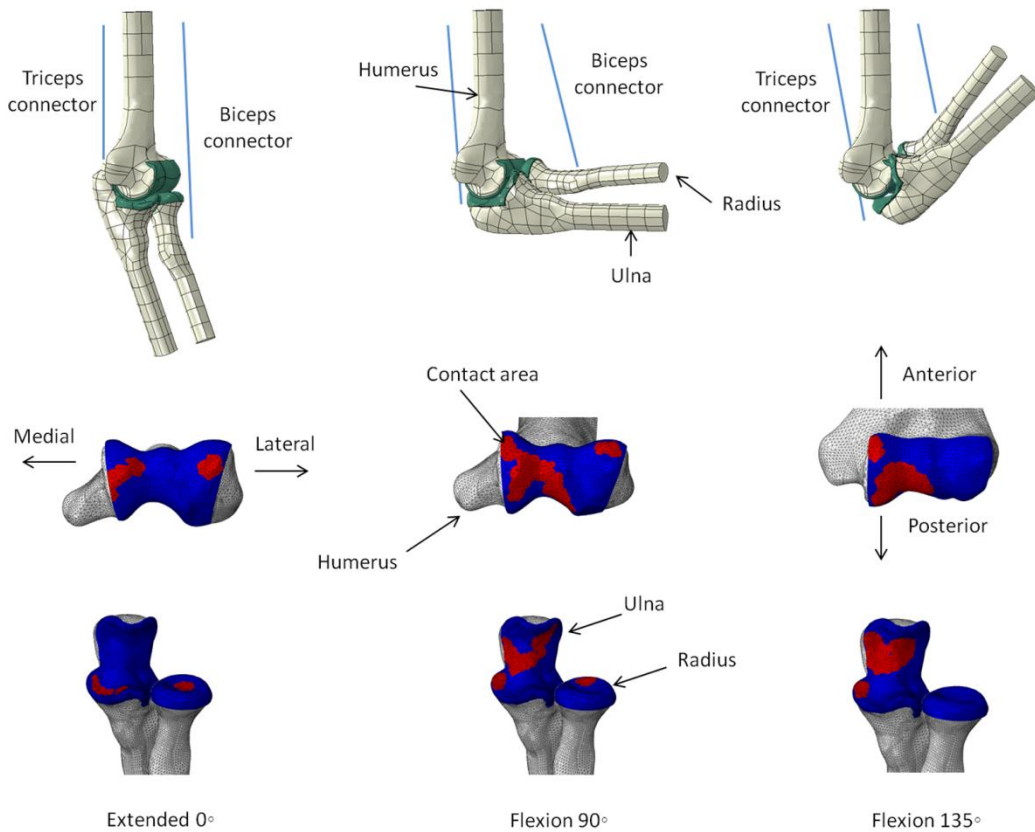
Figure 5.13 Contact area of the elbow joint at three different angles, 0, 90 and 135 degrees: predictions obtained from the finite element model.

5.4   Results

5.4.1   Range of motion of the elbow joint

The range of motion analysis of the elbow joint model was undertaken by applying one load for flexion (152N biceps connector) and another for extension (180N triceps connector). These loads were chosen as they produced a range of motion of approximately 90 degrees in flexion and extension respectively. The anconeus muscle was modelled with a connector element and four different loads were applied to the connector and the range of motion of the joint and articulation area analysed. It was assumed that the anconeus muscle can contribute up to a maximum of 15%

168

(27N) of the total extension force; therefore the first loading condition considered was with 15% (27N) of the total extension force applied as a loading to the anconeus.

The results from this analysis were taken as a reference against which those from the further analyses were compared. Next, to simulate the effect of deactivation of the anconeus, no force was applied to the anconeus connector; this represented the second load condition (0N or 0% of the total extension force). Again, the analysis was run and range of motion and joint contact area calculated. Subsequently, a force of 9N was applied to the anconeus representing 5% of the total force of the triceps brachii. Finally, the fourth force applied to the anconeus connector was 18N. This represented 10% of the total extension force. The effect of the ancones muscle on the elbow was quantified by measuring the change in the range of motion of the joint. The range of motion results obtained from the analysis are presented in Figure 5.14.
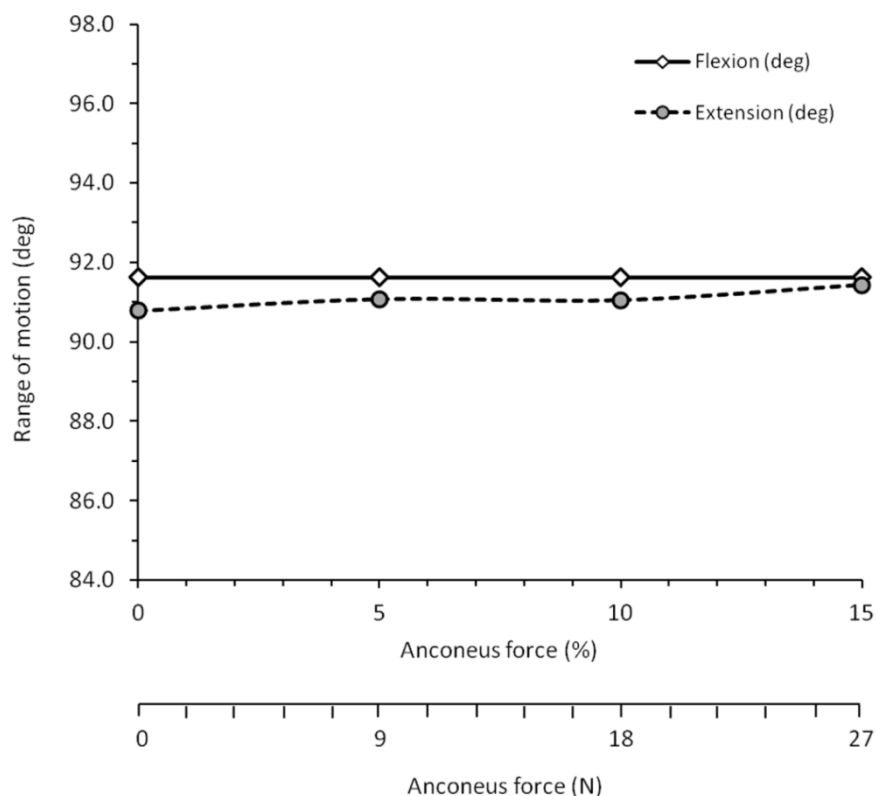

Figure 5.14 Range of motion of the elbow with four different loads applied to the anconeus muscle, 0N, 9N, 18N and 27N. The total force applied to the biceps brachii was 152N and the total force applied to the triceps brachii was 180N.

It is clear upon inspection of Figure 5.14 that the range of motion of the elbow joint changed less than one degree in the extension motion when the anconeus force was lower than 15% of the total force of triceps brachii. Therefore, from the computational analysis, it can be inferred that the effect of the anconeus muscle on the range of motion of the elbow joint is not significant when the force applied to the anconeus is below 15% of the total extension force. This outcome adds further evidence to that provided in chapter four to suggest that the effect of the anconeus muscle in the elbow kinematics is not significant. The range of motion during flexion was kept constant because the analysis of the loading conditions of the anconeus muscle was considered in the extension motion.

5.4.2 Contact area of the joint

The advantage of using connector elements to simulate the concentric contraction of the muscles is that the trochlea notch and the radial head follow the natural path of the flexion extension motion. This modelling decision was undertaken with the aim of representing the natural movement of the joint and the contact area between the cartilages. Figure 5.15 demonstrates that the anconeus muscle had a minor effect on the elbow joint contact area when the muscle force applied to the anconeus was less than 15% of the total extension force.
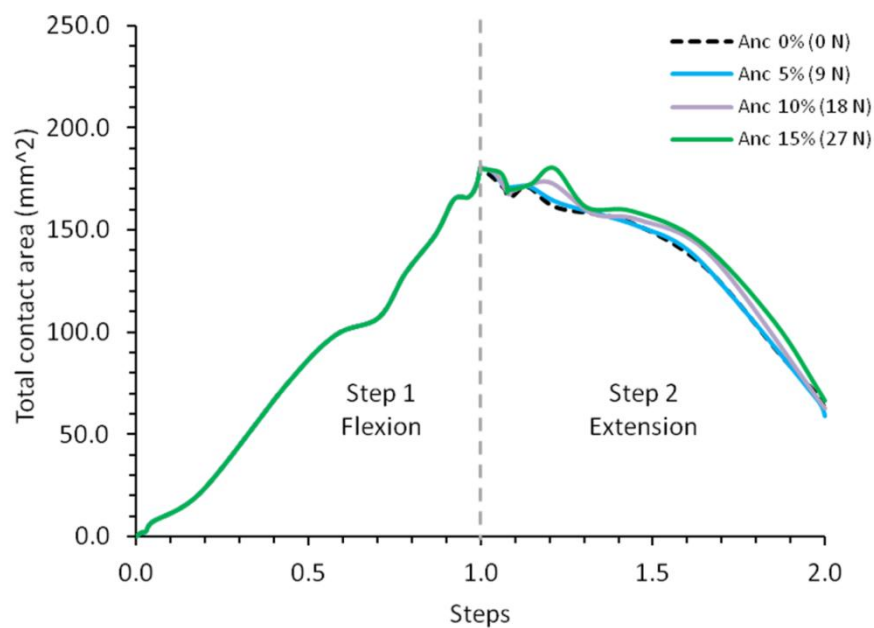
Figure 5.15 Contact area of the elbow joint during flexion and extension motions.

The contact area of the first loading condition (27N) of the anconeus muscle during the extension movement is presented in Figure 5.16. The contact area of the cartilage in the humerus, ulna and radius is presented at three different angles, 120, 90 and 30 degrees.

Figure 5.16 shows that the cartilage of the ulna exhibited a higher contact area during the whole range of motion and that the contact area of the cartilage of the radius changed during the movement. This indicates that the ulna bone has a major contribution to the stability of the articulation. Moreover, the contact area of the head of the radius tends to be at the edge region when the elbow is flexed more than 90 degrees.
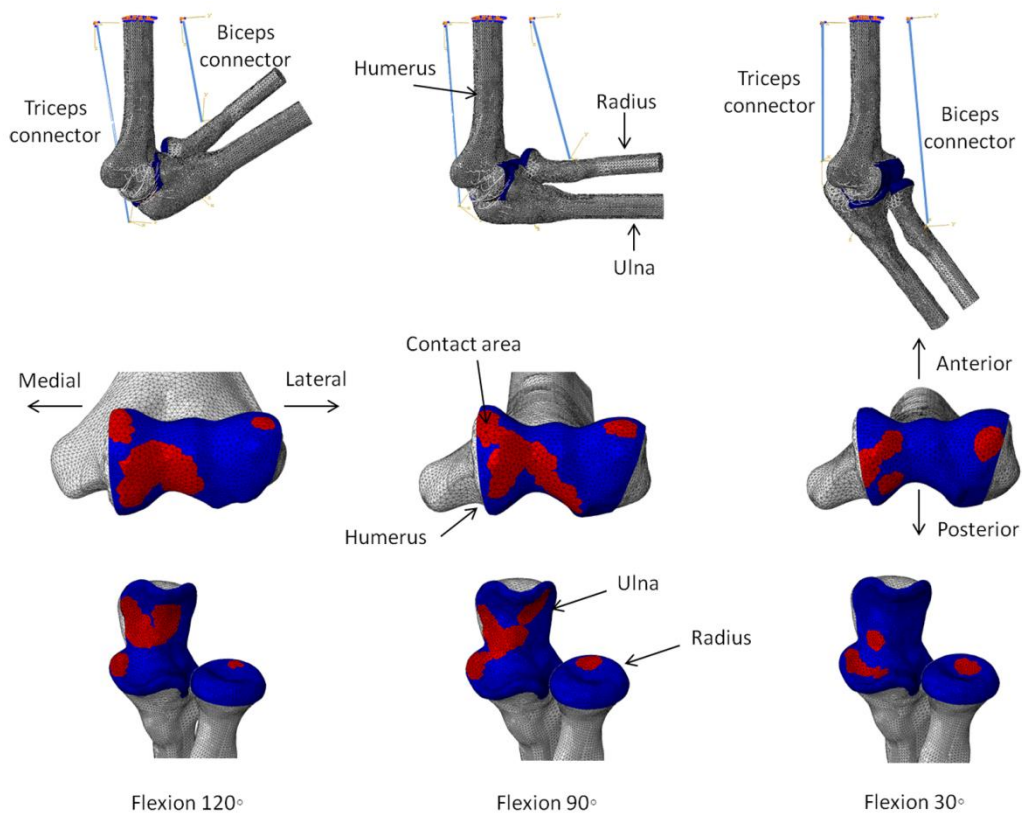
Figure 5.16 Contact area in the humerus, ulna and radius cartilages during extension motion at three different angles, 120, 90 and 30 degrees.

5.4.3 Effect of the anconeus on the elbow joint beyond its maximum reported contribution

In order to ascertain the percentage of the total extension load that the anconeus muscle would need to contribute in order to produce a significant effect on the joint, the elbow model was run with two loads beyond the reported maximum of 15% [34]. Loads representing 20% and 25% of the total extension force were applied to the anconeus connector and the effect on RoM and elbow joint contact area assessed. The outcome from this analysis indicated that the range of motion of the joint increased when the anconeus force was 36N (20%) and 45N (25%), as illustrated in Figure 5.17. In addition, the total contact area in the articulation increased beyond 20% of the total extension force, as shown in Figure 5.18.

Figure 5.17 Range of motion of the elbow with two more loads applied to the anconeus beyond its maximum contribution.
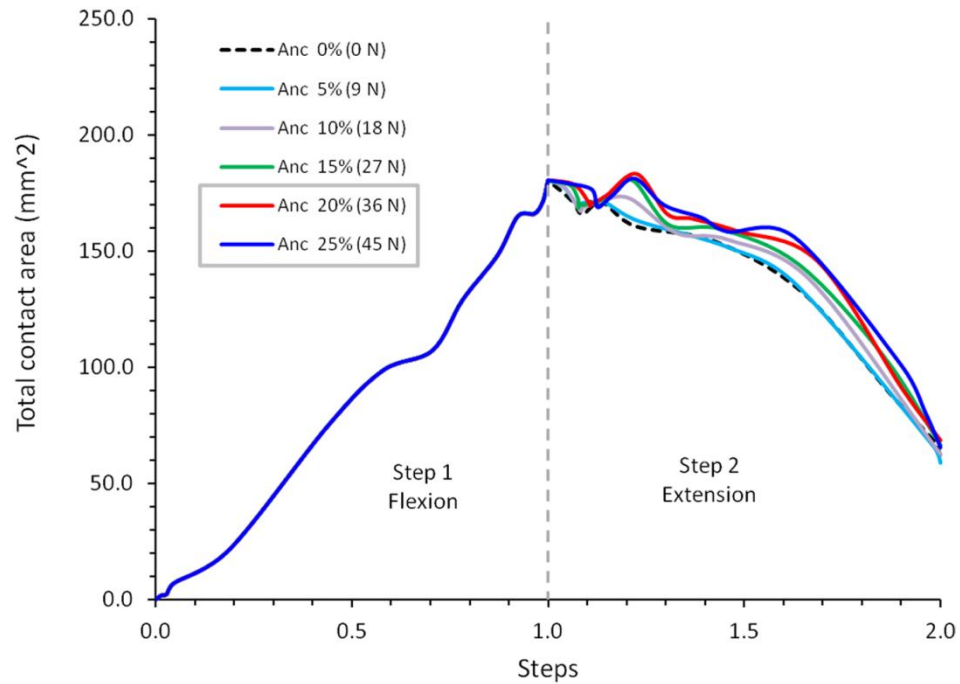
Figure 5.18 Total contact area of the joint with two more loads applied to the anconeus.

5.5   Discussion

This chapter has presented an investigation into the effect of the anconeus muscle by comparing the range of motion and co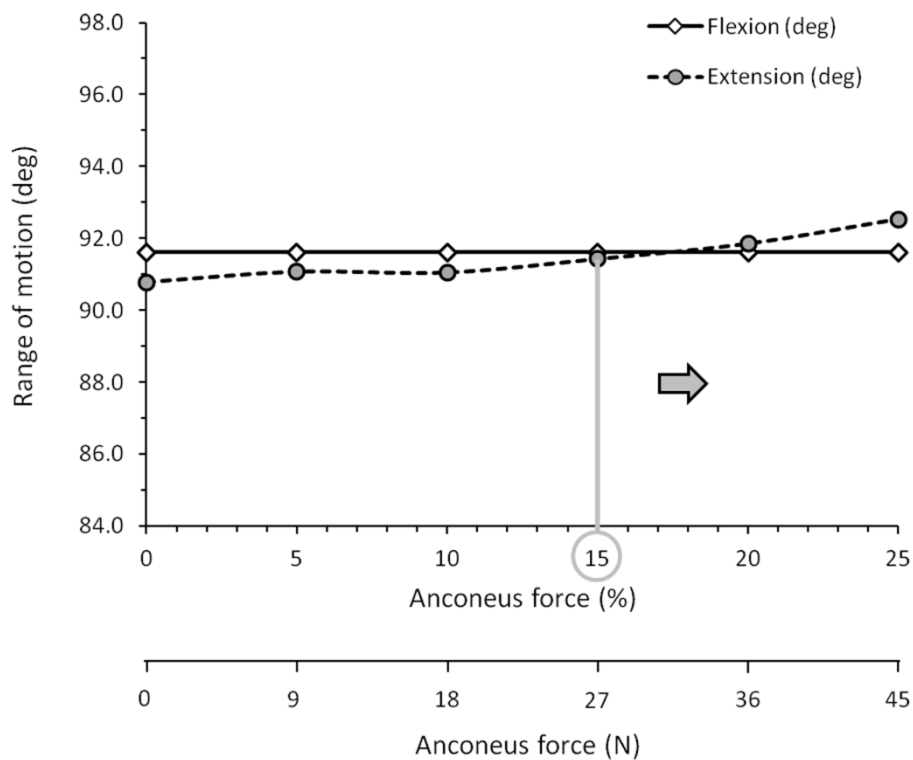ntact area of a computational model of the elbow joint when the anconeus muscle is subject to different loads up to the maximum it has been reported the anconeus can contribute to the overall extension force. It was found that the anconeus muscle did not produce a significant change in the range of motion and contact area in the articulation. These outcomes support the experimental investigation performed in chapter four. However, it was found that the effect of the anconeus muscle on the joint increased when the muscle was simulated with 20% and 25% of the total extension force.

The current chapter has shown the effect of the anconeus muscle on the contact area and range of motion of the elbow joint. However, the results of this study presented some limitations. For example, the force of the anconeus muscle was applied in a single line of action. This implied that the muscle worked like a fusiform muscle instead of a penniform shape. Similarly, the heads of the biceps and triceps brachii were ignored and the forces of the muscles were modelled in a single line of action.

173

Another limitation of this investigation was that the model did not consider all muscles crossing the elbow joint. The model was limited to the main flexor and extensor muscles, biceps brachii, anconeus and triceps brachii. Although this work gave a clear idea of the effect of anconeus on the elbow joint, it would be worth to see the effect of the anconeus muscle in the elbow kinematics considering all muscles crossing the joint. Furthermore, the range of motion during the analysis of flexion-extension was limited to 90 degrees. This range of motion of flexion-extension was from 30° to 120°.

The effect of the anconeus muscle on the contact area and range of motion of the elbow joint was determined from the flexion-extension movement. Nevertheless, the pronation-supination motion was not considered in the model, this mean that the outcomes were limited to the flexion-extension movement. The pronation-supination movement was not studied in the elbow model because the electrical activity of anconeus was negligible.

Finally, the following chapter presents the main conclusions of the different movements evaluated in this investigation and the future work.

CHAPTER SIX

6   CONCLUSIONS AND FUTURE WORK

6.1   Introduction

This thesis focused on the analysis of the electrical activity of the anconeus, biceps brachii and triceps brachii during elbow movement with the aim of elucidating the function and contribution of the anconeus in the kinematics and kinetics of the elbow joint. Healthy participants performed flexion-extension and supination-pronation movements of the elbow in the horizontal and sagittal planes before and after the anconeus was blocked with a local anaesthetic. The selected movements were considered to be representative of those common in daily life activities. Four movements were assessed at different elbow postures in the horizontal and sagittal planes. These movements were chosen so that an analysis of the effect of gravity on the movements could provide more information and insight into the anconeus muscle function. The results of the muscle electrical activity, kinematics and kinetics of the elbow were compared before and after the blocking.

In order to give further information and support the experimental studies, a computational model of the elbow joint was modelled. The elbow model considered the anconeus, biceps brachii, triceps brachii, collateral ligaments, cartilage, trabecular and cortical bone, trying to represent the real structure of the joint as much as possible. The flexion-extension movement of the elbow joint was simulated in a range of motion of 90 degrees from 30° to 120°. The anconeus muscle was modelled with different load conditions, simulating the maximum load contribution and the deactivation of the muscle.

6.2   Experimental studies of the elbow joint: a kinematic, kinetic and electromyographic analysis

The results of the relative electrical activity of the anconeus before blocking clearly indicated that the anconeus behaved as an extensor muscle of the elbow, during flexion-extension in the horizontal plane, in the sagittal plane while standing and during flexion-extension with the spine bent forward 90 degrees. There was no

electrical activity of the anconeus during pronation-supination with the elbow flexed 90 degrees, indicating the anconeus muscle does not contribute to the rotation of the forearm in unloaded conditions. Relative electrical activity of the biceps brachii and triceps brachii was present during the flexion and extension motions, respectively.

In the horizontal flexion-extension movements, the gravity force was perpendicular to the plane of movement. Therefore, the movement of the joint was a result of only muscle activity. The anconeus activity gradually increased in early extension when the net torque was negative and the net power was positive, implying that the dominant muscles at that level of the flexion-extension cycle were extensor muscles working concentrically. It was obvious that the electrical activity of anconeus presented higher amplitude during extension than flexion. These outcomes concur with previous observations reported by other researchers [22-25, 28, 31].

In sagittal plane flexion-extension movements, while standing, gravity was parallel to the plane of motion. Then, gravity created an extensor torque during extension motion and worked against the flexor muscles when the elbow was flexed. As a result, the amplitude of the myoelectric activity of the extensor muscles was reduced during extension movement. Here, it is clear that gravity assisted the function of the anconeus because its electrical activity was reduced, in the sagittal plane during extension, when gravity was producing an extensor torque. Moreover, it was obvious that gravity assisted extension motion because the major extensor muscle of the elbow (triceps brachii) was inactive during the extension motion.

Flexion-extension movements with the spine bent forward 90 degrees were also affected by gravity because the gravitational force was parallel to the plane of motion. The anconeus activity was affected by gravity in a way that indicated it was acting as an extensor muscle. That is, its relative electrical activity increased when the muscle worked against the flexor torque produced by gravity and decreased when the extensor torque produced by gravity assisted it. Moreover, the relative myoelectric activity of the anconeus and triceps brachii presented a similar trend, indicating that they play a similar role. These outcomes are valid for flexion-extension movements in the sagittal and horizontal plane with a range of motion of 90° from 30° to 120°.

The results of the current investigation showed that there was no electrical activity of the anconeus and triceps brachii during pronation and supination motion, suggesting that these muscles do not contribute to forearm rotation when the movement was not resisted. These outcomes agreed with some previous studies, which found that the anconeus was not active during unresisted pronation and supination movement [22-23]. In addition, the activity of the biceps brachii was found to be elevated during the supination motion, which was expected, as the biceps brachii contributes to supinate the forearm when the elbow is flexed at 90 degrees [75, 78, 125].

6.3 Effect of the anconeus muscle to the kinematics of the elbow joint: kinematic and electromyographic study

Several studies have found that the greatest activity of the anconeus muscle appears during extension of the elbow followed by resisted pronation-supination motion [22, 24-25, 31-32, 103]. Others have rejected the idea that the anconeus was an extensor muscle and have suggested that instead the muscle could abduct the ulna during pronation [1, 29-30]. Moreover, it has been proposed that the anconeus could be a stabiliser of the elbow joint [23, 31, 33, 35, 38]. It is clear from the previous investigations that agreement has not yet been reached within the research community about the specific function and contribution of the anconeus on the elbow movement.

Recent studies have found that the anconeus has a penniform structure, which could have a significant contribution in force production [37]. In addition, it has been found that the anconeus produces up to 15% of the extension torque during isometric contractions that require small joint torques [34]. More recent studies have concluded that the anconeus should be considered as a multifunctional muscle at the elbow, which could contribute in extension, stability and abduction of the ulna during pronation [40]. However, it has been suggested that anconeus should be considered as an extension of the triceps brachii muscle and its role in extension is merely an accessory [35].

The relative electrical activity results from the anconeus before blocking clearly indicate that the activity of the muscle is higher during the extension portion of the

flexion-extension cycle. Thus, implying that the anconeus behaves as an extensor muscle of the elbow as it has been reported by previous investigations. However, it was found that the anconeus defunctioning had no effect on the kinematics and kinetics of the elbow. The relationship of the angular velocity of the four movements, before and after deactivating the anconeus, followed a near-linear relationship with a slope close to one. Additionally, the t-test student analysis indicated that the effect of the anconeus on elbow kinematics was insignificant. Furthermore, the spectrum frequency analysis of the angular velocity, in all movements, demonstrates that the frequency components were the same before and after blocking anconeus.

The anconeus defunctioning did not show a significant effect on the net torque and net power of the elbow joint when the muscle was blocked with plain lidocaine. The net power and net torque during flexion-extension and pronation-supination movements in the horizontal and sagittal planes showed similar values before and after the anconeus was blocked with local anaesthesia. Moreover, the total net joint work remained almost the same before and after deactivating anconeus. The paired sample t-test analysis in this study indicated that the anconeus muscle does not have a significant contribution on the kinetics of the elbow joint.

The relative electrical activity of the biceps brachii and triceps brachii was not affected when the anconeus muscle was blocked with lidocaine. Their amplitudes remained almost the same before and after the blocking. The relative electrical activity of the triceps brachii was generally more elevated during the extension motion. However, it was not activated during the rotation of the forearm. The relative myoelectric activity of the biceps brachii was more elevated during the flexion motion and slightly elevated during the supination of the forearm.

6.4 Computational model of the elbow to measure the contribution of the anconeus muscle on the range of motion and contact area of the joint

The model of the elbow joint was created with the aim of investigating the effect of the anconeus muscle during the flexion-extension movement. The analysis was performed by comparing the range of motion and the contact area in the elbow joint.

The study focused on investigating the effect of the anconeus on a range of motion of 90 degrees, starting with the elbow extended at 30 degrees and ending flexed at 120 degrees, approximately. These conditions were similar to the experimental conditions described in chapter four. Four different loads were applied to the anconeus muscle; they represented 0%, 5%, 10% and 15% of the total extension force. The normal function of the anconeus was modelled by applying 15% of the total extension force and deactivation of the muscle was simulated by applying 0% of the load. The analysis of the results indicated that the anconeus muscle did not have a significant effect on the range of motion of the elbow and joint contact area during extension, essentially supporting the findings of the experimental research described in chapter four.

One limitation of the computational model was that the muscles were modelled with a single line of action using connectors sections. However, the biomechanics of the flexion and extension movements of the elbow was represented with accuracy using the connector tools. Furthermore, several studies have modelled the biceps and triceps brachii with a vector force following a line of action [197, 207-208]. Another limitation of the computational model was the number of muscles included in the analysis. Some muscles like brachialis and brachioradialis were ignored in the study. Similarly, the experimental studies of the EMG were limited to the main flexor and extensor muscles (biceps and triceps brachii) of the elbow; brachialis and brachioradialis muscles were ignored in the EMG analysis.

In conclusion, the relative electrical activity resulting from the anconeus before blocking suggested that it behaves as an extensor muscle. However, the results of the blocking trials indicated that the anconeus did not provide a significant contribution to elbow kinematics and kinetics. In addition, after anconeus blocking the relative electrical activity of the biceps brachii and triceps brachii remained essentially unaltered. These findings suggest that the anconeus is a relatively weak extensor. It is likely that the small contribution that the anconeus provided, during extension before blocking, was compensated by the triceps brachii after the anconeus was blocked. In addition, the computational model of the elbow joint supported the outcomes found in the experimental research. It is worth to mention that the main outcomes of this

research are valid for a range of motion of 90 degrees of flexion-extension and pronation-supination of the elbow joint.

6.5   Future work

The current investigation has presented the contribution of the anconeus muscle on the kinematics of the elbow joint and offer further insight into the function of the anconeus muscle at the elbow joint. However, further questions have been raised regarding the contribution of the anconeus muscle to the elbow kinematics in a range of motion of 90° of flexion-extension and pronation-supination. Moreover, this work studied the major flexor and extensor muscles of the elbow and ignored other flexor muscles, such as the brachialis and brachioradialis. With this in main, future work could be done to investigate the effect of the anconeus muscle in a major range of motion of the elbow considering all flexor muscles in the electromyographic, kinematic and kinetic analysis. In a similar way, the pronator and supinator muscles could be studied during the pronation-supination movement in a major range of motion of the elbow.

Furthermore, this work analysed a computational model of the elbow joint to measure the contribution of the anconeus muscle in the range of motion and contact area of the joint. The model evaluated the flexion-extension movement including all collateral ligaments, cartilage, anconeus, biceps brachii and triceps brachii. The analysis was performed simulating similar experimental conditions. Further research can be performed including brachialis, brachioradialis, pronator and supinator muscles in a higher range of motion of the joint.

The aim of this research was to evaluate the effect of the anconeus muscle in the kinematics of the elbow in the sagittal and horizontal plane. Other question raised from this study refers to the contribution of anconeus in the kinematics of the elbow during activities that require high precision, such as painting or gymnastics.

REFERENCES

1.   Duchenne G B A. 1867. Physiology of motion demonstrated by means of electrical stimulation and clinical observation and applied to the study of paralysis and deformities. Philadelphia: J. B. Lippincott Company.

2.   Pankovich A M. 1977. Anconeus approach to the elbow joint and the proximal part of the radius and ulna. J Bone Joint Surg Am 59(1): 124-26.

3.   Almquist E E, Necking L, Bach A W. 1998. Epicondylar resection with anconeus muscle transfer for chronic lateral epicondylitis. J Hand Surg Am 23(4): 723-31.

4.   Schmidt C C, Kohut G N, Greenberg J A, Kann S E, Idler R S, Kiefhaber T R. 1999. The anconeus muscle flap: its anatomy and clinical application. J Hand Surg Am 24(2): 359-69.

5.   Degreef I, Van Raebroeckx A, De Smet L. 2005. Anconeus muscle transposition for failed surgical treatment of tennis elbow: preliminary results. Acta Orthop Belg 71(2): 154-56.

6.   Luchetti R, Atzei A, Brunelli F, Fairplay T. 2005. Anconeus muscle transposition for chronic lateral epicondylitis, recurrences, and complications. Tech Hand Up Extrem Surg 9(2): 105-12.

7.   Nishida K, Iwasaki N, Minami A. 2009. Anconeus muscle flap for the treatment of soft tissue defects over the olecranon after total elbow arthroplasty. J Hand Surg Eur Vol 34(4): 538-39.

8.   Fleager K E, Cheung E V. 2011. The "anconeus slide": rotation flap for management of posterior wound complications about the elbow. J Shoulder Elbow Surg 20(8): 1310-16.

9.   Ng Z Y, Lee S W J, Mitchell J H, Fogg Q A, Hart A M. 2012. Functional anconeus free flap for thenar reconstruction: a cadaveric study. Hand 7(3): 286-92.

10.   Habib M, Tanwar Y S, Jaiswal A, Singh S P, Sinha S, Lal H. 2014. Anconeus pedicle olecranon flip osteotomy: an approach for the fixation of complex intraarticular distal humeral fractures. Bone Joint J 69B(9): 1252-57.

11.   Morrey B F, Schneeberger A G. 2002. Anconeus arthroplasty: a new technique for reconstruction of the radiocapitellar and/or proximal radioulnar joint. J Bone Joint Surg Am 84(11): 1960-69.

12.   Seyahi A, Atalar A C, Demirhan M. 2009. Anconeus arthroplasty: a salvage procedure in recurrent heterotopic ossification. Acta Orthop Traumatol Turc 43(1): 62-66.

13.   Nishida K, Iwasaki N, Funakoshi T, Masuko T, Minami A. 2010. Prevention of instability of the proximal end of the radius after radial head resection using an anconeus muscle flap: level 4 evidence. J Hand Surg-Am 35(10, Supplement): 5-6.

14.   Baghdadi Y M K, Morrey B F, Sanchez-Sotelo J. 2014. Anconeus interposition arthroplasty: mid- to long-term results. Clin Orthop 472(7): 2151-61.

15.   Natarajan V, Velmuregendran C U. 1995. Repetitive nerve stimulation on anconeus muscle. Electromyogr Motor C 97(4): S217.

16.   Kennett R P, Fawcett P R W. 1993. Repetitive nerve stimulation of anconeus in the assessment of neuromuscular transmission disorders. Electromyogr Motor C 89(3): 170-76.

17. Coriolano M D G W S, De Amorim Jr A A, Lins O G. 2007. Repetitive stimulation test on the anconeus muscle for the diagnosis of myasthenia gravis: the mapping of its motor end-plate area. Arq Neuropsiquiatr 65(2 B): 488-91.

18. Maselli R A, Mass D P, Distad B J, Richman D P. 1991. Anconeus muscle: a human muscle preparation suitable for in-vitro microelectrode studies. Muscle Nerve 14(12): 1189-92.

19. Costa J, Evangelista T, Conceição I, Carvalho M d. 2004. Repetitive nerve stimulation in myasthenia gravis relative sensitivity of different muscles. Clin Neurophysiol 115(12): 2776-82.

20. Coel M, Yamada C Y, Ko J. 1993. MR imaging of patients with lateral epicondylitis of the elbow (tennis elbow): importance of increased signal of the anconeus muscle. Am J Roentgenol 161(5): 1019-21.

21. Steinmann S P, Bishop A T. 2000. Chronic anconeus compartment syndrome: a case report. J Hand Surg-Am 25(5): 959-61.

22. Travill A A. 1962. Electromyographic study of the extensor apparatus of the forearm. Anat Rec 144: 373-76.

23. Pauly J E, Rushing J L, Scheving L E. 1967. An electromyographic study of some muscles crossing the elbow joint. Anat Rec 159(1): 47-53.

24. Le Bozec S, Maton B, Cnockaert J C. 1980. The synergy of elbow extensor muscles during static work in man. Eur J Appl Physiol 43(1): 57-68.

25. Le Bozec S, Maton B, Cnockaert J C. 1980. The synergy of elbow extensor muscles during dynamic work in man. I. Elbow extension. Eur J Appl Physiol 44(3): 255-69.

26. Le Bozec S, Maton B. 1982. The activity of anconeus during voluntary elbow extension: the effect of lidocaine blocking of the muscle. Electromyogr Clin Neurophysiol 22(4): 265-75.

27. Praagman M, Chadwick E K J, Van der Helm F C T, Veeger H E J. 2010. The effect of elbow angle and external moment on load sharing of elbow muscles. J Electromyogr Kinesiol 20(5): 912-22.

28. Guillot M, Escande G, Chazal J, Vanneuville G. 1984. The anconeus muscle. Anatomical and electromyographic study. C R Assoc Anat 68(202): 337-43.

29. Ray R D, Johnson R J, Jameson R M. 1951. Rotation of the forearm; an experimental study of pronation and supination. J Bone Joint Surg Am 33 A(4): 993-96.

30. Gleason T F, Goldstein W M, Ray R D. 1985. The function of the anconeus muscle. Clin Orthop 192: 147-48.

31. Basmajian J V, Griffin Jr W R. 1972. Function of anconeus muscle: an electromyographic study. J Bone Joint Surg Am 54(8): 1712-14.

32. Hora B. 1959. O Musculus Anconeus contribuição ao estudo da sua arquitetura e das suas funções. Thesis. The University of Recife, Brazil.

33. O'Driscoll S W, Jupiter J B, King G J W, Hotchkiss R N, Morrey B F. 2000. The unstable elbow. J Bone Joint Surg Am 82(5): 724-24.

34. Zhang L Q, Nuber G W. 2000. Moment distribution among human elbow extensor muscles during isometric and submaximal extension. J Biomech 33(2): 145-54.

35. Molinier F, Laffosse J M, Bouali O, Tricoire J L, Moscovici J. 2011. The anconeus, an active lateral ligament of the elbow: new anatomical arguments. Surg Radiol Anat 33(7): 617-21.

36. An K N, Hui F C, Morrey B F. 1981. Muscles across the elbow joint: a biomechanical analysis. J Biomech 14(10): 659-69.

37. Coriolano M G W S, Lins O G, Amorim M J A A L, Amorim Jr A A. 2009. Anatomy and functional architecture of the anconeus muscle. Int J Morphol 27(4): 1009-12.

38. Pereira B P. 2012. Revisiting the anatomy and biomechanics of the anconeus muscle and its role in elbow stability. Ann Anatomy 195(4): 365-70.

39. Werner S L, Fleisig G S, Dillman C J, Andrews J R. 1993. Biomechanics of the elbow during baseball pitching. J Orthop Sports Phys Ther 17(6): 274-78.

40. Bergin M J G, Vicenzino B, Hodges P W. 2013. Functional differences between anatomical regions of the anconeus muscle in humans. J Electromyogr Kinesiol 23(6): 1391-97.

41. Palastanga N, Field D, Soames R. 2002. Anatomy and human movement: structure and function. 4th ed. Elsevier Health Sciences.

42. Moore K L. 2014. Clinically oriented anatomy. 7th ed. Philadelphia, Pa: London: Wolters Kluwer Health/Lippincott Williams & Wilkins.

43. Kim P T, Isogai S, Murakami G, Wada T, Aoki M, Yamashita T, Ishii S. 2002. The lateral collateral ligament complex and related muscles act as a dynamic stabilizer as well as a static supporting structure at the elbow joint: an anatomical and experimental study. Okajimas Folia Anat Jpn 79(2-3): 55-62.

44. Rizzo D C. 2001. Instructor's manual for Delmar's fundamentals of anatomy & physiology. South Melbourne, Victoria, Australia. Stanford, CT, U.S: Delmar.

45. Lockard M. 2006. Clinical biomechanics of the elbow. J Hand Ther 19(2): 72-81.

46. King G J W, Morrey B F, An K-N. 1993. Stabilizers of the elbow. J Shoulder Elbow Surg 2(3): 165-74.

47. Kingston B. 2001. Understanding joints: a practical guide to their structure and function. Cheltenham: Nelson Thornes.

48. Brabston III E W, Genuario J W, Bell J-E. 2009. Anatomy and physical examination of the elbow. Oper Techn Orthopade 19(4): 190-98.

49. Modi C S, Lawrence E, Lawrence T M. 2012. Elbow instability. Orthop Trauma 26(5): 316-27.

50. Lawry G V, Grigoriadis E. 2010. The elbow. Fam's musculoskeletal examination and joint injection techniques. 2nd ed. Jerome G V L J K A H, Editor. Mosby: Philadelphia. p. 21-28.

51. Murray W M, Buchanan T S, Delp S L. 2000. The isometric functional capacity of muscles that cross the elbow. J Biomech 33(8): 943-52.

52. Martini F. 2006. Fundamentals of anatomy & physiology. 7th ed. San Francisco: Pearson/Benjamin Cummings.

53. Gray H. 1918. Anatomy of the body human. 20th ed. Philadelphia: Lea & Febiger.

54. Bell T H, Ferreira L M, McDonald C P, Johnson J A, King G J W. 2010. Contribution of the olecranon to elbow stability: an in vitro biomechanical study. J Bone Joint Surg Am 92(4): 949-57.

55. Chen N C, Jupiter J B, Steinmann S P, Ring D. 2014. Nonacute treatment of elbow fracture with persistent ulnohumeral dislocation or subluxation. J Bone Joint Surg Am 96(15): 1308-16.

56. Celli A. 2008. Anatomy and biomechanics of the elbow. Treatment of elbow lesions. Springer-Verlag: Milan Italy. p. 1-11.

57. Morrey B F, An K-N. 2005. Stability of the elbow: osseous constraints. J Shoulder Elbow Surg 14(1, Supplement): S174-S78.

58. Charalambous C P, Stanley J K. 2008. Posterolateral rotatory instability of the elbow. J Bone Joint Surg Br 90(3): 272-79.

59. Safran M R, Baillargeon D. 2005. Soft-tissue stabilizers of the elbow. J Shoulder Elbow Surg 14(1): S179-S85.

60. Hannouche D, Bégué T. 1999. Functional anatomy of the lateral collateral ligament complex of the elbow. Surg Radiol Anat 21(3): 187-91.

61. Cohen M S, Hastings H. 1997. Rotatory instability of the elbow. The anatomy and role of the lateral stabilizers. J Bone Joint Surg Am 79(2): 225-33.

62. Bell S. 2008. Elbow instability, mechanism and management. Curr Orthopaed 22(2): 90-103.

63. O'Driscoll S W, Horii E, Morrey B F, Carmichael S W. 1992. Anatomy of the ulnar part of the lateral collateral ligament of the elbow. Clin Anat 5(4): 296-303.

64. Takigawa N, Ryu J, Kish V L, Kinoshita M, Abe M. 2005. Functional anatomy of the lateral collateral ligament complex of the elbow: morphology and strain. J Hand Surg Br 30(2): 143-47.

65. Olsen B S, Henriksen M G, Søjbjerg J O, Helmig P, Sneppen O. 1994. Elbow joint instability: a kinematic model. J Shoulder Elbow Surg 3(3): 143-50.

66. Floris S, Olsen B S, Dalstra M, Søjbjerg J O, Sneppen O. 1998. The medial collateral ligament of the elbow joint: anatomy and kinematics. J Shoulder Elbow Surg 7(4): 345-51.

67. Conway J E, Lowe W R. 2001. Elbow medial ulnar collateralligament reconstruction. Oper Techn Sport Med 9(4): 196-204.

68. Hotchkiss R N, Weiland A J. 1987. Valgus stability of the elbow. J Orthop Res 5(3): 372-77.

69. Tözeren A. 2000. Human body dynamics: classical mechanics and human movement. Washington, DC. USA: New York Springer Science & Business Media.

70. Halls A A, Travill A. 1964. Transmission of pressures across the elbow joint. The Anatomical Record 150(3): 243-47.

71. Narici M. 1999. Human skeletal muscle architecture studied in vivo by non-invasive imaging techniques: functional significance and applications. J Electromyogr Kinesiol 9(2): 97-103.

72. Gonzalez R V, Hutchins E L, Barr R E, Abraham L D. 1996. Development and evaluation of a musculoskeletal model of the elbow joint complex. J Biomech Eng 118(1): 32-40.

73. Amis A A. 2012. Biomechanics of the elbow. Operative elbow surgery. Elsevier Health Sciences: London, UK. p. 816.

74. Neumann D A. 2010. Kinesiology of the musculoskeletal system: fundations for rehabilitation. 2nd ed. St Louis, Missouri, United States: Mosby Inc. .

75. Basmajian J V, Latif A. 1957. Integrated actions and functions of the chief flexors of the elbow: a detailed electromyographic analysis. J Bone Joint Surg Am 39 A(5): 1106-18.

76. Leonello D T, Galley I J, Bain G I, Carter C D. 2007. Brachialis muscle anatomy: a study in cadavers. J Bone Joint Surg Am 89(6): 1293-97.

77.	Basmajian J V, Travill A. 1961. Electromyography of the pronator muscles in the forearm. Anat Rec 139(1): 45-49.

78.	Travill A, Basmajian J V. 1961. Electromyography of the supinators of the forearm. Anat Rec 139(4): 557-60.

79.	Sardelli M, Tashjian R Z, MacWilliams B A. 2011. Functional elbow range of motion for contemporary tasks. J Bone Joint Surg Am 93(5): 471-77.

80.	Morrey B F, Askew L J, An K N, Chao E Y. 1981. A biomechanical study of normal functional elbow motion. J Bone Joint Surg Am 63(6): 872-77.

81.	London J. 1981. Kinematics of the elbow. J Bone Joint Surg Am 63(4): 529-35.

82.	Amis A A, Dowson D, Wright V. 1979. Muscle strengths and musculoskeletal geometry of the upper limb. Eng Med 8(1): 41-48.

83.	Matsuki K O, Matsuki K, Mu S, Sasho T, Nakagawa K, Ochiai N, Takahashi K, Banks S A. 2010. In vivo 3D kinematics of normal forearms: analysis of dynamic forearm rotation. Clin Biomech 25(10): 979-83.

84.	Youm Y, Dryer R F, Thambyrajah K, Flatt A E, Sprague B L. 1979. Biomechanical analyses of forearm pronation-supination and elbow flexion-extension. J Biomech 12(4): 245-51, 53-55.

85.	Robertson D G E. 2004. Research methods in biomechanics. Champaign, III: Human Kinetics.

86.	Dempster W T. 1955. Space requirements of the seated operator: geometrical, kinematic and mechanical aspects of the body with special reference to the limbs. WADC Technical Report 55-159 Wright-Patterson Air Force Base Ohio USA.

87.	Zatsiorsky V M. 2002. Kinetics of human motion. Champaign, IL: Human Kinetics.

88.	Winter D A. 2009. Biomechanics and motor control of human movement. 4th ed. Hoboken, NJ: John Wiley & Sons, Inc.

89.	Sasaki K, Neptune R R, Kautz S A. 2009. The relationships between muscle, external, internal and joint mechanical work during normal walking. J Exp Biol 212(5): 738-44.

90.	Cael C. 2010. Functional anatomy: musculoskeletal anatomy, kinesiology, and palpation for manual therapists. Philadelphia: Wolters Kluwer.

91.	Freivalds A. 2003. Biomechanics of the upper limbs : mechanics, modelling and musculoskeletal injuries. London: Taylor & Francis.

92.	Nordin M. 2004. Basic biomechanics of the musculoskeletal system. 2nd ed. Philadelphia, London:

93.	Hill A V. 1938. The heat of shortening and the dynamic constants of muscle. Proceedings of the Royal Society of London. Series B - Biological Sciences 126(843): 136-95.

94.	Knudson D. 2007. Fundamentals of biomechanics. 2nd ed. California, USA: Springer Science+Business Media, LLC.

95.	Özer H, Açar H I, Cömert A, Tekdemir I, Elhan A, Turanli S. 2006. Course of the innervation supply of medial head of triceps muscle and anconeus muscle at the posterior aspect of humerus (anatomical study). Arch Orthop Trauma Surg 126(8): 549-53.

96.	Garten H. 2013. M. triceps brachii and M. anconeus. The muscle test handbook. Garten H, Editor. Churchill Livingstone. p. 258-61.

97.	Gold R. 2007. Appendix A - Muscle Atlas. Thai massage. 2nd ed. Gold R, Editor. Mosby: Saint Louis. p. 176-217.

98. Hwang K, Han J Y, Chung I H. 2004. Topographical anatomy of the anconeus muscle for use as a free flap. J Reconstr Microsurg 20(8): 631-36.

99. Harwood B, Hamberg C M, Chleboun G S, Rice C L. 2010. Effect of elbow joint angle on anconeus fascicle length and motor unit firing rates. Med Sci Sports Exerc 42(5): 584-85.

100. Scarr G. 2012. A consideration of the elbow as a tensegrity structure. Int J Osteopath Med 15(2): 53-65.

101. Stevens D E, Smith C B, Harwood B, Rice C L. 2014. In vivo measurement of fascicle length and pennation of the human anconeus muscle at several elbow joint angles. J Anat 225(5): 502-09.

102. Chao E Y, Morrey B F. 1978. Three-dimensional rotation of the elbow. J Biomech 11(1–2): 57-73.

103. Basmajian J V, De Luca C J. 1985. Muscles alive: their functions revealed by electromyography. 5th ed. Baltimore, Md.: Williams & Wilkins.

104. Funk D A, An K N, Morrey B F, Daube J R. 1987. Electromyographic analysis of muscles across the elbow joint. J Orthop Res 5(4): 529-38.

105. Naito A, Shimizu Y, Handa Y, Ichie M, Hoshimiya N. 1991. Functional anatomical studies of the elbow movements. I. Electromyographic (EMG) analysis. Okajimas Folia Anat Jpn 68(5): 283-88.

106. Naito A, Handa Y, Handa T, Ichie M, Hoshimiya N, Shimizu Y. 1994. Study on the elbow movement produced by functional electrical stimulation (FES). Tohoku J Exp Med 174(4): 343-49.

107. Davidson A W, Rice C L. 2010. Effect of shoulder angle on the activation pattern of the elbow extensors during a submaximal isometric fatiguing contraction. Muscle Nerve 42(4): 514-21.

108. Kuo K H M, Clamann H P. 1981. Coactivation of synergistic muscles of different fiber types in fast and slow contractions. Am J Phys Med 60(5): 219-38.

109. Le Bozec S, Maton B. 1987. Differences between motor unit firing rate, twitch characteristics and fibre type composition in an agonistic muscle group in man. Eur J Appl Physiol 56(3): 350-55.

110. Burkhart T A, Andrews D M. 2013. Kinematics, kinetics and muscle activation patterns of the upper extremity during simulated forward falls. J Electromyogr Kinesiol 23(3): 688–95.

111. Faro F, Wolf J M. 2007. Lateral Epicondylitis: Review and Current Concepts. J Hand Surg-Am 32(8): 1271-79.

112. Elhassan B, Karabekmez F, Hsu C-C, Steinmann S, Moran S. 2011. Outcome of local anconeus flap transfer to cover soft tissue defects over the posterior aspect of the elbow. J Shoulder Elbow Surg 20(5): 807-12.

113. Magden O, Tayfur V, Edizer M. 2010. Arterial anatomy of anconeus muscle flap. J Exp Clin Med 27(1): 24-25.

114. Duncan S F M. 2012. Reoperative hand surgery New York, NY: Springer.

115. Athwal G S, Rispoli D M, Steinmann S P. 2006. The anconeus flap transolecranon approach to the distal humerus. J Orthop Trauma 20(4): 282-85.

116. Bell S N, Benger D. 1999. Management of radioulnar synostosis with mobilization, anconeus interposition, and a forearm rotation assist splint. J Shoulder Elbow Surg 8(6): 621-24.

117. Daluiski A, Schreiber J J, Paul S, Hotchkiss R N. 2014. Outcomes of anconeus interposition for proximal radioulnar synostosis. J Shoulder Elbow Surg 23(12): 1882-87.

118. Capdarest-Arest N, Gonzalez J P, Türker T. 2014. Hypotheses for ongoing evolution of muscles of the upper extremity. Med Hypotheses 82(4): 452-56.

119. Jenkins F A. 1973. The functional anatomy and evolution of the mammalian humero-ulnar articulation. Am J Anat 137(3): 281-97.

120. Ombregt L. 2013. Applied anatomy of the elbow. A system of orthopaedic medicine. 3rd ed. Ombregt L, Editor. Churchill Livingstone. p. e91-e101.

121. Naito A. 2004. Electrophysiological studies of muscles in the human upper limb: the biceps brachii. Anat Sci Int 79(1): 11-20.

122. Eames M H A, Bain G I, Fogg Q A, Van Riet R P. 2007. Distal biceps tendon anatomy: a cadaveric study. J Bone Joint Surg Am 89(5): 1044-49.

123. Joshi S D, Joshi S S, Sontakke Y A, Mittal P S. 2014. Some details of morphology of biceps brachii and its functional relevance. J Anat Soc India 63(1): 24-29.

124. Segal R L. 1992. Neuromuscular compartments in the human biceps brachii muscle. Neurosci Lett 140(1): 98-102.

125. Naito A, Yajima M, Fukamachi H, Ushikoshi K, Handa Y, Hoshimiya N, Shimizu Y. 1994. Electrophysiological studies of the biceps brachii activities in supination and flexion of the elbow joint. Tohoku J Exp Med 173(2): 259-67.

126. Landin D, Myers J, Thompson M, Castle R, Porter J. 2008. The role of the biceps brachii in shoulder elevation. J Electromyogr Kinesiol 18(2): 270-75.

127. Furlani J. 1976. Electromyographic study of the m. biceps brachii in movements at the glenohumeral joint. Acta Anat (Basel) 96(2): 270-84.

128. Tang Z, Zhang K, Sun S, Gao Z, Zhang L, Yang Z. 2014. An upper-limb power-assist exoskeleton using proportional myoelectric control. Sensors (Switzerland) 14(4): 6677-94.

129. Landin D, Thompson M. 2011. The shoulder extension function of the triceps brachii. J Electromyogr Kinesiol 21(1): 161-65.

130. Maton B, Le Bozec S, Cnockaert J C. 1980. The synergy of elbow extensor muscles during dynamic work in man. II. Braking of elbow flexion. Eur J Appl Physiol 44(3): 271-78.

131. Ali A, Sundaraj K, Ahmad R B, Ahamed N U, Islam A. 2013. Surface electromyography for assessing triceps brachii muscle activities: a literature review. Biocybernetics and Biomedical Engineering 33(4): 187-95.

132. Merletti R, Parker P. 2004. Electromyography - physiology, engineering, and noninvasive applications: John Wiley & Sons.

133. Naito A, Sun Y-J, Yajima M, Fukamachi H, Ushikoshi K. 1998. Electromyographic study of the elbow flexors and extensors in a motion of forearm pronation/supination while maintaining elbow flexion in humans. Tohoku J Exp Med 186(4): 267-77.

134. Sörnmo L, Laguna P. 2005. The electromyogram. Bioelectrical signal processing in cardiac and neurological applications. Academic Press: Burlington. p. 337-410.

135. Weiss L, Weiss J, Gaudino W, Isaac V, Gustafson K. 2004. Chapter 5 Electromyography. Easy EMG. Weiss L W S, Editor. Butterworth-Heinemann: Edinburgh. p. 41-80.

136. Bilodeau M, Arsenault A B, Gravel D, Bourbonnais D. 1991. EMG power spectra of elbow extensors during ramp and step isometric contractions. Eur J Appl Physiol 63(1): 24-28.

137. Bilodeau M, Arsenault A B, Gravel D, Bourbonnais D. 1990. The influence of an increase in the level of force on the EMG power spectrum of elbow extensors. Eur J Appl Physiol 61(5-6): 461-66.

138. Chowdhury R, Reaz M, Ali M, Bakar A, Chellappan K, Chang T. 2013. Surface electromyography signal processing and classification techniques. Sensors 13(9): 12431-66.

139. Hug F. 2011. Can muscle coordination be precisely studied by surface electromyography? J Electromyogr Kinesiol 21(1): 1-12.

140. Farina D. 2006. Interpretation of the surface electromyogram in dynamic contractions. Exerc Sport Sci Rev 34(3): 121-27.

141. De Luca C J. 1997. The use of surface electromyography in biomechanics. J Appl Biomech 13(2): 135-63.

142. Campanini I, Merlo A, Degola P, Merletti R, Vezzosi G, Farina D. 2007. Effect of electrode location on EMG signal envelope in leg muscles during gait. J Electromyogr Kinesiol 17(4): 515-26.

143. Merletti R, Lo Conte L R. 1997. Surface EMG signal processing during isometric contractions. J Electromyogr Kinesiol 7(4): 241-50.

144. Disselhorst-Klug C, Schmitz-Rode T, Rau G. 2009. Surface electromyography and muscle force: limits in sEMG-force relationship and new approaches for applications. Clin Biomech 24(3): 225-35.

145. Inman V T, Ralston H J, De C.M. Saunders J B, Bertram Feinstein M B, Wright Jr E W. 1952. Relation of human electromyogram to muscular tension. Electroencephalogr Clin Neurophysiol 4(2): 187-94.

146. Luttmann A, Jäger M, Laurig W. 2000. Electromyographical indication of muscular fatigue in occupational field studies. Int J Ind Ergonom 25(6): 645-60.

147. Webster J G. 1984. Reducing motion artifacts and interference in biopotencial recording. IEEE Trans Biomed Eng BME-31(12): 823-26.

148. Winter D A, Fuglevand A J, Archer S E. 1994. Crosstalk in surface electromyography: theoretical and practical estimates. J Electromyogr Kinesiol 4(1): 15-26.

149. Lapatki B G, Stegeman D F, Jonas I E. 2003. A surface EMG electrode for the simultaneous observation of multiple facial muscles. J Neurosci Methods 123(2): 117-28.

150. Parker P, Englehart K, Hudgins B. 2006. Myoelectric signal processing for control of powered limb prostheses. J Electromyogr Kinesiol 16(6): 541-48.

151. De Luca C J, Donald Gilmore L, Kuznetsov M, Roy S H. 2010. Filtering the surface EMG signal: movement artifact and baseline noise contamination. J Biomech 43(8): 1573-79.

152. Winter D A. 1980. Report by the Ad Hoc Committee of the international society of electrophysiological kinesiology.

153. Merletti R. 1999. Standards for reporting EMG data. J Electromyogr Kinesiol 9(1): III-IV.

154. Cavalcanti Garcia M A, Vieira T M M. 2011. Surface electromyography: why, when and how to use it. Rev Andal Med Deporte 4(1): 17-28.

155. Phinyomark A, Thongpanja S, Hu H, Phukpattaranont P, Limsakul C. 2012. The usefulness of mean and median frequencies in electromyography analysis. CC BY 3.0 license. © The Author(s).

156. Farina D, Merletti R, Indino B, Graven-Nielsen T. 2004. Surface EMG crosstalk evaluated from experimental recordings and simulated signals reflections on crosstalk interpretation, quantification and reduction. Methods Inf Med 43(1): 30-35.

157. Enderle J D, Bronzino J D. 2011. Introduction to biomedical engineering. 3rd ed. Burlington: Elsevier Science.

158. Roetenberg D. 2006. Inertial and magnetic sensing of human motion. Thesis. Uneverity of Twente, Enschede, the Netherlands.

159. XSens T B V. 2011. MTw user manual. Enschede, Netherlands, 83. Available in www.xsens.com.

160. Cutti A G, Giovanardi A, Rocchi L, Davalli A, Sacchetti R. 2008. Ambulatory measurement of shoulder and elbow kinematics through inertial and magnetic sensors. Med Biol Eng Comput 46(2): 169-78.

161. Luinge H J, Veltink P H, Baten C T M. 2007. Ambulatory measurement of arm orientation. J Biomech 40(1): 78-85.

162. Zhou H, Hu H, Harris N D, Hammerton J. 2006. Applications of wearable inertial sensors in estimation of upper limb movements. Biomed Signal Proces 1(1): 22-32.

163. Djurić-Jovičić M D, Jovičić N S, Popović D B, Djordjević A R. 2012. Nonlinear optimization for drift removal in estimation of gait kinematics based on accelerometers. J Biomech 45(16): 2849-54.

164. El-Gohary M, Holmstrom L, Huisinga J, King E, McNames J, Horak F. 2011. Upper limb joint angle tracking with inertial sensors. Proceedings of the Annual International Conference of the IEEE Engineering in Medicine and Biology Society, EMBS.

165. Zhou H, Hu H. 2005. Inertial motion tracking of human arm movements in stroke rehabilitation. International Conference on Mechatronics & Automation. Niagara Falls, Canada.

166. Roetenberg D, Luinge H a, Slycke P. 2009. XSens MVN: Full 6DOF human motion tracking using miniature inertial sensors. XSens Technologies: 1-7.

167. Brodie M A, Walmsley A, Page W. 2008. The static accuracy and calibration of inertial measurement units for 3D orientation. Comput Methods Biomech Biomed Engin 11(6): 641-48.

168. Brodie M A, Walmsley A, Page W. 2008. Dynamic accuracy of inertial measurement units during simple pendulum motion. Comput Methods Biomech Biomed Engin 11(3): 235-42.

169. Godwin A, Agnew M, Stevenson J. 2009. Accuracy of inertial motion sensors in static, quasistatic, and complex dynamic motion. J Biomech Eng 131(11): 114501-05.

170. Brennan A, Zhang J, Deluzio K, Li Q. 2011. Quantification of inertial sensor-based 3D joint angle measurement accuracy using an instrumented gimbal. Gait Posture 34(3): 320-23.

171. Zhou H, Hu H. 2010. Reducing drifts in the inertial measurements of wrist and elbow positions. IEEE T Instrum Meas 59(3): 575-85.

172. Varesano F. 2011. Using arduino for tangible human computer interaction. Thesis. Universitá degli Studi di Torino, Italy.

173. Luinge H J. 2002. Inertial sensing of human movement. Thesis. University of Twente, Enschede, the Netherlands.

174. Bachmann E R. 2000. Inertial and magnetic tracking of limb segment orientation for inserting humans into synthetic environments PhD. Naval postgraduate school Monterey, California U.S.

175. Kuipers J B. 1999. Quaternions and rotation sequences: a primer with applications to orbits, aerospace, and virtual reality. Princeton, N.J: Princeton University Press.

176. Young A D. 2010. Wireless realtime motion tracking system using localised orientation estimation. PhD. The University of Edinburgh, Edinburgh, Scotlan U.K.

177. Baker R. 2011. Globographic visualisation of three dimensional joint angles. J Biomech 44(10): 1885-91.

178. Woltring H J. 1994. 3-D attitude representation of human joints: a standardization proposal. J Biomech 27(12): 1399-414.

179. Zatsiorsky V M. 1998. Kinematics of human motion. Champaign, Ill: Human Kinetics.

180. Liu G R, Quek S S. 2003. 1 - Computational modelling. Finite Element Method. Liu G R and Quek S S, Editors. Butterworth-Heinemann: Oxford. p. 1-11.

181. Rao S S. 2005. 1 - Overview of Finite Element Method. The Finite Element Method in Engineering. 4th ed. Rao S S, Editor. Butterworth-Heinemann: Burlington. p. 3-49.

182. Ratner B D. 2004. Biomaterials science: an introduction to materials in medicine. 2nd ed. San Diego: Academic Press.

183. Holland P, Davies A M, Cassar-Pullicino V N. 1994. Computed tomographic arthrography in the assessment of osteochondritis dissecans of the elbow. Clin Radiol 49(4): 231-35.

184. Melloni P, Valls R. 2005. The use of MRI scanning for investigating soft-tissue abnormalities in the elbow. Eur J Radiol 54(2): 303-13.

185. Riddlesberger Jr M M, Kuhn J P. 1983. The role of computed tomography in diseases of the musculoskeletal system. J Comput Tomogr 7(1): 85-99.

186. Wessely M A, Hurtgen-Grace K L, Grenier J-M. 2006. Elbow MRI: Part 1. Normal imaging appearance of the elbow. Clinical Chiropractic 9(4): 198-205.

187. Wessely M A, Grenier J-M. 2007. Elbow MRI: Part 2. The imaging of common disorders affecting the elbow region. Clinical Chiropractic 10(1): 43-49.

188. Eng J. 2003. Sample size estimation: how many individuals should be studied? Radiology 227(2): 309-13.

189. Le Bozec S, Evans O M, Maton B. 1987. Long-latency stretch reflexes of the human elbow extensors during voluntary relaxation: differences between agonistic muscles. Exp Neurol 96(3): 516-27.

190. Caldwell G E. 1987. Applied muscle models in prediction of forces at the elbow. Simon Fraser University, Vancouver, Canada

191. SIMULIA. 2012. Abaqus/CAE 6.12 Analysis User's manual Providense RI, USA.

192. Willing R T, Lalone E A, Shannon H, Johnson J A, King G J W. 2013. Validation of a finite element model of the human elbow for determining cartilage contact mechanics. J Biomech 46(10): 1767-71.

193. Lapner M, Willing R, Johnson J A, King G J W. 2014. The effect of distal humeral hemiarthroplasty on articular contact of the elbow. Clin Biomech 29(5): 537-44.

194. Phillips A T M, Pankaj P, Howie C R, Usmani A S, Simpson A H R W. 2007. Finite element modelling of the pelvis: inclusion of muscular and ligamentous boundary conditions. Med Eng Phys 29(7): 739-48.

195. Zou Z, Chávez-Arreola A, Mandal P, Board T N, Alonso-Rasgado T. 2013. Optimization of the position of the acetabulum in a ganz periacetabular osteotomy by finite element analysis. J Orthop Res 31(3): 472-79.

196. Fung Y C. 1981. Biomechanics: mechanical properties of living tissues. New York Inc.:

197. Merz B, Eckstein F, Hillebrand S, Putz R. 1997. Mechanical implications of humero-ulnar incongruity: finite element analysis and experiment. J Biomech 30(7): 713-21.

198. Kim S. 2014. Contact stress analysis of the native radial head and radial head implants. Doctoral Dissertation University of Pittsburgh, Pittsburgh, Pennsylvania.

199. Dunham C E, Takaki S E, Johnson J A, Dunning C E. 2005. Mechanical properties of cancellous bone of the distal humerus. Clin Biomech 20(8): 834-38.

200. Jimenez Cruz D. 2014. Mechanical behaviour of cam-type femoroacetabular impingement. PhD Thesis. The University of Manchester, Manchester, UK.

201. Alonso-Rasgado T, Jimenez-Cruz D, Bailey C G, Mandal P, Board T. 2012. Changes in the stress in the femoral head neck junction after osteochondroplasty for hip impingement: a finite element study. J Orthop Res 30(12): 1999-2006.

202. Brekelmans W A M, Poort H W, Slooff T J J H. 1972. A new method to analyse the mechanical behaviour of skeletal parts. Acta Orthop 43(5): 301-17.

203. Mansour J M. 2003. Biomechanics of cartilage. Lippincott Williams and Wilkins, Philadelphia. p. 66-79.

204. Armstrong A D, Dunning C E, Ferreira L M, Faber K J, Johnson J A, King G J W. 2005. A biomechanical comparison of four reconstruction techniques for the medial collateral ligament-deficient elbow. J Shoulder Elbow Surg 14(2): 207-15.

205. Ahmad C S, Lee T Q, ElAttrache N S. 2003. Biomechanical evaluation of a new ulnar collateral ligament reconstruction technique with interference screw fixation. Am J Sports Med 31(3): 332-37.

206. Regan W D, Korinek S L, Morrey B F, An K N. 1991. Biomechanical study of ligaments around the elbow joint. Clin Orthop (271): 170-79.

207. Spratley E M, Wayne J S. 2011. Computational model of the human elbow and forearm: application to complex varus instability. Ann Biomed Eng 39(3): 1084-91.

208. Fisk J P, Wayne J S. 2009. Development and validation of a computational musculoskeletal model of the elbow and forearm. Ann Biomed Eng 37(4): 803-12.

209. Goto A, Moritomo H, Murase T, Oka K, Sugamoto K, Arimura T, Nakajima Y, Yamazaki T, Sato Y, Tamura S, Yoshikawa H, Ochi T. 2004. In vivo elbow biomechanical analysis during flexion: Three-dimensional motion

analysis using magnetic resonance imaging. J Shoulder Elbow Surg 13(4): 441-47.

210. Stormont T J, An K N, Morrey B F, Chao E Y. 1985. Elbow joint contact study: comparison of techniques. J Biomech 18(5): 329-36.

211. Eckstein F, Löhe F, Hillebrand S, Bergmann M, Schulte E, Milz S, Putz R. 1995. Morphomechanics of the humero-ulnar joint: I. Joint space width and contact areas as a function of load and flexion angle. The Anatomical Record 243(3): 318-26.

APPENDIX I

Podium presentations

Israel Miguel Andres, Teresa Alonso-Rasgado, Alan Walmsley, Adam C Watts. 2013. Function of the Anconeus Muscle: A Kinematic and Electromyographic study of the Elbow. Gold Medal Research Day, Wrightington Hospital Wigan and Leigh NHS, UK.

Israel Miguel Andres, Teresa Alonso-Rasgado, Alan Walmsley, Adam C Watts. 2014. The effect of Blocking the Anconeus Muscle: Kinematic and Electromyographic Study. Gold Medal Research Day, Wrightington Hospital Wigan and Leigh NHS, UK.

Israel Miguel Andres, Teresa Alonso-Rasgado, Alan Walmsley, Adam C Watts. 2015. Contribution of the Anconeus Muscle to the Kinematics of the Elbow. Gold Medal Research Day, Wrightington Hospital Wigan and Leigh NHS, UK.

APPENDIX II

Ethical approval letter

MANCHESTER 1824

The University of Manchester

Faculty of Medical and
Human Sciences
The University of Manchester
Oxford Road
Manchester   M13 9PT

+44(0)161 306 0100
www.manchester.ac.uk

Secretary to Research Ethics Committee 1

Email: katy.boyle@manchester.ac.uk
Phone : 0161 375 1360

Mr Israel Miguel Andres
Postgraduate Student
School of MACE
University of Manchester

Isreal.miguelandres@postgrad.manchester.ac.uk

ref: ethics/11335

26 January 2012

Dear Mr Miguel Andres

Committee on the Ethics of Research on Human Beings
*Miguel Andres, Rasgado, Watts, Mandal, Zou, Walmsley: Function of the anconeus
muscle (ref 11335)*

I write to confirm that the amendments to participant information sheet, consent form, advert
and ethics application form satisfy the concerns of the Committee and that the above project
therefore has ethical approval.

The general conditions remain as stated in my letter of 20th January 2012.

Finally, I would be grateful if you could complete and return the attached form at the end of
the project or by January 2013, whichever is earlier. When completing this form, please
reference your project as:

*Miguel Andres, Rasgado, Watts, Mandal, Zou, Walmsley: Function of the anconeus
muscle (ref 11335)*

We hope the research goes well.

Yours sincerely,
Katy Boyle
Secretary to University Research Ethics Committee

Combining the strengths of UMIST and
The Victoria University of Manchester

APPENDIX III

Raw myoelectric activity

Maximum voluntary contraction (MVC) of anconeus, biceps brachii and triceps brachii muscles (Raw data)

Participant **68136**

Maximum Voluntary Contractions (MVC) of Anconeus, Biceps Brachii and Triceps Brachii
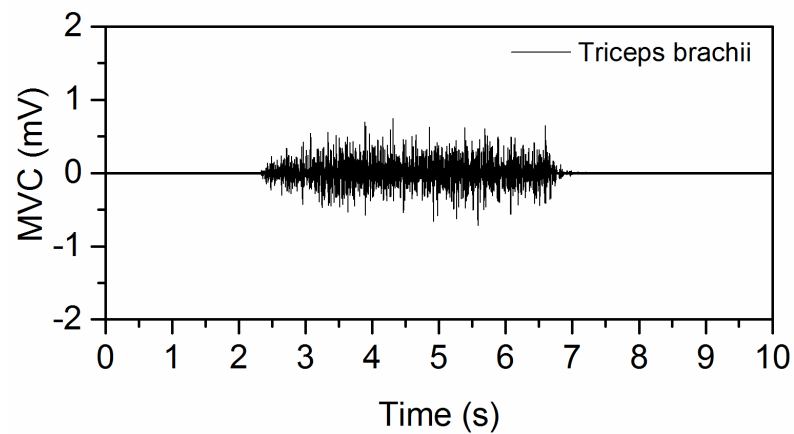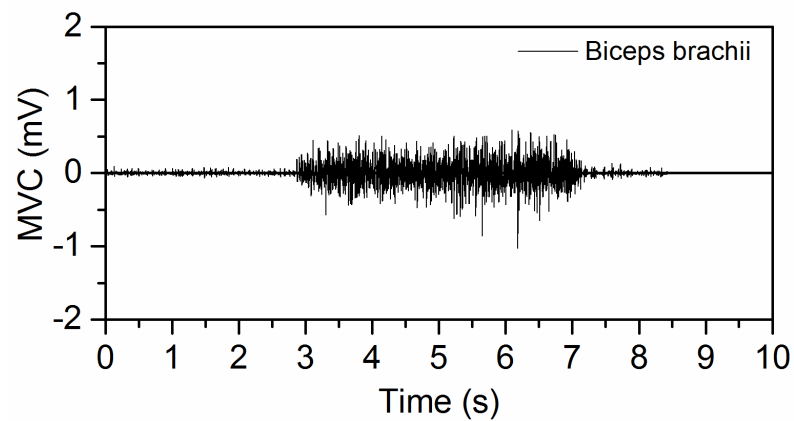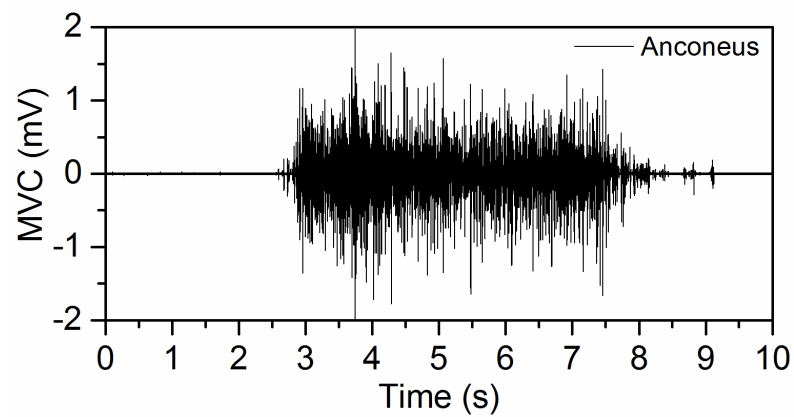
Participant **73799**


Maximum Voluntary Contractions (MVC) of
Anconeus, Biceps Brachii and Triceps Brachii
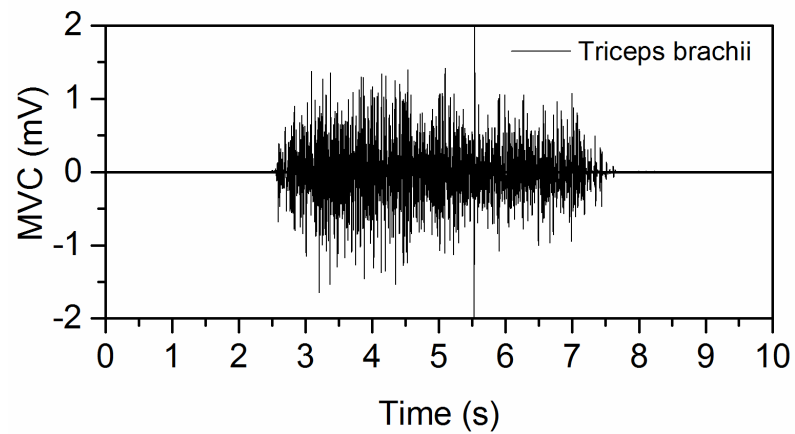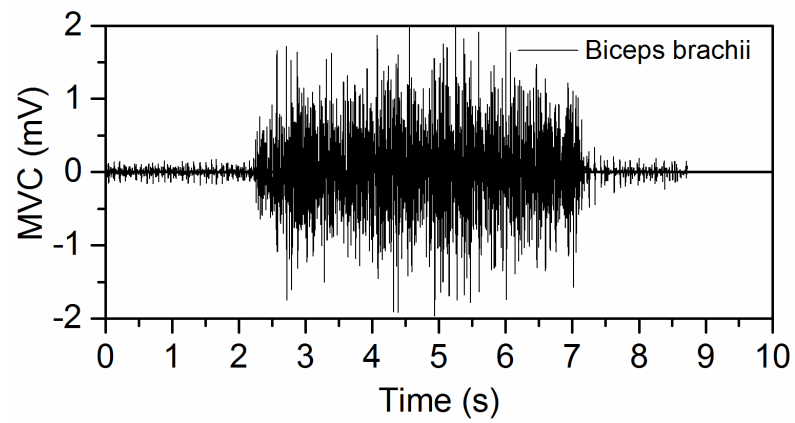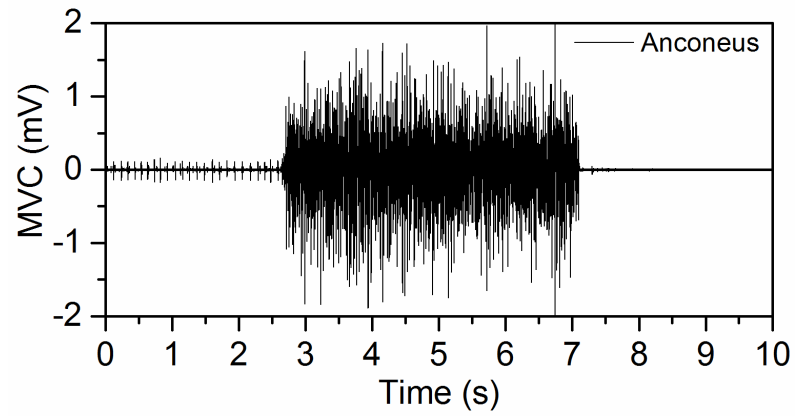
Participant **12632**

Maximum Voluntary Contractions (MVC) of
Anconeus, Biceps Brachii and Triceps Brachii
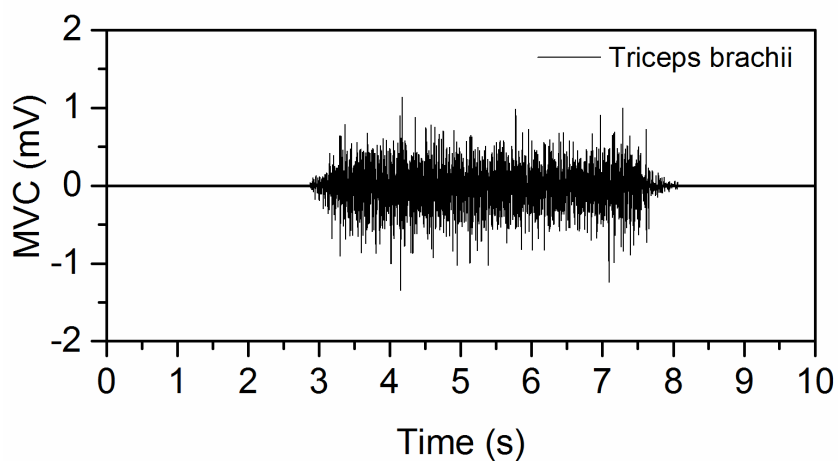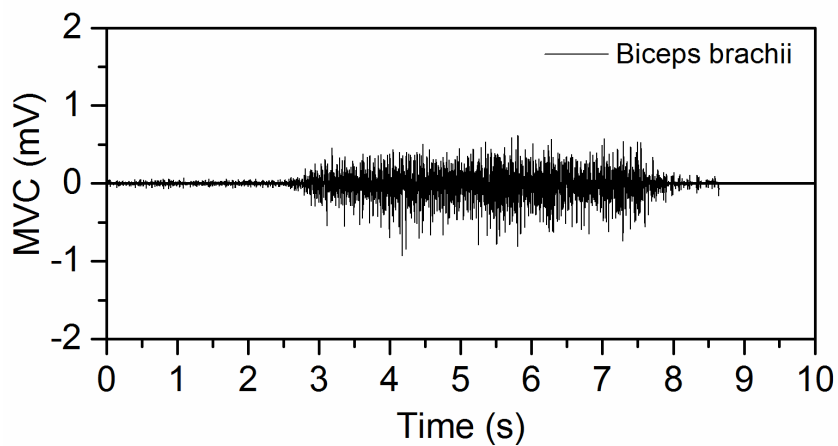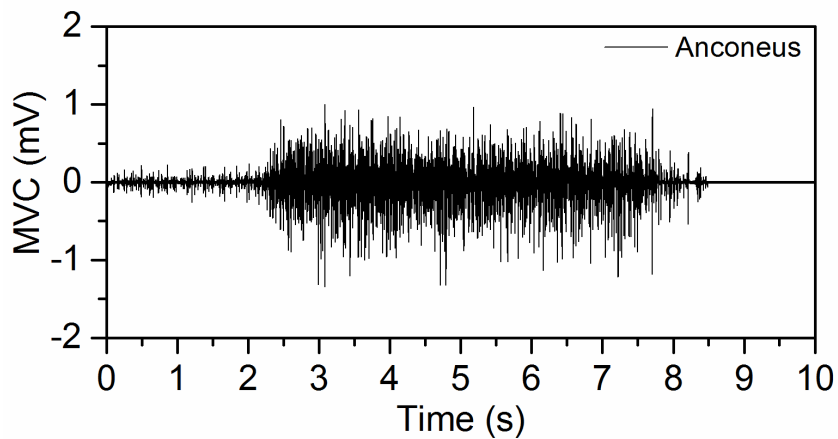
Participant **25106**

Maximum Voluntary Contractions (MVC) of
Anconeus, Biceps Brachii and Triceps Brachii
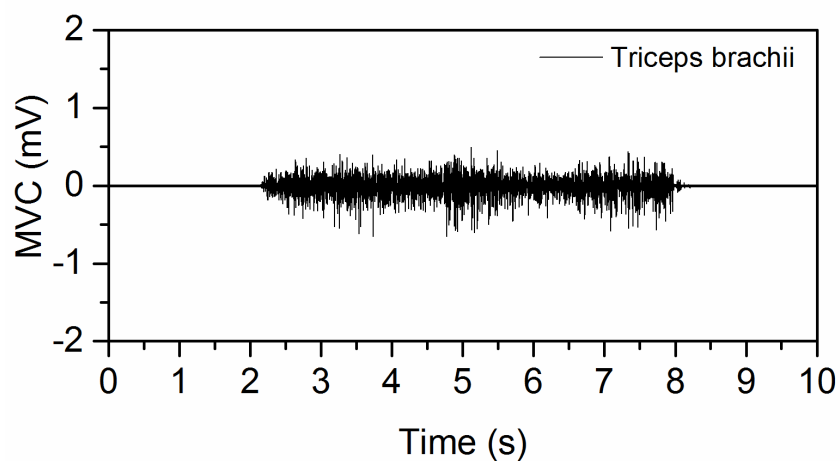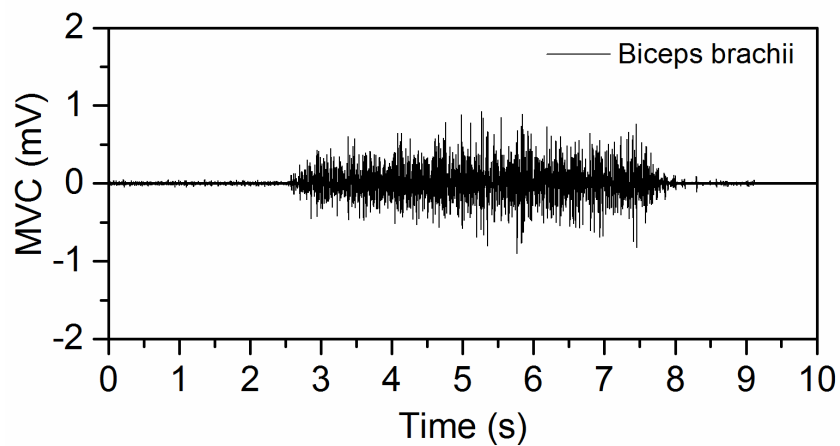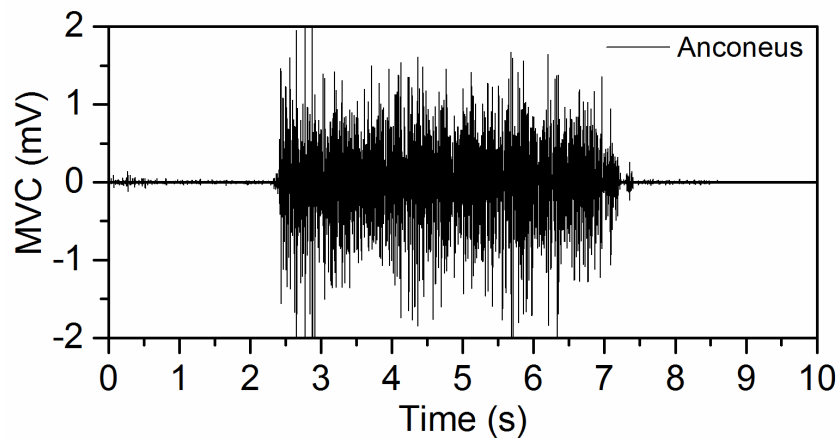
Participant **468N1**

Maximum Voluntary Contractions (MVC) of
Anconeus, Biceps Brachii and Triceps Brachii
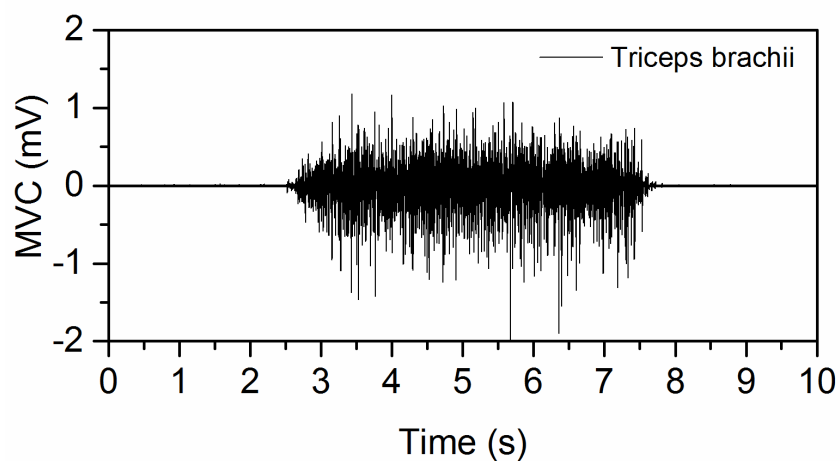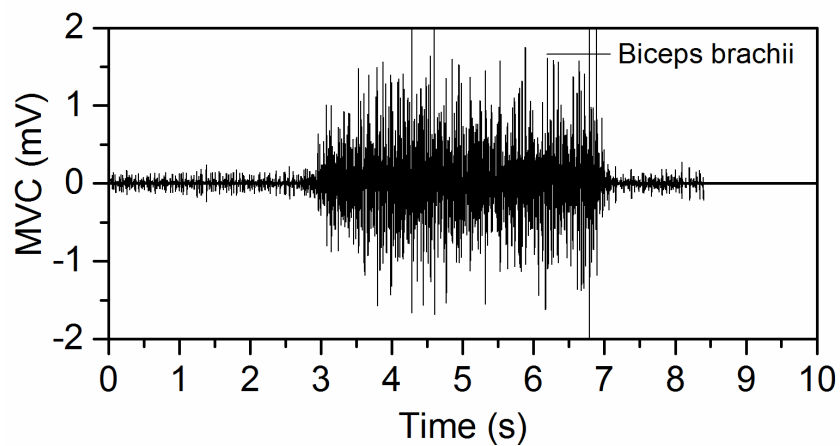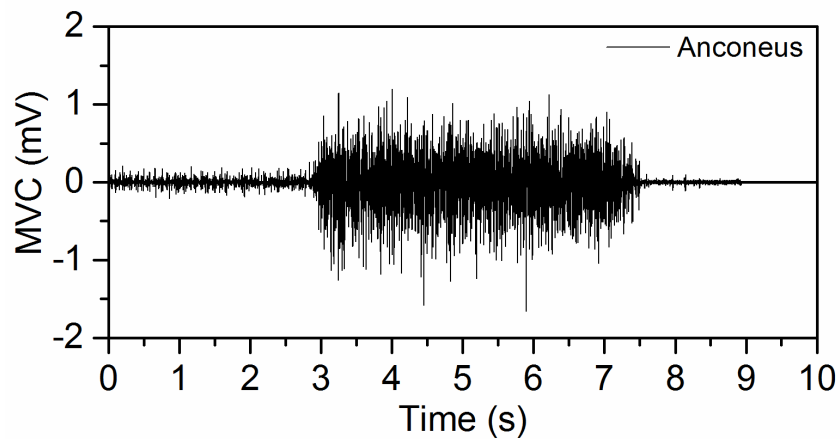
Participant **45636**

Maximum Voluntary Contractions (MVC) of Anconeus, Biceps Brachii and Triceps Brachii
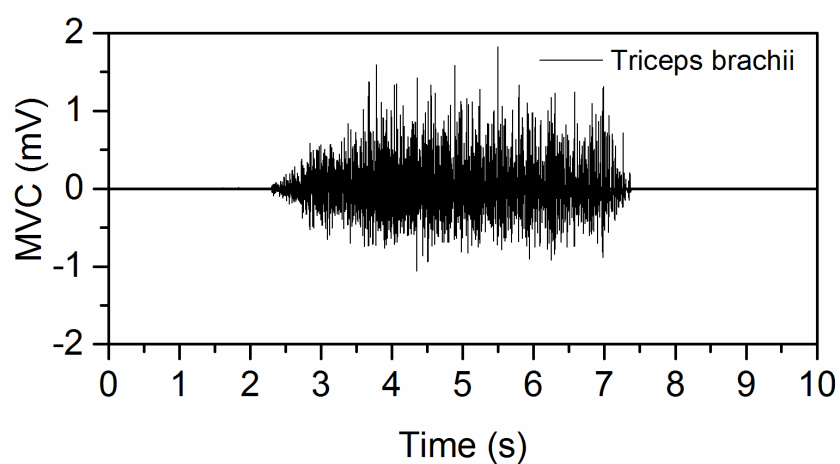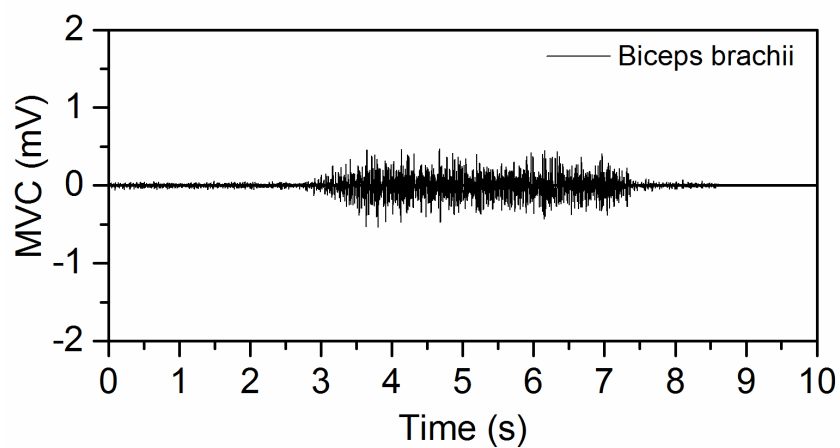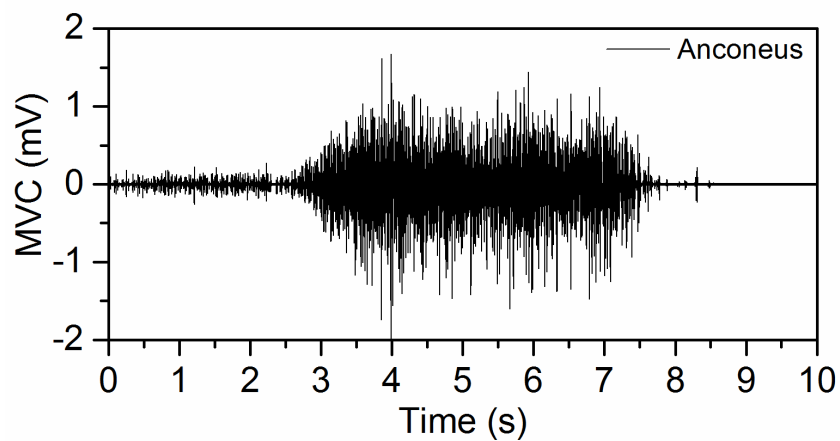
Flexion-extension in the horizontal plane (Raw data)

Participant **68136**

Myoelectric activity of Anconeus, Biceps Brachii and Triceps Brachii
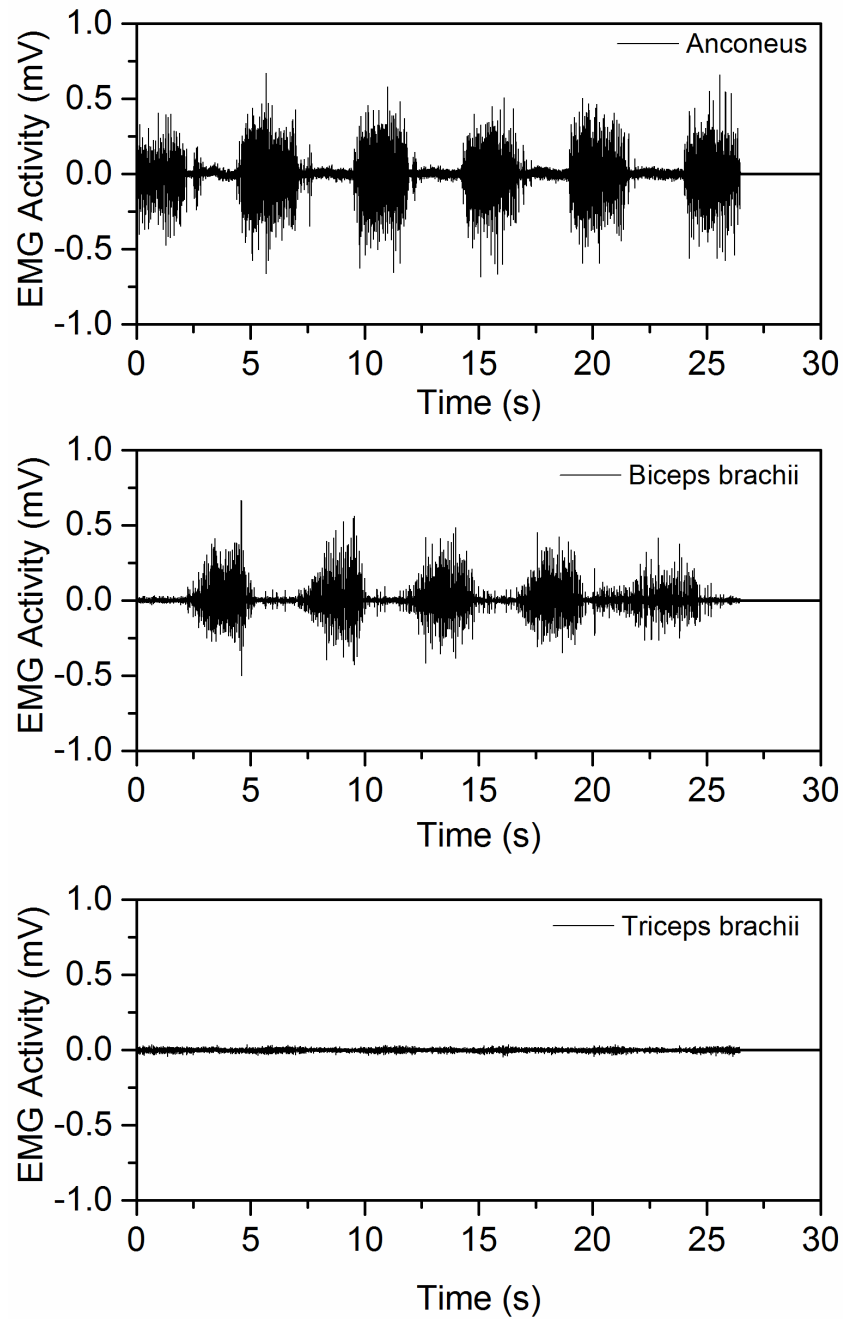
Flexion-extension in the sagittal plane while standing (Raw data)

Participant **68136**

Myoelectric activity of Anconeus,
Biceps Brachii and Triceps Brachii
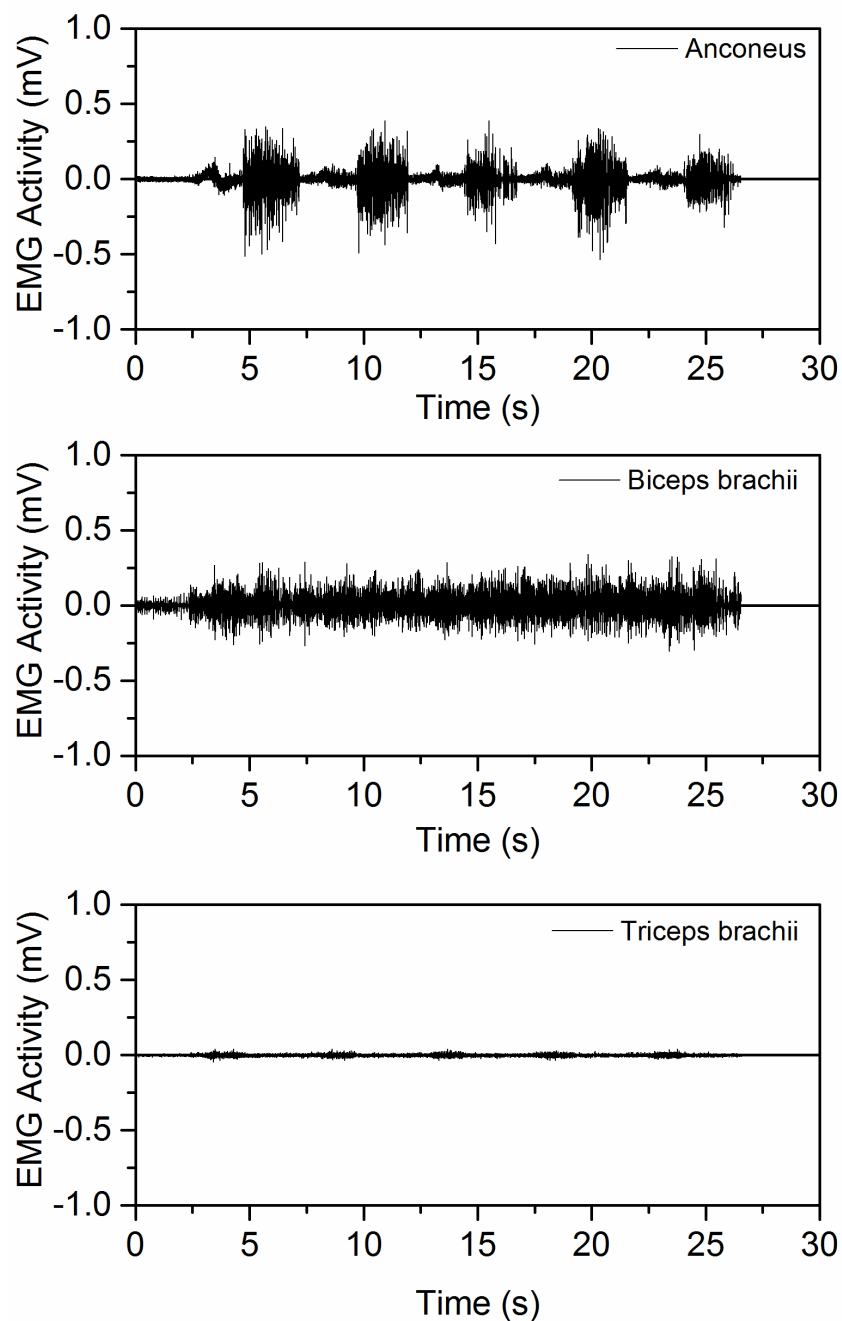
Flexion-extension in the sagittal plane, the spine bent forward 90° (Raw data)

Participant **68136**

Myoelectric activity of Anconeus, Biceps Brachii and Triceps Brachii
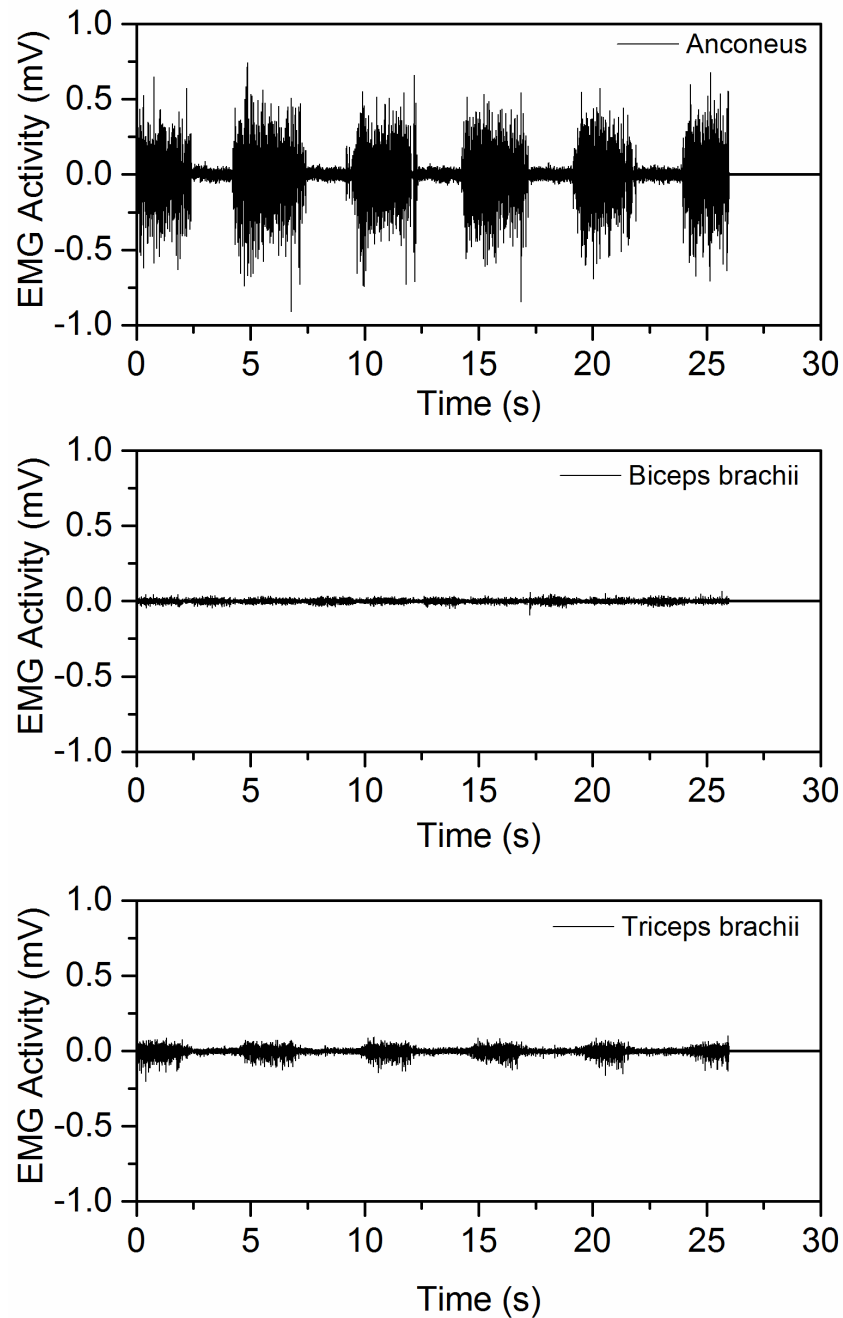
Supination-pronation with the elbow flexed 90 degrees (Raw data)

Participant **68136**

Myoelectric activity of Anconeus, Biceps Brachii and Triceps Brachii
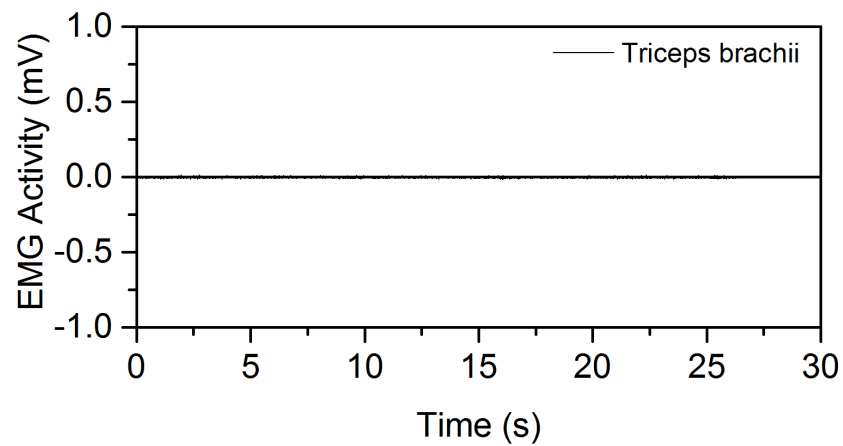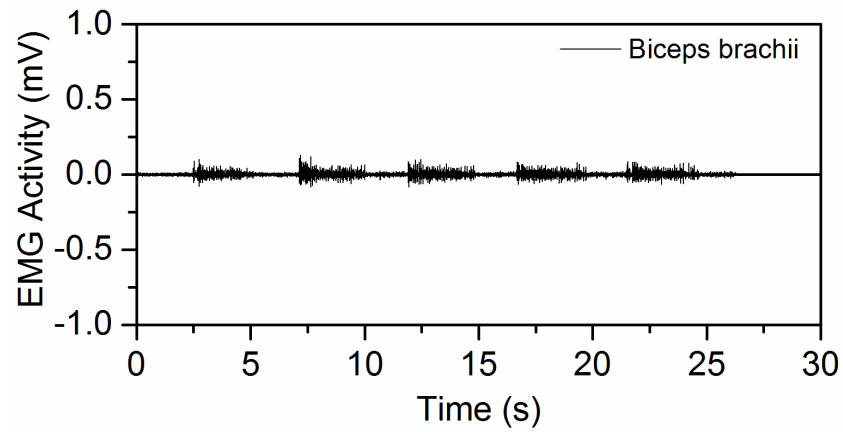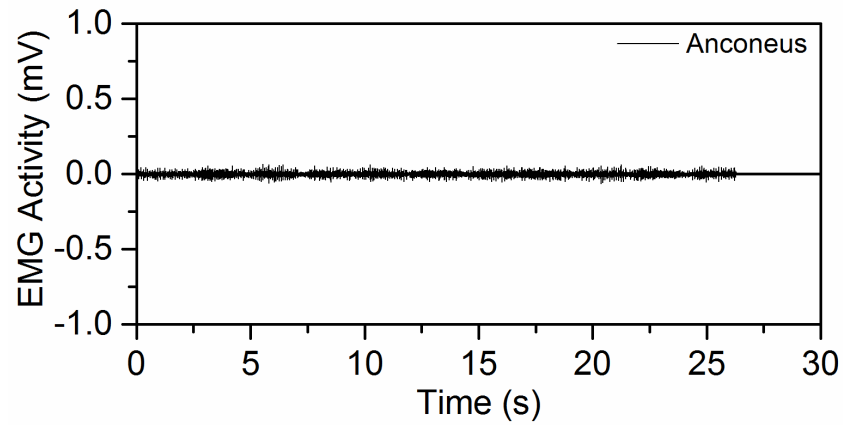
Kinematics, kinetics and EMG activity of anconeus, biceps and triceps brachii

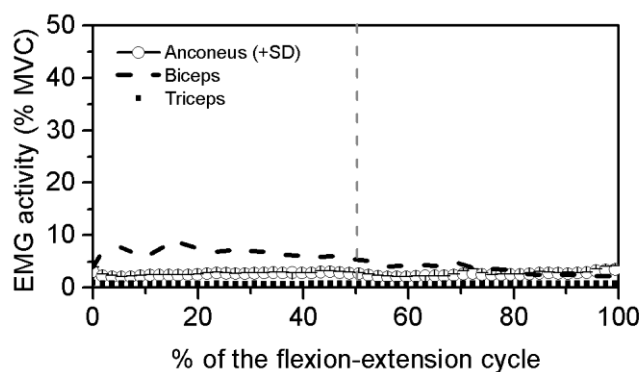Flexion-extension in the horizontal plane

Participant **12632**

a) Angular velocity of the elbow joint, b) Net torque and power of the joint and c) Myoelectric activity of the anconeus, biceps and triceps brachii
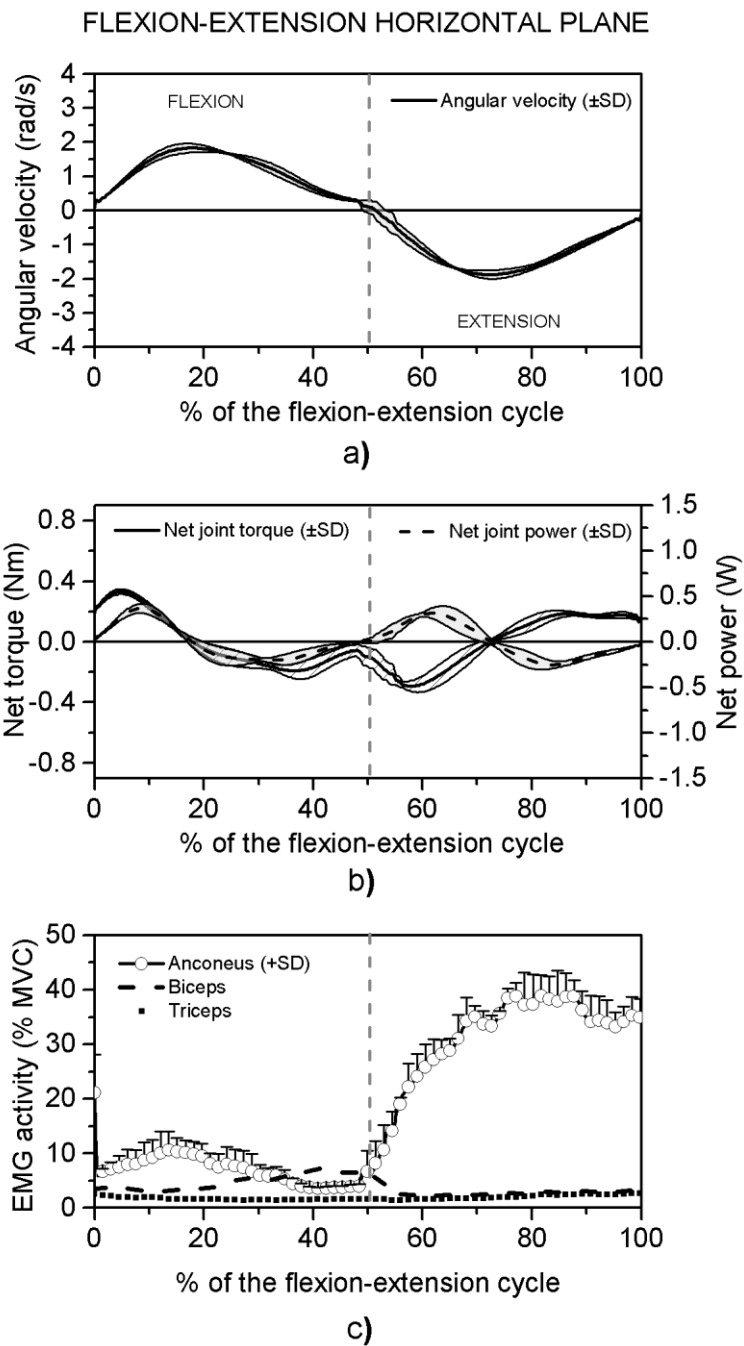

a)

b)

c)

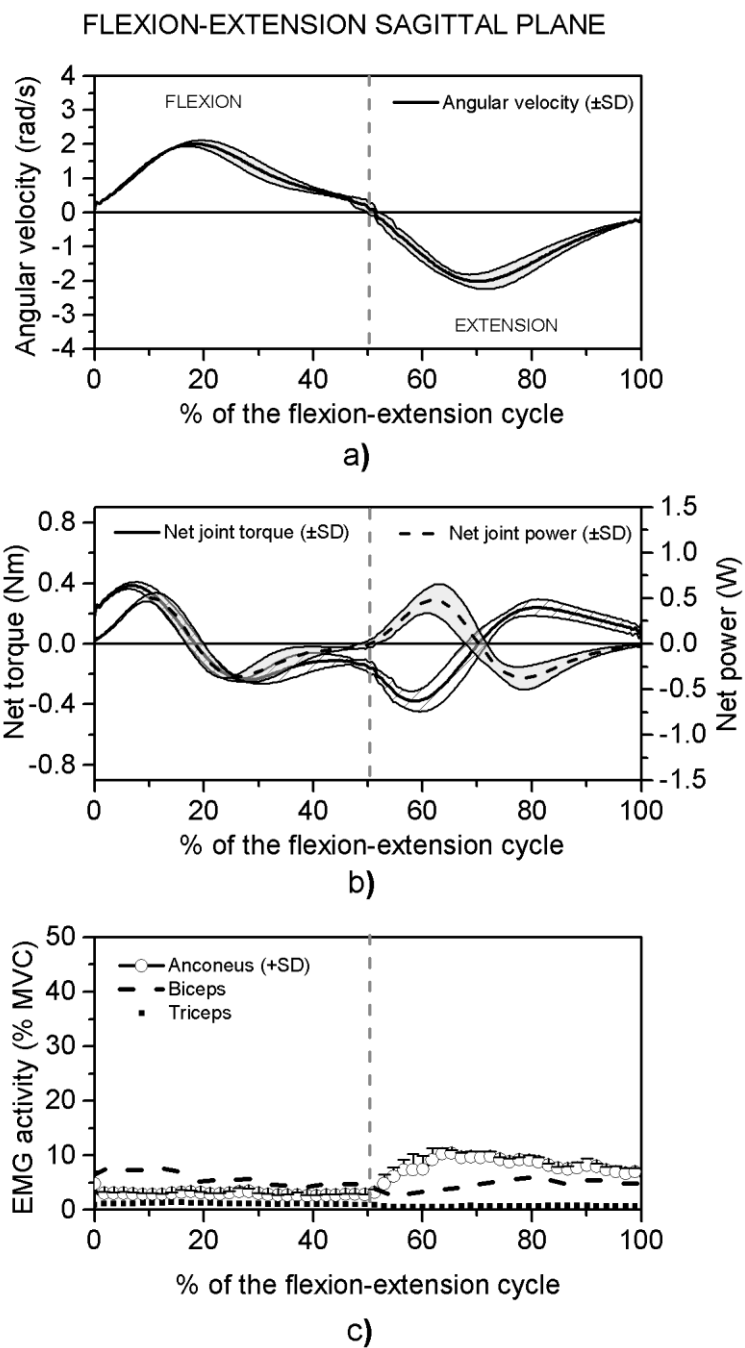Flexion-extension in the sagittal plane while standing

Participant **12632**

a) Angular velocity of the elbow joint, b) Net torque and power of the joint and c) Myoelectric activity of the anconeus, biceps and triceps brachii

FLEXION-EXTENSION SAGITTAL PLANE

a)

b)

c)

Flexion-extension in the sagittal plane, the spine bent forward 90°
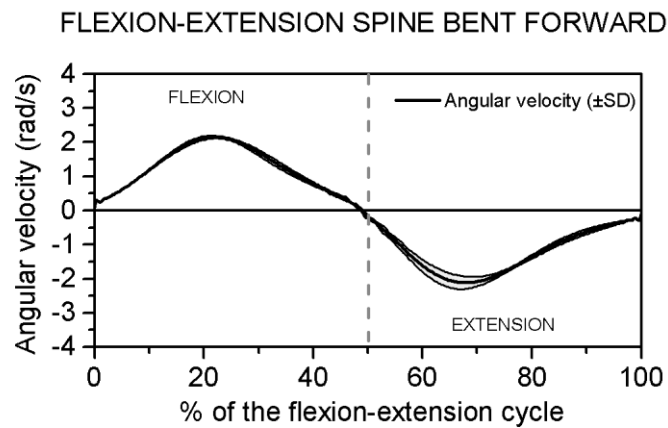
Participant **12632**

a) Angular velocity of the elbow joint, b) Net torque and power of the joint and c) Myoelectric activity of the anconeus, biceps and triceps brachii

FLEXION-EXTENSION SPINE BENT FORWARD

a)

b)

c)
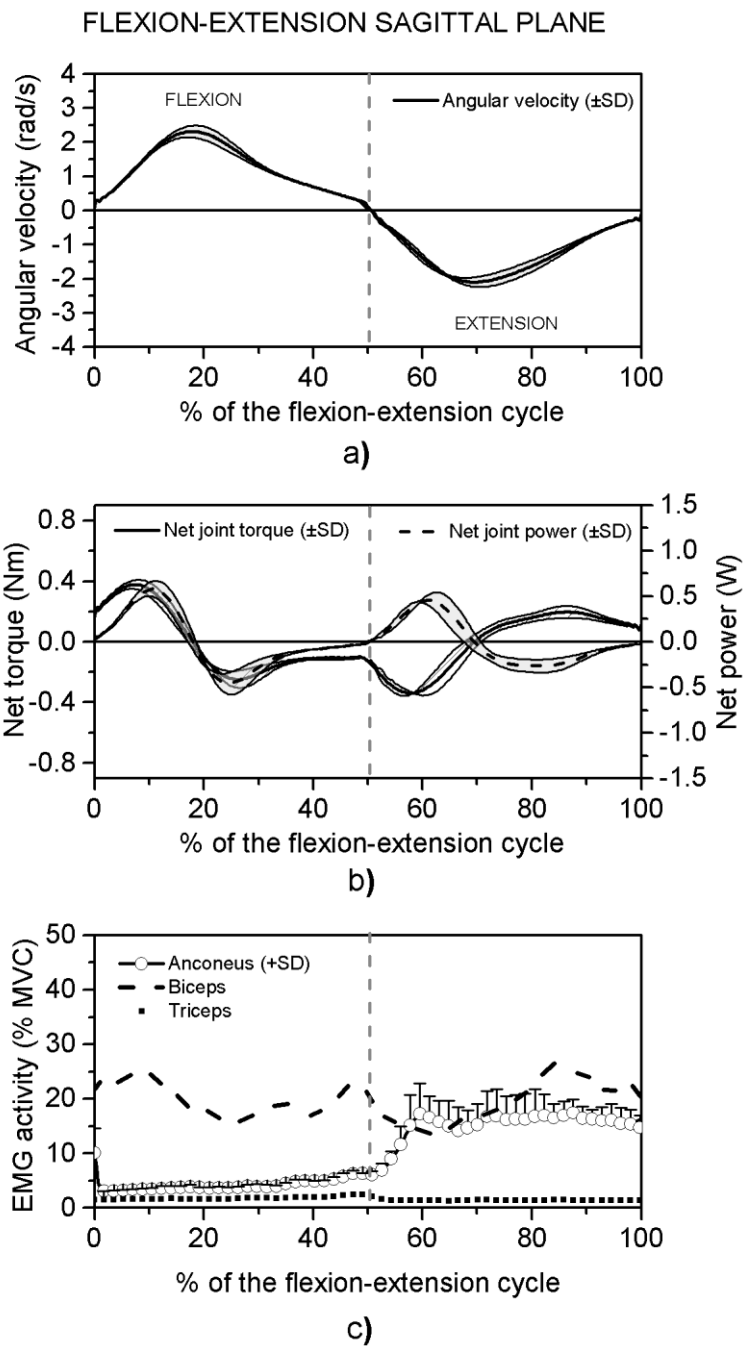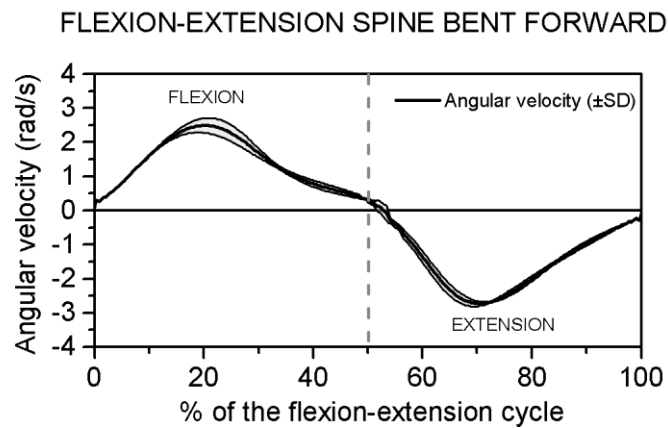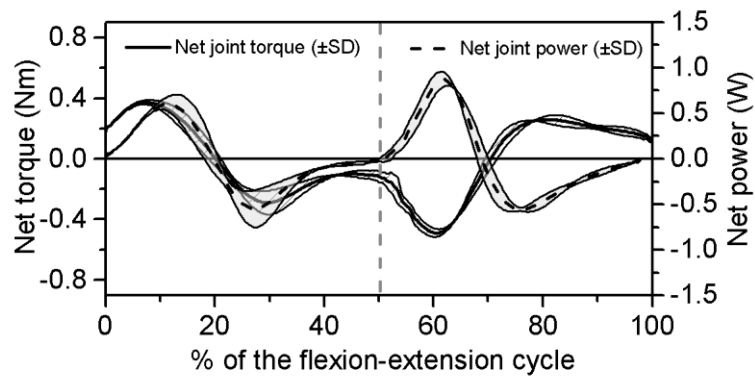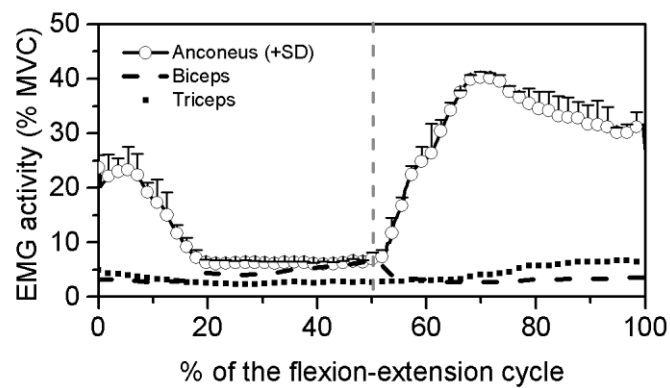
Supination-pronation with the elbow flexed 90 degrees

Participant **12632**

a) Angular velocity of the elbow joint, b) Net torque and power of the joint and c) Myoelectric activity of the anconeus, biceps and triceps brachii
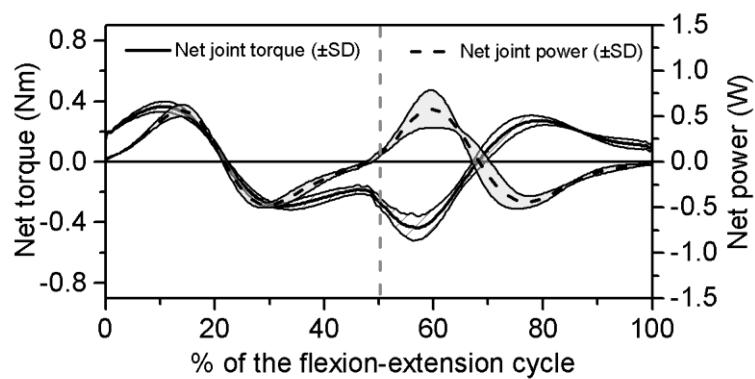
Flexion-extension in the horizontal plane
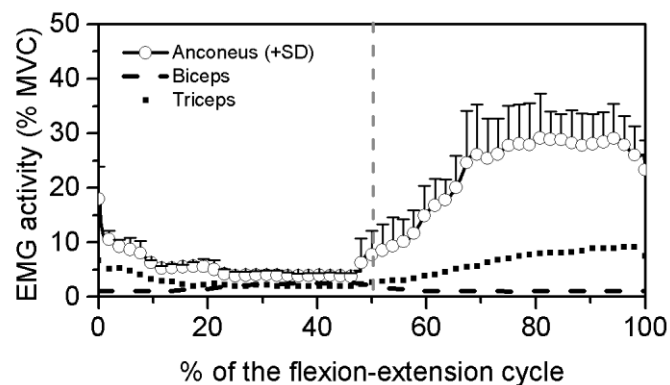
Participant **67214**

a) Angular velocity of the elbow joint, b) Net torque and power of the joint and c) Myoelectric activity of the anconeus, biceps and triceps brachii

FLEXION-EXTENSION HORIZONTAL PLANE

a)

b)

c)

Flexion-extension in the sagittal plane while standing

Participant **67214**

a) Angular velocity of the elbow joint, b) Net torque and power of the joint and c) Myoelectric activity of the anconeus, biceps and triceps brachii

FLEXION-EXTENSION SAGITTAL PLANE

a)

b)

c)

Flexion-extension in the sagittal plane, the spine bent forward 90°

Participant **67214**

a) Angular velocity of the elbow joint, b) Net torque and power of the joint and c) Myoelectric activity of the anconeus, biceps and triceps brachii
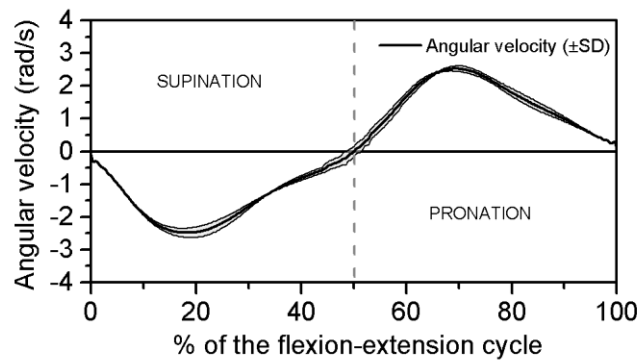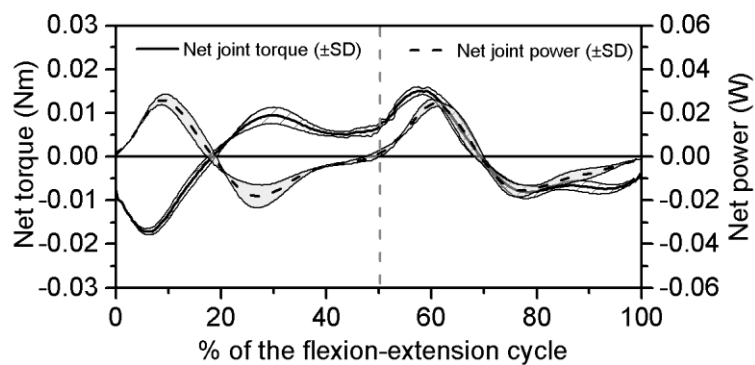
FLEXION-EXTENSION SPINE BENT FORWARD

a)

b)

c)

Supination-pronation with the elbow flexed 90 degrees

Participant **67214**

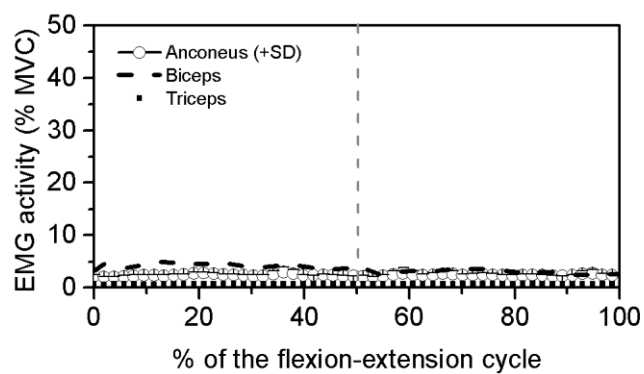a) Angular velocity of the elbow joint, b) Net torque and power of the joint and c) Myoelectric activity of the anconeus, biceps and triceps brachii